ATTENUATION CHARACTERISTICS OF UTTARAKHAND HIMALAYA USING STRONG MOTION DATA

Ph. D. THESIS

by

ASHVINI KUMAR

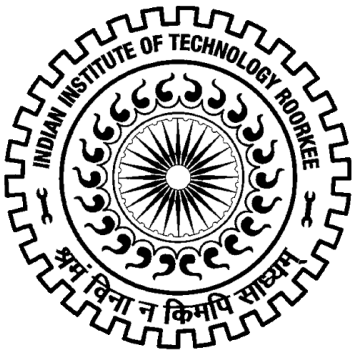

DEPARTMENT OF EARTH SCIENCES
INDIAN INSTITUTE OF TECHNOLOGY ROORKEE
ROORKEE-247 667 (INDIA)

MAY, 2015

ATTENUATION CHARACTERISTICS OF UTTARAKHAND HIMALAYA USING STRONG MOTION DATA

A THESIS
Submitted in partial fulfilment of the
requirements for the award of the degree
of
DOCTOR OF PHILOSOPHY
in
EARTH SCIENCES

by

ASHVINI KUMAR

DEPARTMENT OF EARTH SCIENCES
INDIAN INSTITUTE OF TECHNOLOGY ROORKEE
ROORKEE-247 667 (INDIA)

MAY, 2015

INDIAN INSTITUTE OF TECHNOLOGY ROORKEE
ROORKEE

CANDIDATE'S DECLARATION

I hereby certify that the work which is being presented in the thesis entitled "**ATTENUATION CHARACTERISTICS OF UTTARAKHAND HIMALAYA USING STRONG MOTION DATA**" in partial fulfilment of the requirements for the award of the Degree of **Doctor of Philosophy** and submitted in the **Department of Earth Sciences** of the Indian Institute of Technology Roorkee is an authentic record of my own work carried out during a period from July, 2009 to May, 2015 under the supervision of **Dr. Anand Joshi,** Professor, Department of Earth Sciences and **Dr. Amita Sinvhal**, Professor, Department of Earthquake Engineering, Indian Institute of Technology Roorkee, Roorkee.

The matter presented in the thesis has not been submitted by me for the award of any other degree of this or any other Institute.

(ASHVINI KUMAR)

This is to certify that the above statement made by the candidate is correct to the best of our knowledge.

(ANAND JOSHI)
Supervisor

(AMITA SINVHAL)
Supervisor

Dated:

The Ph.D. Viva-Voce Examination of **Mr. Ashvini Kumar**, Research Scholar, has been held on……

Chairman, SRC

Signature of External Examiner

This to certify that student has made all the corrections in the thesis

Signature of Supervisors

Head of the Department

ABSTRACT

Himalaya is the most seismically active region in the world. This is the results of collision between the Indian and Eurasian plate, which is still, operated. The collision of these continental plates results in crustal shortening along the northern edges of the Indian plate. This process has given rise to three major thrust planes: the Main Central Thrust (MCT), the Main Boundary Thrust (MBT) and the Main Frontal Thrust (MFT) (Gansser, 1964; Molnar and Chen, 1983).The central seismic gap region of the Himalaya which lies in the northern part of the Indian subcontinent is exposed to great seismic hazard. The State of Uttarakhand falls in the central seismic gap and hence any large earthquake in this region will pose great destruction. This region has witnessed two such damaging earthquakes in recent past viz. the Uttarkashi earthquake (Ms 7.1) of 20 October 1991 and the Chamoli earthquake (Ms 6.6) 28 March 1999. Devastation caused by these earthquakes has drawn interest of seismologist to investigate the attenuation characteristics of the medium in this region. It has been seen that the attenuation characteristics of medium plays an important role in the earthquake ground motion at a particular site. Different types of rocks have different attenuating properties. Attenuation characteristics of the medium control the decay of the seismic energy in the lithosphere. Attenuation of the seismic wave is the reduction in the amplitude or energy caused by heterogeneity and anelasticity in the earth. This attenuation can be quantitatively defined by the inverse of the dimensionless quantity known as quality factor Q, this is the ratio of stored to dissipated energy during one cycle of the wave (Johnston and Toksoz 1981).

The strong motion data is fundamental for earthquake engineering studies such as attenuation properties, advance structural analysis, seismic hazard analysis and calibration of ground motion predication relationships. Several strong motions have been observed in the Himalaya region in the past. The destruction of these earthquakes is very high. The State of Uttarakhand has been occupied by the Himalayan mountain chain. The faults in this area are capable of generating large magnitude ground motion that would subject adjacent areas to significant ground shaking. Few studies have been carried out to understand the attenuation characteristics of the subsurface medium in this part of the Himalaya, which is mainly due to the scarcity of strong motion data. The main goal of this study is to improve the scientific

understanding of the physical processes that control strong shaking and to develop reliable estimate of seismic hazard for reduction of loss of life and property during future earthquakes through improved earthquake resistant structure.

Strong motion data is important for seismic hazard assessment in the Uttarakhand Himalaya. In the present study attenuation relations have been developed for the Kumaon and Garhwal Himalaya using strong motion data recorded by two regional networks operated in these regions. Damped least square inversion technique given by Livenberg (1944) has been used for obtaining peak ground attenuation relations. Dependency of the developed attenuation relations on distance parameters has been also checked. Obtained attenuation relation for the Kumaon and Garhwal Himalaya is further used to test the normality and model adequacies, which satisfied this test. Although worldwide attenuation relationships given by various researchers have not been satisfied this test with the Himalaya earthquakes data set. This test confirms the suitability of the developed attenuation relations for regional studies.

To validate the developed attenuation relations, strong ground motion records have been simulated for the 1991 Uttarkashi and the 1999 Chamoli earthquakes which occurred in recent past in the Uttarakhand Himalaya. Semi empirical simulation technique given by Midorikawa (1993) has been used in this study. In the recent years semi empirical simulation technique of strong ground motion has developed as an effective tool to simulate strong motion records. Semi empirical technique has been extensively tested for its applicability in simulation of strong ground motion by Midorikawa (1993), Joshi and Patel (1997), Joshi et al. (1999, 2001), Kumar et al. (1997), Joshi (2001, 2004), Joshi and Midorikawa (2004), Joshi and Mohan (2008). This simulation technique is in turn dependent on attenuation relation of peak ground acceleration. The source parameters of the Uttarkashi and Chamoli earthquakes have been used for earlier studies. Strong motion records of the Uttarkashi and Chamoli earthquakes have been simulated at nine stations, which recorded these earthquakes. Comparison of the observed and simulated peak ground acceleration is made in terms of root mean square error (RMSE). Simulation records of these earthquakes give the good results, which validated developed attenuation relation.

Attenuation study plays an important role for safe deign of engineering structure in seismically active regions. In the present thesis, comparative study of attenuation trend in the

Kumaon and Garhwal Himalaya has been investigated using regional strong motion data. Coda wave quality factor ($Q_c(f)$) has been observed for these regions. Similar strong motion dataset of nine earthquakes recorded at six stations has been used for both regions. Single backscattering technique given by Aki and Chouet (1975) has been used in the present study. Observed coda wave quality factor ($Q_c(f)$) value has been compared with other relations given for the Indian and other worldwide regions, which falls in the range and justified these results. Observed coda wave quality factor ($Q_c(f)$) for both region gives the different trend of attenuation characteristics of seismic wave. The Kumaon Himalaya gives the less coda wave quality factor ($Q_c(f)$) as compared to the Garhwal Himalaya region i.e. the Kumaon Himalaya has high attenuation medium beneath the surface. This attenuation trend has also observed in developed relations of peak ground attenuation in this work.

A modified seismic hazard technique of seismic hazard zonation initially given by Joshi and Patel (1997) has been used for seismic hazard zonation of the Uttarakhand Himalaya region in the present study. This technique has been used in different parts of the Himalaya. Worldwide attenuation relations of peak ground acceleration given by Abrahamson and Litehiser (1989) have been used by earlier researchers for seismic zonation. Modified seismic hazard zonation technique and developed attenuation relations have been used in the present work. Seismic hazard zonation map for probability of exceendance of peak ground acceleration of 100 and 200 gals have been prepared in the present work. These map shows that the many place of the Uttarakhand regions falls in high hazardous zone.

ACKNOWLEDGEMENT

I would like to thank all the following people who have been helping me in one way or in many ways during my Ph.D. study at IIT Roorkee:

It gives me a great pleasure to express my deepest gratitude to my Ph.D. supervisors **Prof. Anand Joshi,** Department of Earth Sciences and **Prof. Amita Sinvhal** from Department of Earthquakes Engineering, for their guidance, encouragement and providing a professional environment in tenure of my research work. I highly appreciate all their contributions of time, ideas, persistence in high quality results, and make my Ph.D. experience productive and stimulating.

I express my sincere thanks to my research committee members SRC Chairman's, **Prof. Sandeep Singh** (Internal Member) and **Prof. M. L. Sharma** (External Member) for providing an insight and constructive suggestions during my research work. I am also thankful to **Prof. R.P. Gupta** (former Head), **Prof. P.K. Gupta** (former Head), **Prof. A.K. Saraf** (former Head), and **Prof. D.C. Srivastva**, Head of the Department of Earth Sciences, Indian Institute of Technology Roorkee, for providing departmental facilities for carrying out my research work.

I sincerely thank **Department of Science and Technology** and **Ministry of Earth Science, Government of India New Delhi** for financial and other supports required for this research work. **National Geophysical Research Institute** Hyderabad and **Department of Earthquake Engineering**, IIT Roorkee are thankfully acknowledged. I sincerely thankfully to **Science of Engineering Research Board (SERB), DST,** New Delhi Government of India for sponsoring project no. SR/S4/ES-596/2011 entitled as "**Crustal attenuation studies of the Garhwal and the Kumaon Himalaya for estimation of seismic hazard**". This research work is an outcome of this project.

I express my sincere thanks to Prof. **R.G.S Sastry,** Sri **S.K. Sharma** and Sri **A.J.G. Nair** for their sincere support and help during my research work. I feel very happy to thank my colleagues and friends, **Chinmoy, Pushpa, Sushil, Parveen, Sandeep Arora, Piu, Monu, Sohan, Vishal, Rahul Dehiya** and **Rakesh** for their sincere support and encouragement through my stay at IIT Roorkee.

I would like to thank my father, Sri. **R.C. Sharma**, mother, Smt. **Darshan Devi**, father In-law Sri. **S.P. Kapil**, mother In-law Smt. **Rakesh Devi** for their constant love and moral support. Thank for my wife Smt. **Gayatri** for extreme help, moral support and my son Master **Parth** for devote infancy time in this study.

Last but not the least, I express my gratitude to the Almighty God for always keeping me in high spirit during all tenure of this work and providing me strength to perform this task successfully.

(Ashvini Kumar)

CONTENTS

LIST OF FIGURES

LIST OF TABLES

LIST OF SYMBOLS AND ABBREVIATIONS

PGA	Peak ground acceleration
GMPE	Ground motion prediction equation
$A(f)$	Acceleration spectra of target earthquake
$A(t)$	Ground motion time history for target earthquake
$a(t)$	Ground motion time history for small earthquake
$a_{ij}(t)$	Filtered acceleration record
$A_{ij}(t)$	Acceleration record after convolution
A_o	Long term flat level of acceleration spectra of target earthquake
A_o'	Long term flat level of acceleration spectra of small earthquake
C	Constant scaling factor
C'	Ratio of stress drop of the target and small earthquake
d	Slip of the small earthquake
D	Slip of the target earthquake
$D(f)$	Filter represent near site attenuation of high-frequencies
$e(t)$	Envelope function
f	Frequency
$F(t)$	Correction function
f_c	Corner frequency of small earthquake
F_c	Corner frequency of target earthquake
f_m	High frequency cutoff range in high-cut filter
$F_R(f, R)$	Filter representing effect of anelastic attenuation
FS	Amplification due to the free surface
$S_D(f)$	Source displacement spectra
$G_i^S(x,t)$	Green's function
i	Angle of incidence
L	Length of the rupture plane of the target earthquake
L_e	Length of the rupture plane of the small earthquake

M	Richter magnitude of an earthquake
m_b	Short-period body-wave magnitude
M_{JMA}	Magnitude scale used by Japan Meteorological Agency
M_o	Seismic moment of the target earthquake
M_o'	Seismic moment of the small earthquake
M_s	Surface-wave magnitude
M_w	Moment magnitude of target earthquake
M_w'	Moment magnitude of small earthquake
N	Number of sub-faults along length or width of the rupture plane
p	Ray parameter
$PRTITN$	Reduction factor
$Q_\beta(f)$	Shear wave Quality factor
$Q_c(f)$	Coda wave Quality factor
R	Hypocentral distance
E	Epicentral distance
r_{ij}	Distance from the observation point to the ijth sub-fault
r_o	Radius of circular crack
$R_{\theta\varphi}$	Radiation pattern coefficient
$S(f)$	Source acceleration spectrum
t	Time
T	Slip duration of the target earthquake
T_d	Duration parameter
t_{ij}	Arrival time
T_d	Rise time of the target earthquake
T_{ss}	Transmission coefficient of incident shear waves
U_o	Long term flat level of displacement spectra of target earthquake
U_o'	Long term flat level of displacement spectra of small earthquake
V	Velocity of propagation
V_r	Rupture velocity
W	Width of the rupture plane of the target earthquake

W_e	Width of the rupture plane of the small earthquake
α	Takeoff angle
β_i	Shear wave velocity in the *i*th layer
δ	Dip of rupture plane
$\delta(t)$	Delta function
λ	Rake
μ_i	Modulus of rigidity in the *i*th layer
ρ	Density of medium
A	Area of rupture plane
τ	Slip duration of the small earthquake
φ	Source-receiver Azimuth
φ_s	Strike of rupture plane
ϕ	Strike of the modelled rupture plane with respect to geographic north
Ω_o	Long term flat level
RMSE	Root mean square error
Rs(f)	Site amplification factor

LIST OF PUBLICATION

1. A. Joshi, **Ashvini Kumar**, C. Lomnitz, H. Castanos and S. Akhtar (2012) **"**Applicability of attenuation relations for regional studies," **Geofisica Internacional Journal**, Vol. 51(4): 349-363

2. A. Joshi, **Ashvini Kumar**, K. Mohan and B. K. Rastogi (2013). "Hybrid Attenuation Model for Estimation of Peak Ground Accelerations in the Kutch Region, India", **Natural Hazard**, Vol. 68: 249-269.

3. Anand Joshi, **Ashvini Kumar**, Heriberta Castanos and Cinna Lomnitz (2013). "Seismic Hazard of the Uttarakhand Himalaya, India, from deterministic modeling of possible rupture planes in the area", **International Journal of Geophysics**, Vol. 2013, article ID 825276, 12 pages, DOI. 10.1155/2013/825276.

4. Sandeep, A. Joshi, Kamal, Parveen Kumar and **Ashvini Kumar** (2014) Effect of frequency-dependent radiation pattern in the strong motion simulation of the 2011 Tohoku earthquake, Japan, using modified semi-empirical method. **Natural Hazard**, Vol 73: 1499-1521.

5. **Ashvini Kumar,** A. Sinvhal, A. Joshi, D. Kumar, Sandeep and Parveen Kumar (2015) Coda wave attenuation characteristics for Kumaon and Garhwal Himalaya, India. **Natural Hazard** Vol. 75:1057-1074.

6. Parveen Kumar, A. Joshi, Sandeep and **Ashvini Kumar** (2014), Three-dimensional attenuation structure of the Kumaon Himalayas, India based on inversion of strong motion data. Pure and applied Geophysics. Vol. 172: 333-358.

7. Sandeep, A. Joshi, Kamal, Parveen Kumar, **Ashvini Kumar** and Piu Dhibar (2015) Modeling of strong motion generation areas of the Niigata, Japan, earthquake of 2007 using modified semi-empirical technique. **Natural Hazard** Vol. 77: 933-957.

8. Parveen Kumar, A. Joshi, Sandeep, **Ashvini Kumar** and R.K. Chadha (2015) Detailed attenuation study of shear waves in the Kumaon Himalaya, India, using the inversion of strong motion data. Bull Seism Soc Am, Vol. 105:1836-1851

9. **Ashvini Kumar** and A Joshi (2015) Semi empirical stochastic simulation of strong motion records of the earthquakes in the Garhwal Himalaya, India using regional attenuation relation. **Natural Hazard** (Under review)

10. Parveen Kumar, A. Joshi, **Ashvini Kumar**, Sandeep, Monu Tomer and Piu Dhibar (2015), A Dense strong motion Instrumentation network in the Kumaon Himalaya, India, **Seismological Research Letters**. (Communicated).

Conferences/ Conventions

1. Joshi A., **Ashvini Kumar,** Amita Sinvhal (2015) Attenuation characteristics of crustal rocks of Garhwal and Kumaon Himalaya, India determined from strong motion data. AOGS Singapore, 2-7 August 2015
2. Mohanty M., Anand Joshi, **Ashvini Kumar,** Parveen Kumar (2015) Attenuation characteristics of Niigata Prefecture, Japan estimated from strong motion data. AOGS Singapore, 2-7 August 2015
3. **Ashvini Kumar**, A. Joshi, Sandeep, Parveen Kumar, Azad Kumar (2014) Estimation of attenuation characteristics using frequency dependent coda wave quality factor of the Niigata prefecture region, Japan. 51st Annual Convention of Indian Geophysical Union on Earth Sciences and Society, India 19-21 November 2014, 142.
4. Sandeep, A. Joshi, Kamal, Parveen Kumar, **Ashvini Kumar** (2014) Strong Motion Generation Areas modelling of the 2011 Tohoku earthquake using modified semi empirical technique. 51st Annual Convention of Indian Geophysical Union on Earth Sciences and Society, India 19-21 November 2014, 151.
5. Parveen Kumar, A. Joshi, Dinesh Kumar, S. S. Teotia, **Ashvini Kumar**, Sandeep (2014) Characterization of shear wave attenuation in the Central Honshu region, Japan from the inversion of strong motion records. 51st Annual Convention of Indian Geophysical Union on Earth Sciences and Society, India 19-21 November 2014, 144.
6. **Ashvini Kumar** and A. Joshi (2013) "Using limited applicability of attenuation relation for simulation of strong motion records of the Uttarkashi Earthquake, India" International Conference on Challenges in Disaster Mitigation and Management 15-17 February, 2013 at Centre of Excellence in Disaster Mitigation and Management, Indian Institute of Technology Roorkee – 247 667, INDIA.
7. A. Joshi, **Ashvini Kumar** and A. Sinvhal (2011). " Attenuation relation for the Kumaon and Garhwal Himalaya, Uttarakhand, India", Proceeding of International symposium on The 2001 Bhuj earthquake and advances in earthquake sciences - AES 2011, ISR, Gandhinagar, Gujarat, India, January 22-24.
8. A. Joshi, A. Sinvhal, **Ashvini Kumar**, Felix Aptikaev and O.O. Erteleva (2010). "Attenuation relation for Garhwal Himalaya obtained using damped least square method", Proceeding of AGU Champman conference on Complexity and Extreme Events in Geosciences – 2010, NGRI Hyderabad, India, Feb 15-19.

CHAPTER - 1

Introduction

The Himalayan orogenic belt is one of the youngest orogens in the world; it was formed as a result of the collision, which is still in progress, between the Indian and Eurasian plates which begun in the Early Eocene (Molnar and Tapponnier 1975; Powell 1979; Norton and Sclater 1979; Patriat and Achache 1984; Searle et al. 1987). Himalayas have witnessed a number of devastating earthquakes in recent past. Most of the seismic activities in the Himalayan region are concerted along shallow north-dipping planes, which indicates under thrusting of the Indian plate (Kumar and Mahajan 2001). Three zones in the entire region of Himalaya in the Indian subcontinent have been demarcated as zones of seismic gaps by Khattri (1987). Uttarakhand state of India lies in one of the three seismic gaps. The Garhwal and Kumaon are the two major parts of the Uttarakhand Himalaya. This region has high density of population, hence attenuation study in these regions plays an important role in characterization of seismic hazards. The region of the Garhwal Himalaya has recently witness two big earthquakes viz. the Uttarkashi earthquake of October 20, 1991 (M_s = 7.1) and the Chamoli earthquake of March 28, 1999 (M_s = 6.6). Although the Kumaon Himalaya has been frequently visited by several earthquakes of small magnitude, it has not experienced any large earthquakes in the recent past. Due to the limited database available in the rough and difficult terrain of the Uttarakhand Himalaya, comparative studies have not been done to estimate attenuation properties of the medium in these parts of the Himalaya.

1.1 Ground Motion Prediction Equations: Literature - Review

The possibility of large earthquakes in the seismically active region can't be ruled out. The construction of protected engineering design depends on various seismic parameters. In almost all the practical cases of seismic hazard analysis, the demand is expressed only as a function of the peak ground acceleration (Shah and Dong 1984). Peak ground acceleration is often treated as an important seismic parameter, which is directly related to the force experienced by a structure during an earthquake. Ground motion prediction equation (GMPE) or attenuation relation explain the dependency of peak ground acceleration parameter observed during any earthquake on various dependent parameters like magnitude, distance, source type, tectonic environment and site type,

respectively. Different attenuation relationships have been developed for different regions worldwide in the past for estimation of peak ground acceleration (Joyner and Boore 1981, 1988; Campbell 1981, 1985; Boore and Joyner 1982; McGuire 1976; Abrahamson and Litehiser 1989; Fukushima and Tanaka 1990; Boore et al. 1997 and Boore and Atkinson 2008). A comprehensive list of the attenuation relations developed between 1969 to 2000 has been given by Douglas (2001) which has been revised in 2010 by Douglas (2011). Very few attenuation relations have been developed for the Himalaya, which are applicable to different parts of Himalaya separately (Singh et al. 1996; Sharma 1998; Nath et al. 2008; Sharma et al. 2009; Joshi et al. 2013).

Seismic hazard assessment of a region requires knowledge and understanding of both the seismicity and the attenuation of strong ground motion. The use of different database and published empirical attenuation relations for peak ground acceleration have resulted in widely varying conclusions. Thus, the use of a particular relationship for an area with different geological and tectonic features may lead to results that differ significantly from the actual values (Shafiee et al. 2011).

An attenuation relationship has been developed by Joyner and Boore (1981) using 182 acceleration records of 23 earthquakes, magnitude ranging between 5 to 7.7, recorded in the Western North America. This analysis uses a magnitude-independent shape, based on geometrical spreading and anelastic attenuation, for the attenuation curve. In this technique, an innovation is introduced by decoupling the distance dependence of the data from the magnitude dependence. The variables used in equation are, PGA is peak ground acceleration, M is the magnitude and ‘r’ is the closest horizontal distance to the surface projection of the rupture plane.

The ground motion prediction equation given by Abrahamson and Litehiser (1989) developed using worldwide dataset of 585 acceleration records from 76 earthquakes. This dataset used 256 records of 28 strike-slip earthquakes, 14 records of 7 normal earthquakes, 42 records of 12 normal oblique earthquakes, 224 records of 21 reverse earthquakes and 49 records of 8 reverse oblique earthquakes. The attenuation model that fits this data has a magnitude dependent shape. The regression uses a two-step procedure that is a hybrid of the Joyner and Boore (1981) and Campbell (1981) regression methods. The standard error of estimation is 0.277.

Fukushima and Tanaka (1990) has developed a new attenuation relation for peak horizontal acceleration applicable to the near source region in the Japan. The database consists of 1372 records of horizontal components from 28 earthquakes in the Japan and 15 earthquakes in the United States and other countries. The data used for the analysis included old uncorrected SMAC-B2 records. The standard deviation of log A is 0.21and the multiple correlation coefficient is 0.89.

Molas and Yamazaki (1995) have derived attenuation relation using wide data recorded by the new JMA-87 type accelerometers. Earthquakes with depths up to 200 km are used to develop the attenuation relation applicable to subduction zone, in the Japan region. Depth and local site effects on the attenuation are considered simultaneously with the distance dependence and magnitude dependence a two stage regression procedure.

Singh et al. (1996) has been developed the attenuation relationship for the Indian Himalaya region, using strong ground motion data from five earthquakes viz. the Dharamsala earthquake (26 April 1986), the Meghalaya earthquake (10 September 1986), the Burma-India earthquake (14 May 1987), the Tripura-Assam earthquake (6 February 1988) and the Guahati earthquake (6 August 1988). Most of the earthquakes occurred in the Northeast (NE) part of the Himalaya region with magnitudes ranging from 5.7 to 7.2.

Attenuation relation for entire Himalaya region has been determined by Sharma (1998), using 66 peak horizontal accelerations data from five Indian earthquakes. This relationship uses 41 recodes at rock sites and 25 records at soil sites. This analysis uses a two-step stratified regression model. The residual sum of squares of the regression analysis is 0.14. It is seen that the proposed relationship give lesser values at shorter distances compared to other relationships.

Gupta and Gupta (2004) developed the attenuation relation for peninsular India using a dataset of 31 three-component accelerograms from the Koyna region of earthquakes in magnitude range 3.5 to 6.5 and hypocentral distance range from 3.5 to 25 kilometre, respectively. Attenuation relation is obtained by performing a two step regression analysis using the peak ground acceleration values of the largest two horizontal components and vertical component of selected accelerograms.

Iyenger and Raghukant (2004) have developed the attenuation relationship for the peninsular India. This relationship is based on statistically simulated strong motion records using seismological model which clearly lacks actual observational data. It has been observed that attenuation of strong motion in peninsular India is similar to that in other intraplate regions of the world.

Nath et al. (2005) have obtained an attenuation relation using a semi empirical approach by minimizing the difference between the observed and the estimated values of peak ground motion for the Sikkim Himalaya, India. The first-order attenuation law for the Sikkim Himalaya is developed using the data for 80 local earthquakes ($3 \leq M \leq 5.6$) recorded during 1998-2003 with epicentral distance ranging from 10 to 100 kilometre. This is a mean attenuation relationship without considering local site conditions for hypocentral distances less than 100 km. The first order attenuation relation is further used for developing a second-order spectral attenuation relationship taking into the consideration local site condition in terms of site amplification, elevation, source azimuth and spectral acceleration. This relation uses both the recorded and simulated events, with local site conditions incorporated in the simulation.

Atkinson and Boore (2006) developed ground motion prediction equations for the rock and soil sites in Eastern North America (ENA) using stochastic finite fault modeling technique. They suggested that stochastic ground motion prediction equations provide a basis for estimating peak ground motions and response spectra for earthquakes of magnitudes range 4.0 to 8.0, at distances from 1 to 200 kilometer.

Nath et al. (2008) has developed an attenuation relation for the Garhwal Himalaya region. They used a similar algorithm as used for the Sikkim Himalaya region i.e. semi empirical approach by minimizing the difference between the observed and estimated values of peak ground motion. They have used data of selected 61 well-recorded aftershocks out of many events with magnitude greater than 2.4 for this study.

Mandal et al. (2009) have developed attenuation relation for Gujarat, India. In this study they used peak ground acceleration from the records of seismic response recorder (SRR) of Bhuj earthquake ($M_w = 7.7$) of 26 January, 2001. A total of 239 records of 32 significant aftershocks of magnitude range $3.1 \leq M_w \leq 5.6$, at epicentral distance range of $1 \leq R \leq 288$ km have been used.

They used the Joyner-Boore's method for a magnitude-independent shape based on geometrical spreading and anelastic attenuation for the attenuation curve. Developed peak ground attenuation relation is valid for magnitude range $3.1 < M_w \leq 7.7$ with standard deviation (σ): ± 0.8243.

Ulutas and Ozer (2010) have developed an attenuation relation of peak ground acceleration for the Marmara region of north-western Turkey. The database consists of 751 horizontal components of peak ground acceleration recorded from 78 earthquakes, including the Izmit (M_w = 7.4) and Duzce (M_w = 7.2) earthquakes of 1999. Multiple regression analysis have been used to calculate the coefficients of regression relationship. The horizontal peak ground acceleration has been found to be log-normally distributed with a standard error representing a 0.392 percent increase in terms of natural logarithm.

Deif et al. (2011) developed a ground motion attenuation relationship for the Aswan area Egypt. The magnitude range $4.0 \leq M_w \leq 7.0$ and distance to the surface projection of fault up to 100 km for Aswan based on a statistically simulated seismological model. They generated suites of ground motion time histories using stochastic technique. The proposed model of Joyner and Boore (1981) has been selected for this study.

Joshi et al. (2013) has developed a hybrid attenuation model for estimation of the peak ground accelerations in Kutch region, India. This regression model uses both actual and simulated database. The database consist of 569 peak ground acceleration values in which 89 peak ground acceleration values are obtained from observed records and 480 from simulated records. The dataset consists of earthquake magnitude in range 3.0 to 8.2 and hypocentral distance 12 to 120 kilometer. The standard deviation of the attenuation model is: (σ) ± 0.5.

1.2 Synthetic Generation of Ground Motion – Review

Synthetic generation of ground motion is a topic of interest in seismic prospecting as well as seismology. Several techniques have been proposed in seismic prospecting to generate synthetic seismogram for prospecting of oil and gas reservoirs (Domenico 1977; Castagna et al. 1985; Rao et al. 2006; Singh et al. 2014a, 2014b). Synthetic generation of ground motion is equally important in seismological studies especially that deal with high frequency strong ground motion. Strong ground motion is a basic tool for designing safe structure by an engineers. Strong motion data is

observed by an accelerogarph near the source region. Some of the techniques used for synthetic generation of ground motion parameters are (i) Composite Source modeling technique (Zeng et al. 1994; Yu 1994; Yu et al.1995; Saikia and Herrman 1985; Somerville et al. 1991 and Saikia 1993) (ii) Empirical Green Function technique (Hartzell 1978, 1982; Kanamori 1979; Hadley and Helmberger 1980; Mikumo et al. 1981; Hadley et al. 1982; Irikura and Muramatu 1982; Irikura 1983, 1986; Coats et al. 1984; Munguai and Brune 1984; Hutchings 1985; Kamae and Irikura 1998) (iii) Stochastic simulation technique (Housner and Jennings 1964; Hanks and McGuire 1981; Lai 1982; Boore 1983; Boore and Atkinson 1987) (iv) Semi empirical simulation technique (Midorikawa 1993; Joshi 2001; Joshi and Midorikawa 2004). These techniques have some advantages as well as disadvantages compared to each other. These techniques have been discussed in following section.

1.2.1 Composite Source Modeling Technique

The composite source modeling technique has been given by Zeng et al. (1994) and Yu (1994). This technique uses the synthetic Green's function for simulation of strong motion records. This technique is quite successful in representing strong ground motion. Modeling the features of earthquake source process and application of wave propagation theory synthetic accelerograms are simulated in this technique. However, the fault plane solution, the detail velocity Q structure of the region and stress drop parameters is required. All these parameters are not easily available for interested site. Zeng et al. (1994) presented a composite source model for convolution with the synthetic Green's function, in order to simulate strong ground motion due to a complex rupture process of an earthquake. Yu et al. (1995) have simulated 1991, Himalayan earthquake of magnitude 7.1 by using composite source model defined by Zeng et al. (1994). Kumar et al. (2011) presented a simple and efficient hybrid technique for simulating earthquake strong ground motion. This procedure is the combination of the techniques of envelope function (Midorikawa 1993) and composite source model (Zeng et al. 1994). The applicability of the technique has demonstrated by successful modeling of Uttarkashi earthquake (M_s = 7.1) of 1991 by Kumar et al. (2011).

1.2.2 Empirical Green's Function Technique

Empirical Green's function technique uses the record of aftershock of the main event to simulate ground motion at the observation point (Hartzell 1978, 1982). It is observed that simulation of synthetic records using earth model involve two major problems. The first one is associated with the description of source and the second one with estimation of earth response (Hartzell 1978). Summation of point sources has used in media ranging from full space (Aki 1968) to layered half space (Heaton and Helmberger 1977). Empirical Green Function technique has the advantage of not requiring the computation of propagation and the local site effects compared to other techniques. The main limitation of this technique is that it can be applied in case only where appropriate records of small events considered as Green function in the area of study are available. Unfortunately, it is rare to have good records of such small events, especially in the source area of a large earthquake (Kamae et al. 1998). Irikura (1986) proposed the method of Empirical Green's function which is consistent with spectral scaling at high frequencies. The method of Empirical Green's Function technique given by Irikura (1986) uses both target and small events having spectral characteristics that can be predicted by ω^{-2} model.

1.2.3 Stochastic Simulation Technique

Stochastic simulation technique initiated by Housner and Jenning (1964) was among earliest techniques of simulation which uses statistical properties of strong motion records. Housner and Jenning (1964) simulated records of earthquakes which had pertinent properties of recorded strong motion earthquakes. In the stochastic simulation technique, a band limited random white Gaussian noise is passed through number of filters, representing earthquake process to get a synthetic ground motion (Housner and Jennings 1964). Inspite of success of this technique it is also well known that the point source model breaks down in some cases, particularly near the source of great earthquakes. The limitation of technique of modeling is that; it does not include conceptual model of earthquake source and propagation of energy in the medium.

1.2.4 Semi empirical Simulation Technique

The method of semi empirical modeling technique was initially proposed by Midorikawa (1993) and later modified by Joshi and Midorikawa (2004). In semi empirical technique synthetic records from different sub-faults within the rupture plane are used in place of aftershock records as Green's function. This technique is based on stochastic simulation of high frequency ground motion which was introduced by Hanks and McGuire (1981); Boore (1983); McGuire et al. (1984); Boore and Joyner (1991) and Lai (1982). Boore (1983) used the filtered random white Gaussian noise with zero mean and unit variance for simulation of strong ground motion. This method takes advantage of both stochastic simulation technique of Boore (1983) and Empirical Green's function technique of Irikura (1986).

Midorikawa (1993) proposed a simplified method for synthesizing ground acceleration from a large earthquake for engineering use. This method is based on semi-empirical method of Irikura (1986) in which the fault of the target earthquake is divided into small sub faults. The simulation of synthetic records is controlled by various factors including attenuation relation, model of the rupture plane, model of the earth and the geometry of rupture propagation.

Joshi and Patel (1997) modeled the three dimensional rupture along identified active lineaments. Peak ground accelerations were obtained by using semi empirical method of Irikura (1986), which was used by Midorikawa (1993). The efficacy of this simulation technique for the Himalayan region was established by simulating peak ground accelerations for modeling of the Uttarkashi earthquake of October 20, 1991 and comparing it with recorded one.

Semi empirical technique of simulation given by Midorikawa (1993) is used by Kumar et al. (1999) for calculating synthetic accelerograms for a wide range of earthquake magnitudes. The validity of this technique was confirmed by modeling of the observed accelerograms, the Dharmsala (M_s = 5.3) 1986 and the Uttarkashi (M_s = 7.1) 1991 earthquakes at relatively shorter distances. The method has applications where seismic hazard needs to be estimated and empirical data sets including accelerograms, velocity Q models and earthquake focal mechanisms are sparse or not available at all (Kumar et al. 1999).

The final output of the modeling technique used by Midorikawa (1993), Joshi and Patel (1997) was the envelope of accelerogram which only gives the idea about peak ground acceleration at a particular site and the total duration of the record but not the complete representation of the time series (Joshi et al. 1999). The realistic earthquake time series were simulated from the modeled rupture plane in a layered earth model given by Joshi et al. (1999), by multiplying filtered white noise with the envelope of accelerogram at a particular observation point. The filters through which white noise is passed include effect of geometrical spreading, anelastic attenuation and near site attenuation of high frequencies.

An attempt was made by Joshi et al. (2001) to check the effect of layered earth model in the technique of semi empirical modeling. In this approach, Joshi et al. (2001) modified the envelope of acceleration record to take into account the transmission of energy and travel time taken by energy at various boundaries within the layered earth model. The simulated resultant envelope is used for generating synthetic accelerograms by multiplying filtered white noise with the envelope of accelerogram at a particular site. This modified technique has tested for its applicability to simulate the strong motion records of the Uttarkashi earthquake of 20 October, 1991.

Joshi and Midorikawa (2004) presented a simplified method to simulate strong ground motion for a realistic representation of a finite earthquake source buried in a layered earth medium. Joshi and Midorikawa (2004) simulated ground motion data of the Geiyo, Japan earthquake (M_w = 6.8) of 24 March 2001 using stochastic method of Boore (1983) with the help of shaping window based on the finite source model of the rupture plane. This shaping window is depended on the geometry of the earthquake source and the propagation characteristics of the energy released by various sub-faults. The shaping window was modified by Joshi and Midorikawa (2004) to take into account the effect of the transmission of energy released from the finite fault at various boundaries of the layered earth model above the source. Strong motion records have simulated at eight near-field stations and compared with the observed data and the simulated record by using empirical Green's function method of Irikura (1986). Through comparison the efficacy of this method has been established to simulate strong ground motion data by assuming a finite rupture plane.

Joshi and Mohan (2008) modified semi empirical technique initially started by Midorikawa (1993) for simulation of strong ground motion due to a rupture buried in the earth medium consisting of several layers of different velocities and thicknesses. Simulations in the semi empirical technique were made by considering, transmission of energy at each layer, frequency filtering properties of medium and earthquake source, correction factor for slip of large and small magnitude earthquakes and site amplification ratio at various stations (Joshi and Mohan 2008). To test the efficacy of the developed technique, strong motion records were simulated by Joshi and Mohan (2008) at different stations that recorded the 2004 Niigata-ken Chuetsu, Japan earthquake (M_s = 7.0). The comparison of synthetic with observed records over wide range of frequencies showed that the present technique is effective to predict various strong motion parameters from simple deterministic model which is based on simple regression relations and modeling parameters (Joshi and Mohan 2008).

1.3 Frequency Dependent Attenuation Studies - Review

The attenuation relations are mostly used by engineers to estimate peak ground acceleration at different sites. Empirical regression equations have advantages in terms of being convenient, efficient, and economical, there is a notable drawback (Kuo et al. 2011). Although attenuation relation provide useful information about attenuation characteristics of the medium, it still lakes basis seismological understanding. The attenuation characteristics of a region provide essential information regarding the seismic hazard of the region. In terms of seismic hazard assessment the characterization of this frequency dependence can have important practical implications (MalischewskyAuning et al. 2006). Various techniques have been developed to study the attenuation characteristic of seismic waves using different parts of the seismogram (e.g., Aki 1969; Aki and Chouet 1975; Hermann 1980; Mitchell 1995). Most studies use decay of the coda wave to determine attenuation in the earth's crust, (Aki 1969; Aki and Chouet 1975; Sato 1977; Roecker et al. 1982; Pulli 1984; Reha 1984; Jin and Aki 1986; Ibanez et al. 1990; Kanao and Ito 1992; Gupta et al. 1995; Gupta and Kumar 2002; Paul et al. 2003; Kumar et al. 2005; Sharma et al. 2012, Singh et al. 2012). The backscattering method is the most frequently methods which is used to measure the attenuation characteristic using coda wave. It has been given by Aki (1969) and Aki and Chouet (1975). The seismic coda waves are backscattering waves from numerous randomly

distributed heterogeneities in the earth (e.g., Aki 1969; Aki and Chouet 1975; Rautian 1976; Rautian and Khalturin 1976). Aki and Chouet (1975) proposed two extreme models for back-scattered waves to calculate the coda wave quality factor (Q_c).The first single scattering model considers the scattering as a weak process without loss of seismic energy by scattering and in the second one the seismic energy transfer is considered to be a diffused process. The single backscattering model proposed by Aki and Chouet (1975) was a frequently used model for describing the behavior of the coda waves from small local earthquakes. According to this model the coda waves are interpreted as backscattered body waves generated by the numerous heterogeneities present in the earth's crust and upper mantle.

Gupta et al. (1995) have determined quality factor of coda waves ($Q_c(f)$) by analyzing coda waves of vertical component of velocity sensor of the seven local earthquakes recorded in the Garhwal Himalaya region. They have been used single backscattering model in this study. The obtained frequency dependent coda wave relationship as $Q_c(f) = 126f^{0.95}$ for the Garhwal Himalaya.

Mandal and Rastogi (1998) have estimated the frequency dependent coda wave ($Q_c(f)$) values from 30 local earthquakes around the Koyna-Warna region, India. The recorded seismic network consists of short-period seismometers, broadband seismometers, digital accelerographs and analog portacorders. Single scattering method has been used for obtaining frequency dependent coda quality factor ($Q_c(f)$). They obtained frequency dependent coda wave quality factor for the Koyna-Warna region as $Q_c(f) = 169f^{0.77}$.

Gupta et al. (1998) have estimated frequency dependent coda wave relationship for the Koyna region, India using 13 local earthquakes recorded during July to August 1996. The dataset was recorded using three-component short-period seismometers. They obtained average frequency-dependent attenuation relationship, $Q_c(f) = 96f^{1.09}$ using a single back scattering model.

Zelt et al. (1999) have estimated the frequency-dependent coda wave $Q_c(f)$ relation for Southwestern British Columbia, Canada region. Single-scattering method was used to calculated frequency dependent quality factor using the data of 122 local earthquakes. The frequency dependent relation $Q_c = 110f^{0.72}$ was estimated, which is applicable in frequency range 2-16 Hz.

Mandal et al. (2001) have estimated frequency-dependence $Q_c(f)$ relationship for the Chamoli region, India. They have used 48 well-located aftershocks data of the Chamoli earthquake in this work. Scattering method has been used to obtain frequency-dependence coda $Q_c(f)$ relationship. The frequency dependent coda wave relationship $Q_c(f) = (30\pm0.8)f^{(1.21\pm0.03)}$ has been estimated in this study.

Gupta and Kumar (2002) have estimated the seismic wave attenuation characteristics of the Garhwal Himalaya, Koyna region and Northeast regions of India. Frequency dependent coda wave quality factor was determined by implementing the single backscattering model for the three regions. Digitally recorded earthquakes were used to estimate $Q_c(f)$ for the Garhwal and Koyna region while strong motion data was used for the Northeast India region. Frequency dependent coda wave quality factor was obtained as $(110\pm5.15)f^{(1.02\pm0.025)}$, $(97\pm7.18)f^{(1.09\pm0.036)}$ and $(86\pm4.04)f^{(1.01\pm0.026)}$ for the Garhwal Himalaya, Koyna region and Northeast India, respectively.

Paul et al. (2003) have calculated coda wave quality factor for the Kumaon Himalaya using eight events recorded on digital telemetered seismic network. Single backscattering model given by Aki and Chouet (1975) has been used in this study. Coda wave quality factor $Q_c(f) = (92\pm4.73)f^{(1.07\pm.023)}$ was computed for the Kumaon region in this study.

Dutta et al. (2004) have studied the coda wave attenuation using the strong motion data in the South Central Alaska region. They estimated coda wave quality factor (Q_c) by single backscattering methods. They computed $Q_c^{-1}(f) = 0.0063\ f^{-0.79}$ and $Q_c^{-1}(f) = 0.0066\ f^{-0.84}$ for the transverse and radial component, respectively for the South-central Alaska region.

Kumar et al. (2005) have estimated the coda wave quality factor $Q_c(f)$ for the NW Himalaya, India using single backscattering method. A total of 36 local earthquakes of magnitude range 2.1 to 4.8 have been used for Q_c estimation at central frequencies 1.5, 3.0, 6.0, 9.0, 12.0 and 18.0 Hz through eight lapse time windows from 25 to 60 sec starting at double the time of the primary shear wave from the origin time. The estimated average frequency dependence quality factor gives the relation, $Q_c(f) = 158f^{1.05}$.

Kumar et al. (2007) have studied the attenuation characteristics of the Dharwar Craton, the Cuddapah basin and Godawari graben, India. Broadband data was used to determine the coda wave

quality factor for the three regions. Single scattering method given by Aki and Chouet (1975) has been used for estimation of coda $Q_c(f)$ relations. Coda $Q_c(f)$ relations i.e. $Q_c(f) = (730.62 \pm 0.09)\ f^{(0.54 \pm 0.01)}$, $Q_c(f) = (535.06 \pm 0.13)\ f^{(0.59 \pm 0.01)}$ and $Q_c(f) = (150.56 \pm 0.08)\ f^{(0.91 \pm 0.01)}$ was calculated for the Dharwar Craton, the Cuddapah basin and Godawari graben region, respectively.

Sharma et al. (2007) have computed the coda wave ($Q_c(f)$) quality factor for the Koyna region, India. Total 37 local earthquakes recorded on short-period three-component seismometers were used in this study. The single back-scattering method was used to determine coda wave (Q_c). The obtained relationship for the Koyna region is $Q_c(f) = (117.0 \pm 2.0)\ f^{(0.97 \pm 0.07)}$.

Sharma et al. (2008) have estimated the coda wave ($Q_c(f)$) quality factor for the Kachchh region, Gujarat India by using the broadband data. The single backscattering method was used to determine frequency dependent coda wave quality factor. The obtained relationship for coda wave is $Q_c(f) = (148.0 \pm 3.0)\ f^{(1.01 \pm 0.02)}$.

Sahin (2008) has estimated the quality factor $Q_c(f)$ in the Southwest Anatolia region using coda wave normalization method. Broad band data of the KOERI array (Kandilli Observatory and Earthquake Research Institute) recorded at two stations was used for the computation in this work. The coda $Q_c(f)$ relation for this region is expressed by $Q_c(f) = (102\pm8)f^{0.82\pm0.07)}$.

Mukhopadhyay et al. (2008) have used 30 aftershock data of the Chamoli earthquake 28th March 1999 to estimate the $Q_c(f)$ values by using single back scattering model. Data used in this work was recorded on the network of short-period seismometers. They determined the coda wave quality factor as $Q_c = (33\pm2)\ f^{(1.17\pm0.03)}$, $Q_c = (55\pm6)\ f^{(1.16\pm0.05)}$, $Q_c = (78\pm15)\ f^{(1.12\pm0.08)}$, $Q_c = (93\pm18)\ f^{(1.07\pm0.08)}$ and $Q_c = (122\pm20)\ f^{(0.98\pm0.07)}$ for average lapse time 19.1, 24, 29.3, 34.0 and 40.7sec , respectively.

Rahimi et al. (2009) have estimated the coda wave quality factor for the South East Sabalan Mountain, NW Iran by using 65 local events recorded on five accelerographs. Single backscattering method has been used in this study. They obtained frequency dependent $Q_c(f)$ relationship viz. $(48\pm6)f^{(0.88\pm0.05)}$, $(49\pm5)f^{(0.97\pm0.03)}$, $(51\pm7)f^{(1.02\pm0.06)}$, $(53\pm7)f^{(0.97\pm0.03)}$ and $(44\pm5)f^{(0.96\pm0.03)}$ for Sarein, Ardebil, Kariq, Islamabad and Nir stations, respectively.

Ma'hood and Hamzehloo (2009) hava estimated coda wave attenuation in the East Central Iran using single backscattering model given by Aki and Chouet (1975). The $Q_c(f)$ relation for the entire region of east central Iran, from all data (both seismograms and accelerograms) is obtained as $Q_c(f) = (101\pm6)f^{(0.94\pm0.11)}$

Mukhopadhyay and Sharma (2010) have estimated the coda wave quality factor $Q_c(f)$ for the Garhwal-Kumaon Himalaya region India by using digital data of 81 events. The range of magnitude, epicentral distance and focal depth of the dataset are 2.1 to 4.0, 10 to 140 km and 0 to 40 km, respectively. The single back-scattering method was used to determine coda $Q_c(f)$. The frequency dependent coda wave relationship of form $119f^{0.99}$ is obtained in this study.

Gupta et al. (2012) have studied the attenuation characteristics of coda waves for the Mainland Gujarat, India. In this work, single backscattering method was used on the broadband data to determine the coda $Q_c(f)$. The computed average coda $Q_c(f)$ relations are: $(87.0\pm13.0)f^{(1.01\pm0.06)}$, $(112.0\pm20.0)f^{(0.94\pm0.08)}$ and $(120.0\pm22.0)f^{(0.76\pm0.07)}$ for the lapse time of 30 sec, 40 sec and 50 sec, respectively.

Brahma (2012) has estimated coda wave attenuation using the single backscattering model for the Northeast India. Frequency dependent coda $Q_c(f)$ relation was estimated as (21.49 ± 1.17) $f^{(1.48\pm0.08)}$, (48.6 ± 1.11) $f^{(1.29\pm0.06)}$ and (88.86 ± 1.12) $f^{(1.19\pm0.06)}$ for the time window of 20 sec, 30 sec and 40 sec, respectively.

Sharma et al. (2012) have estimated the attenuation characteristics based on coda waves of two areas Jamnagar and Junagarh of the Saurashtra, Gujarat India, using single back scattering model. They used broadband waveforms of the vertical components of 33 earthquakes (M_w 1.5 to 3.5) recorded at six stations and 68 earthquakes (M_w 1.6 to 5) recorded at five stations of the Jamnagar and Junagarh area, respectively. They estimated frequency dependent coda wave quality factor for the Junagarh and Jamnagar are as $(170 \pm 4.4)f^{(0.97\pm0.02)}$ and $(224 \pm 6)f^{(0.98\pm0.06)}$, respectively.

1.4 Seismic Hazard Zonation- Review

Seismic hazard zoning can be defined as a process of demarcating or mapping areas of same seismicity or equal hazard related to a characteristic of strong ground shaking and of site or structural response (Todorovska et al. 1995).The concept of seismic hazard in India was introduced by scientists of Geological Survey of India in 1935 immediately after the great Bihar Nepal earthquake of 15th January 1934 (Auden 1959).The ground motion parameters that first used in seismic zoning was the intensity of shaking (e.g. Modified Mercalli Intensity, MMI). Although the intensity scale is not based on instrumental data yet the places where instrumental data is lacking or is insufficient, zoning in terms of site intensity is the only choice (Todorovska et al. 1995). Chen et al. (1988) has given the fuzzy recurrence relationship for seismic hazards analysis or seismic zonation. In many studies, the seismic intensity has been also correlated to instrumentally measured parameters of strong ground motion like peak ground acceleration. The peak ground acceleration is the most widely used ground motion parameters for seismic hazard zoning (Algermissen and Parkins 1976; Kiremidjian et al. 1982; Khattri et al. 1984; Lin et al. 2014).

The first seismic regionalization map of the India show areas of different kind of damage was compiled by Geological Survey of India in 1935 (Auden 1959). Similar map was prepared by West (1937); Tandon (1956); Krishna (1959); Mithal and Srivastava (1959) and Srivastava (1969). The Bureau of Indian Standards (BIS) published the recommendations for earthquake-resistant design of structures in the shape of a code in 1962 (IS: 1893-1962). This code included a seismic zoning map of the India. In this seismic zoning map, the observed intensity values during the major past earthquakes were used as the main parameter. However the zoning map did not reflect the seismotectonic setup of the region, where major earthquakes are expected due to ongoing geotectonic processes (Todorovska et al. 1995). In 1966 (IS: 1893-1966), this map was revised and again in 1970 (IS: 1893-1970, 1975, 1984 and 2002) including the additional data on earthquake occurrence, geology and tectonics.

Guha (1962) prepared a seismic zoning map of India in 1962 based on modified Mercalli Intensity for 35 major earthquakes in a period from 1827 to 1950. This seismic map was demarcated as very heavy, heavy, moderate, minor and no damage area, keeping the compatibility with the geology and tectonics of the country. Entire peninsular shield region was demarcated as

stable zone in this map. This map was further modified for the peninsular shield after occurrence of Koyna earthquake of 1967, Bhadrachalam earthquake of 1969 and Broach earthquake of 1970 (Verma et al. 1970).

Gubin (1968) prepared a map of seismogenic zones of the Indian peninsula in 1968 and updated the map in 1970 aftermath of the occurrence of the Bhadrachalam (13^{th} April 1969) and Broach (23^{rd} March 1970) earthquakes. This map shows sixteen seismogenic zones which correspond to areas with differential tectonic motions. The width of each seismogenic zone is arbitrarily assumed to be 5 km greater than the width of the fault, taking into account possible sloping extensions into depth. In this map out of 16 zones, zone 16 can experience earthquake with intensity VI-VII where as zones 4, 5 and 15 with intensity V.

Kaila et al. (1972) have prepared three quantitative seismicity maps of the India, viz., the *a* value, *b* value and return period maps for earthquakes with magnitude six or above from 1954-1967. This map shows a very good match of seismicity with the regional tectonic features. Kaila and Rao (1979) prepared seismic zoning map of India taking data from 1954-1975 within 2°×2° grid averages for seismic risk, expected maximum magnitude (M_{max}), Intensity (I_{max}) and peak horizontal acceleration. In this map, the seismic risk values R_D (M) was estimated on the basis of Gumble's theory of largest values and a and b-values are estimated from the cumulative regression curve defined by log N = a - bM, where N is the cumulative number of earthquakes which occur in a given region during a certain time interval and whose magnitudes equal or exceed M. The seismic risk map shows the probability of occurrence of earthquakes capable of producing accelerations exceeding 10% of acceleration due to gravity in a design period of 50 years.

Using the method of probabilistic seismic hazard analysis, Basu and Nigam (1977, 1978) have prepared a zoning map of the India which shows peak ground acceleration contour for a life period of 100 years. They used the approach given by Cornell (1968). The entire Indian subcontinent has been divided into a grid of 2°×2°. They considered two different earthquake sources (the area and volume source), focal depth and distribution of earthquake occurrence. The magnitude, focal depth and occurrences were determined using January 1917 to December 1972 data from Indian Meteorological department (IMD). Using this data a contour map of peak ground acceleration for 100 years has been prepared. Basu and Nigam (1977, 1978) modified the zoning

map IS: 1893-1984 and divided the Assam region in two different zones (Zone IV and V) which was the single zone (Zone V) in IS code map. In their map they have expanded the zone II upto Central India.

Kiremidjian et al. (1982) have prepared seismic hazard map of the Honduras in terms of an iso-acceleration map. Such a map is developed for a return period of peak ground acceleration of 500 years. They used OASES (1978) attenuation relation for the seismic hazard analysis. The highest hazard is observed in the southwestern and western regions of the country which are closest to the junction of the Benioff Zone, the Caribbean Plate Boundary and the Shallow Focus Volcanic province.

Khattri et al. (1984) have prepared seismic zoning map showing peak ground acceleration for the India and neighboring areas having 10% probability of exceedence in 50 years. They used probabilistic seismic hazard approach given by Cornell (1968). In this map, India and adjoining region have been divided into 24 source zone based on similar generalized geological features and similar seismogenic processes. The seismicity of each source zone has been estimated by fitting a frequency-magnitude relation using the data with the longest possible time base and correcting the data in each magnitude interval for incompleteness using the procedure developed by Stepp (1973). They have used the attenuation relationship given by Algermissen and Perkins (1976) with some modifications for Indian conditions. In this map the Indian shield and the western coastal area is characterized by peak ground acceleration value of 0.05g and 0.4g, respectively. The north western and north eastern region shows the expected peak ground acceleration value of around 0.7g. The maximum peak ground acceleration value of 0.8g is obtained in the area of Bharamputra valley and Quetta region in the northwestern part of Indian subcontinent.

Joshi and Patel (1997) developed a technique for modeling the three dimensional rupture along identified active lineaments. Peak ground accelerations were obtained by using semi-empirical method given by Midorikawa (1993). The efficacy of this modeling technique is established by comparing observed and simulated peak ground accelerations data of the Uttarkashi earthquake of 20 October, 1991 (Joshi and Patel 1997). The zonation map for great earthquakes ($M \geq 8$) has been prepared by modeling a rupture in the central seismic gap region of the Uttarakhand

Himalaya. Seismic study of the region showed that it was prone to moderate as well as great earthquakes.

Bhatia et al. (1999) have prepared a seismic hazard zonation map for India and adjoining region under the Global Seismic Hazard Assessment Program (GSHAP). This map is based on the probabilistic approach of Cornell (1968). The peak ground acceleration computed in this work has 10% probability of exceedence in 50 years, at location defined by a grid of 0.5°×0.5°. In this work they have used the attenuation relation of Joyner and Boore (1981) which was defined for California and Western United States to obtain the seismic hazard map based on peak ground acceleration values. The entire study region has been divided into 86 seismogenic source zones based on major tectonic features and seismicity trends to compute the seismic hazard. In this map, the northern Indian plate boundary region and Tibetan Plateau region have been assigned the value of the order of 0.25g. The value of the order of 0.35-0.4g is assigned to more active region like Burmese arc, Northeastern Indian and Hindukush region. In the Indian shield the seismic hazard has been of the order of 0.05-0.1g is shown in this map.

Parvez et al. (2003) have prepared a first order deterministic seismic zonation map of India and adjoining region based on the technique of Costa et al. (1993). They computed synthetic seismograms at frequency of $1H_z$ and at a regular grid of 0.2°×0.2° by model summation technique proposed by Panza (1985). Parvez et al. (2003) have divided the India and surrounding region into 15 polygons defining different structural models and 4 of seismogenic zones based on various geophysical and geological data. A regional fault plane solution has been defined for each seismogenic zone depending on the mechanism of the strongest event or with the best obtained event, or the most frequent event. The earthquake database from 1819 to 1998 has been used in this study. In this work they have expressed the seismic hazard in terms of maximum displacement, maximum velocity and design ground acceleration which have been extracted from the synthetic signals and mapped on a regular grid. In the map for design ground acceleration the value of 0.6-1.3g has been assigned to the region of great Assam earthquake. The value of the order of 0.3-0.6g has been assigned to the central and western Himalaya region whereas the value of the order of 0.3-0.6g has been assigned to Andaman-Nicobar Islands.

Mohan et al. (2008) prepared a seismic hazard map of two seismically active regions of Himalaya, India. In this work, they have modeled the finite rupture along several lineaments using semi empirical technique given by Midorikawa (1993).The zonation map is prepared for magnitude $M \geq 6.0$, for these regions. The area has been divided into different zones on the basis of expected peak ground acceleration. The range of zones follows the similar peak ground acceleration as proposed by Bureau of Indian standard map (BIS 2002).

Joshi and Mohan (2010) prepared expected peak ground acceleration map for different zones similar to zones proposed by the Bureau of Indian standard (BIS 2002). The proposed technique has been applied to the Kumaon Himalaya area and the surrounding region for earthquakes of magnitude $M \geq 6.0$. Approximately 56000 km^2 study area is classified into the highest hazard zone V with peak accelerations of more than 400 cm/s^2. The prepared map shows that epicentres of many past earthquakes in this region lie in zone V.

Mahajan et al. (2010) has developed probabilistic seismic hazards of NW Himalaya and its adjoining area, India. They apply standard method of PSHA given by Cornell (1968) for computing the peak ground acceleration (PGA) for 10% probability of exceedance in 10 and 50 years at locations defined in the grid of 0.25°×0.25°.

1.5 Research Gaps

The state of Uttarakhand in India lies in central seismic gap demarcated by Khattri (1987). The possibility of a great earthquake in this seismically active region cannot be ruled out. In any seismically active region construction of safe engineering design depends on various seismic parameters. Attenuation study plays an important role in visualizing the seismic hazard of any region. The literature survey revealed that there are several methods which can be used to determine attenuation property of a region using broadband, teleseismic, strong motion and micro earthquake data. Comparative studies related to attenuation prosperities of the Uttarakhand Himalaya can be divided into two steps. (1) Study of peak ground attenuation relation and (2) Frequency dependent coda wave quality factor.

Inspite of seismically high status of the Uttarakhand Himalaya, this region does not have sufficient amount of strong motion data required for preparation of reliable attenuation relation. As

most strong motion data show that peak ground acceleration in vertical component usually is less than the horizontal component (Wen et al. 2006). Recent studies related to the estimation of seismic hazard in India shows that the attenuation relations used for seismic hazard studies in this area are basically those that are developed by different workers using worldwide data.

The available relations in this region have used data from entire Himalaya irrespective of the nature and properties of earthquake occurring in different parts of the Himalaya. It is seen that earthquakes in NW Himalaya are occurring mostly along shallow dipping plane of detachment (Ni and Barazangi, 1984), while earthquakes in north east Himalaya are occurring mostly at a depth of 10 to 30 km (Kayal and De 1991). Therefore any attenuation relation that includes entire dataset of Himalayan earthquakes can give large deviation from observed peak ground acceleration when applying it to the different parts within Himalaya. Further large heterogeneities and complexities in the Himalayan crust always present chances of strong regional variation of attenuation characteristics of the medium.

Attenuation characteristics of the region can be determined from dimensionless parameter known as quality factor Q. Different types of rocks have different attenuating properties which controls the decay of seismic energy released during an earthquakes. Different estimates of quality factor have been given by different workers for Himalayas (Gupta et al. 1995; Mandal et al. 2001; Paul et al. 2003; Joshi et al. 2009, 2010b). The literature studies of this region give some research gaps:

1. Strong motion data are important for seismic study in any seismically active region. Dense strong motion network is required for the detailed study of any region. Deficiency of strong motion data is a major constrain of the attenuation study in the Uttarakhand Himalaya.

2. Different attenuation properties exist for different parts of the Himalaya. Any attenuation relation that includes entire dataset of the Himalayan earthquakes can give large deviation from observed peak ground acceleration. So there is a need of developed of region specific attenuation relation, which can provide more realistic picture of attenuation property of the region.

3. In the past many researchers had estimated different quality factors for the Kumaon and the Garhwal Himalayas. Most of these studies had used limited data sets from this region. Dense data sets for the study region can provide better understanding of quality factor in this region.

4. Study of existing relation of shear wave quality factor indicates that the attenuation rate in both the Kumaon and Garhwal Himalaya is different. However, attenuation properties in this region have not been estimated using near field strong motion data.

5. Detail seismic studies of the region indicate that the Garhwal Himalaya has been devastated by two large earthquakes in recent past viz. the Uttarkashi and the Chamoli earthquakes. However no such major earthquake has been reported in the Kumaon Himalaya. Possible causes for such drastic change in seismicity pattern in almost similar tectonic regime have been not investigated.

6. Many researchers have simulated records of major earthquakes in the Garhwal Himalaya using semi empirical simulation technique and worldwide attenuation relation given by Abrahamson and Litehiser (1989). Use of this worldwide attenuation relation for study of Himalayan earthquakes is questionable.

7. Seismic hazards zonation of the Uttarakhand Himalaya had been made using worldwide attenuation relations.

1.6 Research Objective

Strong motion data is the first requirement of the engineer and seismologist for safe design of structure. Himalaya region has experienced many small as well as moderate earthquakes in the past. Maintenance of strong motion array is the major problem in this region due to its rough topography and high attitude. Without strong motion data seismic hazards assessment is not possible in this area. In the Uttarakhand Himalaya a network is operating in the Garhwal region since 1976, but in Kumaon region there is a strong requirement of such network. For solve this problem, a dance network of eight strong motion accelerographs has been installed by the

Department of Earth Sciences, Indian Institute of Technology Roorkee and National Geophysical Research Institute Hyderabad, India under the seismicity project since 2006. Parameters extracted from the recorded strong motion records from these two networks have provided an opportunity to compare regional attenuation properties of this region. The objective of this work is to use strong motion parameters from data recorded by these two networks to study attenuation characteristics of both the Kumaon and Garhwal Himalaya.

Anelastic attenuation studies performed by Gupta et al. (1995) and Paul et al. (2003) for the Garhwal and the Kumaon Himalaya indicate high attenuation rate for the Kumaon Himalaya as compare to the Garhwal Himalaya. Both researchers have determined frequency dependent coda wave attenuation relation for these regions using back scattering technique of Aki (1968). However the dataset are entirely different for two studies. Completely different trends in attenuation rates of strong ground motion in the Garhwal and the Kumaon region has motivated a strong need to look insight into the detail attenuation characteristics of the Garhwal and Kumaon region. In order to maintain consistency in the approach, the study needs to be done by similar technique using dataset having similar constraints. On the basis of literature survey and research gaps the research work in the Ph.D degree is targeted to achieve following objectives:

1. Development of regression relation of peak ground acceleration for the Uttarakhand Himalaya using strong motion data of similar parametric constraints of independents variables.

2. Checking of the suitability of developed attenuation relation to simulate large earthquake in this region.

3. Development of frequency dependent coda wave quality factor for both the Kumaon and Garhwal Himalaya using similar strong motion data with similar techniques.

4. Preparation of seismic hazard map on the basis of obtained attenuation relation for the Uttarakhand Himalaya.

1.7 Thesis Layout

Total seven Chapters are included in the present thesis. The literature review regarding the attenuation relation, technique of simulation, frequency dependent coda wave quality and seismic hazards zonation studies is presented in Chapter 1. Different relations developed by various researchers to determine the attenuation property are discussed in this Chapter. Literature survey for seismic hazards zonation of the Indian region is also discussed in this Chapter. Various research gaps are identified on the basis of literature survey and objectives of present work have been discussed in this Chapter.

Strong motion data and study area are discussed in Chapter 2. The strong motion networks operated in the Uttarakhand Himalaya has been discussed in this Chapter. Methodology used for developing attenuation relation for the Kumaon and Garhwal Himalaya region using regional strong ground motion data is described in Chapter 3. This Chapter also describes normality and model adequacies with developed attenuation relation. Validity of these attenuation relations are checked by modeling of the Uttarkashi and Chamoli earthquakes and is discussed in Chapter 4. Determination of frequency dependent coda wave quality factor using single backscattering technique is presented in Chapter 5. This Chapter also discusses the regional average relationships for the Kumaon and Garhwal Himalaya.

The seismic hazard zonation map of the Uttarakhand Himalaya region, have been prepared in this work and is given in Chapter 6. Summary and conclusion of present research work is given in Chapter 7. This Chapter summarizes the whole research work, which reveals the important conclusions for future research work.

CHAPTER – 2

Parameterization of Strong Motion Data

2.1 Introduction

Strong motion data is a major requirement for designing earthquake resistant structures in a seismically active region. Himalayan is one of the most seismically active regions in the world. Numbers of major earthquakes have visited this region during the last hundred years. However, very few strong motion records of these earthquakes are available today. The major difficulty in getting regional strong motion records is that this region is quite inaccessible and it is also difficult to maintain strong motion stations in this rough mountainous terrain. In the resent years, strong motion networks have been installed in the region of the Uttarakhand Himalaya. These networks have recorded strong motion data of several small events in this region. This Chapter discussed about the study area, processing and source parameters of strong motion data recorded by the networks operated in the Kumaon and Garhwal Himalaya.

2.2 Geology and Tectonic of Study Area

The Himalaya orogen, which extends over 2500 km from Kashmir in the northwest to Arunachal Pradesh in northeast India, is believed to be a result of collision of the Indian and Eurasian plates (Gansser 1964; Holmes 1965; Seeber et al. 1981; and Lyon and Molnar 1983). Himalayan mountain chain is characterized by a marked concentration of interplate seismicity and high rate of upliftment as well as convergence (Molnar and Chen 1983; Nakata 1989; Demets et al. 1990). Many thrust faults lie in the Himalayan regions which are capable of producing earthquakes of magnitude 8.0 or greater (Gitis et al. 2008). Fourteen major earthquakes of magnitude $\geq$ 7.5, including five great earthquakes of magnitude $\geq$ 8, have occurred in the Himalayan region during 1897 to 1992 (Gupta et al. 1995; Satyabala and Gupta 1996). Many historical earthquakes have been recorded in this region which are mostly concentrated between main boundary thrust (MBT) and main central thrust (MCT) (Seeber and Armbruster 1984).

The Uttarakhand Himalaya falls under the highest zone IV and V of seismic zoning map of India. This area has witnessed two major earthquakes i.e. the Uttarkashi earthquake of 1991 (M_s = 7.1) and the Chamoli earthquake of 1999 (M_s = 6.6) in the recent past. The northeastern part of the study area is occupied by the Tibetan Plateau while the southwestern sector is occupied by the Indo Genetic plains. The northeastern part of the study area exposes rocks of the Trans Himalayan tectogen along with late to post tectonic granitoid and ophiolite bodies (GSI 2000). South of this, the belt between the Karakoram Fault and the Indian suture zone is occupied by cover rocks, affected by Himalayan orogeny, late to post tectonic granitoid ophiolite and lithopackets of the accretionary complex (GSI 2000). The foothill belt constitutes foredeep sediments affected by the terminal phases of the Himalayan orogeny. South of foothills the tract is covered by the alluvial fill of the Gangetic foredeep. The northern most tectonic element is the dextral Karakoram Fault, which is sub parallel to the Indus Suture Zone (ISZ), occurring to the South. The Indus Suture Zone (ISZ) is an important tectonic zone, which demarcates the northern boundary of the Indian Plate (GSI 2000). Within the main Himalayan belt the high grade complex of the central crystalline is bound to the north and south by the Martoli Thrust and the Main Central Thrust (MCT) respectively. A similar high grade complex, the Almora crystalline, is delimited on either side by the North Almora Thrust (NAT) and South Almora Thrust (SAT). The main Himalayan belt is represented from the Tertiary frontal fold belt by the Main Boundary Thrust (MBT) and the southern limit of the frontal belt is marked by the Main Frontal Thrust (MFT), which has its surface manifestation at places (GSI 2000). A number of N-S to NNE-SSW faults of limited spatial extension has also been mapped from the area. Seismicity of this region from 1973 to 2014 along with tectonic map is shown in Fig. 2.1.

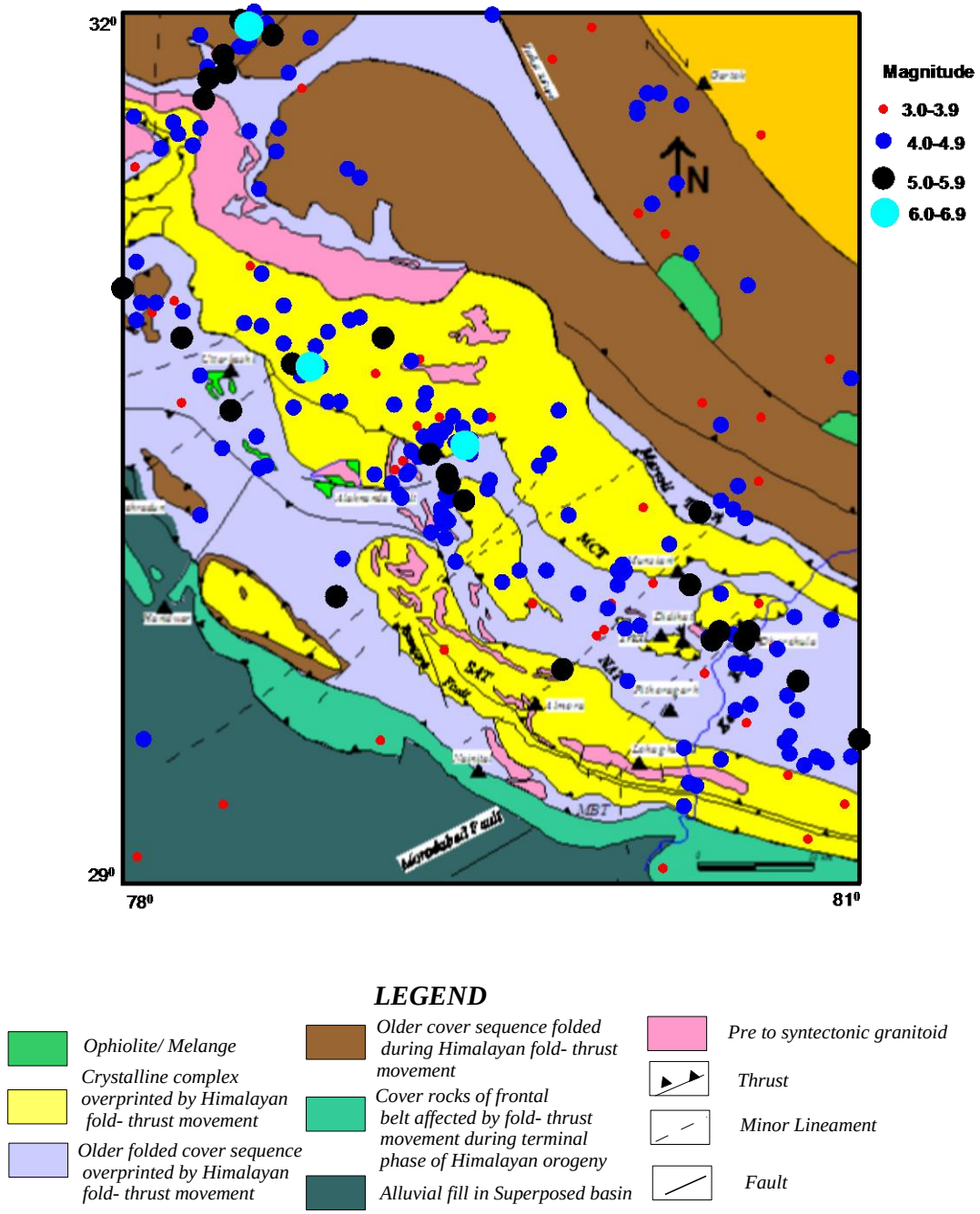

Figure 2.1: Locations of various events in the Garhwal and Kumaon Himalaya during 1973 to 2014 reported by USGS. The geology and tectonics of the region is after GSI (2000).

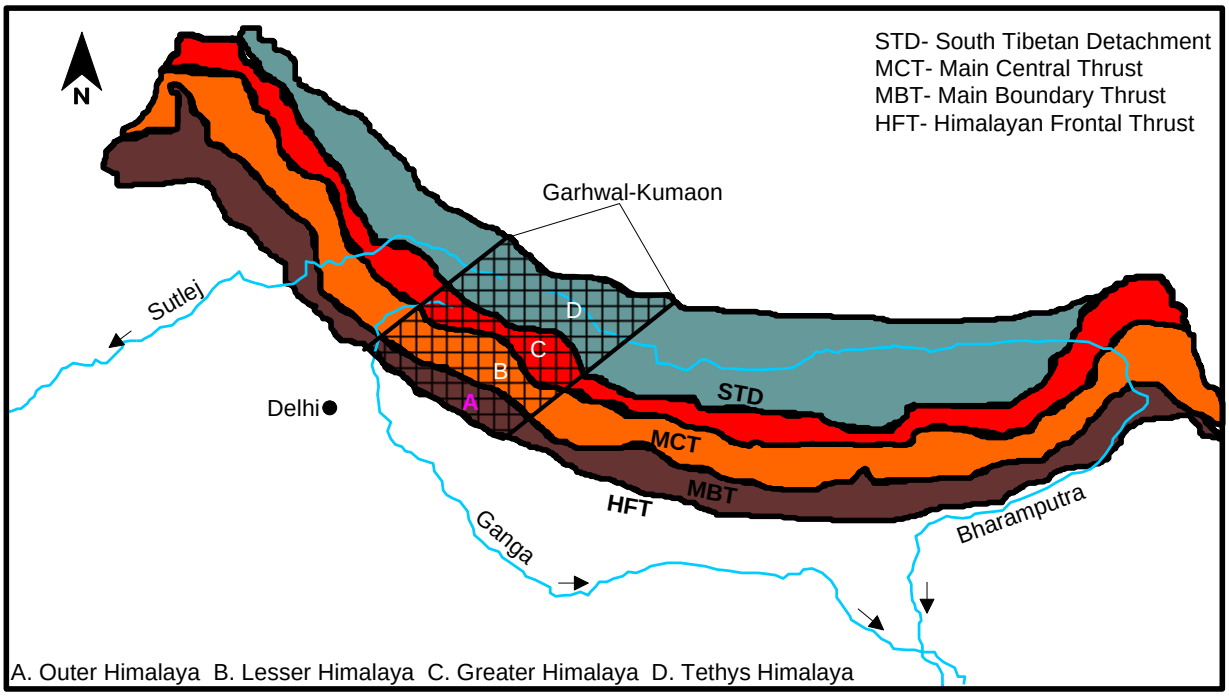

Figure 2.2: Geological sketch map of the Himalaya. A - Outer Himalaya, B - Lesser Himalaya, C - Greater Himalaya and D - Tethys Himalaya (Figure modified after Bhattacharya 2008).

Himalaya has been geologically divided into four lithotectonic subdivisions as shown in Fig. 2.2. From south to north these are defined as (Gansser 1964):

(1) Outer Himalaya: - This part mostly includes the molassic Siwalik Supergroup of Mio-Pliocene ages and is demarcated by two tectonic planes, the Himalayan Frontal Thrust (HFT) to the south and the Main Boundary Thrust (MBT) to the north (Bhattacharya 2008).

(2) Lesser Himalaya: - This part exposes a thick pile of highly folded Proterozoic sedimentary strata together with a few outcrops of older crystalline rocks; this subdivision is bounded by the MBT in the south and the Main Central Thrust (MCT) in the north. The Main Central Thrust (MCT) is defined by the contact between the Lesser and the Higher Himalayas (Bhattacharya 2008).

(3) Greater or Higher Himalaya: - This part exposes a massive, north-dipping pile of metamorphic rocks – the Central Crystalline Zone and is demarcated by the MCT to its south and the Dar-Martoli Fault or Tethys Fault or the South Tibetan Detachment (STD) to the north (Bhattacharya 2008).

(4) Tethys Himalaya: - This part includes a thick pile of sedimentary rocks of Cambrian to Lower Eocene ages (Bhattacharya 2008).

2.3 Strong Motion Networks

Under a major seismicity project funded by the Department of Science and Technology, Government of India, a dense network of eight stations has been installed in the highly mountainous terrain of the Kumaon Himalaya since March 2006 by Department of Earth Sciences, Indian Institute of Technology Roorkee and National Geophysical Research Institute, Hyderabad, India. Additional six strong motion accelerographs have been deployed by the Department of Earth Sciences Indian Institute of Technology Roorkee, in another project funded by Ministry of Earth Science, New Delhi, Government of India, since 2008. Because of high seismic activity and seismic gap present in this region, this strong motion network has great importance in recording recent seismic activities of the region.

On recommendation of International Workshop on strong motion measurements held in Honolulu, the Department of Earthquake Engineering, Indian Institute of Technology Roorkee established three strong motion arrays in India, funded by the Department of Science and Technology, New Delhi, Government of India (Chandrasekaran and Das 1993), which is still operating. Under this project 284 strong motion accelerographs have been installed in the three strong motion arrays. These are Kangra array (NW Himalaya), Uttar Pradesh array (North Himalaya) and Shillong array (NE Himalaya) India. The instruments used in these arrays are analogue strong motion accelerographs (SMA-1). The Uttar Pradesh array has 40 strong motion accelerographs. This array has recorded several earthquakes in the entire Himalayan belt. This array also covers various parts of the Garhwal Himalaya, India and continuously monitoring the seismic activities in this region.

Location of stations of the Kumaon and Garhwal Himalaya networks along with the geology and tectonics in the Uttarakhand Himalaya which data used is in the present work shown in Fig 2.3. The minimum inter station distance of Kumaon array is approximately 11 km, while for Garhwal array it is approximately 20 km. Strong motion data of the earthquakes in the Garhwal Himalaya are available from the website maintained by the Department of Earthquake Engineering, Indian Institute of Technology, Roorkee, India.

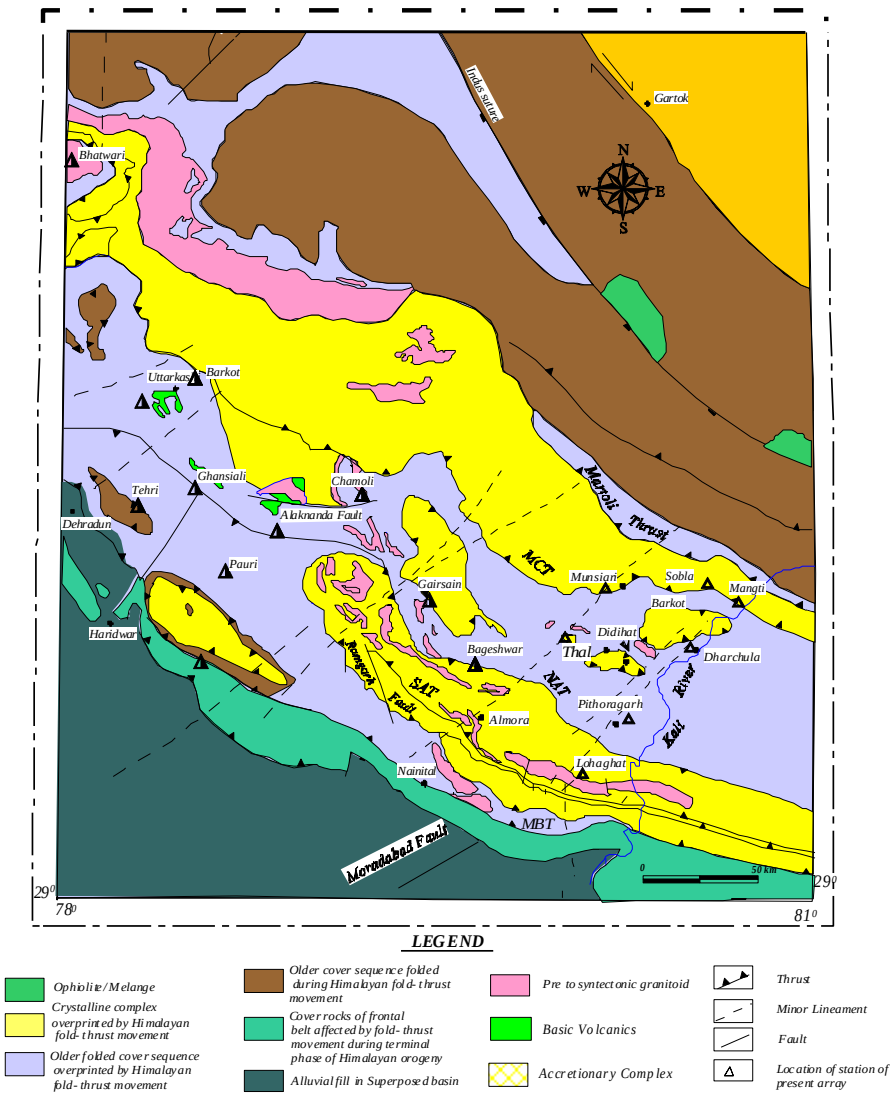

Figure 2.3 Locations of strong motion recorders in the Kumaon and Garhwal Himalaya which data used. Half filled triangle denotes the station maintained by the Department of Earthquake Engineering, Indian Institute of Technology Roorkee and empty triangle denotes the stations maintained by the National Geophysical Research Institute and Department of Earth Sciences, Indian Institute of Technology Roorkee. Tectonic map has been taken after GSI (2000).

2.3.1 Data from Kumaon Network

The sites for installation of strong motion accelerographs (SMA) in the Kumaon array have been selected on the basis of historical seismic activities. The historical events during 1973 to 2014 shown in Fig. 2.1 indicate a cluster of events in between Main Central Thrust (MCT) and North Almora Thrust (NAT) in the Kumaon Himalaya region. Hence most of the strong motion accelerographs are installed between MCT and NAT to record maximum earthquakes occurring in this region. Details of all stations in the Kumaon array are given in Table 2.1. Some stations of this network are mobile and hence Table 2.1 has a total of 16 stations. This network is installed in highly mountainous terrain of the Kumaon Himalaya as shown in Fig. 2.4 where elevation of recording stations from mean sea level lie between 612 to 2239 meter. This network is one of the dense networks monitoring strong motion seismic activity in highly mountainous terrain of the Himalaya, India. Three-component accelerograph has been installed at each station as shown in Fig. 2.5. The stations Jouljibi and Munsyari have minimum and maximum elevation of 612 m and 2239 m, respectively.

Table 2.1: Name, code and location of the recording stations in the Kumaon array.

Sr. No.	Station Name	Station Code	Latitude (Degree)	Longitude (Degree)	Elevation of the stations from mean sea level (meter)
1	Didihat	DID	29.80	80.25	1628
2	Pithoragarh	PIT	29.58	80.21	1574
3	Tejam	TEJ	29.95	80.12	968
4	Dharchula	DHA	29.84	80.53	935
5	Munsyari	MUN	30.06	80.25	2239
6	Askot	ASK	29.76	80.33	1258
7	Kamedidevi	KAM	29.84	79.96	1811
8	Jouljibi	JOL	29.75	80.38	612
9	Baluakot	BAL	29.79	80.42	644
10	Knalichhina	KNA	29.67	80.27	1656
11	Muavani	MUA	29.74	80.13	822
12	Berinag	BER	29.77	80.05	1684
13	Mangti	MAN	30.00	80.71	1609
14	Sobla	SOB	30.06	80.59	1628
15	Thal	THL	29.82	80.14	784
16	Bageshwar	BHA	29.83	79.77	873

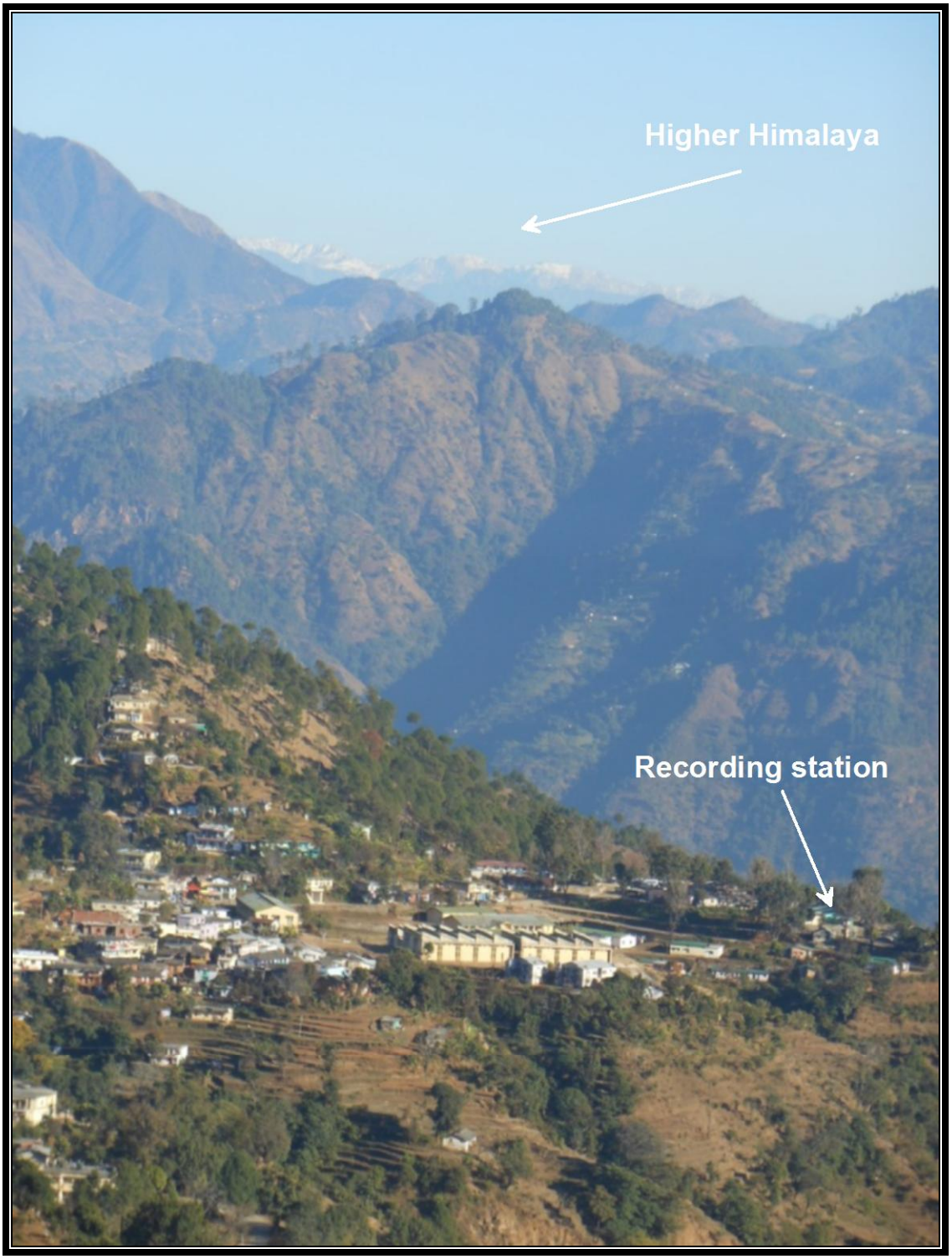

Figure 2.4 Location of recording station in mountainous terrain of Himalaya. Figure showing location of the Askot station installed at the elevation of 1258 meter from mean sea level.

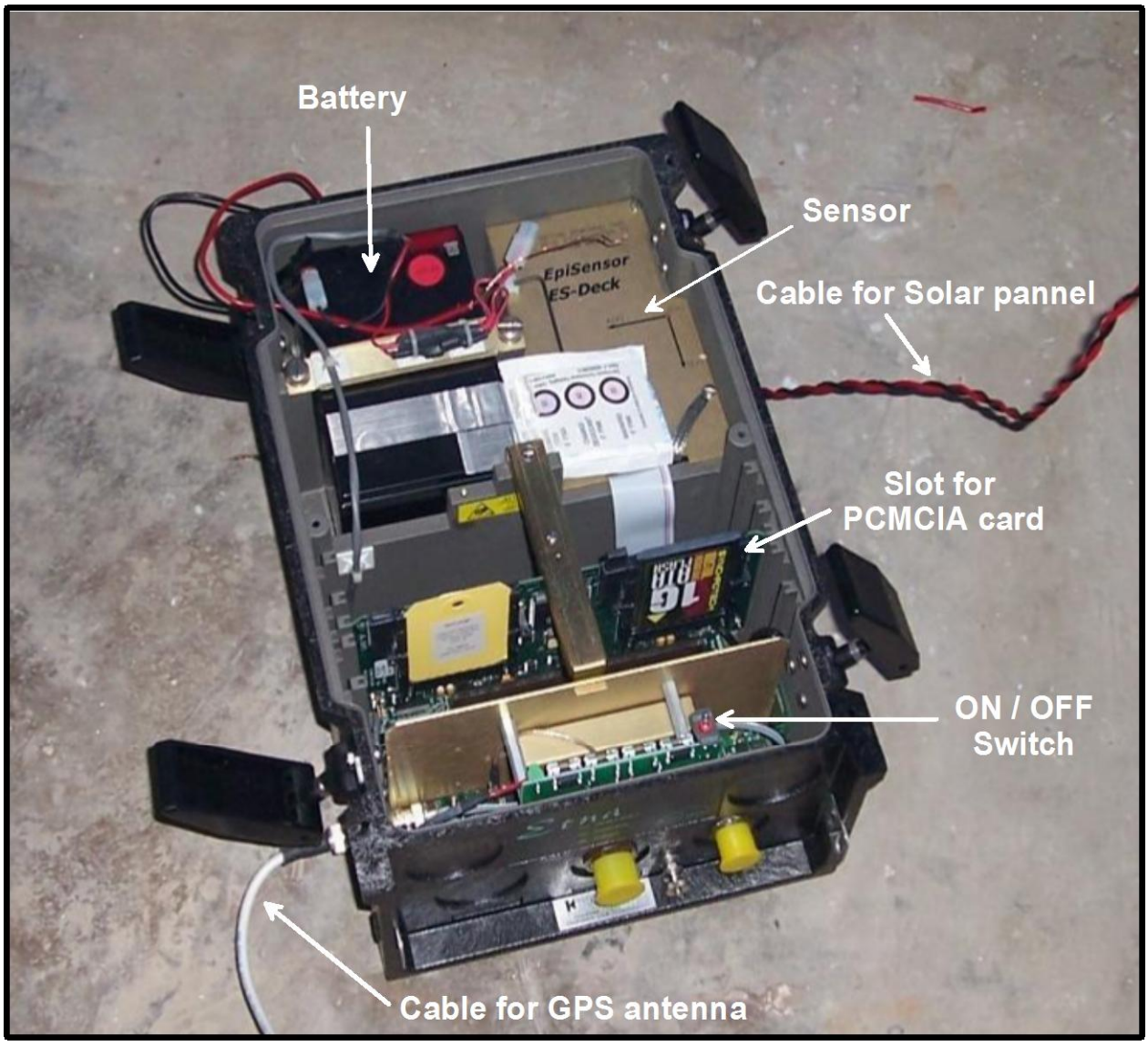

Figure 2.5 Strong motion accelerograph made by Kinemetrics, U.S.A. installed at each site.

This network had recorded two hundred ninety four events in this region since March, 2006 to December 2014. Three-component force balance, accelerometer of Etna model make by Kinemetrics, U.S.A. have been installed at all stations of this network. In order to record events with low energy, the threshold level of instruments were set at very low level of 0.005% of full scale. The sensitivity of instrument is 1.25 V/g and full scale measurement is 2.5V. Sampling interval of digital data is kept at 0.01 sec. Purpose of such low threshold level is to record almost every possible local events occurring in this region. The major components of entire accelerograph unit are the Sensor, Global positioning system (GPS) antenna, Solar panel, Battery and PCMCIA card and is shown in Fig. 2.6 and 2.7. The entire instrument is in a compact form and consists of sensor, recording unit and battery. Global positioning system (GPS) antenna is connected through a cable to the main unit and is used to provide accurate geographical location and time. Solar panel and battery is used to supply the power backup to the accelerograph. Data can be retrieved from the PCMCIA card or through a cable connected with laptop as shown in Fig 2.8. PCMCIA is the memory card which is used to store the data. The data retrieved from the card is obtained in EVT format. The ASCII conversion of this format give three files with extension .001, .002 and .003, respectively which represent the longitudinal, transverse and vertical components, respectively of acceleration record. Three components of accelerogram of recorded at Dharchula station is shown in Fig. 2.9.

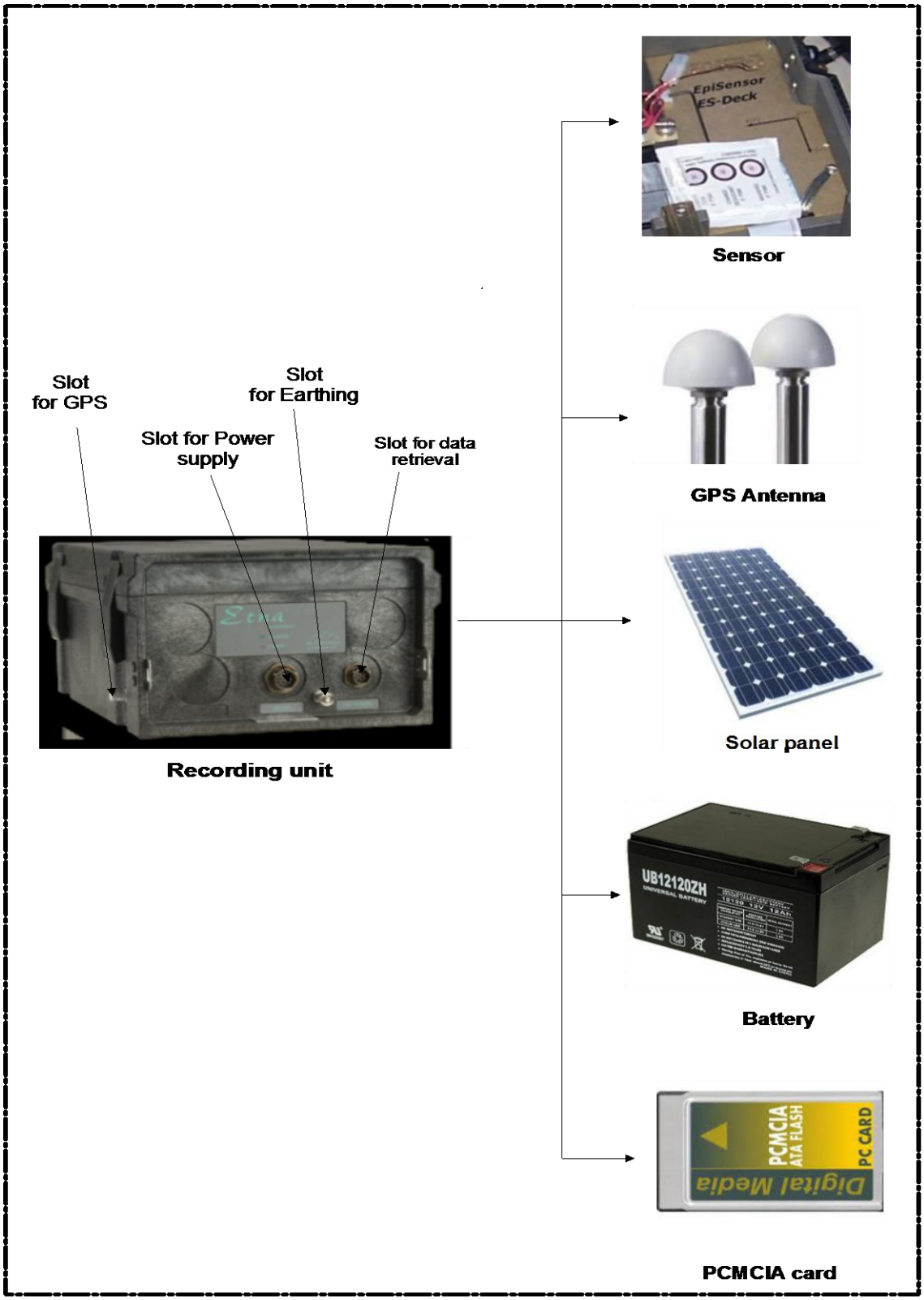

Figure 2.6 Major components of the strong motion accelerograph.

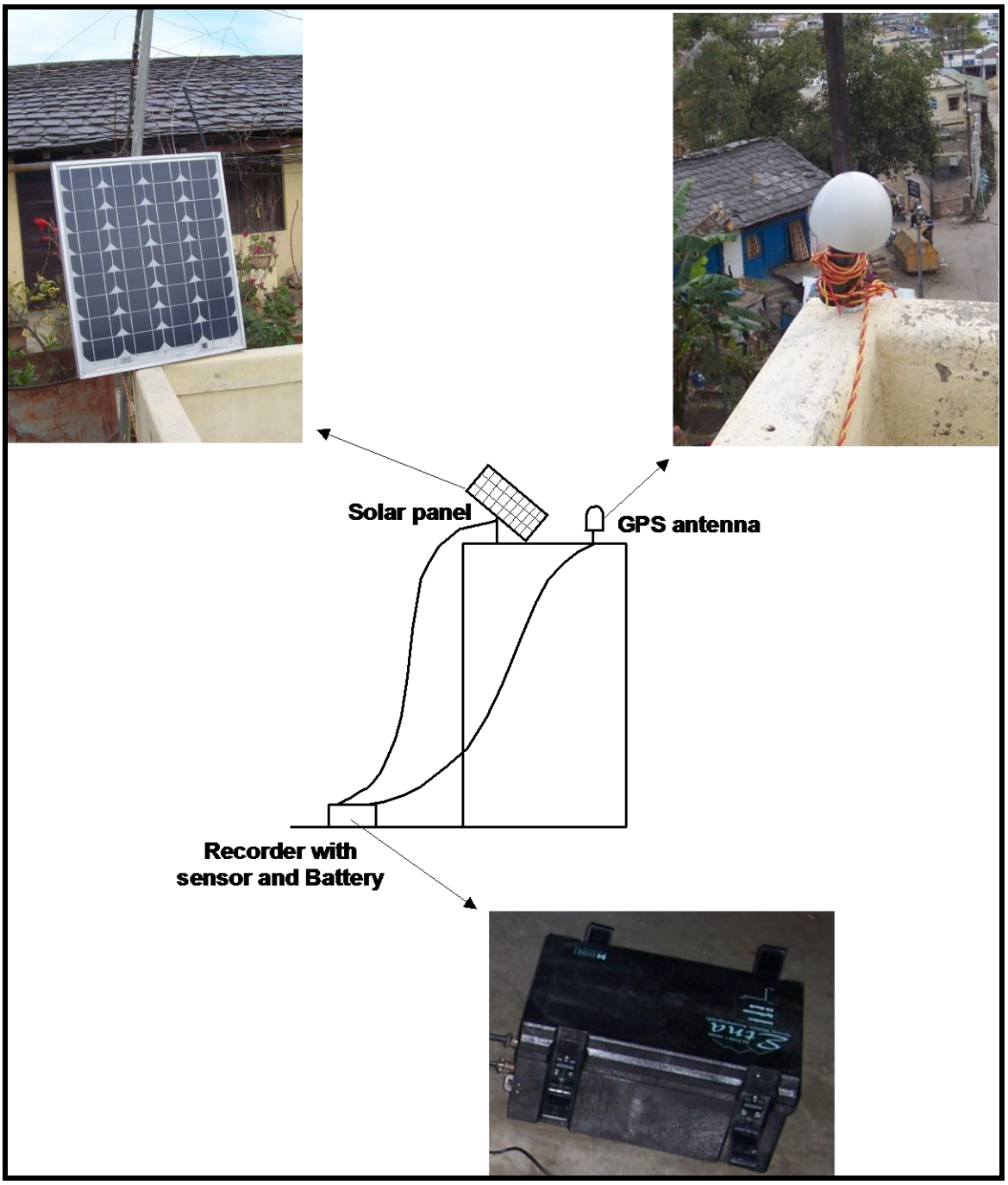

Figure 2.7 A figure showing the major component of accelerograph installed in the field.

Figure 2.8 Retrieval of data recorded in the strong motion accelerograph through a cable by using the laptop.

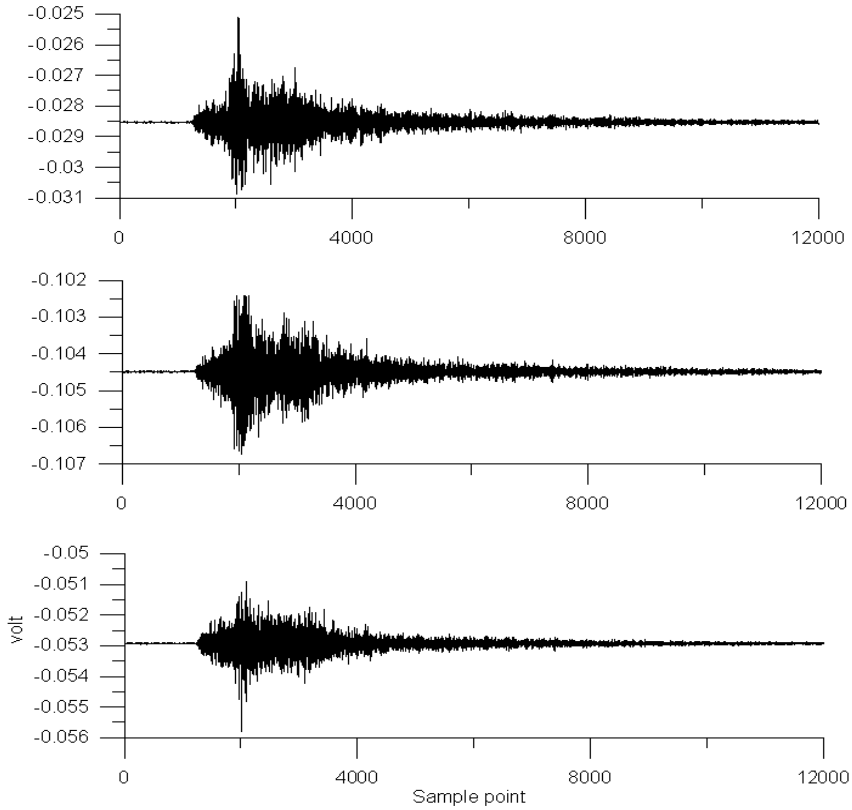

Figure 2.9 Recorded three component of unprocessed accelerogram of an event occurred on 4-09-2008 at the Dharchula station.

The hypocentral parameters of events recorded at three or more than three stations have been determined using HYPO71 software originally developed by Lee and Lahr (1972). Input parameters for the software are: station coordinates, arrival time of P-wave and S-wave, and velocity model of the region. The velocity model given by Yu et al. (1995) has been used for localization of events. Those events which are recorded at one and two stations are also used in the present work for calculation of source parameters using displacement spectra after estimating hypocentral distance from S-P time in the record. The records collected from the accelerograph have been processed using the procedure suggested by Boore and Bommer (2005). The processing steps involve baseline correction, instrumental scaling and frequency filtering which are defined in following section.

2.3.2 Data from Garhwal Network

A strong motion network of two hundred analog accelerographs had been installed by the Department of Earthquake Engineering Indian Institute of Technology Roorkee. This network covers various parts of the Himachal Pradesh, Punjab, Haryana, Uttar Pradesh, Uttarakhand (Table 2.2), Bihar, West Bengal, Sikkim, and northeastern India. Inter spacing distance is about 20 to 40 km of this network of strong motion instruments were located only in the Himachal Pradesh, Uttarakhand, and Shillong regions. Some strong motion accelerographs were installed in the seismic zone III of India. Due to its large population density this region has high seismic vulnerability. These strong motion networks are monitoring seismic activities and providing good quality strong motion data. However, due to the unavailability of components/spare parts and to obsolete technology, most of the strong motion accelerographs installed in the early 1980s are no longer functional. To overcome this problem, a division of the Government of India, sanctioned a project titled “National Strong Motion Instrumentation Network” to the Indian Institute of Technology, Roorkee (Kumar et al. 2012).

In February 2004, under a another seismicity project funded by the Department of Science and Technology, New Delhi about 300 digital strong motion accelerographs were installed in northern and northeastern India to monitor seismic activity. In 2007 this network was further strengthened by 20 digital strong motion accelerographs by installing in the Delhi region under another project sanctioned by the Department of Science and Technology (Kumar et al. 2012).

Typically, the instruments are installed in a room on the ground floor of (preferably) a government-owned one or two story building where proper logistics are available, which means that the instrument is protected from tampering and 220 v AC power supply is available. In Delhi, however, free field instruments were installed inside a specially fabricated housing. All 300 strong motion accelerographs consist of internal AC-63 GeoSIG triaxial force-balanced accelerometers and GSR-18 GeoSIG 18-bit digitizers with external GPS. The 12 strong motion accelerographs installed in the Delhi are K-2 (Kinemetrics K-2s) with internal accelerometer (model episensor) and 18-bit digitizer. The recording for all instruments is in trigger mode at a sampling frequency of 200 sps. The recording is done on a 256-MB GeoSIG or 1-GB Kinematics compact flash card (Kumar et al. 2012). Major components of instrument installed in the Garhwal Himalaya regions are shown in Fig. 2.10. A diagram showing the networking of instruments installed in remote area to the central station Roorkee is shown in Fig. 2.11.

Table 2.2 List of strong motion accelerographs stations with name and coordinates installed in the Garhwal Himalaya (after Mittal et al. 2012)

S. No.	Station name	Latitude (Degree)	Longitude (Degree)
1.	Chamoli	30.41	79.32
2.	Pauri	30.15	78.78
3.	Tehri	30.37	78.43
4.	Uttarkashi	30.73	78.44
5.	Barkot	30.81	78.25
6.	Dhanaulti	30.43	78.23
7.	Garsain	30.05	79.29
8.	Ghansali	30.43	78.66
9.	Joshimath	30.57	79.58
10.	Lansdown	29.84	78.68

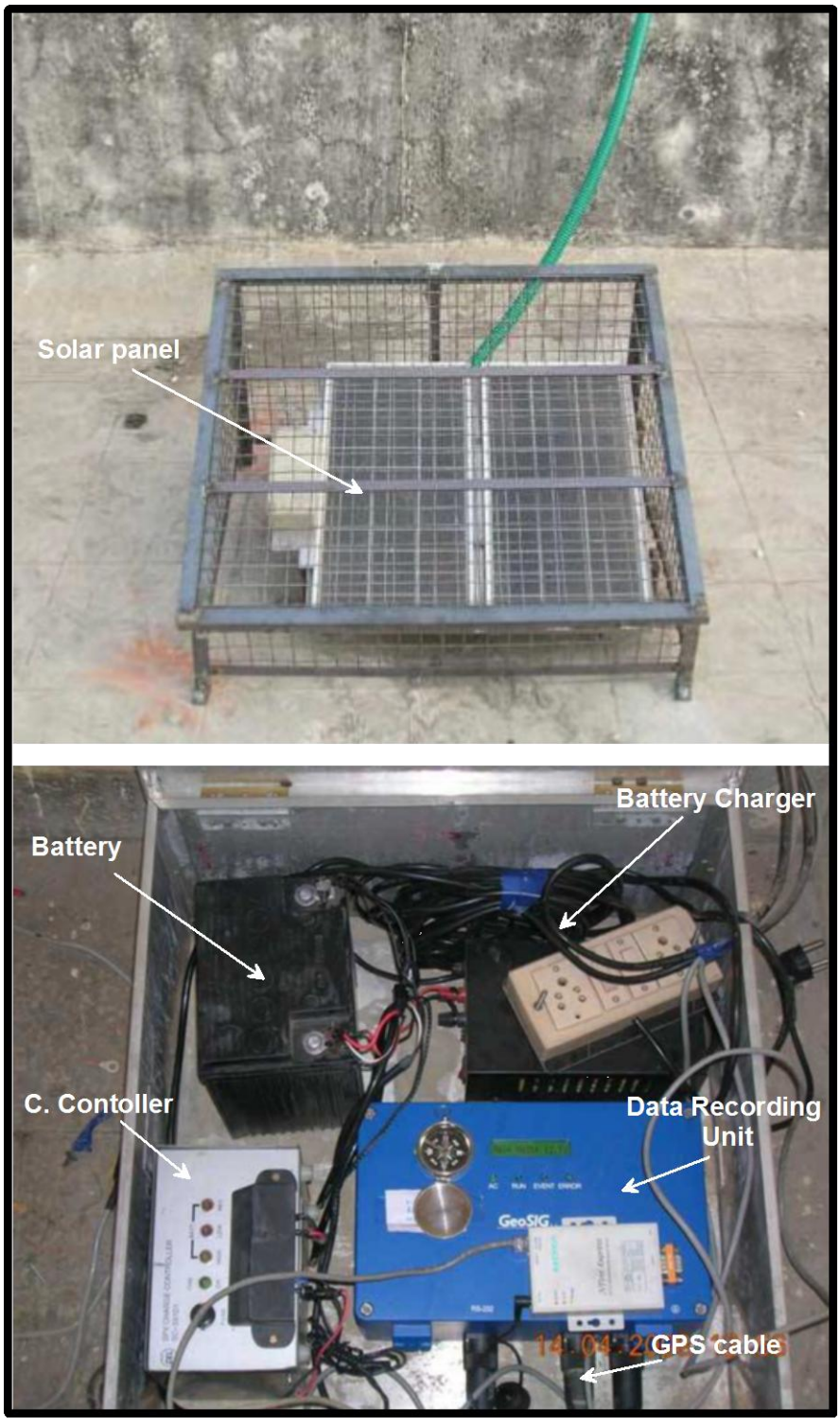

Figure 2.10 Major components of instrument installed in the Garhwal Himalaya regions (modified after www.pesmos.in).

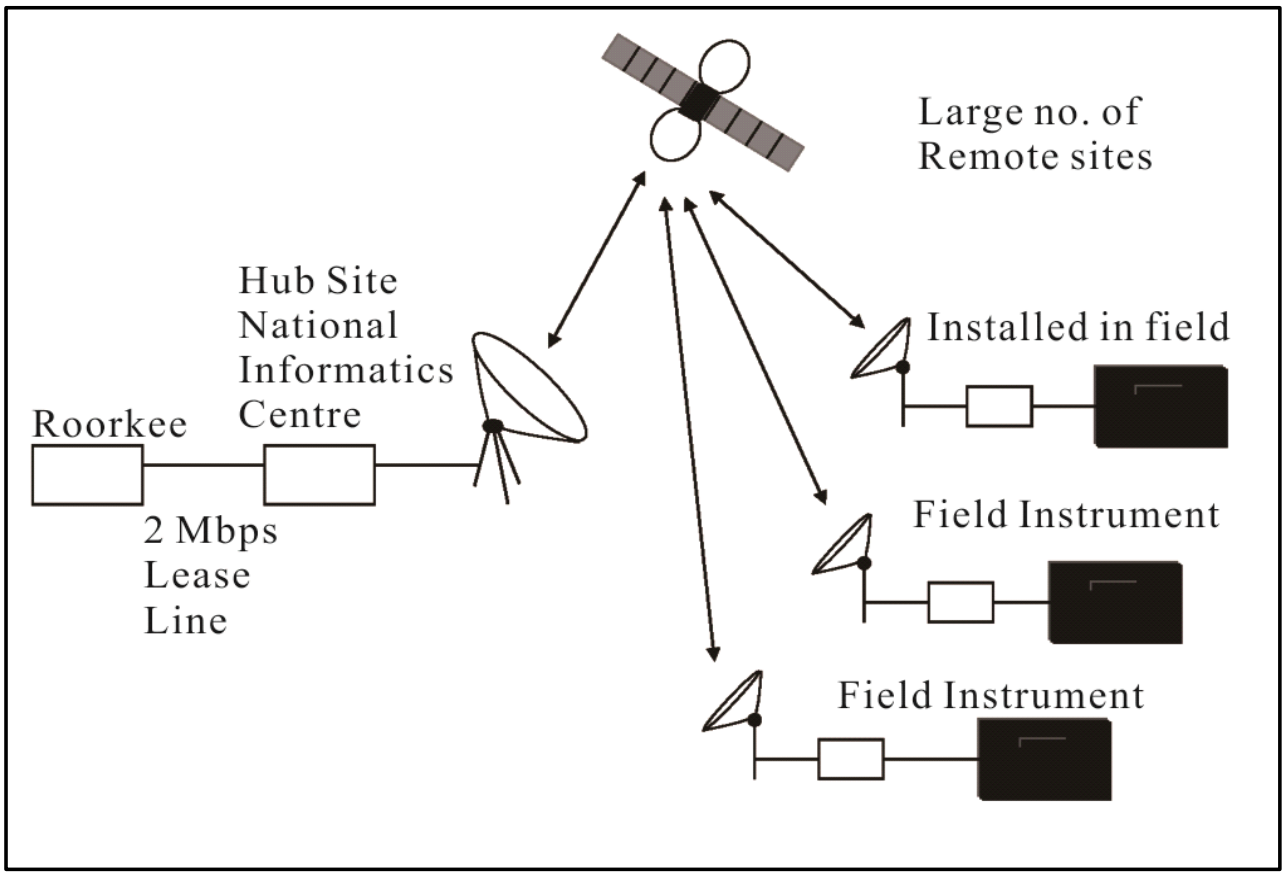

Figure 2.11 A diagram showing the networking of instruments installed in field to Roorkee (the central station). This figure has been taken after Kumar et al. (2012).

2.4 Processing of Strong Motion Data

2.4.1 Instrument scaling: This is an important correction, which converts counts or milivolt recorded by the instrument into actual ground acceleration in gals (cm/sec^2). For strong motion accelerographs installed in Kumaon array, the instrument correction for longitudinal transverse and vertical component is 1.25 volt/g, respectively. The recorded data has been converted into acceleration form as shown in Fig. 2.12.

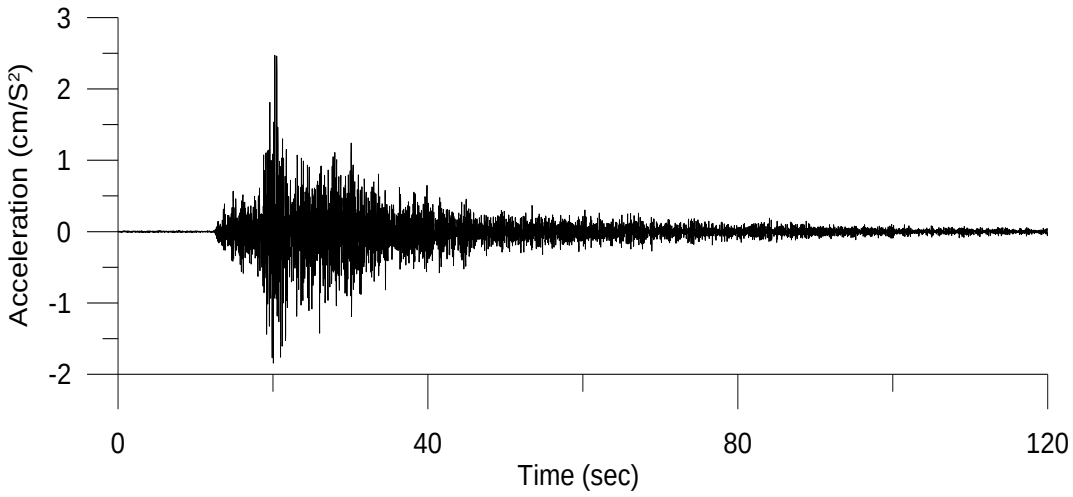

Figure 2.12 Processed (Baseline corrected) NS component of at the Dharchula station after instrument scaling correction. Records taken from strong motion data of earthquake occurred on 4.09.2008.

2.4.2 Baseline correction: This step necessitates subtraction of straight line from the input of time series. The line can be linear least square fit to the time series or the mean value of time series. The mean value is determined from the mean of suitable portion of accelerogram. Basically the portion of record prior to P- wave is taken for calculating mean and in case of absence of pre event memory in the recorder, entire record can be used. In the time series of the accelerogram, it is very difficult to see the effect of linear correction and is evident on the velocity record obtained from the integration of acceleration record. It is seen that velocity record of unprocessed accelerogram clearly shows long period undulation due to abrupt change in the linear trend of velocity record as shown in Fig. 2.13. This is removed clearly in the accelerogram processed for baseline correction shown in Fig. 2.13.

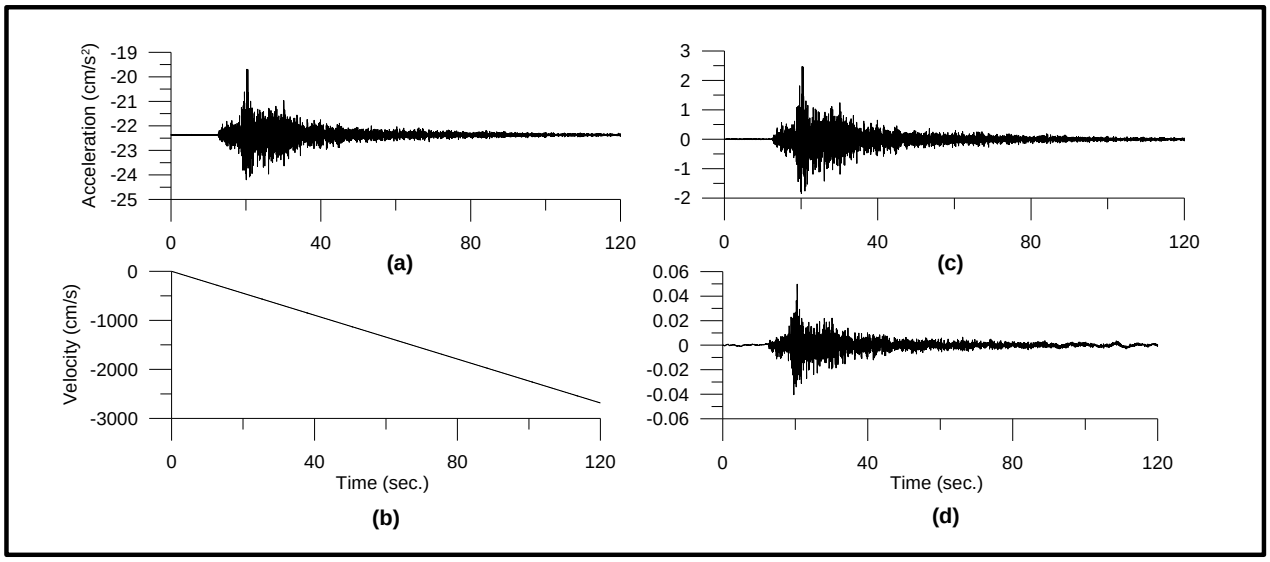

Figure 2.13 An example of (a) Digitized acceleration record without baseline correction, (b) Velocity record obtained from the integration of acceleration record, (c) Digitized acceleration record with baseline correction, (d) Velocity record obtained from the integration of acceleration record.

2.4.3 Padding: This step extends the time series in both directions by adding zeros to the leading and trailing ends of the record. This step is used before application of low cut frequency filtering. The zero pads are added symmetrically to both ends of the records in order to accommodate the filter transient. The length of zero pad 't_{pad}' at each end is calculated using following empirically determined formula:

$$T_{pad} = 1.5 * nroll / f_c \quad (2.1)$$

Where, nroll is the rolloff of the acausal low cut Butterworth filter and f_c is the low cut frequency of the filter. The effect of padding is visible in the integrated displacement record obtained from accelerogram. A long term away from zero at the end of the velocity or displacement time series indicates that there may be insufficient padding. The integrated displacement record shows that without padding there is long term away from zero at the end of displacement record and this is removed in the zero padded processed record shown in Fig. 2.14.

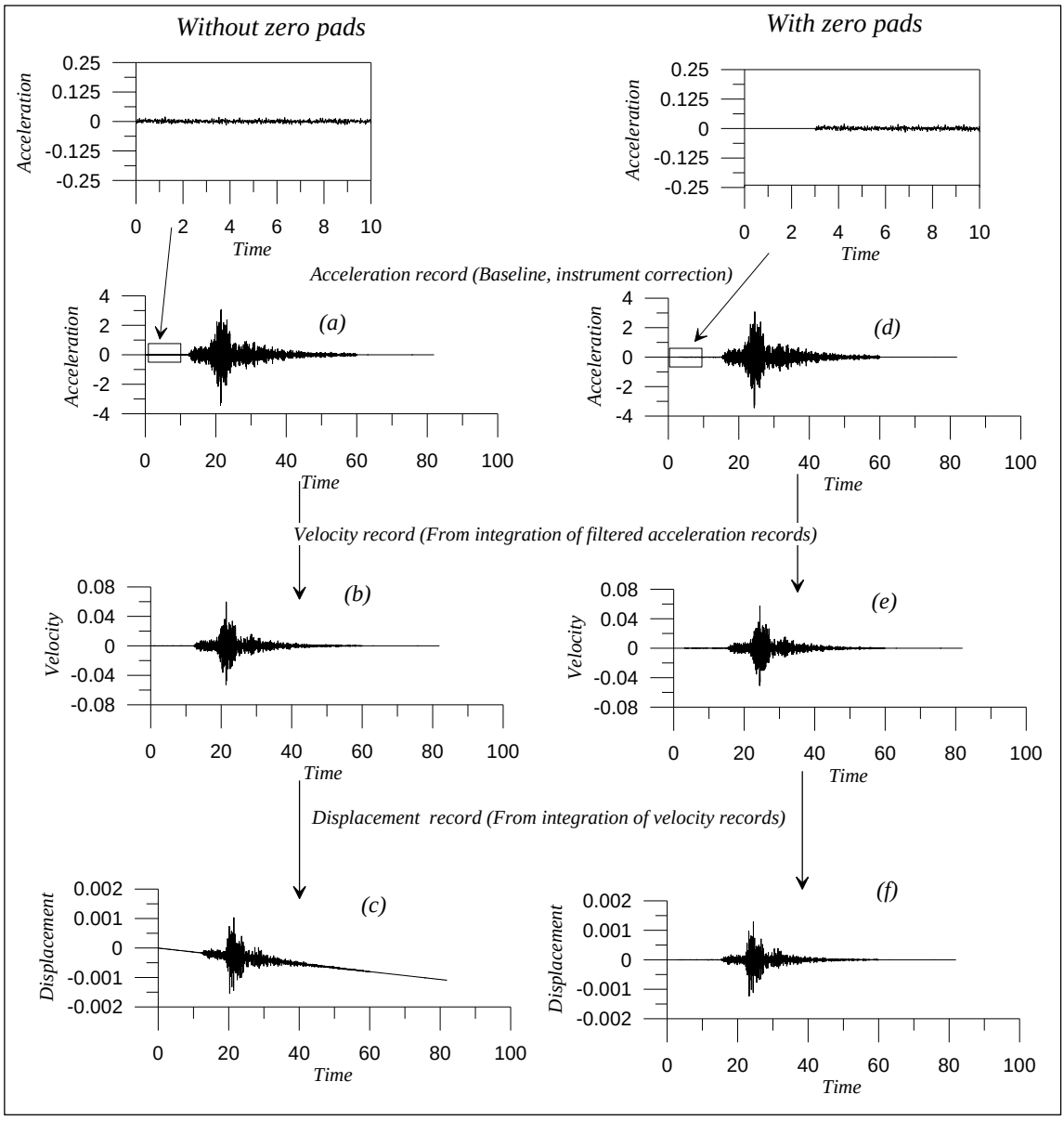

Figure 2.14 An example of (a) Acceleration record without zero pads. The portion of record marked by rectangle is shown above this plot, (b) Velocity record obtained from integration of acceleration record, and (c) Displacement record obtained from the integration of velocity record. (d) Acceleration record with zero pads. The portion of record marked by rectangle is shown above this plot (e) Velocity record obtained from integration of acceleration record, and (f) Displacement record obtained from the integration of velocity record.

2.4.4 Frequency Filtering: After baseline and instrument correction a filter is applied to remove high frequency noise. The usual processing of digital records uses Butterworth filter with a corner frequency near 80% of final sampling rate (Shakal et al. 2004). In the present work, we have used the having sampling rate of 0.01 sec, therefore high frequency corner of Butterworth filter is assumed as 40 H_z for 50 H_z nyquist frequency. Selection of low frequency cutoff of Butterworth filter remains the most difficult part of strong motion processing, because the effect of earthquake magnitude is to raise the response spectrum at low frequencies. The selection of cutoff of the Butterworth filter is based on the criteria so that the crossing with noise spectrum may not occur in the usual strong motion processing band. The selection of low frequency cutoff of the Butterworth filter is based on the characteristics of the noise and event present in the record. In this work we have selected noise from pre event memory of the digital record. The selection of low cutoff of the Butterworth filter is made in such a way that the ratio of the Fourier amplitude spectrum of record to that of noise is greater than 3 (Boore and Bommer 2005). In this work, we have used following criteria for selection of low frequency cut offs of the Butterworth filter which are based on the work done by Boore and Bommer (2005) and Shakal et al. (2004):

(i) This criteria for selection of low frequency cutoff of the Butterworth filter uses the velocity response spectrum of the record and the noise. The selection of low frequency cutoff of the Butterworth filter based on the property of logarithm of velocity response spectrum was first suggested by Trifunac (1977). The logarithm of velocity response spectrum of record increases from low values at short period until it reaches a maximum at intermediate periods, beyond which it starts decreasing. However, the logarithm of noise spectrum increases in long period ranges. The frequency at which the ratio of logarithm of response spectrum of event and noise is less than 3 is selected as low frequency corner of the Butterworth filter. This criterion is shown in Fig. 2.15(g).

(ii) This criteria for selection of low frequency cut offs of Butterworth filter uses the ratio of Fourier amplitude spectrum of record with that noise. The low frequency cut offs of Butterworth filter is taken as that frequency, where this ratio is less than 3. This criterion is shown in Fig. 2.15(h). Criteria for selection of low frequency cut-off of the Butterworth filter are shown in Fig. 2.15.

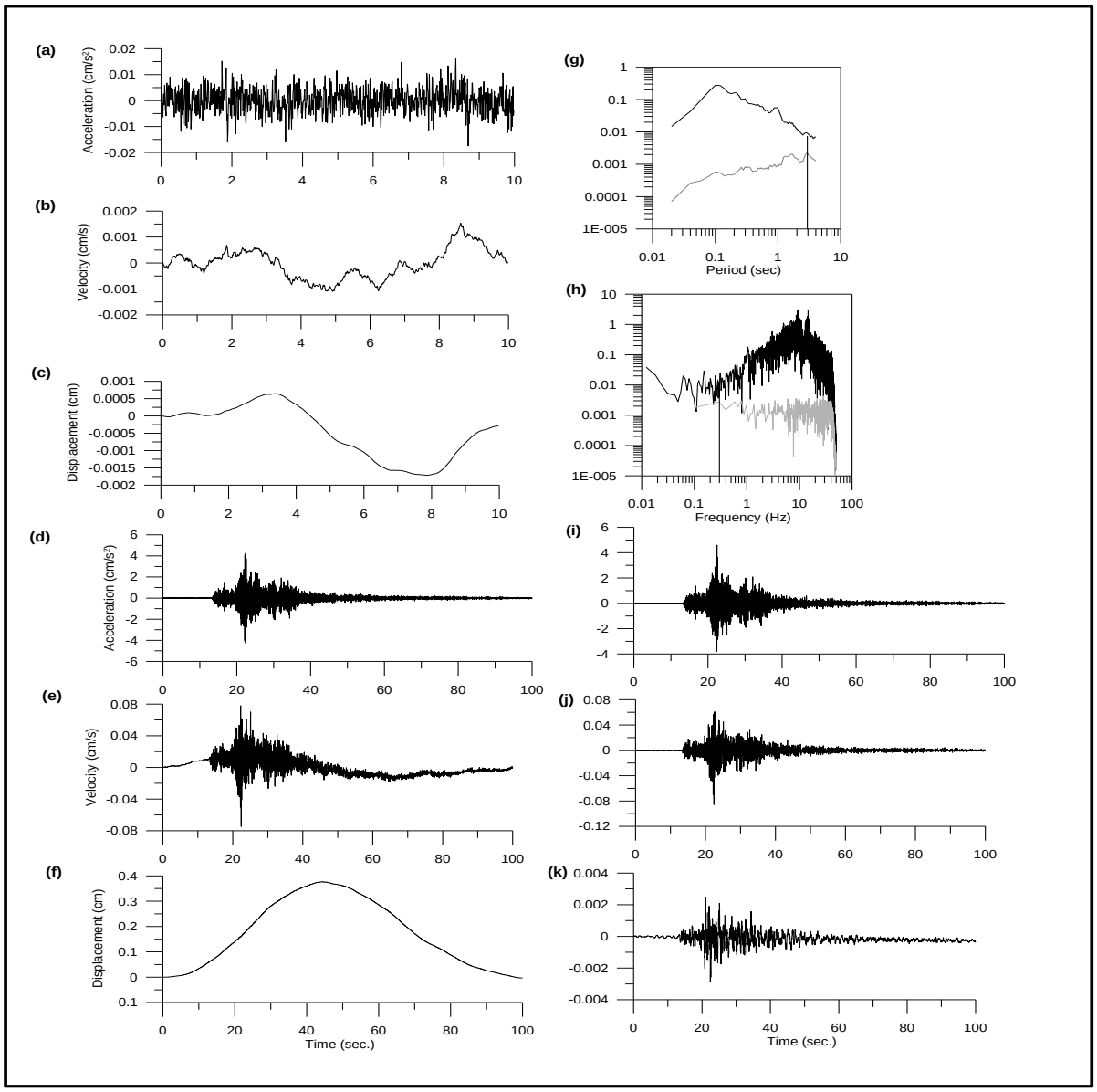

Figure 2.15 An example of (a) Acceleration, (b) velocity and (c) displacement waveform of the digitized record of noise taken from prevent memory of the record of event recorded at the Dharchula station (d) Acceleration, (e) velocity, and (f) displacement record of signal corrupted with noise. (g) The Pseudo velocity response spectra at 5% damping of noise and signal with noise. (h) Amplitude spectra of acceleration record of noise and signal corrupted with noise. (i) Acceleration, (j) velocity, and (k) displacement record of signal after filtering. The spectrum of noise is shown by grey colour while the spectrum of signal corrupted with noise is shown by black. Vertical line in the spectra denotes the lower frequency range.

2.5 Estimation of Source Parameters

Once the record is processed, the next step is the calculation of source parameter from that record for proper parameterization of event. The calculation of source spectra from acceleration record is based on the spectral property of acceleration record. The acceleration spectra of shear waves recorded at a distance R due to an earthquake of seismic moment M_o can be given as (Boore 1983; Atkinson and Boore 1998):

$$A(f) = CM_o S(f) D(f) R_s(f) \quad (2.2)$$

Where, C is a constant for a particular station; S(f) represents the source acceleration spectra; $R_s(f)$ denotes the site amplification factor and D(f) denotes a frequency-dependent diminution function which takes into account the anelastic attenuation and attenuation due to geometrical spreading and is given as (Boore and Atkinson 1987):

$$D(f) = [e^{-\pi fR/\ Q(f)\beta} G(R)] P(f, f_m) \quad (2.3)$$

In the above equation $P(f, f_m)$ is a high-cut filter that accounts for the observation that acceleration spectra often show a sharp decrease with increasing frequency, above some cutoff frequency f_m, that cannot be attributed to whole path attenuation (Boore 1983). Due to the rapid fall of acceleration spectra after 25 Hz in most of the acceleration records used in the present work, f_m is used as 25 H_z in the analytical form of $P(f, f_m)$ suggested by Boore (1983). The function G(R) represents the geometrical attenuation term and is taken to be equal to 1/R for R < 100 km and equal to $1/\left(10\sqrt{R}\right)$ for R > 100 km (Singh et al. 1999). The term $e^{-\pi fR/\ Q(f)\beta}$ represent anelastic attenuation term and in this term Q(f) is the frequency-dependent shear wave quality factor. Using equation (2.2) the source acceleration spectra $S_A(f)$ can be calculated as:

$$S_A(f) = A(f)/D(f) \quad (2.4)$$

The source displacement spectra '$S_D(f)$' can be calculated from source acceleration spectra '$S_A(f)$' by using differential property of the Fourier transform. This gives the following equation:

$$S_D(f) = S_A(f)/ (2\pi f)^2 \quad (2.5)$$

Source displacement spectra obtained from equation (2.5) gives idea about 'f_c' and 'Ω_0'. The seismic moment (M_o) which determines the source strength is calculated using long term flat level (Ω_0) and corner frequency (f_c) from the source displacement spectra. An example of obtained source displacement spectra obtained from acceleration records is shown in Fig. 2.16. The source displacement spectra '$S_D(f)$' can be theoretically computed from following expression given by Brune (1970):

$$S_D(f) = 1/(1+(f/f_c)^2) \quad (2.6)$$

In the above expression 'f_c' is corner frequency. The match of theoretical source spectra with observed source spectra gives an estimate of corner frequency 'f_c' and long term flat level Ω_0. Corner frequency and long term flat level (Ω_o) is used to calculate the variation of source parameters. Seismic moment (M_0) and long term flat level (Ω_o) are related by following relation (Brune 1970, 1971):

$$M_o = 4\pi\rho\beta^3\, \Omega_o\, R/\, FS*R_{\theta\phi}*PRTITN \quad (2.7)$$

Where, ρ and β are the density and the S-wave velocity of the medium, respectively, FS is the free surface effect, PRTITN is the reduction factor, Ω_o is the long term flat level of the source displacement spectrum at a hypocentral distance of R and $R_{\theta\phi}$ is the radiation-pattern coefficient. The value of density and shear wave velocity as 2.7 gm/cm^3 and 3.5 km/sec, respectively have been used. The radiation pattern coefficient '$R_{\theta\phi}$' was approximately taken as 0.55 for S wave (Atkinson and Boore 1995).

The other parameter representing the source is its size, which is defined by the radius of circular rupture. The corner frequency 'f_c' of the source spectra is related to the radius 'r_o' of the equivalent circular crack by the following relation. The relation between 'r_o' and the corner frequency 'f_c' is given as (Brune 1970, 1971):

$$r_o = 2.34\beta/2\pi f_c \quad (2.8)$$

Stress drop ($\Delta\sigma$) is one of the important parameters of an earthquake source and the static stress drop is the simplest measure of the overall reduction in shear stress due to slip on the fault zone. It is the difference between the average shear stress on the fault zone before and after the

earthquake (Ruff 1999). For a circular crack of radius 'r_o' the stress drop '$\Delta\sigma$' is given as (Papageorgiou and Aki 1983):

$$\Delta\sigma = 7M_o /16\ r_o^3 \qquad (2.9)$$

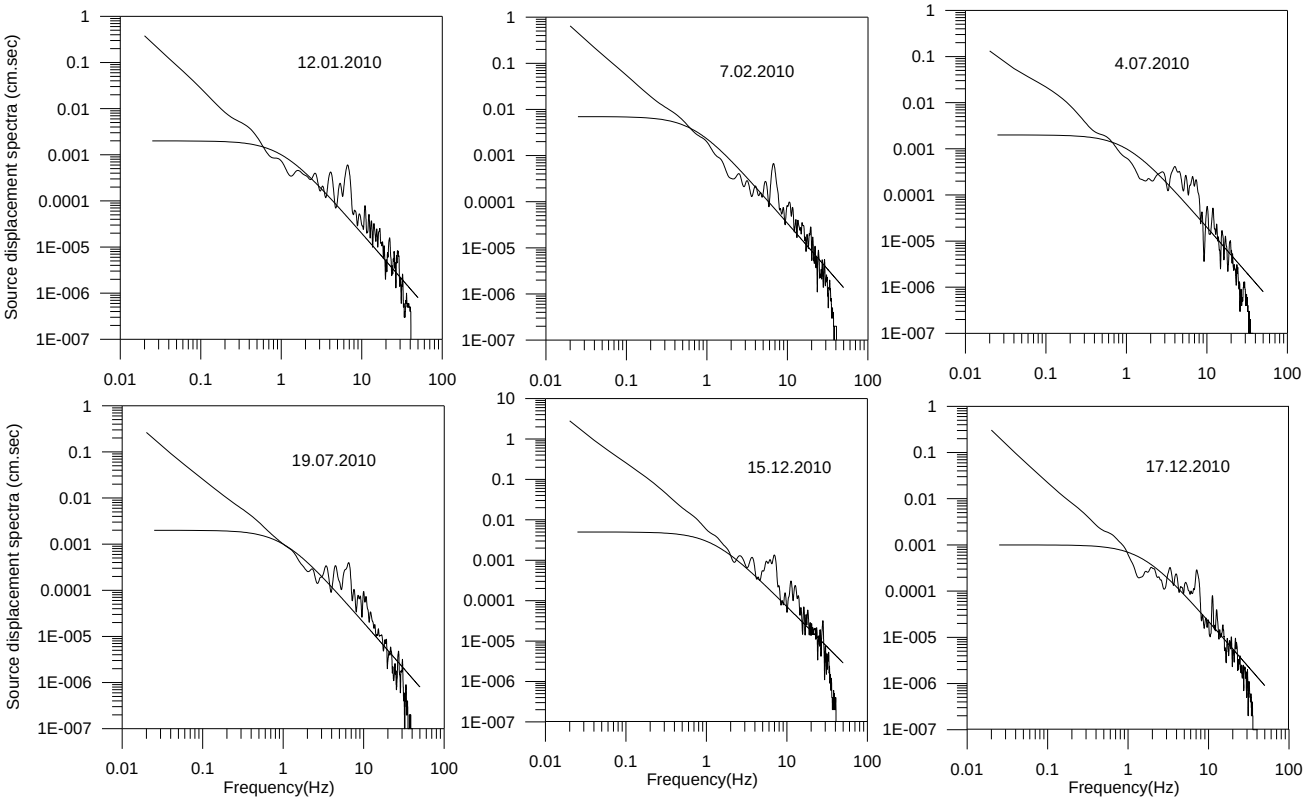

Figure 2.16 Source displacement spectra of different earthquakes recorded at the Dharchula station. Theoretical Brune's spectrum is shown by solid line.

The seismic moment of an earthquake is directly related to the moment magnitude of an earthquake. Keeping in view of the saturation of m_b, M_s and M_L magnitude scales, moment magnitude (M_w) have been determined in the present work. Following relation given by Hanks and Kanamori (1979) has been used in the present work:

$$M_w = \frac{2}{3} L\text{og}_{10}(M_o) - 10.7 \tag{2.10}$$

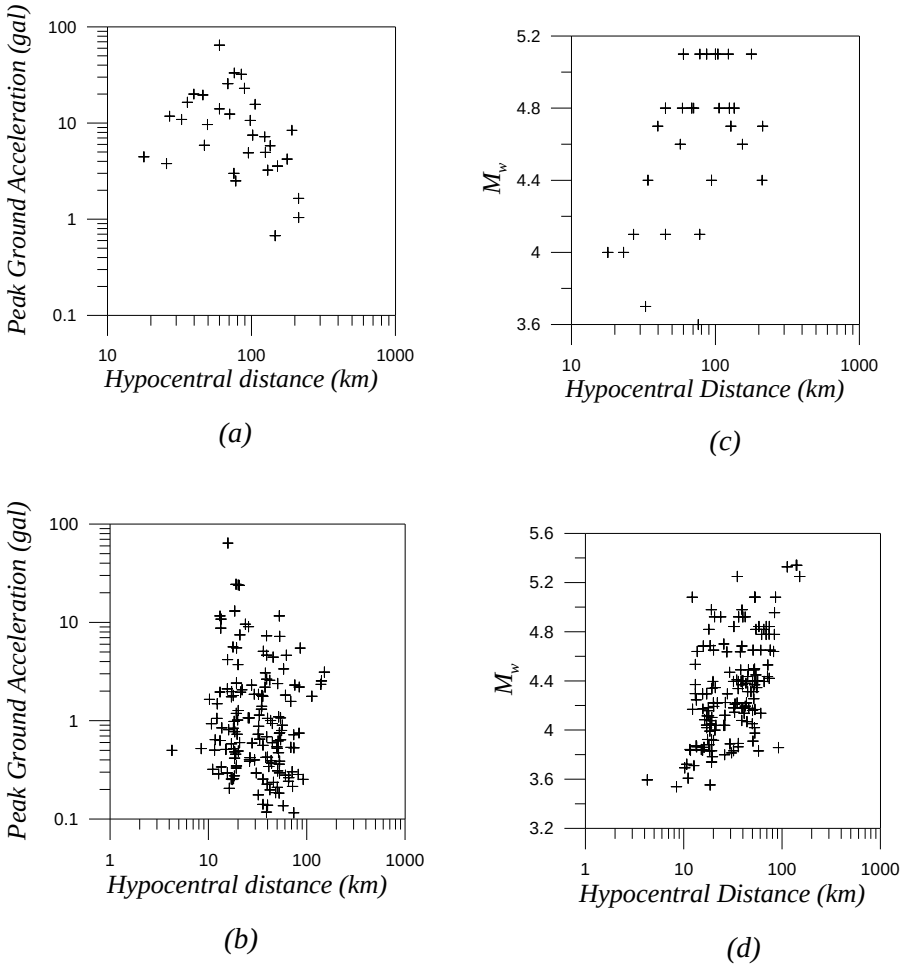

Figure 2.17 Distribution of peak ground acceleration with hypocentral distance for (a) Garhwal data (b) Kumaon data and (c) Moment magnitude with hypocentral distance of the recorded data of Garhwal array (d) Moment magnitude with hypocentral distance of the recorded data of Kumaon array.

Distribution of peak ground acceleration with hypocentral distance for the Garhwal and the Kumaon data is shown in Fig. 2.17(a) and (b), respectively. This shows that the range of hypocentral distance of the data set is between 4 to 151 km and maximum data lies in the range of 10 to 100 km. Distribution of magnitude with hypocentral distance for the Garhwal and the Kumaon Himalaya is shown in Fig. 2.17(c) and (d), respectively. This shows that data of both regions lies between the magnitude range $3.5 \leq M_w \leq 5.3$. For developing regression relation of peak ground acceleration for the Garhwal and Kumaon Himalaya, the moment magnitude and the hypocentral distance are selected as independent variables. In order to have consistency in the range of independent variable, we have used similar range of distance and magnitude, respectively for both of the regions.

2.6 Conclusion

This Chapter discusses strong motion data obtained in the Kumaon and Garhwal Himalaya, respectively. Various processing steps used to process strong motion records have been discussed in the present Chapter. The processed acceleration records are further used to obtained source parameters of earthquakes recorded by networks operating in the Garhwal and Kumaon Himalaya, respectively.

CHAPTER-3

Attenuation Relations for the Kumaon and Garhwal Himalaya

3.1 Introduction

Peak ground acceleration during an earthquake plays an important role in safe design of engineering structures. Peak ground acceleration attenuates with respect to the epicentral and hypocentral distance. This decay is explained by attenuation relation. An attenuation relation is a mathematical expression relating specific parameters of an earthquake (Campbell 2001) with the desired engineering parameters. In the present work, strong motion data has been used for developing attenuation relation using Damped least square inversion method. This Chapter discussed the methodology of regression analysis to determine the attenuation relation of the Kumaon and Garhwal Himalaya. Various statistical tests on the developed regression relation is presented in this Chapter.

3.2 Methodology of Regression Analysis

Attenuation relation is one of the major requirements for estimations of seismic hazard of an area. Attenuation relations are generally derived from regression analysis. The first step in the regression analysis is the selection of regression model. In the present work regression model has been selected on the basis of dependency of peak ground acceleration on magnitude and distance parameters. Various functional dependencies have been checked and regression model that gives the best correlation and minimum error is selected for final regression model. Most of the earthquakes in the Uttarakhand Himalaya originate at a shallow dipping plane of detachment at approximate depths of about 10-15 km. Therefore in order to include the effect of earthquake originating from the plane of detachment a term 'R^b' is introduced in the present work which is equal to (R+15), which coincide with the approximate depth of plane of detachment. Following regression model has been selected in the present work:

$$ln(PGA) = a + bf_1(R) + cf_2(M_w) + df_3(R^b) \quad (3.1)$$

Where, PGA is horizontal peak ground acceleration in gals, M_w is moment magnitude, 'R' is hypocentral distance in kilometer, R^b is distance parameter which can be hypocentral (R+15) or epicentral (E+15) distance in kilometer, E is epicentarl distance and a, *b*, *c* and *d* are regression coefficients, respectively. Following set of equations is obtained from different values of peak ground acceleration (PGA_{mk}) obtained at different stations due to earthquake of magnitude (M_m) and hypocentral distance (R_{mk}):

$$ln(PGA_{11}) = a + bf_1(R_{11}) + cf_2(M_1) + df_3(R^b{}_{11})$$
$$ln(PGA_{12}) = a + bf_1(R_{12}) + cf_2(M_1) + df_3(R^b{}_{12})$$

: : :

$$ln(PGA_{1k}) = a + bf_1(R_{1k}) + cf_2(M_1) + df_3(R^b{}_{1k})$$

: : :

$$ln(PGA_{1n}) = a + bf_1(R_{1n}) + cf_2(M_1) + df_3(R^b{}_{1n})$$

For peak ground acceleration data of m^{th} earthquake recorded at k^{th} stations following set of equations is obtained:

$$ln(PGA_{m1}) = a + bf_1(R_{m1}) + cf_2(M_m) + df_3(R^b{}_{m1})$$
$$ln(PGA_{m2}) = a + bf_1(R_{m2}) + cf_2(M_m) + df_3(R^b{}_{m2})$$

: : :

$$ln(PGA_{mk}) = a + bf_1(R_{mk}) + cf_2(M_m) + df_3(R^b{}_{mk})$$

The above set of equations can be written in matrix form as:

$$\begin{vmatrix} \ln(PGA_{11}) \\ \ln(PGA_{12}) \\ : \\ \ln(PGA_{1n}) \\ : \\ \ln(PGA_{m1}) \\ \ln(PGA_{m2}) \\ : \\ \ln(PGA_{mk}) \end{vmatrix} = \begin{vmatrix} 1 & f_1(R_{11}) & f_2(M_1) & f_3(R^b_{11}) \\ 1 & f_1(R_{12}) & f_2(M_1) & f_3(R^b_{12}) \\ & : & : & \\ 1 & f_1(R_{1n}) & f_2(M_1) & f_3(R^b_{1n}) \\ & : & : & \\ 1 & f_1(R_{m1}) & f_2(M_m) & f_3(R^b_{m1}) \\ 1 & f_1(R_{m2}) & f_2(M_m) & f_3(R^b_{m2}) \\ & : & : & \\ 1 & f_1(R_{mn}) & f_2(M_m) & f_3(R^b_{mk}) \end{vmatrix} \begin{vmatrix} \\ a \\ b \\ c \\ d \\ \\ \\ \\ \\ \end{vmatrix}$$

The above matrix equations can be further simplified as:

$$d = Gm \tag{3.2}$$

Where, ‘d’ is the column matrix having peak ground acceleration data at various stations due to different earthquakes, ‘G’ is a rectangular matrix defining the dependency of independent parameters of magnitude and hypocentral distance and ‘m’ is the model matrix having coefficient of regression analysis. The model matrix ‘m’ is obtained by following expression using least square inversion method:

$$m = (G^T G)^{-1} G^T d \tag{3.3}$$

In this expression, matrix ‘G^T’ define the transpose of matrix *G*. In actual case some of the eigen values of ‘G^TG’ are very small so that the variance of solution becomes unacceptably large (Joshi et al. 2010a). To avoid this difficulty, we used the damped least squares method given by

Levenberg (1944), which does not require eigen values analysis. The inversion using damped least square method is can be expressed as:

$$m^{est} = (G^T G + \lambda I)^{-1} G^T d \tag{3.4}$$

In above equation, matrix 'I' is the identity matrix and 'λ' is the damping factor. Addition of large damping factor stabilizes the matrix by enhancing small eigen values but at the cost of losing resolution. It is therefore essential to keep the damping factor as small as possible as one approaches final solution (Manglik and Verma 1998). The solution of above equation can be obtained by minimizing $|d\text{-}Gm| + m^T(\lambda I)m$ instead of $|d\text{-}Gm|^2$, where (λI) is a diagonal matrix with damping factors. In order to choose the value of λ we have to check various possibilities of eigen values. The criteria of selection used in the present work is that based on modification of that, given by Dimri (1992) and applied by Joshi et al. (2010a). In the present work we have checked various possibilities of damping factors starting from one tenth of the largest eigen value. In order to find smallest damping factor giving minimum root mean square error (RMSE), we have performed several iterations and in each iteration the damping factor is reduced by half of its earlier value. The power and inverse power methods have been used in the present work for calculation of largest and smallest eigen values. For numerical implementation of this scheme we have started with damping factor equal to 0.1 of the largest eigen value and reduced it further in a stepwise manner by half of its initial value for next 20 iterations. The root mean square error in each of the iteration has been computed by using following formula. Several such iterations have been performed to select damping factor corresponding to minimum root mean square (RMS) error.

$$(RMSE)_{PGA} = \sqrt{\frac{\sum_{i=1}^{N} \left\{ (P_{obi} - P_{cai}) / P_{obi} \right\}^2}{N}} \tag{3.5}$$

Where, P_{obi} is observed and P_{cai} is calculated peak ground acceleration respectively and N is the number of sample. The magnitude of an earthquake depends on logarithm of maximum ground motion. Therefore, in the present study regression model that has logarithmic dependency of peak ground acceleration on magnitude has been used. Various dependency of logarithm of peak ground acceleration on distance parameter gives various possibilities of regression models. These models

explain linear, power and logarithmic dependency of dependent variables on various independent variables like R, R^b and M_w, respectively. The obtained coefficients of the regression relation from these models are compared. The comparison of statistical parameters from all possible models which gives minimum error and maximum correlation in terms of best fit is selected as final model.

3.3 Data Used

Under a major seismicity project funded by the Department of Science and Technology, and Ministry of Earth Science, Government of India New Delhi, a network has been installed in the highly mountainous terrain of the Kumaon Himalaya by National Geophysical Research Institute, Hyderabad and Department of Earth Sciences, Indian Institute of Technology Roorkee, India. The Department of Earthquake Engineering, Indian Institute of Technology Roorkee has installed an another strong motion arrays in the Garhwal Himalaya, India under a major project funded by Department of Science and Technology, Government of India. Detail of these networks is described in Chapter 2. These arrays had recorded several earthquakes in the entire Himalayan belt.

Strong motion networks installed in the Kumaon and Garhwal Himalaya region has given opportunity to record small to major earthquakes occurred in these regions. One hundred thirty strong motion records from the Kumaon and twenty nine strong motion records from the Garhwal Himalaya have been used in the present work as input data. Consistency in the data set has been maintained by selecting data from earthquakes of similar magnitude and distance range. Since our database contains very few earthquakes having hypocentral distance less than 15 km, we have rejected that data. The maximum data is lies in the distance range between 15 to 100 kilometer, while magnitude (M_w) range is from 3.5 to 5.3, respectively.

3.4.1 Case-I: Attenuation Models for the Kumaon Himalaya

Most of the earthquakes in this part of Himalaya are originating from the basement thrust lying at an average depth of 15 km. Assuming the logarithmic dependency of magnitude scale on the amplitude of the ground motion we have assumed following four possible models for the regression analysis:

Model- I $ln(PGA) = a + b\ln R + cM_w + d\ln(R^b)$

Model- II $ln(PGA) = a + bR + cM_w + d\ln(R^b)$

(3.6)

Model -III $ln(PGA) = a + bR + cM_w + d(R^b)$

Model- IV $ln(PGA) = a + b\ln R + cM_w + d(R^b)$

These models explain linear, power and logarithmic dependency of dependent variables on various independent variables like R, M_w and R^b. Using the damped least square inversion scheme regression coefficients has been computed for each regression model. The obtained coefficients of the regression relation from these models for the Kumaon Himalaya are given in Table 3.1. The comparison of statistics from all four models indicates that model II gives minimum error and maximum correlation of observed and calculated data. The elements of the resolution and the correlation matrix for each model indicates high resolution and low error for coefficients of regression analysis for model II. The damping factor giving the minimum root mean square error (RMSE) between observed and calculated data set is 0.87. The developed attenuation relation for the Kumaon Himalaya on the basis of inversion of data and obtained values of regression coefficient is given as:

$$\ln(PGA) = -0.336 + 2.58M_W + 0.018R - 2.96\ln(R+15) \quad (3.7)$$

Where, PGA is peak ground acceleration in cm/sec^2, M_w is moment magnitude, and R is the hypocentral distance in kilometer. The comparison of actual and computed peak ground acceleration is shown in Fig. 3.1(a).The resolution matrix obtained from the inversion algorithm is shown in Fig. 3.1(b). Distribution of residual with respect to peak ground acceleration is shown in Fig. 3.1(c) which indicates that the parameter is predicted properly and are not over or under estimated. Distribution of residual with respect to magnitude and distance parameter is shown in Fig. 3.1(d) and 3.1(e), respectively and it shows that the residual is within permissible limits for selected magnitude and distance ranges.

Table 3.1 Statistics of the obtained coefficients from different regression relations for Kumaon data using hypocentral distance.

Model	Regression coefficients	Mean of observed log(PGA)	Standard deviation of observed log(PGA)	Mean of log(PGA) computed from relation	Standard deviation of log(PGA) computed from relation	Correlation coefficient	SSE (Sum of square error)	SSR (Sum of square residual)
I	a = -8.78; b = -2.3; c = 2.6, d = 1.48	-0.05	1.26	0.19	0.90	0.71	0.90	0.93
II	a = -0.336; b = .018; c = 2.58, d = -2.96	-0.05	1.26	-.045	0.91	0.72	0.87	0.90
III	a = -10.41; b = -0.029; c = 2.6, d = -0.004	-0.05	1.26	-0.48	0.89	0.69	1.03	0.98
IV	a = -5.87; b = -1.6; c = 2.5, d = 0.007	-0.05	1.26	-0.25	0.87	0.70	0.89	0.90

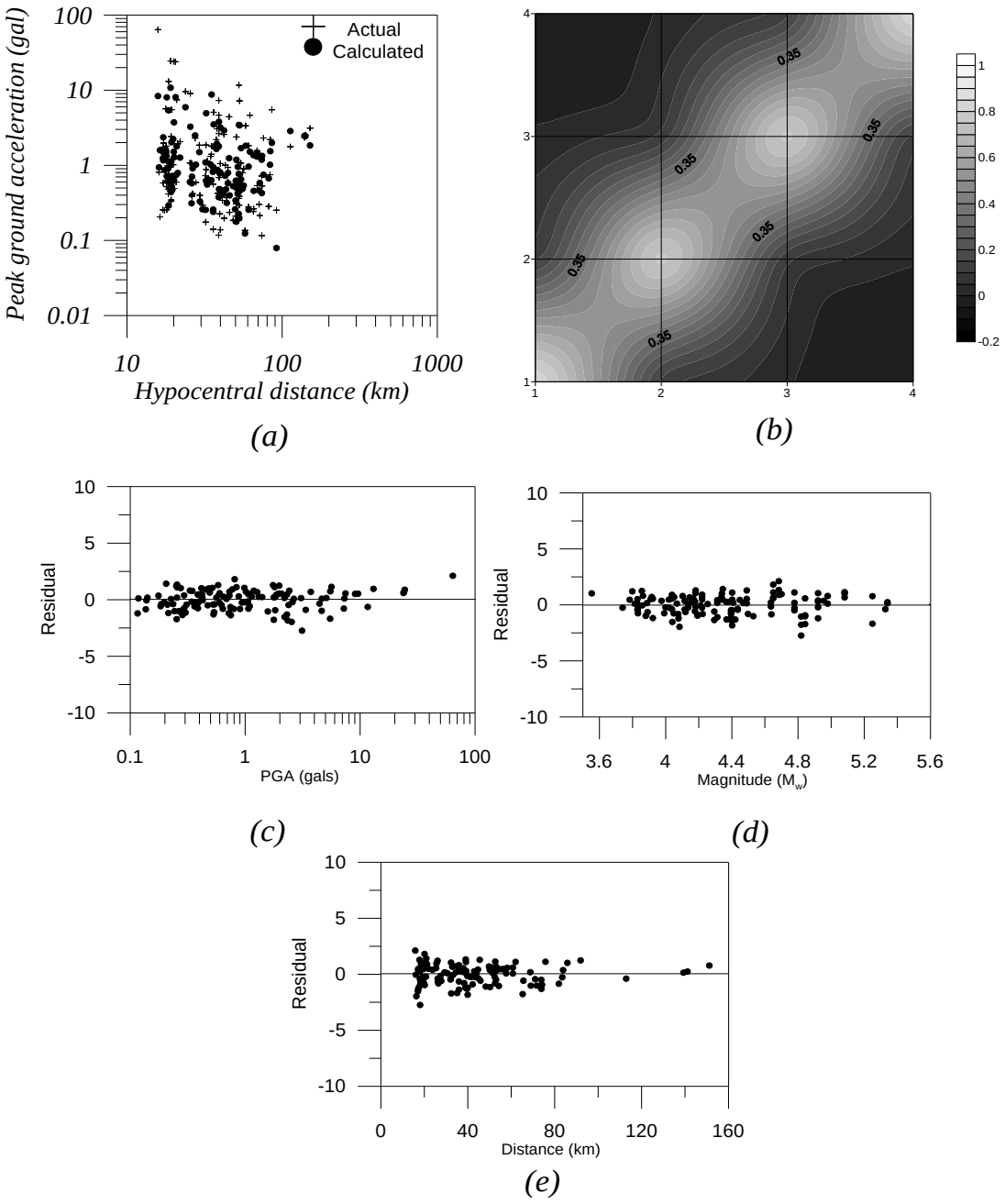

Figure 3.1 Using selected attenuation model (a) Comparison of observed peak ground acceleration with calculated one. The cross and solid circle represent observed and calculated peak ground acceleration, respectively, (b) Resolution matrix of regression coefficients (c) Distribution of residual with respect to peak ground acceleration. (d) Plot of residual versus magnitude and (e) Plot of residual versus hypocentral distance. Residual is difference of logarithm of observed peak ground acceleration with calculated.

In an attempt to check the dependency of attenuation relation on distance parameter, we have introduced term epicentral distance '(E+15)' in place of '(R+15)' in the regression models given in equation (3.6). This new parameters gives following four possible models:

$$\begin{aligned}
&\text{Model- V} && ln(PGA) = a + b\ln R + cM_w + d\ln(R') \\
&\text{Model- VI} && ln(PGA) = a + bR + cM_w + d\ln(R') \\
&\text{Model -VII} && ln(PGA) = a + bR + cM_w + d(R') \\
&\text{Model- VIII} && ln(PGA) = a + b\ln R + cM_w + d(R')
\end{aligned} \tag{3.8}$$

Where, PGA is peak ground acceleration in cm/sec^2, M_w is the moment magnitude, 'R' is the hypocentral distance and R' shows the distance parameter and is equal to (E+15). These models explain linear, power and logarithmic dependency of dependent variables on various independent variables like R, M_w and R'. Using the damped least square inversion scheme regression coefficients has been computed for each regression model. The obtained coefficients of the regression relation from these models (Model V to VIII) for the Kumaon Himalaya are given in Table 3.2. The compressions of statistics from all four models indicate that model V gives the minimum error and maximum correlation. This gives following attenuation model from similar dataset for Kumaon Himalaya:

$$\ln(PGA) = -5.8 + 2.62M_w - 0.16\ln R - 1.33\ln(E+15) \tag{3.9}$$

Where, PGA is peak ground acceleration in cm/sec^2, M_w is the moment magnitude, 'R' is the hypocentral distance and E is the epicentral distance in kilometer. Root mean square error between logarithm observed and estimated peak ground acceleration (PGA) obtained for this model is 0.87 and standard deviation is 0.42, which has less than that observed in attenuation relation given in equation (3.7). Comparison of actual and computed peak ground acceleration is shown in Fig. 3.2(a). Resolution matrix obtained from the inversion algorithm is shown in Fig. 3.2(b). Plot of resolution matrix in Fig. 3.2(b), shows that the regression coefficients are properly

resolved. Distribution of residual with respect to peak ground acceleration (PGA) is shown in Fig. 3.2(c) and indicates that the parameter is predicted properly and is not over or under estimated. Distribution of residual with respect to magnitude and distance parameter is shown in Fig. 3.2(d) and 3.2(e), respectively and it shows that the residual is within permissible limits for selected magnitude and distance ranges.

Table 3.2 Statistics of the obtained coefficients form different regression relation for Kumaon data using epicentral distance.

Model	Regression coefficients	Mean of observed log(PGA)	Standard deviation of observed log(PGA)	Mean of log(PGA) computed from relation	Standard deviation of log(PGA) computed from relation	Correlation coefficient	SSE (Sum of square error)	SSR (Sum of square residual)
V	a = -5.8; b = -0.16; c = 2.62, d = -1.33	-0.05	1.26	-0.04	0.91	0.72	0.87	0.90
VI	a = -4.6; b = 0.006; c = 2.57, d = -1.8	-0.05	1.26	-0.03	0.91	0.72	0.87	0.90
VII	a = -9.48; b = 0.069; c = 2.55, d =-0.089	-0.05	1.26	-0.09	0.88	0.70	0.89	0.88
VIII	a = -6.21; b = -1.52; c = 2.61, d = 0.004	-0.05	1.26	-0.05	0.90	0.71	0.87	0.90

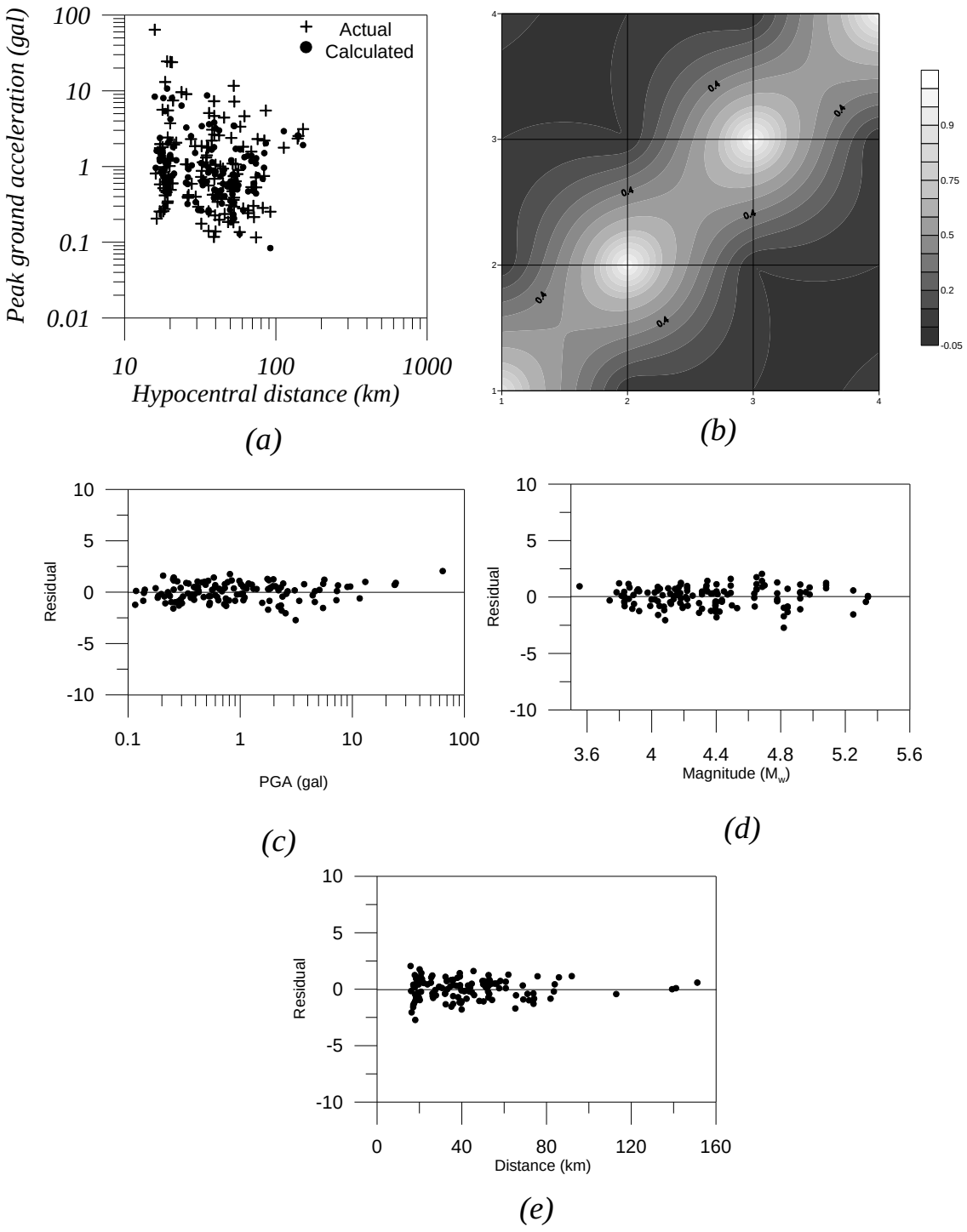

Figure 3.2 An attenuation relation using epicentral distance (a) comparison of observed peak ground acceleration with calculated one. (b) Resolution matrix of regression coefficients (c) Distribution of residual with respect to peak ground acceleration. (d) Plot of residual versus magnitude and (e) Plot of residual versus distance. Residual is difference of logarithm of observed peak ground acceleration with calculated.

3.4.2 Case-II: Attenuation Relations for the Garhwal Himalaya

In the present work regression relation for the Garhwal Himalaya is developed using strong motion data recorded by network operating in the Garhwal Himalaya. This data set consists of limited event due to high threshold of recording. This data set consists of peak ground acceleration from 29 records of horizontal component. Four different regression model given in equation (3.6) has been selected for regression analysis. Damped least square algorithm has been used for obtain coefficients of regression analysis. The obtained regression coefficients for all four models (Model I to IV in equation 3.6) are given in Table 3.3. This indicates high resolution and low error for coefficients of regression analysis for model I. Model I also gives minimum root mean square error. The diagonal elements of resolution and correlation matrix indicate that model II is also giving minimum error however resolution matrix corresponding to this model is very poor. Therefore model I has been retained for defining attenuation relation for the Garhwal Himalaya. The attenuation relation for this model is given as:

$$\ln(PGA) = 2.29 + 2.07M_w + 1.95\ln R - 4.03\ln(R+15) \tag{3.10}$$

Where, PGA is peak ground acceleration in gals observed in the horizontal component, M_w is moment magnitude, and R is hypocentral distance in km. The damping factor corresponding minimum root mean square error is 0.017 and the root mean square error (RMSE) between observed and calculated data set is 0.46. The comparison of actual and computed peak ground acceleration is shown in Fig. 3.3(a). The resolution matrix obtained from inversion algorithm is shown in Fig. 3.3(b) and shows that the regression coefficients have been properly resolved. Distribution of residual with respect to peak ground acceleration (PGA) is shown in Fig. 3.3(c). This indicates that the data is predicted properly and is not over or under estimated. Distribution of residual with respect to magnitude and distance parameter is shown in Fig. 3.3(d) and 3.3(e), respectively and it shows that the residual are within permissible limits for selected magnitude and distance ranges.

Table 3.3 Comparisons of statistics for obtained values from different models using hypocentral distance for the Garhwal Himalaya region.

Model	Regression coefficients	Mean of Observed (PGA) data	Standard deviation of observed (PGA) data	Mean PGA data computed from relation	Standard deviation of PGA data computed from relation	Correlation coefficient	SSE (Sum of square error)	SSR (Sum of square residual)
I	a = 2.29; c = 2.07; b = 1.95; d = -4.03	2.03	1.04	2.0	0.91	0.88	0.46	0.89
II	a = -4.17; c = 1.96; b = -0.012; d = -0.38	2.03	1.04	2.06	0.91	0.88	0.47	0.90
III	a = -0.03; c = 1.63; b = 0.25; d = -0.27	2.03	1.04	1.64	1.0	0.84	0.67	1.08
IV	a = -4.61; c = 1.92; b = -0.18; d = 0.013	2.03	1.04	2.1	0.89	0.87	0.48	0.88

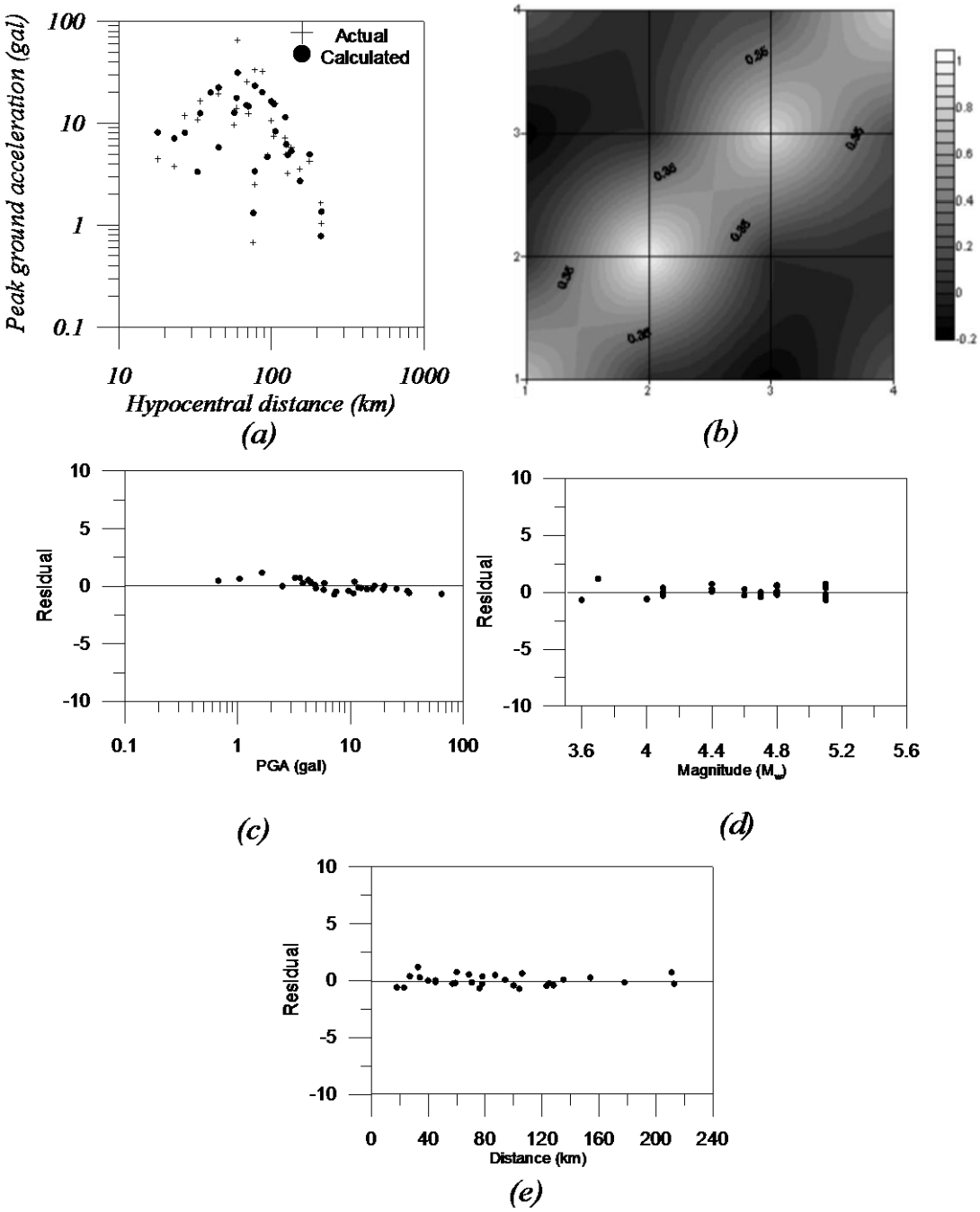

Figure 3.3 For selected regression model using hypocentral distance (a) Comparison of observed peak ground acceleration with calculated one. The cross and solid circle represent observed and calculated peak ground acceleration, respectively, (b) Resolution matrix of regression coefficients (c) Distribution of residual with respect to peak ground acceleration. (d) Plot of residual versus magnitude and (e) Plot of residual versus hypocenter distance. Residual is difference of logarithm of observed peak ground acceleration with calculated.

Dependency of regression model on different distance parameters have been also checked for the Garhwal Himalaya. The obtained coefficients from these models (Model V to VII in equation 3.8) are given in Table 3.4. Comparison of correlation coefficient, sum of square error (SSE), sum of square residual (SSR) and other statistical parameters of used and calculated dataset indicate that model VI gives high correlation coefficient and low error as compared to other models. This regression model is given as:

$$\ln(PGA) = -4.8 + 1.92M_w - 0.014R - 0.17\ln(E + 15) \tag{3.11}$$

Where, PGA is peak ground acceleration, M_w moment magnitude, R is hypocentaral distance and E is epicentral distance in kilometer. Comparison of actual and computed peak ground acceleration is shown in Fig. 3.4(a) and it shows that the regression model is capable of predicting the dataset. The resolution matrix obtained from the inversion algorithm is shown in Fig. 3.4(b). Distribution of residual with respect to peak ground acceleration (PGA) is shown in Fig. 3.4(c) and it indicate that the parameter is predicted properly and is not over or under estimated. Distribution of residual with respect to magnitude and distance parameter is shown in Fig. 3.4(d) and 3.4(e), respectively and it shows that the residual are within permissible limits for selected magnitude and distance ranges.

Table 3.4 Comparisons of statistics for obtained values from different regression models using epicentral distance for the Garhwal region.

Model	Regression coefficients	Mean of observed PGA data	Standard deviation of observed PGA data	Mean PGA data computed from relation	Standard deviation of PGA data computed from relation	Correlation coefficient	Sum of square error	Sum of square residual
V	a = -0.54;c = 2.09; b = 0.34; d = -1.9	2.03	1.04	2.03	0.89	0.86	0.52	0.88
VI	a = -4.8; c = 1.92; b=-.014;d= -0.17	2.03	1.04	2.03	0.92	0.88	0.47	0.90
VII	a = -5.2; c = 1.89; b = -.013;d= -.001	2.03	1.04	2.24	0.87	0.86	0.52	0.88
VIII	a = -4.8; c = 1.91; b= -0.12; d= -.014	2.03	1.04	2.05	0.92	0.88	0.47	0.90

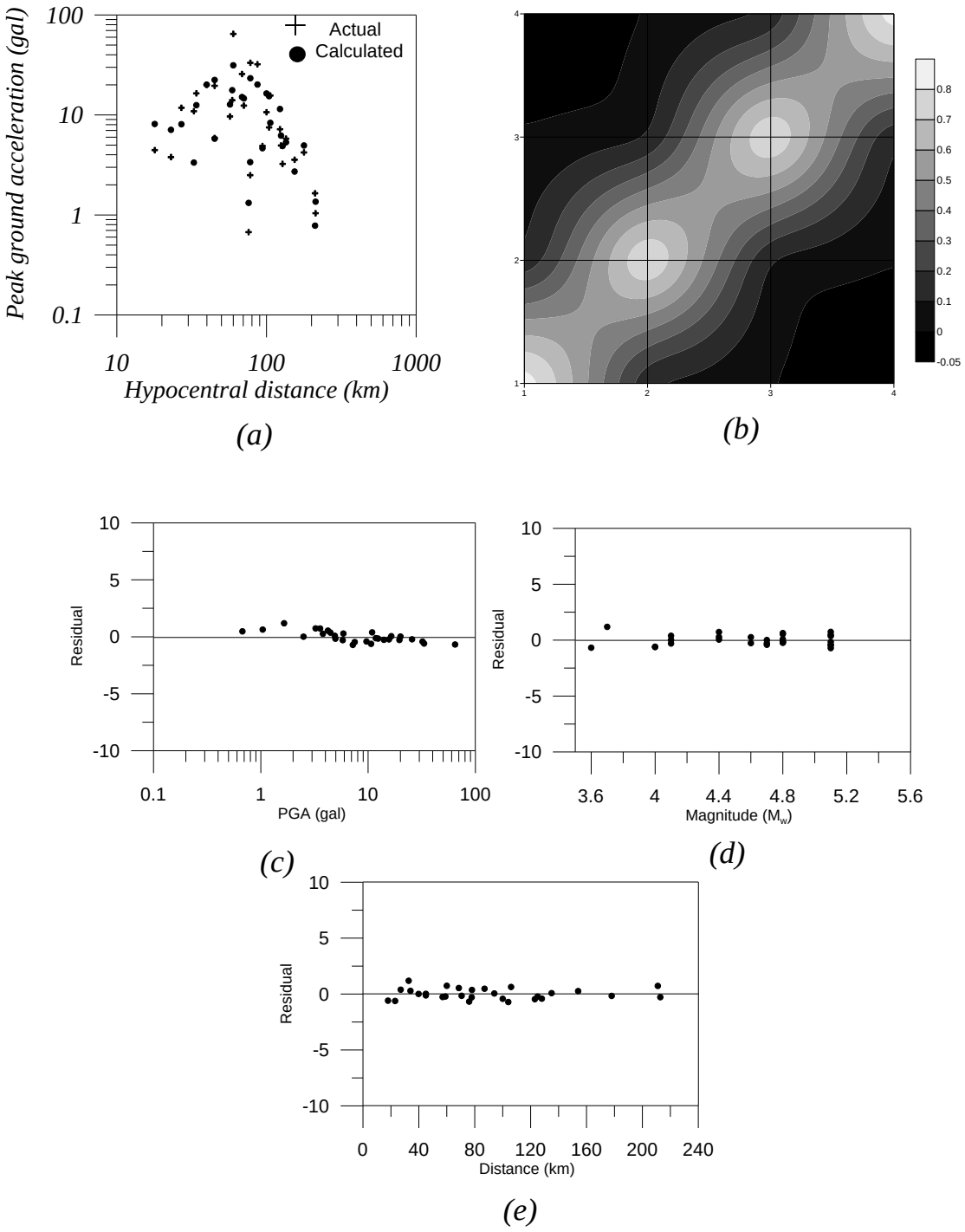

Figure 3.4 Attenuation relation using epicentral distance (a) comparison of observed peak ground acceleration with calculated one. (b) Resolution matrix of regression coefficients (c) Distribution of residual with respect to peak ground acceleration. (d) Plot of residual versus magnitude and (e) Plot of residual versus distance. Residual is difference of logarithm of observed peak ground acceleration with calculated.

3.5 Numerical Experiment

Attenuation relation is major input for estimation of seismic hazard using probabilistic seismic hazard assessment (PSHA) technique. It is seen that the computation of seismic hazard depends on the distribution of random variable called as residual from the attenuation relation. The random residual is defined as difference of logarithm of actual and predicted values. The random residual is usually assumed to be log normally distributed (Campbell 1981). A posteriori empirical justification in support of a lognormal distribution for random residual comes from statistical tests on the observed scatter about the predicted value of peak ground acceleration (Esteva 1970; Donovan 1973; McGuire 1977, 1978; Campbell 1981). It is assumed that random residuals behave normally for all computations related to the ground motion variability. Deviation of this random residual with respect to normality is one of the main causes of presence of fat tail in the distribution function, which may effect in the computation of the seismic hazard of the region. A simple method of checking nonlinearity assumption is to construct a plot of cumulative probability with respect to residuals plotted in an increasing order. Figure 3.5 shows the example of nonlinearity assumption. This graph is a straight line for normal distribution as shown in Fig. 3.5(a). A sharp upward and downward curve at both ends in Fig. 3.5(b) indicates that the tail of this distribution is too heavy to be considered as normal distribution. Flattening at the extreme end is shown in Fig. 3.5(c), which is a typical pattern from a distribution with thinner tail. The patterns associated with positive and negative skew are shown in Fig. 3.5(d) and 3.5(e), respectively. Small departures from normality assumption do not affect the model greatly, but gross nonlinearity is potentially more serious. If the errors come from a distribution with thicker or heavier tails than the normal, the least square fit may be sensitive to a small subset of data. Heavy tail distribution often generates outliers that pull the least square fit too much in their direction. The random residual also plays an important role in deciding several types of model inadequacies. The model inadequacies in the attenuation relation are checked by plotting random variable versus predicted parameter. If the plot of random residuals versus predicted parameter shows the data points within a horizontal band then there are no obvious model defect. An example of the model inadequacies in the plots by with deviation are shown in Fig.3.5.

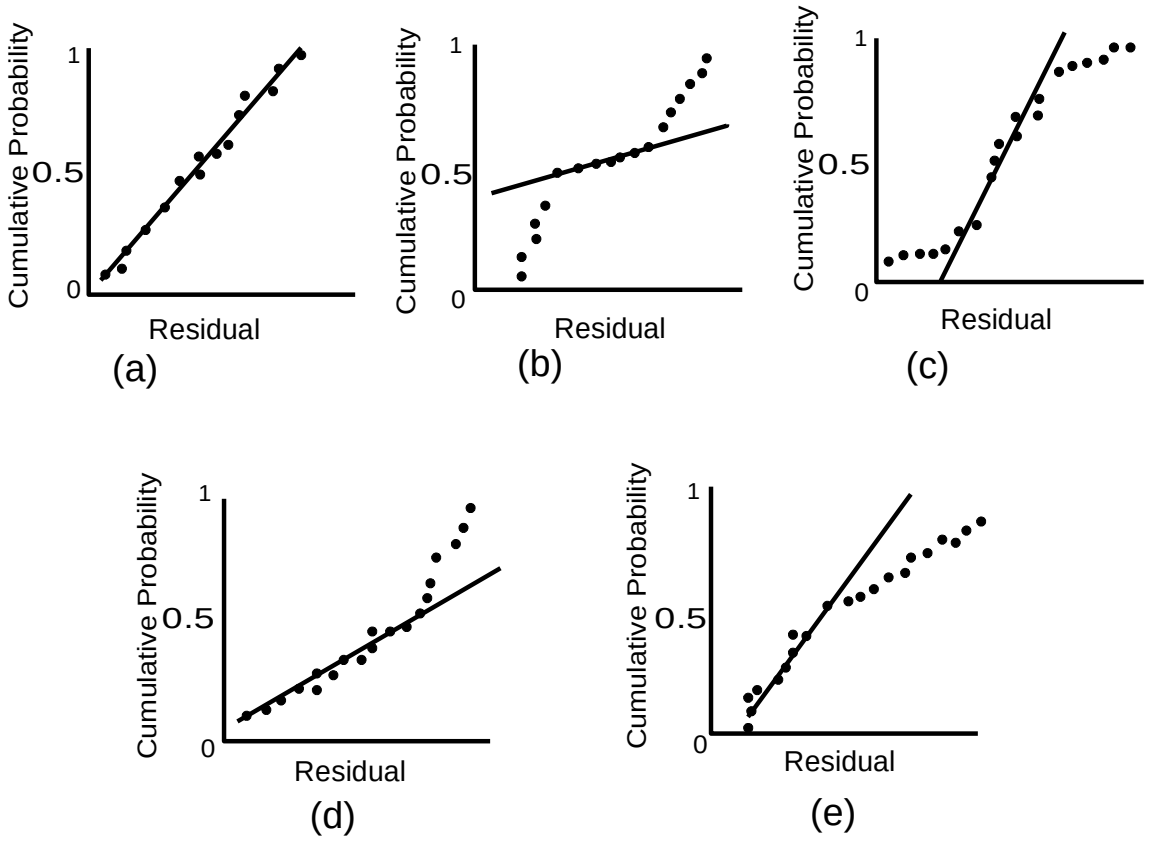

Figure 3.5 Normal probability plots (a) ideal; (b) heavy-tailed distribution; (c) light-tailed distribution; (d) positive skew; (e) negative skew. (Modified after Montgomery et al. 2003)

A very simple method for checking the normality assumption in attenuation relation is to construct a cumulative probability plot of the residuals. First step in this process is calculation of random residuals. The random residuals are arranged in an increasing order and are plotted against cumulative probability in order to make cumulative probability plot. The ideal normal probability plot of random residual follows a straight line. Substantial departures from a straight line indicate that the distribution is not normal. The model inadequacies in the ground motion prediction equation (GMPE) are checked by the plot of random residual versus observed value. In the present work model adequacies present in the developed ground motion prediction equation (GMPE) are checked by plotting random residuals versus observed peak ground acceleration values. It is seen that as long as the plot of random residuals versus observed values follows horizontal band there are no model inadequacies. Strong deviations of random residuals from this band and strange patterns often resulted due to the model inadequacies (Montgomery et al. 2003).

Various studies done by Joshi and Patel (1997), Joshi et al. (2001), Joshi (1997, 1998, 2001), Kumar et al. (1999) regarding modeling of strong motion data for the Himalayan earthquakes shows that the attenuation relation of Abrahamson and Litehiser (1989) is suitable to predict peak ground acceleration parameters in this region. The GMPE given by Abrahamson and Litehiser (1989) has been tested for normality and model inadequacies in the present work. This relation which is hereby referred in the text as AL89 and is given as:

$$Log_{10}\, a(g) = -0.62 + 0.177M - 0.982\log_{10}(R + e0.284M) + 0.132F - 0.0008ER \qquad (3.12)$$

In this expression, M is the magnitude of the earthquake represented by an element, R is the distance in km to the closest approach of the zone of energy release and a(g) is the horizontal peak ground acceleration. The variable E is a dummy variable and is 1 for interplate events and zero for intraplate events. The dummy variable F is 1 for reverse or reverses oblique events and zero otherwise. The observed and predicted value of peak ground acceleration using AL89 relationship is shown in Fig. 3.6(a). The plot of normality and model inadequacies is shown in Fig. 3.6(b) and 3.6(c), respectively. The relation between predicted value of the peak ground acceleration used in the dataset and observed value obtained from this relation is shown in Fig. 3.6(a). The linear trends of plot in Fig. 3.6(a) denote that GMPE is capable of predicting the data which has been used for its generation. The plot of random residual versus cumulative probability in Fig. 3.6(b) shows

presence of weak tail in the cumulative probability plot. The horizontal band of residual in all range of actual data defend that the model is adequate to predict peak ground acceleration values.

The attenuation relation developed by Joyner and Boore (1981) has been used for preparing seismic hazard map of India and adjoining region by Bhatia et al. (1999) under Global Seismic Hazard Assessment Program (GSHAP). The ground motion prediction equation (GMPE) given by Joyner and Boore (1981) is tested normality and model inadequacies in the present work. The GMPE given by Joyner and Boore (1981) is hereby referred as JB81 in the text and is given as:

$$Log\,a(g) = -1.02 + 0.249M - \log r - 0.00255r \tag{3.13}$$

$$r = (d_2 + h_2)^{1/2}, h = 7.3$$

In this expression, 'r' is the hypocentral distance, 'M' is the magnitude of earthquake and a(g) is peak ground acceleration in g. This relation is restricted to the data of Western North American shallow earthquakes with depth less than 20 km and magnitude more than 5.0 and includes 183 records. Estimated and observed peak ground acceleration values using JB81 relationship is shown in Fig. 3.7(a). Plot of cumulative probability function versus random residual is shown in Fig. 3.7(b) and residual versus peak ground acceleration plot are shown in Fig.3.7(c).

In the present work ground motion prediction equations have been developed from database of networks installed in the Uttarakhand Himalayan region. The developed ground motion prediction equations (GMPEs) have been used to check the assumption of normality and model inadequacies. Figure 3.8 and Fig. 3.9 shows the test of normality and model inadequacies of GMPEs given in equation (3.7) and (3.9), respectively. The cumulative probability plot of random variable also falls in straight line indicating it to be following normality assumption. However some weak tails are also evident at the extreme ends.

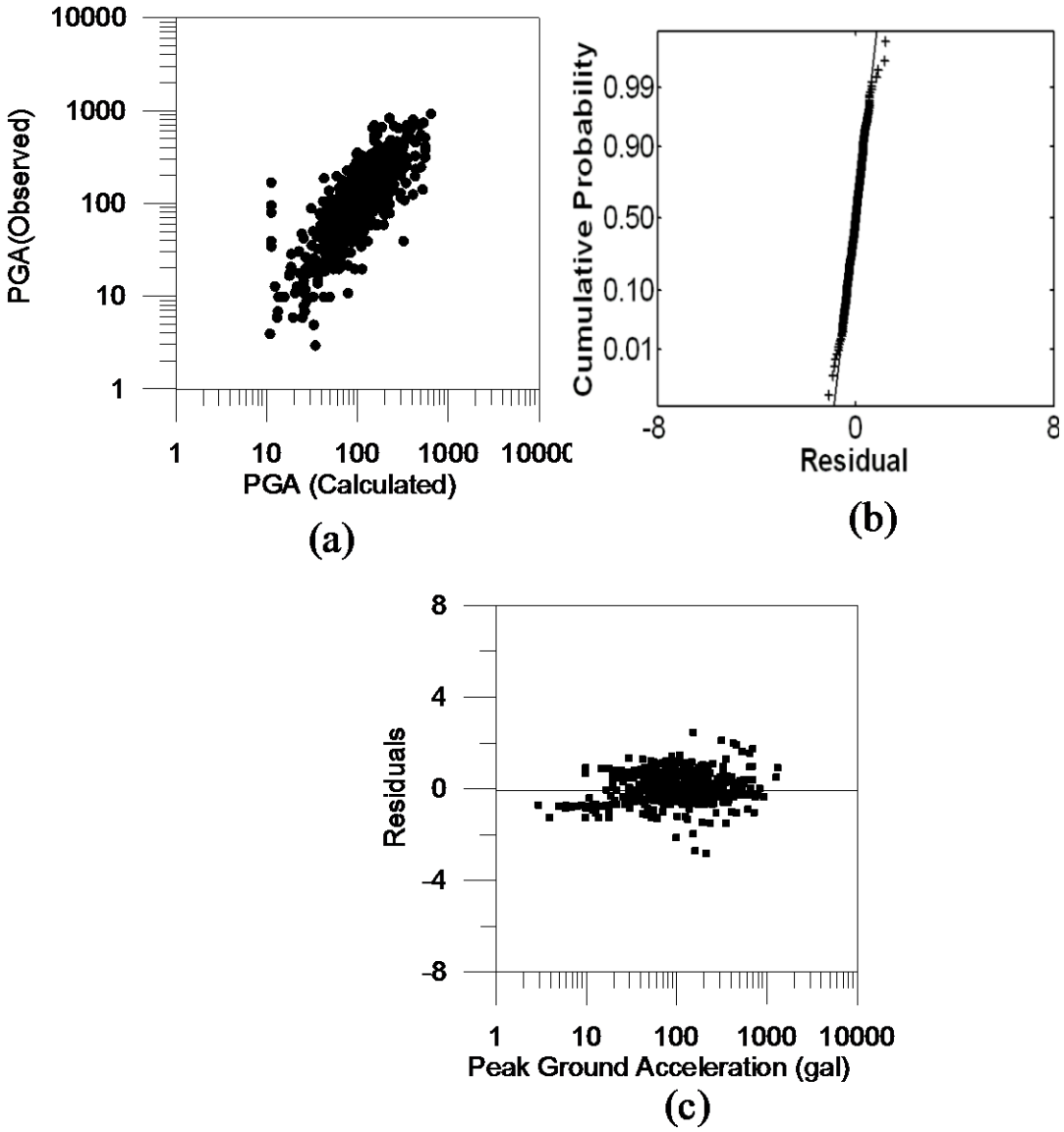

Figure 3.6 (a) Comparison of peak ground acceleration obtained from GMPE of Abrahamson and Litehiser (1989) with the data used in developing this GMPE, (b) its cumulative probability function plot with respect to random residual of estimation, (c) random residual plot with respect to peak ground acceleration parameter.

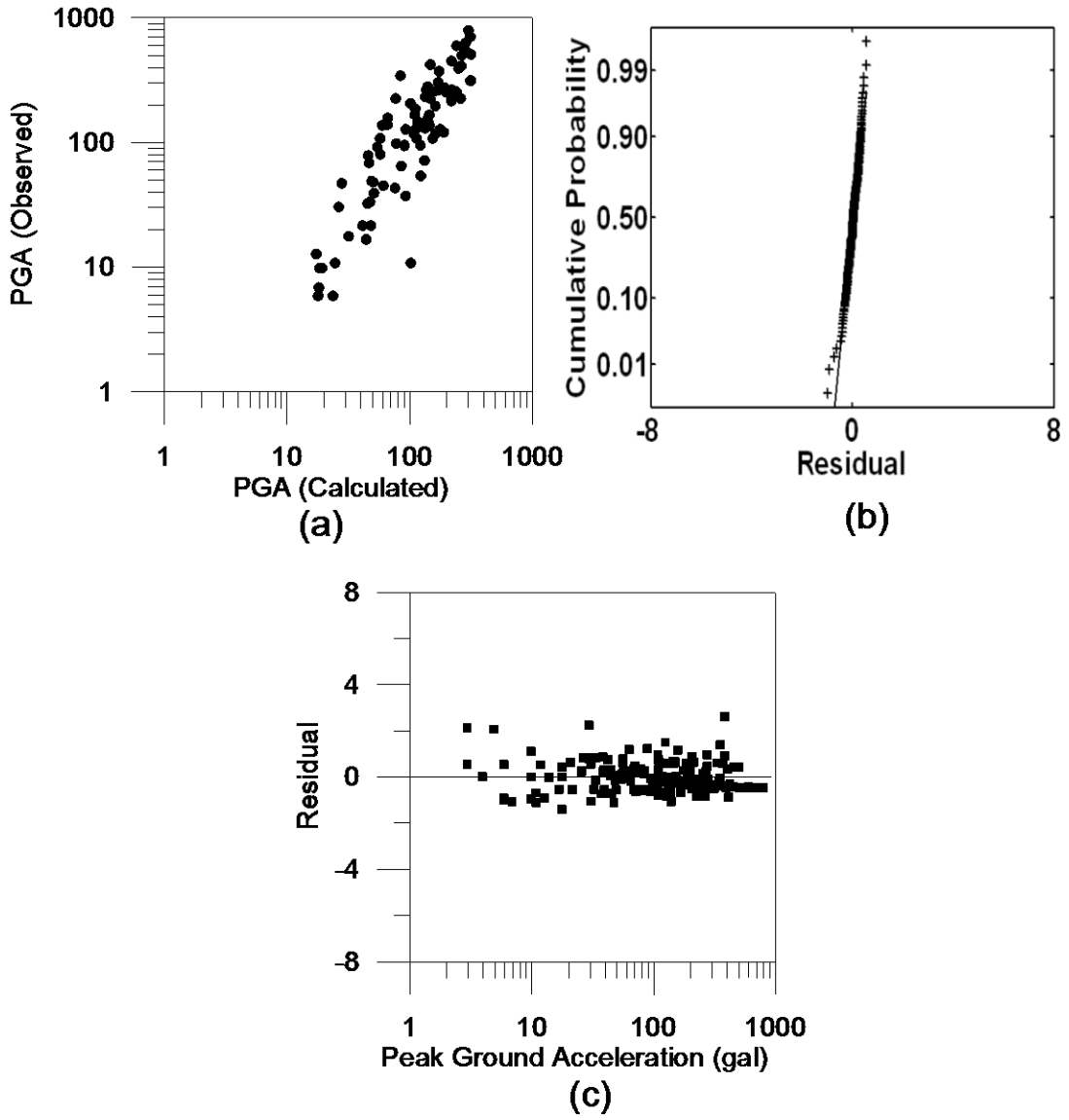

Figure 3.7 (a) Comparison of peak ground acceleration obtained from regression relation of JB81 with the data used in developing this GMPE, (b) its cumulative probability function plot with respect to random residual of estimation, (c) random residual plot with respect to PGA parameter.

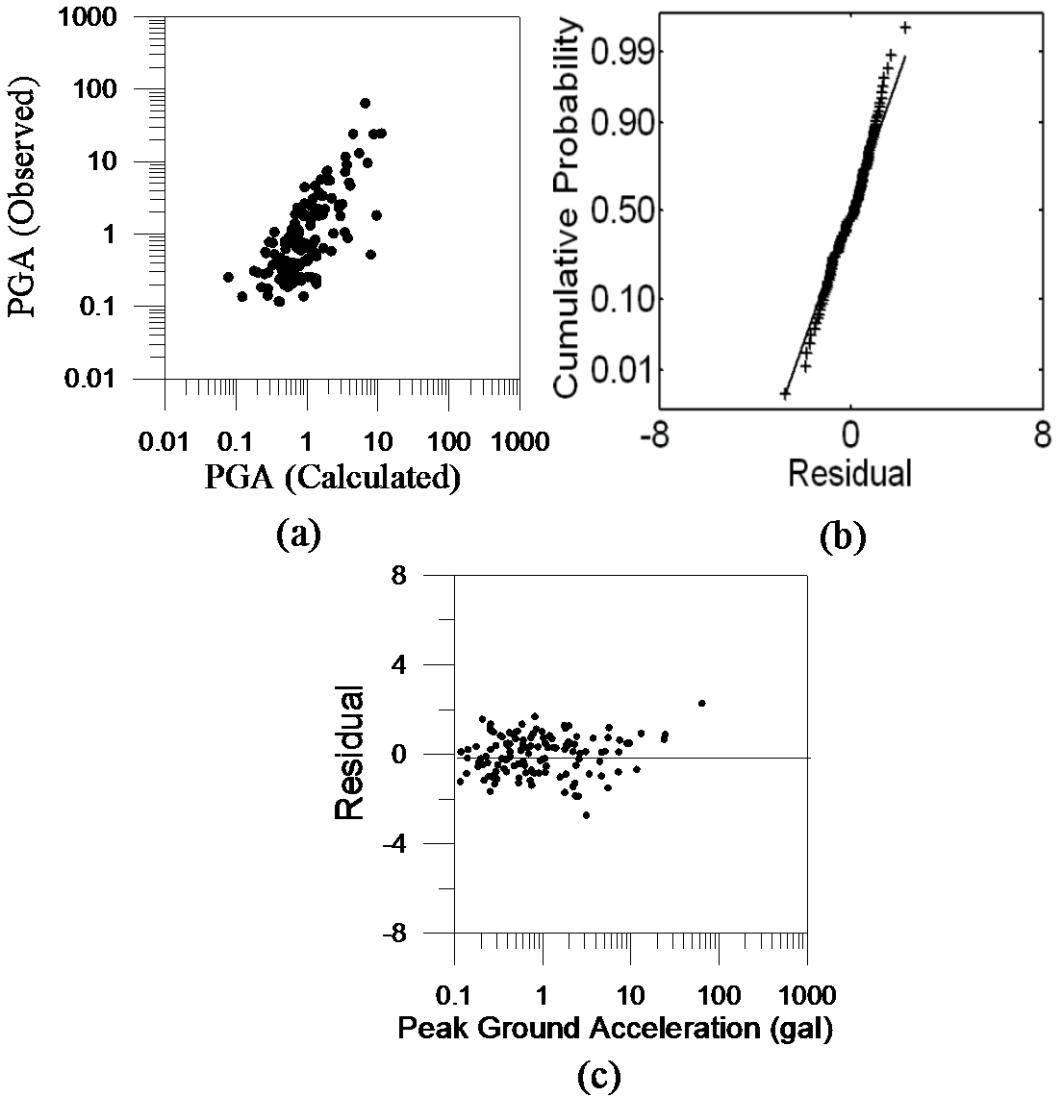

Figure 3.8 (a) Comparison of PGA obtained from regression model (equation 3.7) with the data used in developing this GMPE, (b) its cumulative probability function plot with respect to random residual of estimation, (c) its random residual plot with respect to PGA parameter.

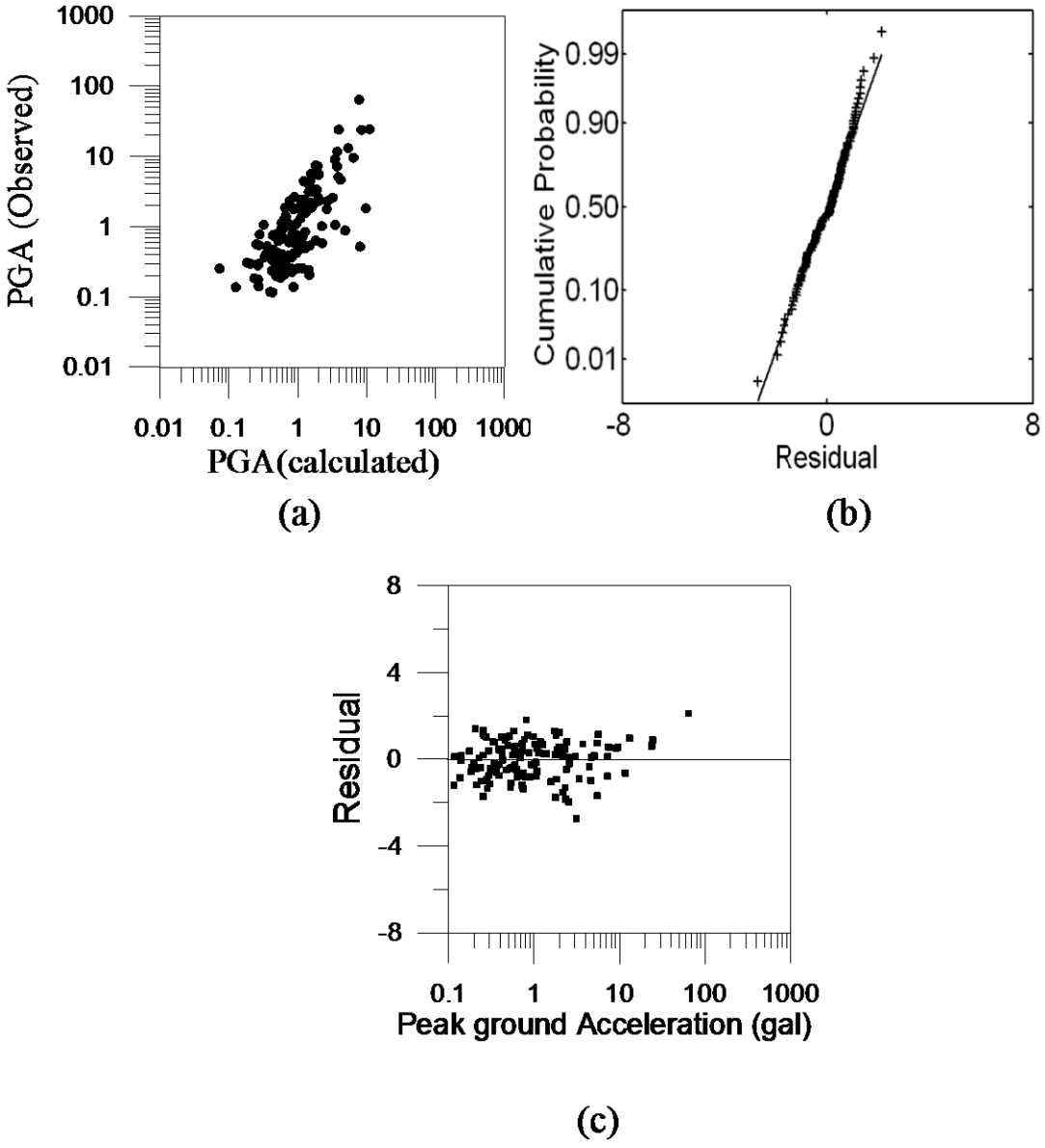

Figure 3.9 (a) Comparison of PGA obtained from regression model (equation 3.9) with the data used in developing this GMPE using epicenteral distance as one of the distance dependent parameter, (b) its cumulative probability function plot with respect to residual of estimation, (c) its residual plot with respect to peak ground acceleration

The test on normality and model inadequacies on various ground motion prediction equations shows that GMPE behave almost similar to its dataset which is used for its prediction. However in actual practice attenuation relation is used to predict values in the region that have limited or no strong motion data. This situation is same as using ground motion prediction equation to create data set other than that used in development of GMPE. In order to check the effect of normality for predicting data set other than that used for developing GMPE, a test is performed on the data set of Abrahamson and Litehiser (1989) using GMPE given by Joyner and Boore (1981) and that of Joyner and Boore (1981) using GMPE given by Abrahamson and Litehiser (1989). Clear deviation from normality is observed in this test which is shown in Fig. 3.10. These cumulative probability plots show that the mean is a negative value which means there is problem of underestimation. The problem of underestimation can also be due to the difference in the variable used in two ground motion prediction equation models. It is seen that the deviation from cumulative probability plot on predicting the data of Abrahamson and Litehiser (1989) by Joyner and Boore (1981) is less because of the large amount of data used by Abrahamson and Litehiser (1989) as compared to Joyner and Boore (1981).

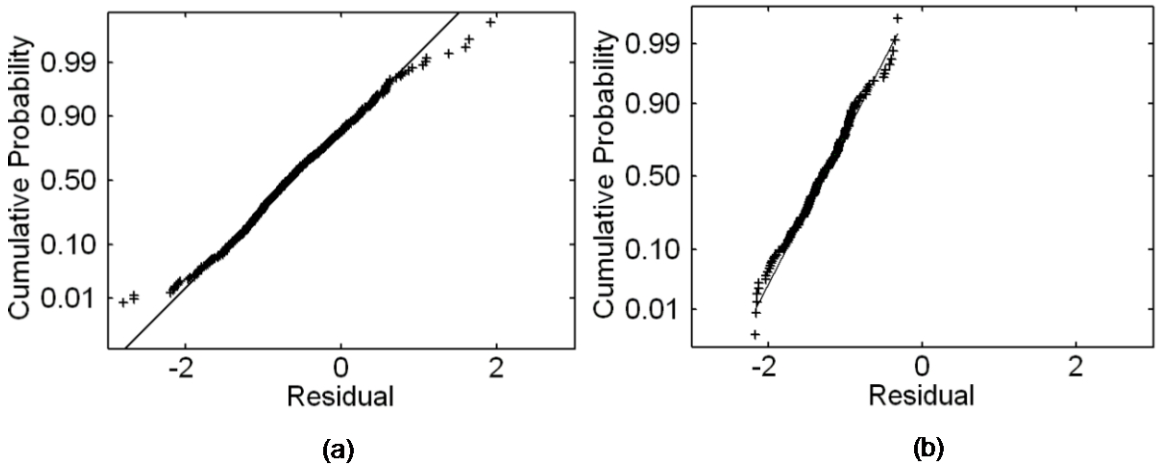

Figure 3.10 Cumulative probability plots of random residual produced by using (a) GMPE defined by Joyner and Boore (1981) for predicting data used in Abrahamson and Litehiser (1989) (b) GMPE given by Abrahamson and Litehiser (1989) for predicting data used in Joyner and Boore (1981).

The effect on the assumption of normality and model inadequacies in the ground motion prediction equation (GMPE) used for predicting regional Himalayan data from Kumaon Himalaya is numerically tested in the present work. In this test ground motion prediction equation of Abrahamson and Litehiser (1989), Joyner and Boore (1981) are included because of its frequent use in strong motion modeling of the Himalayan earthquakes (Joshi, 2006; Kumar et al. 1999) and seismic hazard estimation of the region (Bhatia et al. 1999). This test also includes other ground motion prediction equation (GMPE) given by Boore et al. (1997) and Boore and Atkinson (2008). The ground motion prediction equation given by Boore and Atkinson (2008) and Boore et al. (1997) is now hereby referred in the text as BA08 and BO97, respectively. The test checks the distribution of random residual with respect to peak ground acceleration and deviation of random residuals from normality. These tests are shown in Fig. 3.11. It is seen that the attenuation relations given by Abrahamson and Litehiser (1989), Boore and Atkinson (2008) and Joyner and Boore (1981) overestimate the value of peak ground acceleration when applied to predict data from the Kumaon Himalaya, thus clearly emphasizing the need to develop a new ground motion prediction equation for the region. Although Boore et al. (1997) gives comparable match in terms of predicted parameter, strict deviation from normality is clearly seen in the ground motion prediction equation when used for predicting data from the Kumaon Himalayan. It is seen from this test that when these relations are used for predicting values of peak ground acceleration of data from the Kumaon Himalaya fat tail or heavy tail is clearly seen in the normality plot of random residual which clearly indicates deviation of ground motion prediction equation from normality. This type of deviation from normality is expected to affect probabilistic seismic hazard assessment technique where we use 10% of probability of exceedence of peak ground acceleration in 50 years as a major parameter for seismic hazard zonation.

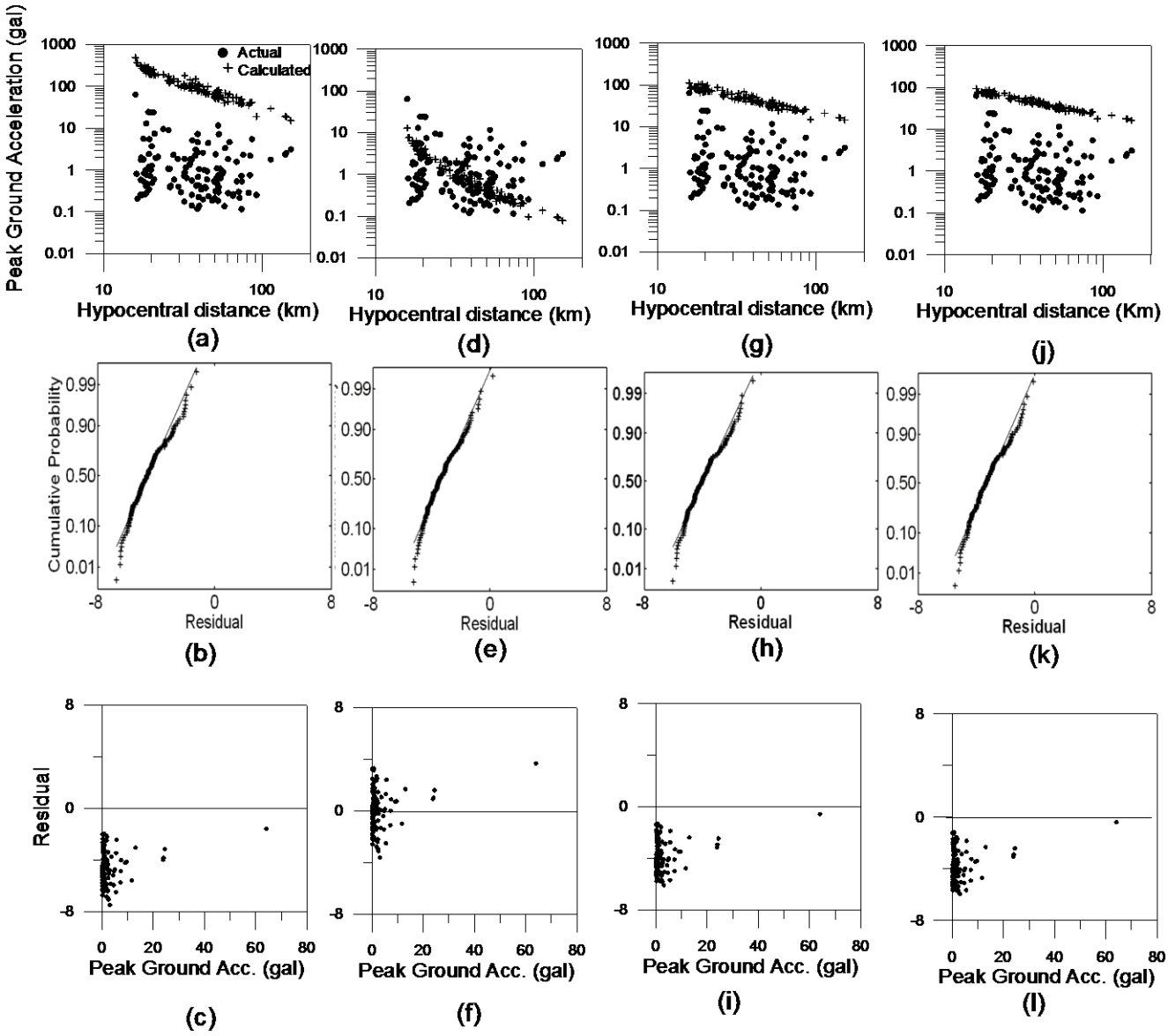

Figure 3.11(a) Comparison of PGA obtained from GMPE defined by Boore and Atkinson (2008) with the dataset of Kumaon Himalaya, (b) its cumulative probability function plot with respect to random residual of estimation, (c) its random residual plot with respect to PGA parameter, (d) Comparison of PGA obtained from GMPE of BO97 with the dataset of Kumaon Himalaya, (e) its cumulative probability function plot with respect to random residual of estimation, (f) its random residual plot with respect to PGA parameter. (g) Comparison of PGA obtained from GMPE of AL89 with the dataset of Kumaon Himalaya, (h) its cumulative probability function plot with respect to random residual of estimation, (i) its random residual plot with respect to PGA parameter. (j) Comparison of PGA obtained from GMPE of JB81 with the dataset of Kumaon Himalaya, (k) its cumulative probability function plot with respect to random residual of estimation, (l) its random residual plot with respect to PGA parameter.

3.6 Discussion

Regression relations have been developed in the present work for the Kumaon and Garhwal region. Regional strong motion data set has been used for developing regression relation. Distance parameter depending on the hypocentral and epicentral distance has been included in the regression model. It is seen that regression relations depending on epicentral as distance parameter give the minimum root mean square error. Attenuation curve of peak ground acceleration has been obtained using developed attenuation relations for both cases and different attenuation trend for the Kumaon and Garhwal Himalaya has been observed. Obtained attenuation curve for the Kumaon and Garhwal Himalaya are shown in Fig. 3.12. These curves shows that attenuation of peak ground acceleration is high in the Kumaon Himalaya as compare to the Garhwal Himalaya.

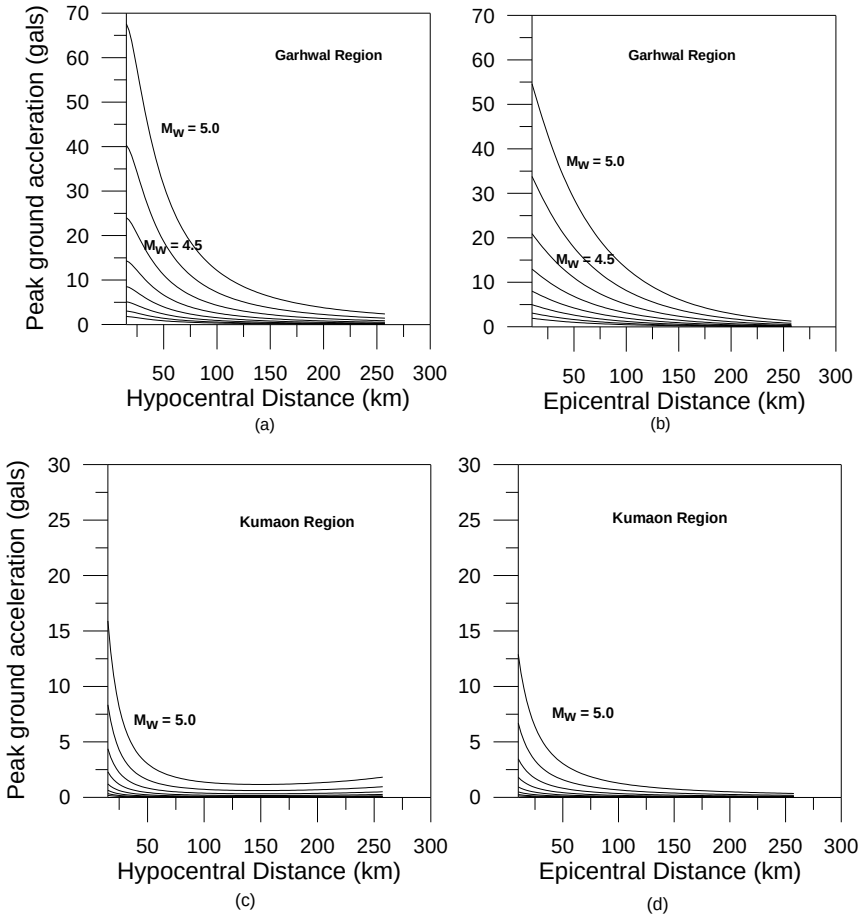

Figure 3.12 Attenuation curve for (a) and (b) Garhwal region, (c) and (d) Kumaon region using developed attenuation relation using hypocentral and epicentral distance, respectively.

3.7 Conclusion

This Chapter discusses the methodology of the regression relation analysis. Attenuation relations have been developed using damped least square inversion method. Dependency of developed attenuation relation on distance parameters also check in this study. The attenuation relations using epicentral distance in place of hypocentral distance gives the minimum root mean square error. The data for the Himalayan earthquake are predicted by using the attenuation relations developed for the Himalayan region with hypocental and epicentaral distance parameters. These attenuation relations obey normality and do not reflect any model inadequacies. The worldwide attenuation relations which are frequently used in Indian regions have been also checked for the assumption of normality and models inadequacies. It is seen that these attenuation relation shows presence of fat tails together with large model inadequacies when they are used for predicting Himalayan data. It is seen that as long as the data set is similar to that used for generating ground motion prediction equation (GMPE) the normality and model adequacies are broadly satisfied. However, clear deviation from normality is observed when using GMPE for predicting different data sets.

CHAPTER - 4

Modeling of Finite Earthquake Source using Semi-empirical Technique

4.1 Introduction

The technique of simulation of strong ground motion is useful tool where strong motion data is not available. Many techniques which have been used for synthesis of strong motion data have been discussed in Chapter 1. One of the widely used techniques is the semi empirical simulation technique given by Midorikawa (1993). The semi empirical simulation technique is dependent on attenuation relation. Joshi et al. (2012) have demonstrated the applicability of attenuation relation in this technique for regional studies. In this Chapter, semi empirical technique has been used for simulation of strong ground motion due to the Uttarkashi and Chamoli earthquakes

4.2 Method of Finite Modeling of Earthquake Source

Developed attenuation relation of limited applicability can be used for deterministic modeling of the rupture plane using semi empirical technique, initially proposed by Midorikawa (1993) and later modified by Joshi and Midorikawa (2004). This technique requires attenuation relation applicable in the study area for simulation of strong ground motion using deterministic model of the rupture plane. The method was initially proposed by Midorikawa (1993) and is used to model rupture plane buried in a homogenous earth model. Modification in this technique has been made by Joshi and Midorikawa (2004) to include the effect of buried rupture plane in the layered earth model. This technique has been used to simulate accelerogram due to rectangular rupture source. The semi empirical technique of simulation is based on the concept of dividing the finite rupture of the target earthquake into several subfaults representing small earthquakes. This technique uses attenuation relation for scaling the envelope of accelerogram which are treated as Green's function. This simulation technique is controlled by various factors like attenuation relation, geometry of the rupture plane, velocity model of the earth crust, geometry of the rupture

propagation and source parameters of small earthquakes. The basic concept of the release of synthetic record from various subfaults and their summation at the observation point considering the rupture propagation and propagation of the energy in the medium is same as that was initially given by Midorikawa (1993) in his envelope summation technique. The scaling relation between the parameters of the target and small earthquakes is based on the self similarity laws given by Kanamori and Anderson (1975).

4.2.1 Self-Similarity

Division of rupture plane of target earthquake into sub-faults in this simulation technique is based on the self-similarity law of the source parameter given by Kanamori and Anderson (1975) and other the self-similarity law of source spectra given by Aki (1967). Scaling relationship of source parameters such as rupture length, rupture width, slip, slip duration and magnitude are defined by the self-similarity laws given by Kanamori and Anderson (1975) and is defined as follows:

$$L/L_e = W/W_e = T/\tau = D/d = \left(M_o \big/ C' M_o'\right)^{1/3} = N \tag{4.1}$$

where,

L and L_e = length of the rupture plane of the target and small earthquakes, respectively;
W and W_e = width of the rupture plane of the target and small earthquakes, respectively;
T and τ = slip duration of the target and element earthquakes, respectively;
D and d = slip of the target and small earthquakes, respectively;
M_o and M_o' = seismic moment of the target and small earthquakes, respectively and
N = total number of sub-faults along the length or width of the target rupture plane.

Above relation was modified by considering following empirical relationship between seismic moment and the earthquake magnitude given by Kanamori (1977):

$$\log_{10} M_o = 1.5 M_w + 16.1 \tag{4.2}$$

Where, M_o and M_w are the seismic moment and moment magnitude of an earthquake, respectively. Using equation (4.1), following relation has been obtained:

$$M_o = 10^{1.5M_w+16.1} \tag{4.3}$$

$$M_o' = 10^{1.5M_w'+16.1} \tag{4.4}$$

Dividing equation (4.3) with (4.4) we get:

$$N = 10^{0.5\left(M_w - M_w'\right)} \tag{4.5}$$

Where, M_w and M_w' are the moment magnitude of the target and small earthquakes, respectively. Above equation has been also used by Midorikawa (1993) for fixing parameters of target and subfault events, respectively. The scaling laws mentioned above are required for defining the parameter of rupture plane responsible for causing target earthquake. The other scaling relation which is used in the simulation technique is based on the spectral scaling model given by Aki (1967) and Brune (1970) and is called as Omega square (ω^{-2}) spectral scaling model. According to ω^{-2} model (Aki 1967; Brune 1970), the theoretical shapes of source spectrum is given as:

$$U(f) = \frac{M_o}{\left[1+\left(f/f_c\right)^2\right]} \tag{4.6}$$

The source displacements spectra of both the target and small earthquakes can be defined as follows:

$$U_o(f) = \frac{M_o}{\left[1+\left(f/F_c\right)^2\right]} \tag{4.7}$$

$$U_o'(f) = \frac{M_o'}{\left[1+\left(f/f_c\right)^2\right]} \tag{4.8}$$

Where, F_c and f_c are the corner frequency of the target and small earthquakes, respectively

According to ω^{-2} model, Irikura (1986) have proposed following approximation:

$$U(f \to 0) \approx \omega^o, U(f \to \infty) \approx \omega^{-2} \tag{4.9}$$

The self-similarity law for spectral parameter of the target and small earthquakes is formulated as follows:

$$\frac{U_o}{U_o'} = \frac{M_o}{M_o'} = N^3 \tag{4.10}$$

Where, U_o and U_o' are the constant levels of the source displacement spectra of the target and small earthquakes, respectively. This scaling relation is called as ω^{-2} spectral scaling model (Aki 1967; Brune 1970). If the average stress drop is independent of M_o, self-similarity exists among these earthquakes (Aki 1967). Under such cases high-frequency acceleration flat level A_o is proportional to $M_o^{1/3}$, which gives the following form of the spectral relationship between the target and small earthquakes (Irikura 1986):

$$\left(A_o / A_o'\right) = \left(M_o / C' M_o'\right)^{1/3} = N \tag{4.11}$$

Where, A_o and A_o' are the high-frequency flat level of the acceleration spectra of the target and small earthquakes, respectively. The constant stress drop model gives following scaling relation between the corner frequency of the target and small earthquakes (Boore 1983):

$$F_c / f_c = \left(M_o' / M_o\right)^{1/3} = 1/N \tag{4.12}$$

Where, F_c and f_c are the corner frequency of the target and small earthquakes, respectively. The condition of constant stress drop does not always hold for wide magnitude range (Joshi and Midorikawa 2004). Therefore, Irikura (1986) has introduced a flexible condition for ω^{-2} model, having shape of ω^{-2} source spectrum but not constant stress. In such cases the self-similarity law of source spectra for including stress drop ratio C' of the target and small earthquakes is given as (Irikura 1986):

$$\frac{U_o}{U_o'} = \frac{M_o}{M_o'} = C'N^3 \tag{4.13}$$

$$\left(A_o / A_o'\right) = \left(M_o / C' M_o'\right)^{1/3} = N \tag{4.14}$$

Where, C' is the stress drop ratio between the target and small earthquake, N and C' can be derived from constant levels of the source displacement and acceleration spectra of the target and small earthquakes, respectively. In this case other scaling laws parameters are given as:

$$L/L_e = W/W_e = T/\tau = D/d = \left(M_o \big/ C'M_o'\right)^{1/3} = N \tag{4.15}$$

$$D/d = \left(A_o \big/ A_o'\right) = N \tag{4.16}$$

Where, C' is the ratio of stress drop of the target and the small earthquake.

The procedure of simulation of the strong ground motion is illustrated in Fig. 4.1. White Gaussian noise shown in Fig. 4.1(a) is passed through filters representing the basic spectral shape defined by Boore (1983) and shown in Fig. 4.1(b). These filters represent source spectrum, near site attenuation of high frequency and anelastic attenuation. The cut-off frequency of high cut filter assumed in this work is 40 Hz and the shear wave quality factor in the filter representing anelastic attenuation is assumed as $Q_\beta(f) = 112f^{.97}$ (Joshi 2006). This is the relation of shear wave quality factor derived for Garhwal region by Joshi (2006). The filtered white noise shown in Fig. 4.1(c) is windowed by the envelope of accelerogram released by a particular element shown in Fig. 4.1(d) to obtain accelerogram shown in Fig. 4.1(e). The accelerogram arriving at the observation point is convolved with the correction factor F(t) to account the slip distribution of large and small events Fig. 4.1(f). Summation of all accelerogram arriving at the observation point at different time lags (Fig. 4.1g) gives the resultant accelerogram shown in Fig. 4.1(h). Stepwise procedure of simulation is given as below:

(i) The rupture responsible for the target event is identified.

(ii) Rupture is divided into several sub faults on the basis of self similarity laws.

(iii) Parameters of rupture plane are decided on the basis of earlier studies and source parameters of target events.

(iv) One element is treated as starting point of energy which acts as a nucleation point or the starting point of rupture. The rupture from nucleation point travels in all directions with an assigned rupture velocity.

(v) On arrival of rupture front at the centre of an element energy is released in the form of envelope function defined by Kameda and Sugito (1978) and modified by Joshi et al. (2001) as:

$$e(t) = T_{ss}\left\{((PGA)t)/T_d\right\}\exp(1-t/T_d) \tag{4.17}$$

In this expression, PGA is the peak ground acceleration, T_{ss} represents transmission factor (Joshi et al. 2001) and T_d the duration parameters, respectively. The parameter PGA is determined using attenuation relation.

(vi) White Gaussian random noise of zero mean and one standard deviation (Fig. 4.1a) is passed through several of filters given by Boore (1983) having basic shape of acceleration spectra given in Fig. 4.1(b).

(vii) This is windowed using the envelope function defined in equation (4.17) and given in Fig. 4.1(d).

(viii) In order to compensate the slip duration of target and small event the windowed filtered record is convolved with a correction function given by Irikura (1986) and shown in Fig. 4.1(f). We have used following form of correction function given by Irikura et al. (1997) :

$$F(t) = \delta(t) + \left\{(N-1)/T(1-\exp(-1))\right\}\exp(1-t/T) \tag{4.18}$$

Where, $\delta(t)$ is the delta function, N is the total number of subfaults along the length or width, T is rise time of the target earthquake.

(ix) The geometry of rupture propagation decides the time at which record is released from different elements.

(x) The acceleration records released from each subfault reaches the observation point depending upon the rupture propagation from the nucleation point to a particular subfault and the travel time of energy in the layered earth from that subfault to the observation point. Appropriate summation of all records gives resultant acceleration record at the observation point (Fig. 4.1g). The procedure of simulation of strong ground motion is illustrated in Fig. 4.1.

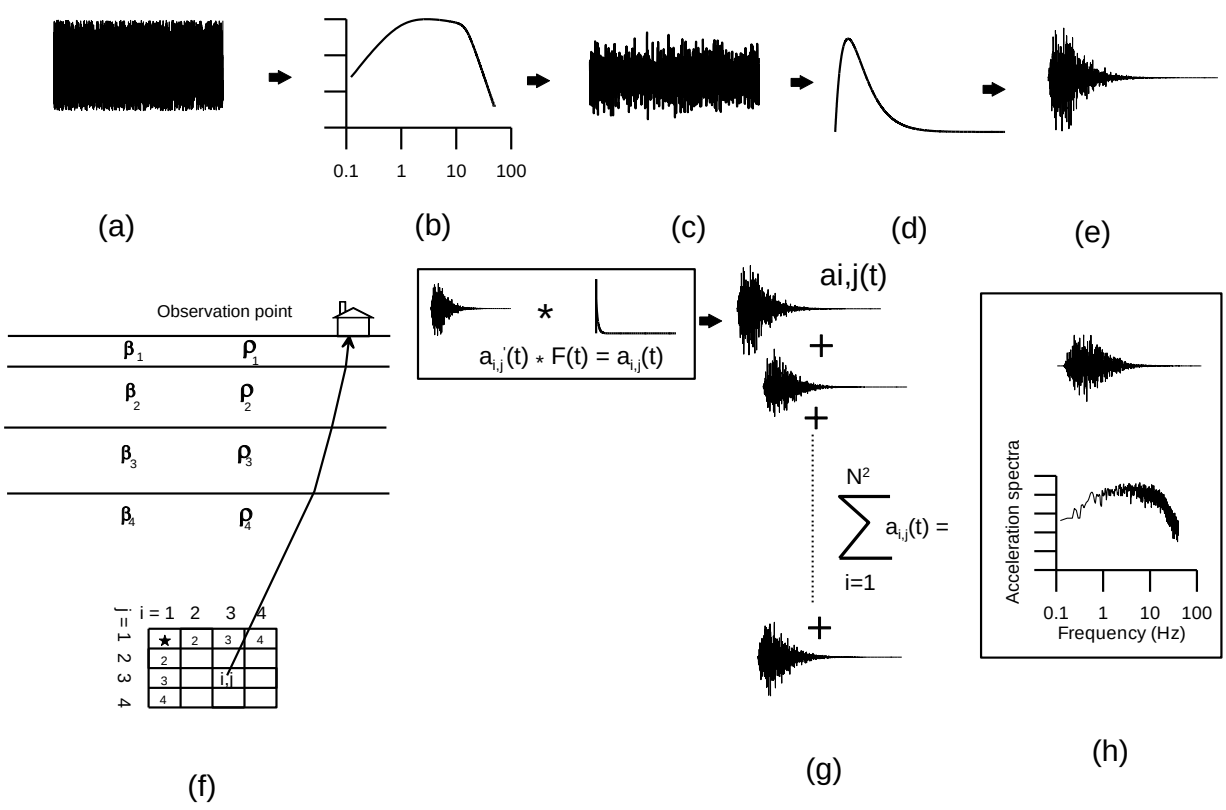

Figure 4.1 Method of simulation of the strong ground motion showing (a) White Gaussian noise, (b) Filter representing actual earthquake process, (c) Filtered white noise, (d) Envelope of accelerogram released by i, j element within the rupture plane shown in figure f, (e) Multiplication of the envelope with filtered white noise, (f) Rupture plane divided into 4×4 elements in the layered earth with i,j, element releasing record which is convolved with the correction factor F(t), (g) Summation of all accelerogram from various element according to their arrival time at the observation point and (h) The simulated acceleration record and its acceleration spectrum.(after Joshi 2004)

4.4 Simulation of the Uttarkashi and Chamoli Earthquakes

The region of the Garhwal Himalaya has been visits by recently two earthquakes viz. the Uttarkashi earthquake (M_s = 7.1) 20th October 1991 and Chamoli earthquake (M_s = 6.6) 28th March 1999. The parameters of the Uttarkashi and Chamoli earthquakes are given in Table 4.1. The Uttarkashi region which lies in the northern part of Indian subcontinent was rocked by a moderately strong earthquake. Thirteen stations had recorded strong motion data of this earthquake. Maximum peak acceleration of horizontal component was recorded at the Uttarkashi station and the vertical component at the Bhatwari station. The most probable causative fault for this earthquake has been identified on the basis of location of isoseismal, isoacceleration, aftershocks distribution in regional tectonic maps (Joshi 1994). The Uttarkashi earthquake was associated with the very complex Alpine Himalayan tectonic setup. The most prominent tectonic feature in this picturesque region is the Main Central Thrust (MCT), which exists as three northeast-dipping crystalline thrust sheets, separated by Vaikrita, Munsiari and Bhatwari Thrusts. Other lineaments in the vicinity are North Almora, Tons Nayar, Dunda, Krol and Garhwal thrusts (Joshi 2004).

The region of the Garhwal Himalaya was rocked by the Chamoli earthquake on 28th March, 1999. The Chamoli earthquake was felt at far off places like Kanpur (440 km southeast of the epicentre), Shimla (220 km northwest) and Delhi (280 km southwest). A strong motion network of 28 stations is operated in the source regions of this earthquake. The instruments are Kinemetrics SMA-1 accelerographs, which are triggered accelerographs with threshold level of 1% of g (Chandrasekaran and Das 1992) recording three orthogonal components of acceleration on 70mm film. Detail knowledge of the site conditions is unavailable; however most of the stations of this array are located on the hard rock site (Sharma 1998). At the time of earthquake the strong motion array operational in the epicentral area recorded the Chamoli earthquake at eleven stations (Joshi 2004). At the far field stations like Lansdown and Roorkee, the processed record does not have clear phase and entire coda length. Due to this reason record from these two stations are not used in the present study. The region surrounding the epicenter of the Chamoli earthquake is marked by various tectonic faults and lineaments. In the region of the Western Garhwal the Main Central Thrust (MCT) forms a 12 km thick NNE dipping shear zone. The MCT zone of deformation is bounded in this region by the Munsiari thrust in the south and Vaikrita thrust in northward

direction (Metcalfe 1993). The Chamoli earthquake lies in the same seismo-tectonic belts as the 1991 Uttarkashi earthquake. This belt of moderate seismicity with 6 to 7 magnitude earthquakes is located within the nortern part of the Lesser Himalaya and lies immediate south of the higher Himalayas (Mahajan and Virdi 2001). Tectonics of the region surrounding the epicenters of the Uttarkashi and Chamoli earthquakes with location of rupture planes responsible for these earthquakes is shown in Fig. 4.2.

The suitability of developed attenuation relations in this work has been checked by simulating strong motion records of these two earthquakes at nine near field stations. The attenuation relation developed for the Garhwal Himalaya has been used to simulate records of these earthquakes using semi empirical technique. The semi empirical technique has been previously used by Joshi et al. (2001) and Joshi (2004) for simulating the strong motion records of these earthquakes using attenuation relation of worldwide applicability given by Abrahamson and Litehiser (1989). In this work the rupture model considered for the modeling the Uttarkashi and Chamoli earthquakes are assumed to be similar to that modeled by Joshi (2004). The parameters of rupture model of the Uttarkashi and Chamoli earthquakes are given Table 4.2 and Table 4.3, respectively. In order to test the applicability of developed attenuation relation, we have modeled the ruptures of these two earthquakes and records have been simulated at the sites that have recorded these earthquakes.

Table 4.1 Parameters of (a) Uttarkashi earthquake of 20th Oct, 1991. (b) Chamoli earthquake of 28th March, 1999.

Hypocenter	Size	Fault Plane Solution	Reference
(a) 20.10.1991 21:23:14.3(GMT) 30.78° N, 78.77° E 10 km	m_b = 6.5, M_s = 7.1, M_o = 1.8 x 10^{26} dyne-cm M_W = 6.8	NP1: φ= 296°, δ= 5°, λ= 90° NP2: φ= 116°, δ= 85°, λ= 90°	USGS
(b) 28.03.1999 19:05:11.00 (GMT) 30.51°N, 79.40°E 15.0 km	m_b = 6.4 M_s = 6.6 M_0 = 7.7x10^{25} dyne-cm	NP1: φ= 282°, δ= 9°, λ= 95° NP2: φ = 97°, δ= 81°, λ= 89°	USGS

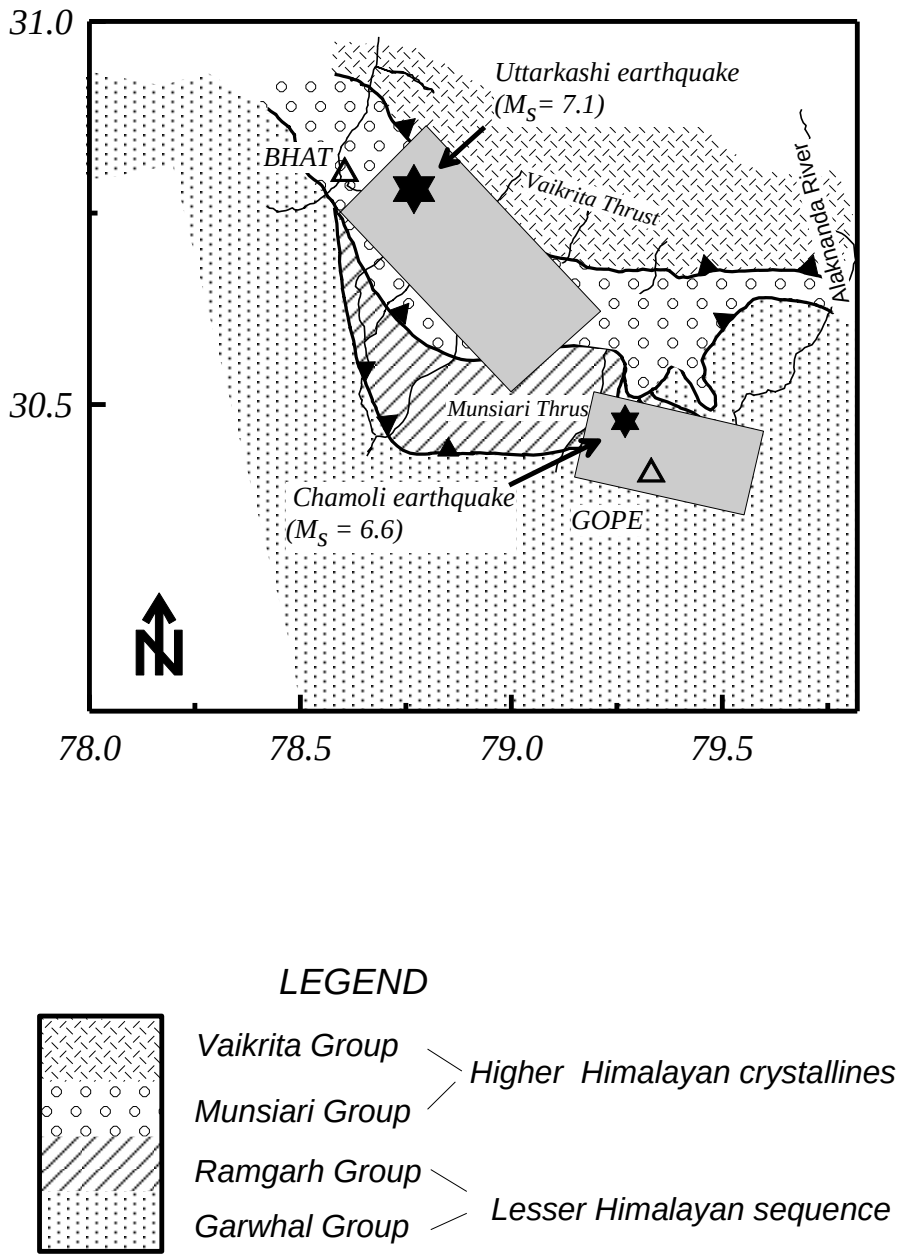

Figure 4.2 Tectonics of the region surrounding the epicenters of the Uttarkashi and Chamoli earthquakes (after Metcalfe 1993 and Valdiya 1977). Location of rupture planes responsible for the Uttarkashi and Chamoli earthquakes have been after Joshi (2004). The location of near field stations recording these events is shown by empty triangle.

Table 4.2 Modeling parameters of rupture plane of the Uttarkashi earthquake.

Modeling parameters	Source
Length = 33 km	Wells and Coppersmith (1994)
Width = 15 km	Wells and Coppersmith (1994)
Dip = 14^0	CMT (Harvard)
Strike = 317^0	CMT (Harvard)
$Q_\beta(f) = 112f^{.97}$	Joshi (2006)
Number of elements = 225	Kanamori and Anderson (1975)

Table 4.3 Modeling parameters of rupture plane of the Chamoli earthquake.

Modeling parameters	Source
Length = 22 km	Wells and Coppersmith (1994)
Width = 11 km	Wells and Coppersmith (1994)
Dip = 9^0	CMT (Harvard)
Strike = 282^0	CMT (Harvard)
$Q_\beta(f) = 112f^{.97}$	Joshi (2006)
Number of element = 16	Kanamori and Anderson (1975)

The strong motion records of the Uttarkashi and Chamoli earthquakes have been simulated at nine near field stations, respectively. Locations of these stations are shown in Fig. 4.3. The pseudo acceleration response spectra is prepared from simulated and observed records after band-passing them through a Butterworth filter with 1 to 10 Hz bandwidth. The simulated records are compared with actual records in terms of peak ground acceleration values for the Uttarkashi and Chamoli earthquakes are given in Table 4.4 and Table 4.5, respectively. Root mean square error between the observed and obtained peak ground acceleration is obtained using following relation:

$$Err_{PGA} = (P_{obi} - P_{cai}) / P_{obi} \tag{4.19}$$

Where, P_{obi} and P_{cai} is the observed and calculated peak ground acceleration respectively.

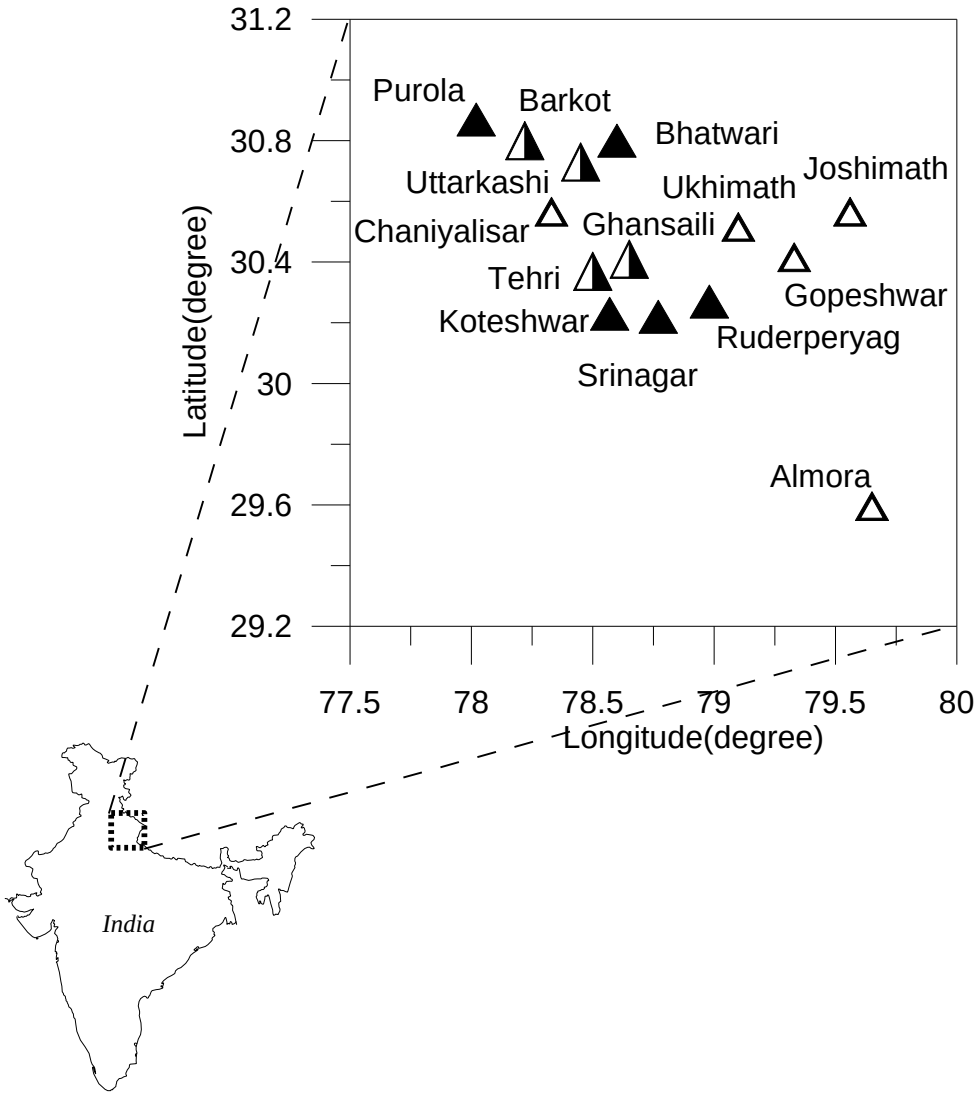

Figure 4.3 Location of strong motion array that have recorded the Uttarkashi and Chamoli earthquakes. The stations recording only the Uttarkashi and Chamoli earthquakes are shown by a solid filled and hollow triangle, respectively. Those stations which recorded both the Uttarkashi and Chamoli earthquakes are shown by half filled triangle.

4.3.1 Simulation for the Uttarkashi earthquake

A comparison of simulated and observed acceleration records and pseudo acceleration spectrum for the Uttarkashi earthquake is shown in Fig. 4.4 and 4.5, respectively. Station wise comparison of simulated and observed records is summarized below:

***Bhatwari*:** The simulated record match with the observed records at this station. The simulated response spectrum matches effectively with that of the observed.

Uttarkashi: Maximum ground acceleration was recorded at this station during the Uttarkashi earthquake. The simulated peak ground acceleration value is very closer to observed value. A good match of the simulated and observed response spectra is observed at periods from 0.1 to 0.4 sec.

Ghansaili: The simulated peak ground acceleration and observed peak ground acceleration value similar, 120 and 121 cm/s^2 at this station which is the best match of two records. The simulated response spectrum matches effectively with that of the observed one.

Barkot: At this station simulated and observed record very much resembles each other. The simulated response spectrum is also showing good match with observed spectrum.

Rudrapryag: The simulated peak ground acceleration value is higher than observed peak ground acceleration value at this station. The simulated response spectrum have good match at the period more than 0.5 sec.

Srinagar: The simulated peak ground acceleration and observed peak ground acceleration value at this station is 88 cm/s^2 and 49 cm/s^2, respectively. The simulated response spectrum is showing good match with observed spectrum between the period 0.3 sec to 1sec.

Purola: The simulated and observed record nearly matches at this station. Also response spectra for the period 0.3 to 0.5 sec are showing a good match.

Koteswar: The close approximation of peak ground acceleration values for simulated with observed shows good match between the records. The simulated acceleration spectrum has low value at this station compared to observed spectrum.

Tehri: The simulated peak ground acceleration matches effectively with the recorded data. The simulated response spectrum have good match with observed at the period more than 0.2 sec.

The comparison of peak ground acceleration values from simulated and observed records at nine stations is made in terms of Err_{pga} error. This is given in Table 4.4. Error between simulated and observed peak ground acceleration vary from 0.008 to 1.14. Err_{pga} error is minimum at the Ghansaili and is maximum at the Srinagar station.

Table 4.4 Comparisons of observed peak ground acceleration values with that simulated for the Uttarkashi earthquake.

Recording station	Observed longitudinal peak ground acceleration (cm/sec^2)	Observed transverse peak ground acceleration (cm/sec^2)	Simulated peak ground acceleration (cm/sec^2)	Err_{pga} computed from longitudinal and simulated PGA	Err_{pga} computed from transverse and simulated PGA
Bhatwari	235	238	270	.14	.13
Ghansaili	129	120	121	.06	.008
Uttarkashi	245	309	252	.02	.18
Rudraparyag	48	51	81	.68	.58
Barkot	85	80	79	.07	.01
Srinagar	41	49	88	1.14	.79
Purola	66	87	50	.24	.42
Tehri	74	66	82	.10	.24
Koteshwar	100	61	81	.19	.32

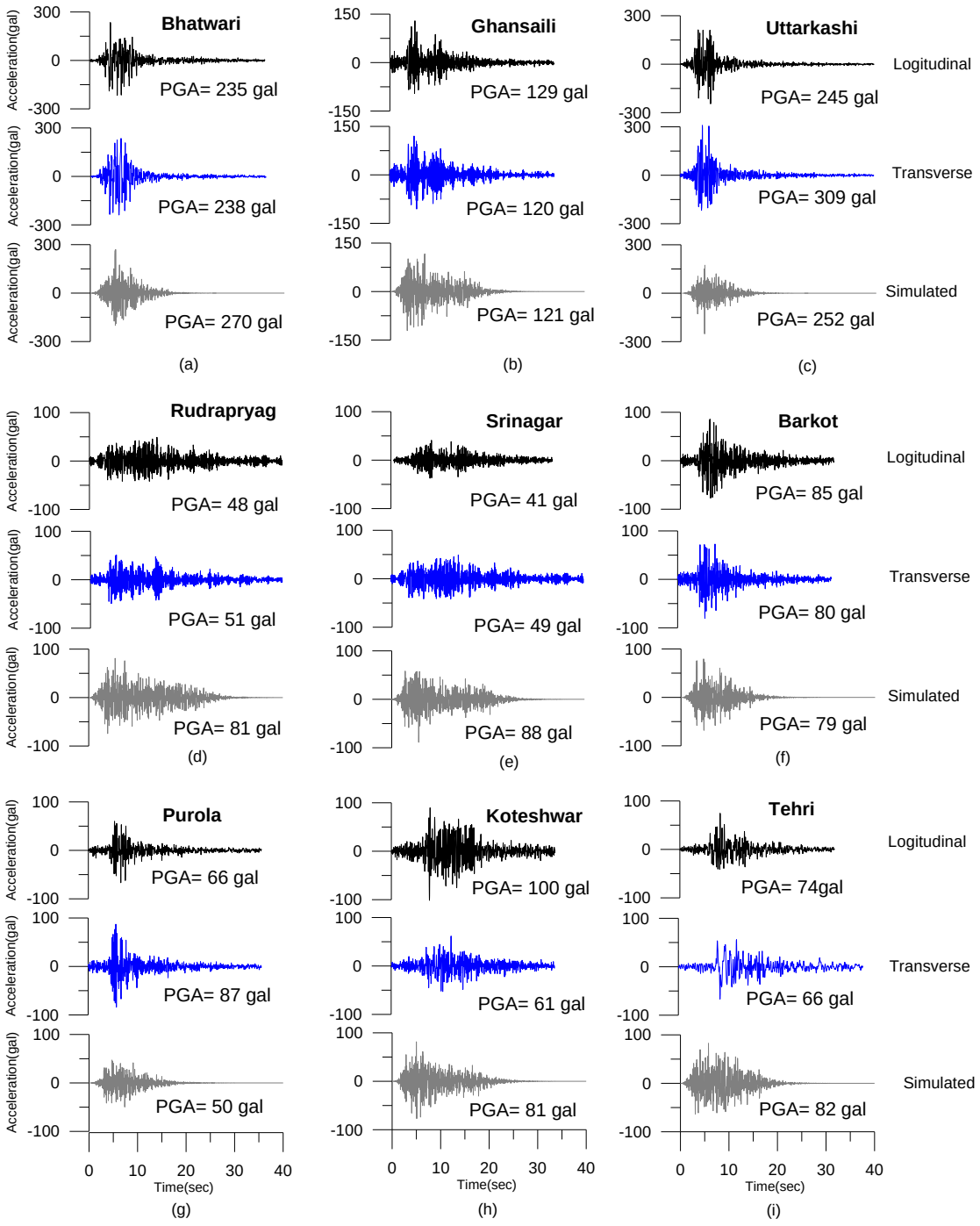

Figure 4.4 Comparison of observed and simulated acceleration records at various stations for the Uttarkashi earthquake using developed attenuation relation with recorded longitudinal and transverse component.

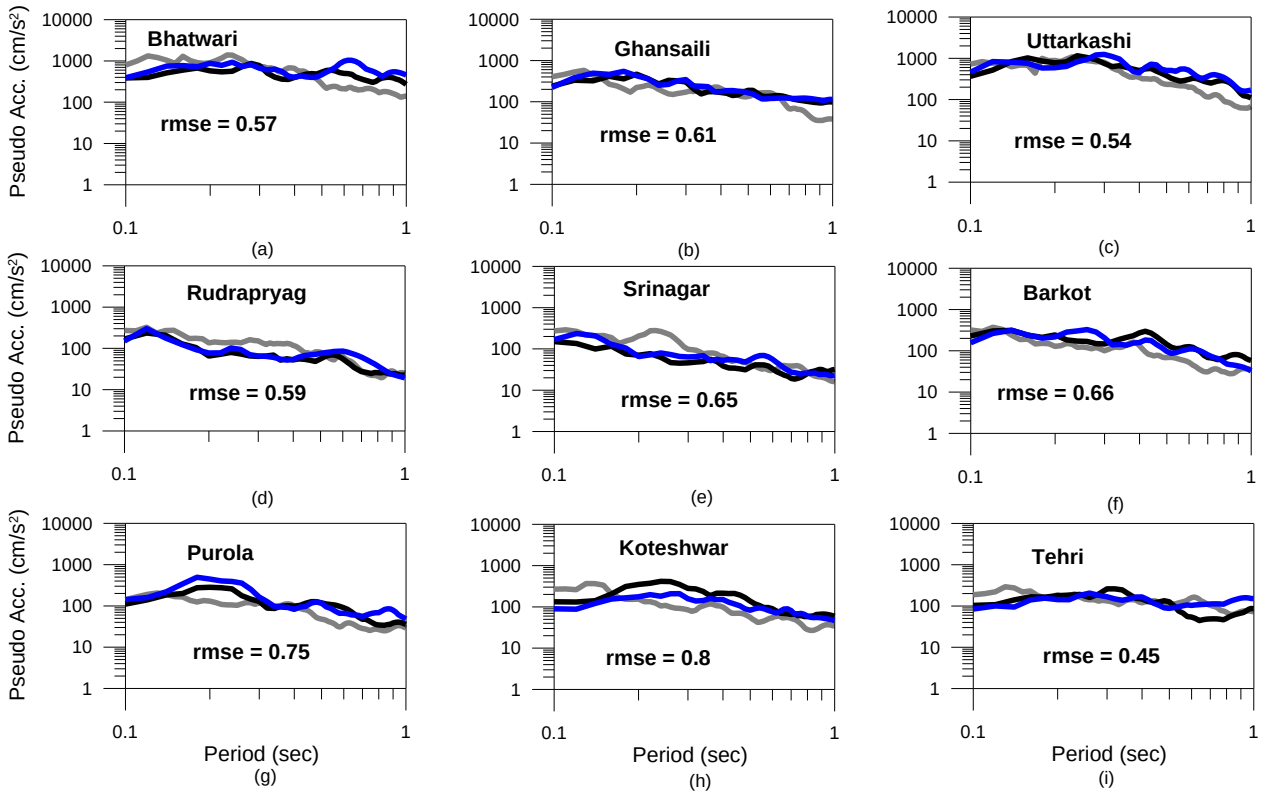

Figure 4.5 Comparison of response spectra obtained from observed and simulated records at nine stations for the Uttarkashi earthquake. The black, blue and gray lines represent the observed two horizontal records, simulated records respectively, using developed attenuation relation.

4.3.2 Simulations for the Chamoli earthquake

A comparison of simulated and observed acceleration records and pseudo acceleration spectrum for the Chamoli earthquake is shown in Fig. 4.6 and 4.7, respectively. Station wise comparison of acceleration records is summarized below:

Gopeshwar: The simulated record match well with the observed records at this station. The simulated response spectrum matches effectively with that of the observed spectrum.

Joshimath: The simulated peak ground acceleration and observed peak ground acceleration value at this station is 109 cm/s^2 and 65 cm/s^2, respectively. The simulated response spectrum is also little bit deviating from observed spectrum.

Barkot: At this station simulated and observed records are showing close matching. The simulated response spectrum is very much identical with observed spectrum.

Ghansaili: The simulated peak ground acceleration and observed peak ground acceleration value at this station is 87 cm/s^2 and 83 cm/s^2, respectively which are a good match. The simulated response spectrum matches effectively with that of the observed.

Ukhimath: This station having not good observed records. The simulated and observed peak ground acceleration values are 131 cm/s^2 and 89 cm/s^2, respectively. The simulated response spectrum have good match with observed at the period more than 0.2 sec.

Uttarkashi: The simulated peak ground acceleration value is low at this station as compare to observed value. The simulated response spectrum have good match with observed spectrum at the low and high period ranges.

Chinyalisar: The close approximation of peak ground acceleration values for simulated with observed shows good match between the records. The simulated acceleration spectrum also shows a good match with observed spectrum between period 0.1 to 0.2sec.

Almora: The simulated record match well with the observed records at this station. The simulated response spectrum matches effectively with that of the observed spectrum.

Tehri: The simulated peak ground acceleration value is low compare to observed peak ground acceleration value at this station. The simulated response spectrum have not good match with observed spectrum at the period more than 0.3 sec.

The comparison of peak ground acceleration values from simulated and observed records at nine stations is made in terms of Err_{pga} error and is given in Table 4.5. Error between simulated and observed acceleration record vary from .04 to .84. Minimum root mean square error is obtained at the Ghansiali while maximum Err_{pga} error is obtained at the Joshimath station. The comparison shows that simulate records have peak ground acceleration closer to the actual values. The comparison of simulated with observed response spectra of the Uttarkashi and Chamoli earthquakes is shown in Fig. 4.5 and 4.7 respectively. This confirms the suitability of attenuation relation developed in the present work.

Table 4.5 Comparisons of observed peak ground acceleration values with that simulated for the Chamoli earthquake.

Recording station	Observed longitudinal peak ground acceleration (cm/s^2)	Observed transverse peak ground acceleration (cm/s^2)	Simulated peak ground acceleration (cm/s^2)	Err_{pga} computed from longitudinal and simulated PGA	Err_{pga} computed from transverse and simulated PGA
Gopeshwar	187	369	308	.64	.16
Joshimath	65	59	109	.67	.84
Barkot	15	21	20	.33	.04
Ghansiali	72	83	87	.20	.04
Ukhimath	89	73	131	.47	.79
Uttarkashi	48	64	31	.35	.51
Chaniyalisar	49	43	35	.28	.18
Almora	25	29	32	.28	.10
Tehri	56	65	39	.30	.40

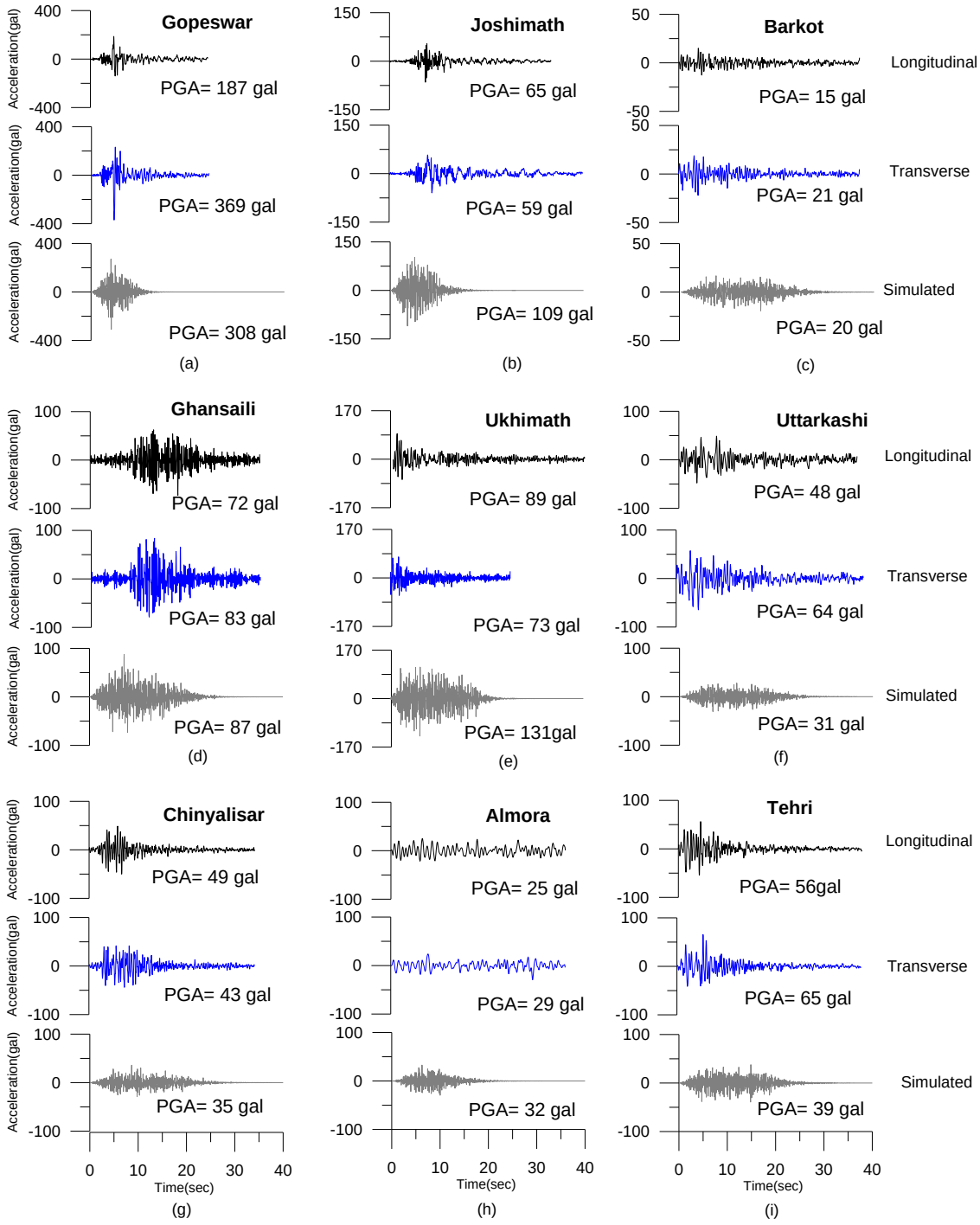

Figure 4.6 Comparison of the observed and simulated acceleration records at various stations for the Chamoli earthquake using developed attenuation relation.

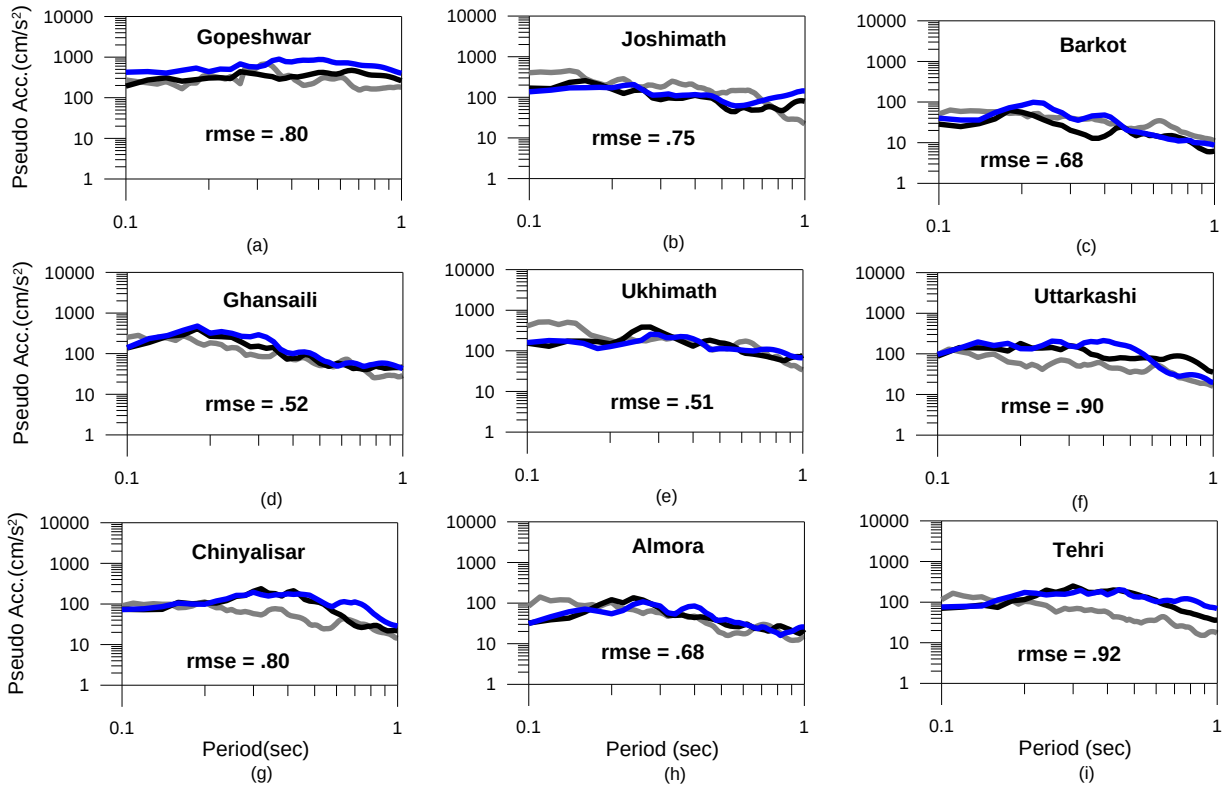

Figure 4.7 Comparison of response spectra is obtained from observed and simulated records at nine stations for the Chamoli earthquake. The black, blue and gray lines represent the observed two horizontal records, simulated records using developed attenuation relation, respectively.

4.4 Conclusion

Finite modeling of source of the Uttarkashi and Chamoli earthquakes using the semi empirical simulation technique given by Midorikawa (1993) has been discussed in this Chapter. Developed attenuation relation has been used in the present work for simulation of acceleration records of these earthquakes at those stations which has recorded these earthquakes. Comparison of simulated record is made with the observed records. It is seen that the simulated record of these earthquakes have a good match with observed records which confirms the suitability of developed attenuation relations in this work to model earthquakes in this region.

CHAPTER - 5

Coda Wave Attenuation Characteristics of the Kumaon and Garhwal Himalaya

5.1 Introduction

Frequency dependent coda wave attenuation characteristics of the Kumaon Himalaya and Garhwal Himalaya region has been studied using single backscattering method given by Aki and Chouet (1975). Single backscattering method is one of the most frequently used techniques. Strong motion data of nine earthquakes recoded on six stations for the Kumaon and Garhwal Himalaya region respectively has been used. This Chapter discussed the methodology and numerical experiment, which gives the comparable evidence of attenuation characteristics for both regions.

5.2 Frequency Dependent Coda Wave (Q_c)

The energy content in a strong motion record is highly affected by attenuation characteristic of the medium. The study of attenuation characteristic of a medium, using strong motion data, is important for seismologists and engineers for seismic hazard analysis. Attenuation characteristic of a medium is defined by anelastic attenuation of seismic waves. This in turn, is characterized by a dimensionless quantity known as quality factor Q (Knopoff 1964). Anelastic attenuation property can be estimated using different parts of an accelerogram. Most studies use decay of coda wave to determine attenuation characteristic of the earth's crust, (Aki 1969; Aki and Chouet 1975; Sato 1977; Roecker et al. 1982; Pulli 1984; Reha 1984; Jin and Aki 1986; Ibanez et al. 1990; Kanao and Ito 1992; Gupta et al. 1995; Gupta and Kumar 2002; Paul et al. 2003; Kumar et al. 2005; Sharma et al. 2012). Coda wave quality factor estimates for the Kumaon and the Garhwal Himalaya region have been made in high frequency range using single backscattering model given by Aki and Chouet (1975). Coda waves of 30 sec window length, filtered at six different frequency bands, centered at 1.5, 3.0, 6.0, 12.0, 20.0 and 28.0 Hz, have been analyzed using the single backscattering method. In the present work strong motion data recorded within an epicentral distance of 100 km have been used for estimation of coda wave quality factor. Strong motion data recorded by the networks operational in the Kumaon and Garhwal Himalaya region, within the State of Uttarakhand, India have been used to determine regional attenuation characteristics.

5.3 Data Used

A major seismicity project funded by the Department of Science and Technology and Ministry of Earth Sciences, Government of India, a network of Strong Motion Accelerograph (SMA) has been installed in the Pithoragarh region of the Kumaon Himalaya by the National Geophysical Research Institute and Department of Earth Sciences, Indian Institute of Technology Roorkee, India. Instrument specification of this network, operational in the Kumaon Himalaya has been described in Chapter 2. Strong motion data recorded on this network has been used to determine attenuation properties of the Kumaon Himalaya. The strong motion data recorded in the Garhwal Himalaya are available through website **www.pesmos.in** maintained by the Department of Earthquake Engineering, Indian Institute of Technology, Roorkee, India. Fig. 5.1 shows epicenters of events used in this work, station location of those strong motion recorders which recorded these events, and tectonics of the region. Geographical coordinates of stations are given in Table 5.1.

Table 5.1 Strong motion stations in the Kumaon and Garhwal Himalaya, with their geographical coordinate. Strong motion data from these stations was used in the present analysis.

Sr. No.	Kumaon Array			Garhwal Array		
	Station Name	Latitude (Degree)	Longitude (Degree)	Station Name	Latitude (Degree)	Longitude (Degree)
1.	Dharchula	29.84N	80.53E	Uttarkashi	30.730N	78.445E
2.	Didihat	29.80N	80.25E	Chamoli	30.412N	79.320E
3.	Pithoragarh	29.58N	80.21E	Barkot	30.809N	78.256E
4.	Thal	29.82N	80.14E	Tehri	30.374N	78.430E
5.	Tejam	29.95N	80.12E	Dhanaulti	30.427N	78.288E
6.	Askot	29.76N	80.33E	Gairsain	30.051N	79.288E

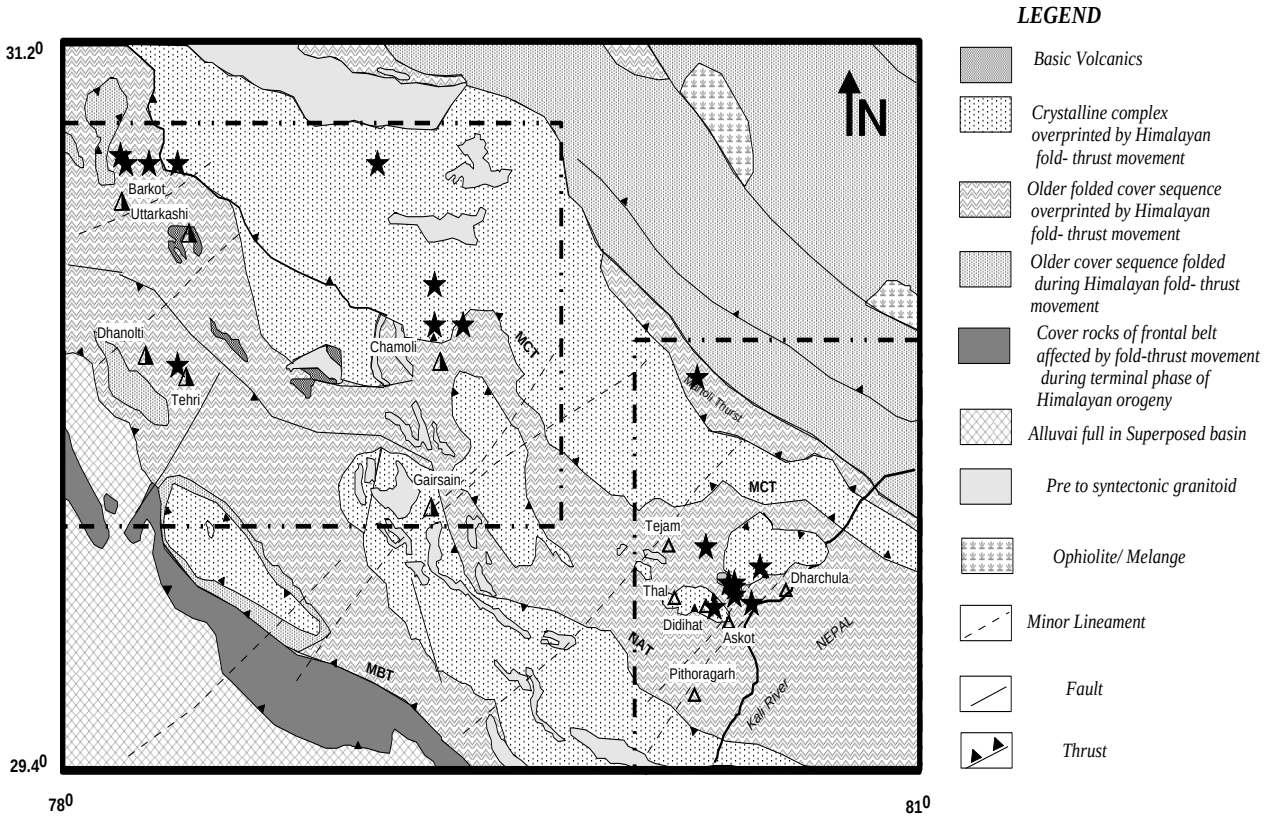

Figure 5.1 Location of strong motion recorders installed in the Kumaon and Garhwal Himalaya. Empty triangles and half filled triangles denote stations in the Kumaon and Garhwal array, respectively. Stars show the epicenter of the earthquakes. Tectonics of the region is taken after GSI (2000).

Determination of frequency dependent coda wave quality factor from acclerograms requires a processed record. Acceleration records were processed as per the procedure suggested by Boore and Bommer (2005). The processing steps involve baseline correction; instrumental scaling and frequency filtering are discussed in Chapter 2. In the present work strong motion data of nine events of similar magnitude and depth range, recorded at six stations for the Kumaon Himalaya and Garhwal Himalaya region, respectively, have been used to determine coda wave quality factor (Q_c). Those earthquakes were selected in both regions, which had maximum coverage of the entire region.

5.4 Methodology

The single backscattering model given by Aki and Chouet (1975) is a commonly used method for describing the behavior of the coda wave from small regional earthquakes. According to this method, the coda waves are interpreted as backscattered body waves generated by numerous heterogeneities present in the earth's crust and upper mantle. This implies that the scattering is a weak process and outgoing waves are scattered only once before reaching the receiver (Gupta et al. 1995). In the single backscattering model, the coda wave's amplitude *A(f, t),* for central frequency *'f'* over a narrow bandwidth signal and lapse time *'t'* measured from earthquake origin time is described as (Aki 1980):

$$A(f,t) = S(f)t^{-a}\exp(-\pi ft/Q_c) \tag{5.1}$$

Where *S(f)* represent the source function at frequency '*f*' and '*a'* is geometrical spreading factor and taken as unity for body waves and Q_c is the quality factor representing the average attenuation characteristics of the medium. Equation (5.1) is linearised by taking its logarithm. The logarithm of equation (5.1) gives following form of linear equation:

$$\ln[A(f,t)] = \ln S(f) - a\ln(t) - \frac{\pi ft}{Qc}$$

$$\ln[A(f,t)] + a\ln(t) = \ln S(f) - \frac{\pi ft}{Qc}$$

$$\ln[A(f,t)t] = C - bt \tag{5.2}$$

Equation (5.2) represent an equation of line in which constant 'C' is equal to *ln S(f),* '*a'* is the geometrical spreading factor and taken as one for body waves and slope of the line is defined as b ='$\pi f/Q_c$'. Parameter Q_c is the quality factor representing the average attenuation characteristics of the medium. Value of parameters 'b' and 'C' in equation (5.2) is determined by using least square fit and 'Q_c' can be obtained from slope of the *ln*[*A(f,t)t]* verses *'t'* curve.

In the process of determination of frequency dependent coda 'Q_c', the processed accelerogram are filtered at different central frequency over narrow bandwidths. Six different frequency bands have been considered in the present work. Filtered accelerogram is used to determine frequency dependent coda wave quality factor (Q_c). P-wave and S-wave are identified from accelerogram. Normally, lapse time '*t*' is taken as twice the *S*-wave travel time (Rautian and Khalturian 1978), but in case of strong motion records, '*t*' is taken from the point where regular decay of coda waves in the strong motion records start (Gupta and Kumar 2002). The root mean square amplitudes of filtered accelerograms are estimated using a moving time window of 2.56 sec wide with 1.28 sec interval. This amplitude is further use to obtain curve define in equation (5.2). Slope of *ln[A(f,t)t]* verses *'t'* curve give the value at different central frequencies. Slope *ln[A(f,t)t]* of best fit line give the value of coda *'Q_c'* at different central frequencies.

5.5.1 Case Study: Coda Wave Quality Factor for the Kumaon Himalaya

In the present work strong motion data of nine events, comprising 30 accelerograms, recorded at six stations have been used to determine coda wave quality factor (Q_c). Those earthquakes were selected which had maximum coverage of the entire region; their parameters are listed in Table 5.2. Figure 5.2 shows epicenters of located earthquakes, stations which recorded these earthquakes and source-receiver geometry for earthquake occurring in the Kumaon Himalaya.

Table 5.2 Hypocentral parameters and moment magnitude of the events used in the present study from the Kumaon Himalaya and the error obtained in its localisation. ERH and ERZ define the horizontal and vertical error in the location of hypocenter, respectively.

Date	Origin time (GMT)	Epicenter	Depth (km)	No. of Stations	ERH (km)	ERZ (km)	Seismic moment M_o (dyne cm)	Moment magnitude M_w
30/05/06	18:25:18.03	29º54.14',80º 26.95'	03	03	0.9	1.9	$3.0x10^{21}$	3.8
27/10/06	7:55:01.39	29º57.46',80º 15.23'	13	04	5.6	3.1	$2.1x10^{22}$	3.8
08/12/09	07:05:16.70	30º22.39',80º 13.22'	13	03	8.4	5.6	$5.5x10^{22}$	4.5
11/01/10	05:15:14.61	29º48.68',80º 25.06'	12	03	0.2	0.6	$4.3x10^{22}$	4.4
12/01/10	09:35:21.62	29º51.73',80º 21.30'	05	03	0.4	7.2	$2.3x10^{21}$	3.4
26/01/10	06:51:13.30	29º51.82',80º 19.89'	03	03	2.3	1.5	$8.8x10^{21}$	3.9
4/07/10	02:35:57.50	29º51.28',80º 21.16'	13	04	2.4	1.9	$2.0x\ 10^{22}$	4.1
6/07/10	19:08:21.96	29º50.05',80º 21.59'	12	03	0.3	0.2	$5.3x\ 10^{22}$	4.4
17/12/10	12:14:50.84	29º48.45',80º 16.91'	16.4	04	3.1	2.5	$1.3x\ 10^{21}$	3.3

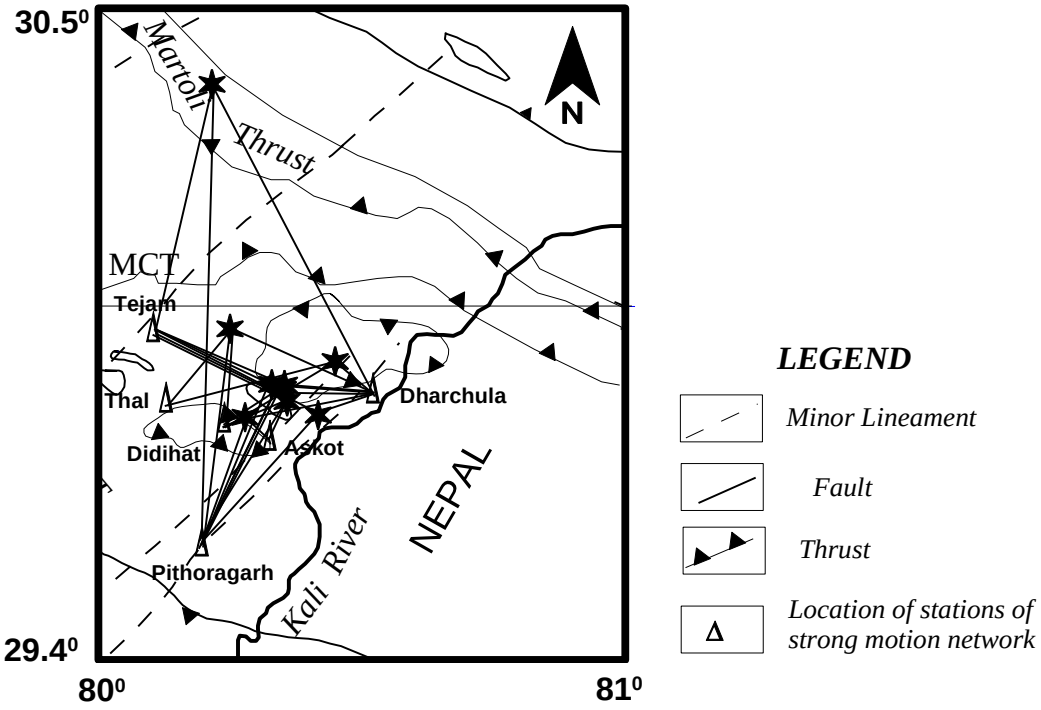

Figure 5.2 Projection of ray path of events recorded at different stations in the Kumaon region. Star shows epicenters of studied events and hollow triangles show recording stations. Tectonics of the region has been taken after GSI (2000).

Figure 5.3 shows P wave, S wave and coda wave of an accelerogram recoded on 27/10/2006 at the Pithoragarh station. Strong motion accelerograms were filtered at six different central frequencies and are shown in Fig. 5.4. The low cutoff, high cutoff and central frequencies of these bands are given in Table 5.3. The filtered accelerogram was used to determine frequency dependent coda wave quality factor $Q_{c.}$ Root mean square amplitude of filtered accelerogram of each event was estimated from time window 2.56 sec of 1.28 sec interval. This amplitude was further used to obtain *ln[A(f, t) t]* versus *t* curve, defined in equation (5.2). Slope of *ln[A(f, t) t]* versus '*t'* curve gives the value of Q_c for different central frequencies for one event recoded at the Pithoragrah station and is shown in Fig. 5.5. Thirty accelerograms, filtered at six different central frequencies, yield an ensemble of 180 plots of *ln[A(f, t) t]* versus *t* for determining frequency dependent $Q_{c.}$ This was further used to obtain a plot of average Q_c versus frequency. Obtained coda

Q(f) relationship at various stations of the Kumaon Himalaya region is given in Table 5.4 and is shown in Fig. 5.6. The best fit curve gives an estimate of frequency dependent Q_c, at different central frequencies for the Kumaon region, and is shown in Fig. 5.7(a). Equation of best fit line of mean value shown in Fig. 5.7(b) gives $Q_c = (65 \pm 2.4) f^{(1.07 \pm .04)}$ for the Kumaon Himalaya.

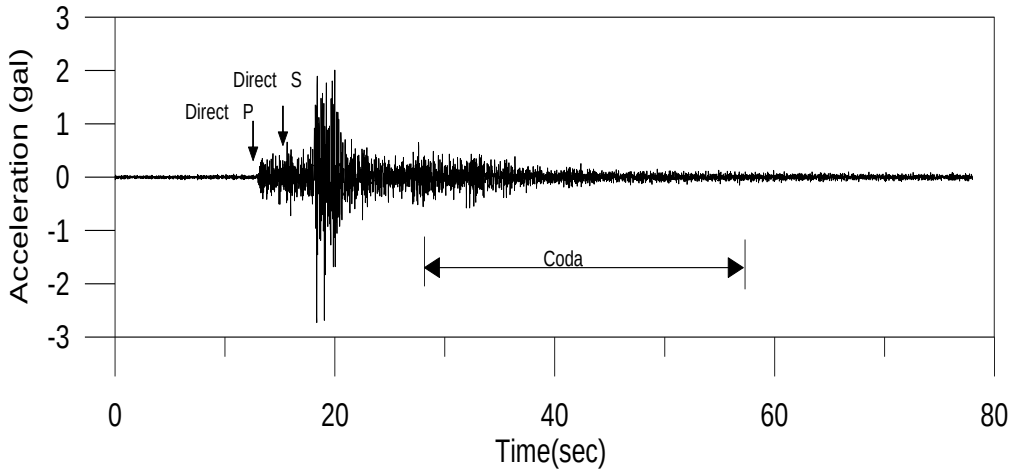

Figure 5.3 An example of observed acceleration record for an earthquake recorded at the Pithoragarh station of Kumaon array.

Table 5.3 Low and high cutoff frequencies of Butterworth band pass filter used for filtering strong motion data.

Low cutoff	Central frequency (Hz)	High Cutoff
1.0	1.5	2.0
2.0	3.0	4.0
4.0	6.0	8.0
8.0	12.0	16.0
16.0	20.0	24.0
24.0	28.0	32.0

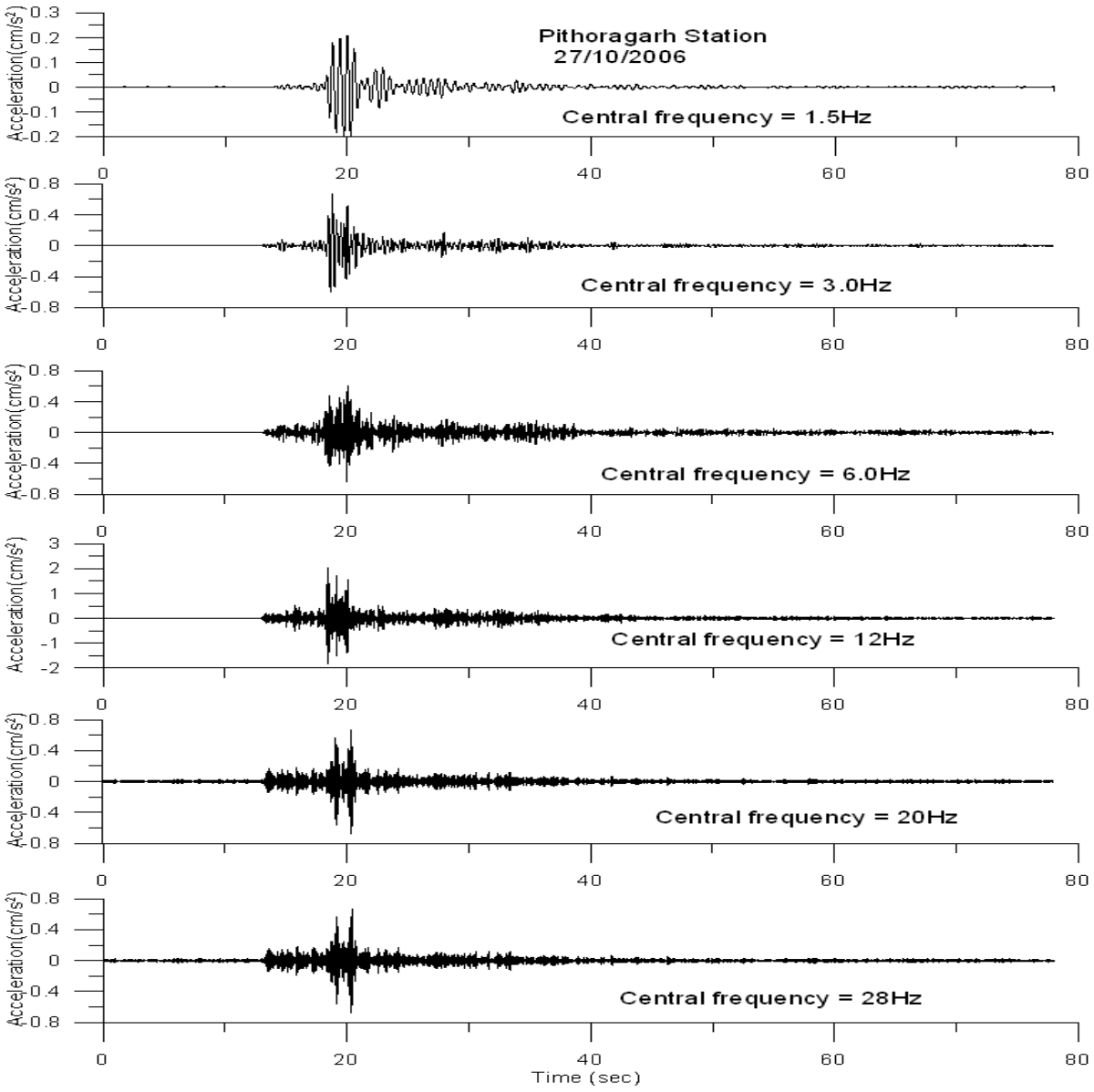

Figure 5.4 Strong motion record of the Pithoragarh station for the event that occurred on 27/10/2006, filtered at different central frequencies.

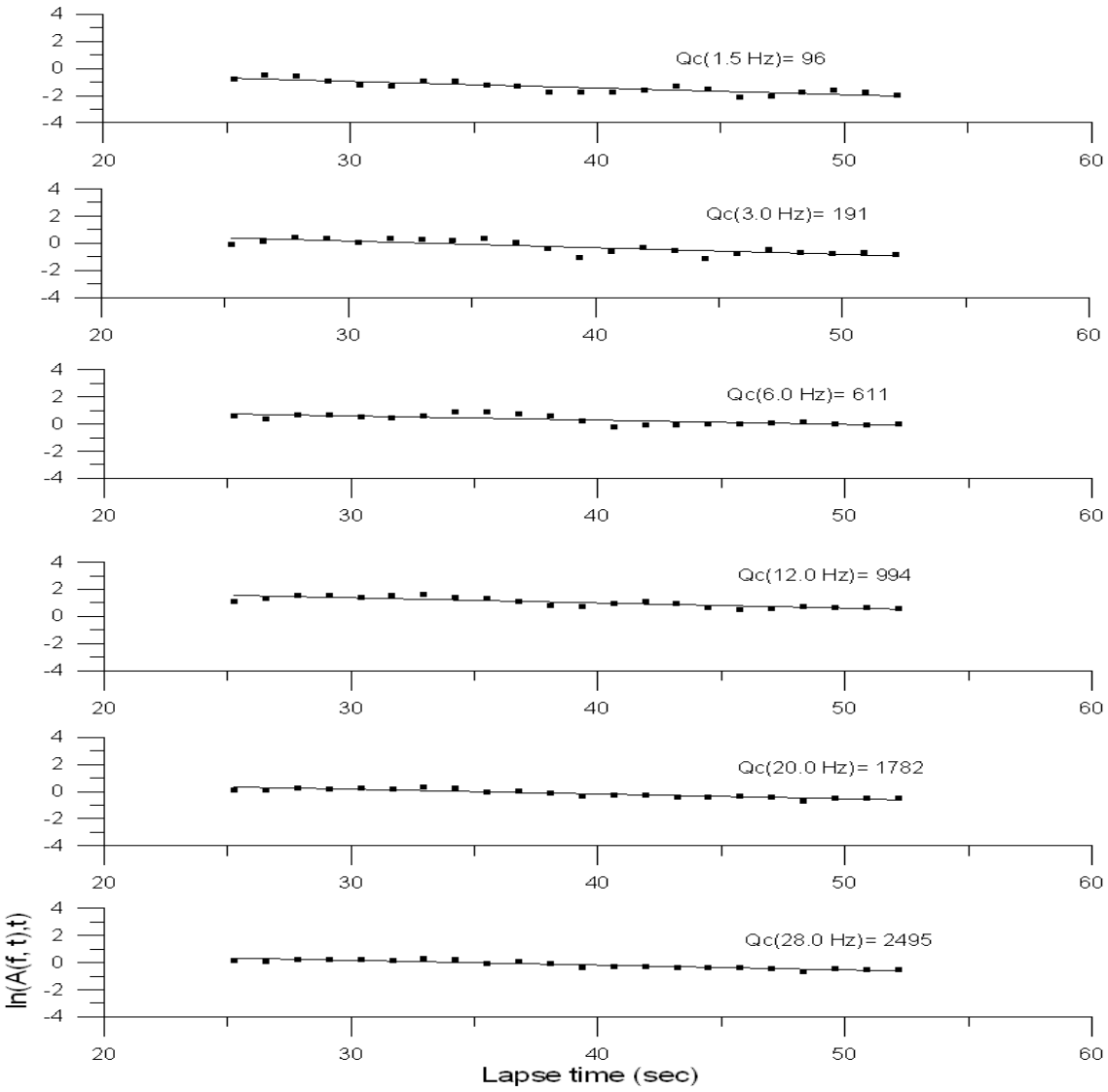

Figure 5.5 Linear equation fitted between logarithmic coda amplitude and lapse time, for estimation of coda Q_c for different central frequencies at the Pithoragarh station for the event recoded on 27/10/2006.

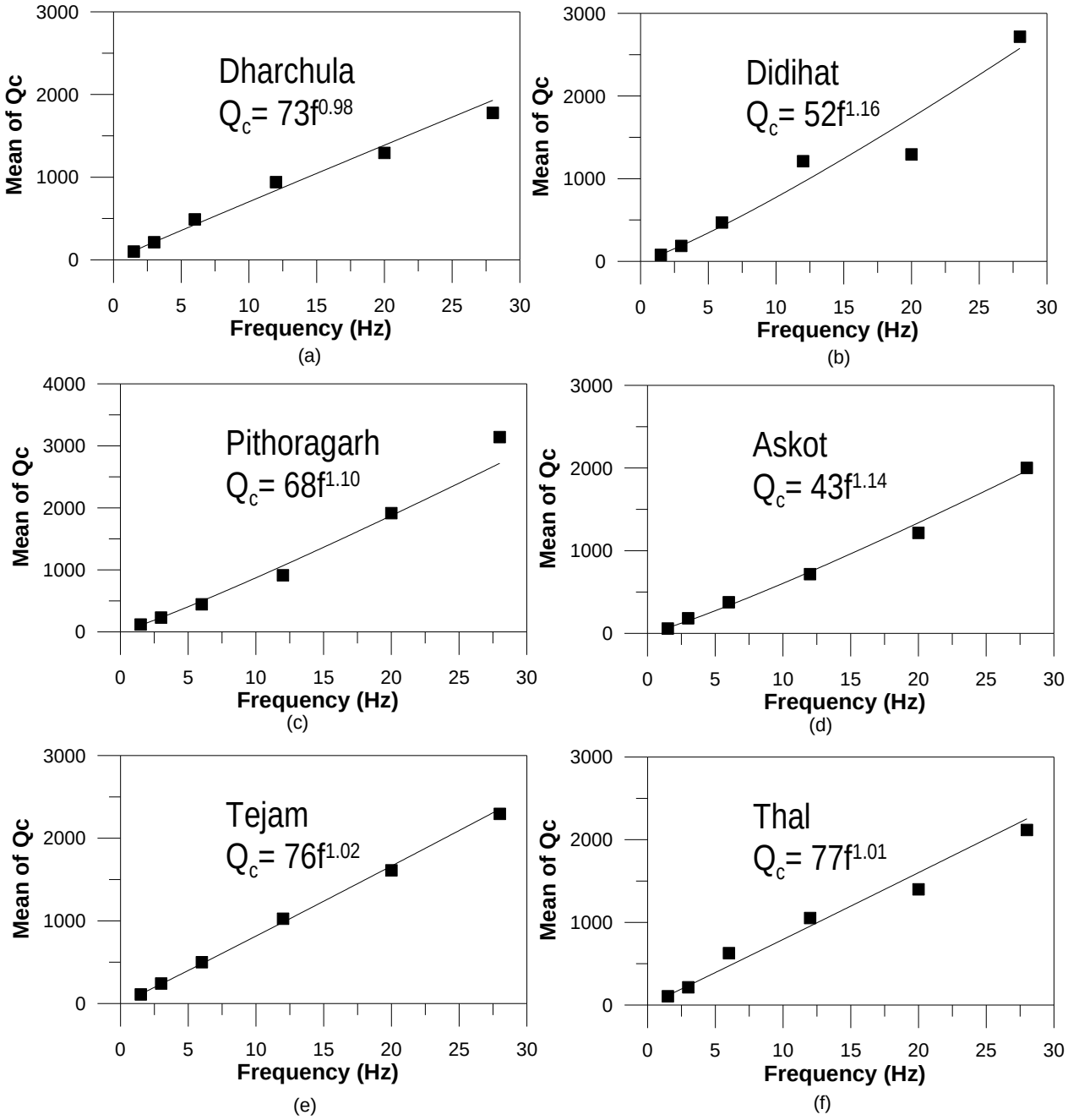

Figure 5.6 Plot for obtained frequency dependent coda $Q_c(f)$ relationship for various stations of the Kumaon Himalaya region.

Table 5.4 Obtained coda $Q_c(f)$ relationship for various stations of the Kumaon Himalaya region.

S.N.	Station Name	Coda Qc Value
1.	Dharchula	$73f^{0.98}$
2.	Didihat	$52f^{1.16}$
3.	Pithoragarh	$68f^{1.10}$
4.	Askot	$43f^{1.14}$
5.	Tejam	$76f^{1.02}$
6.	Thal	$77f^{1.01}$

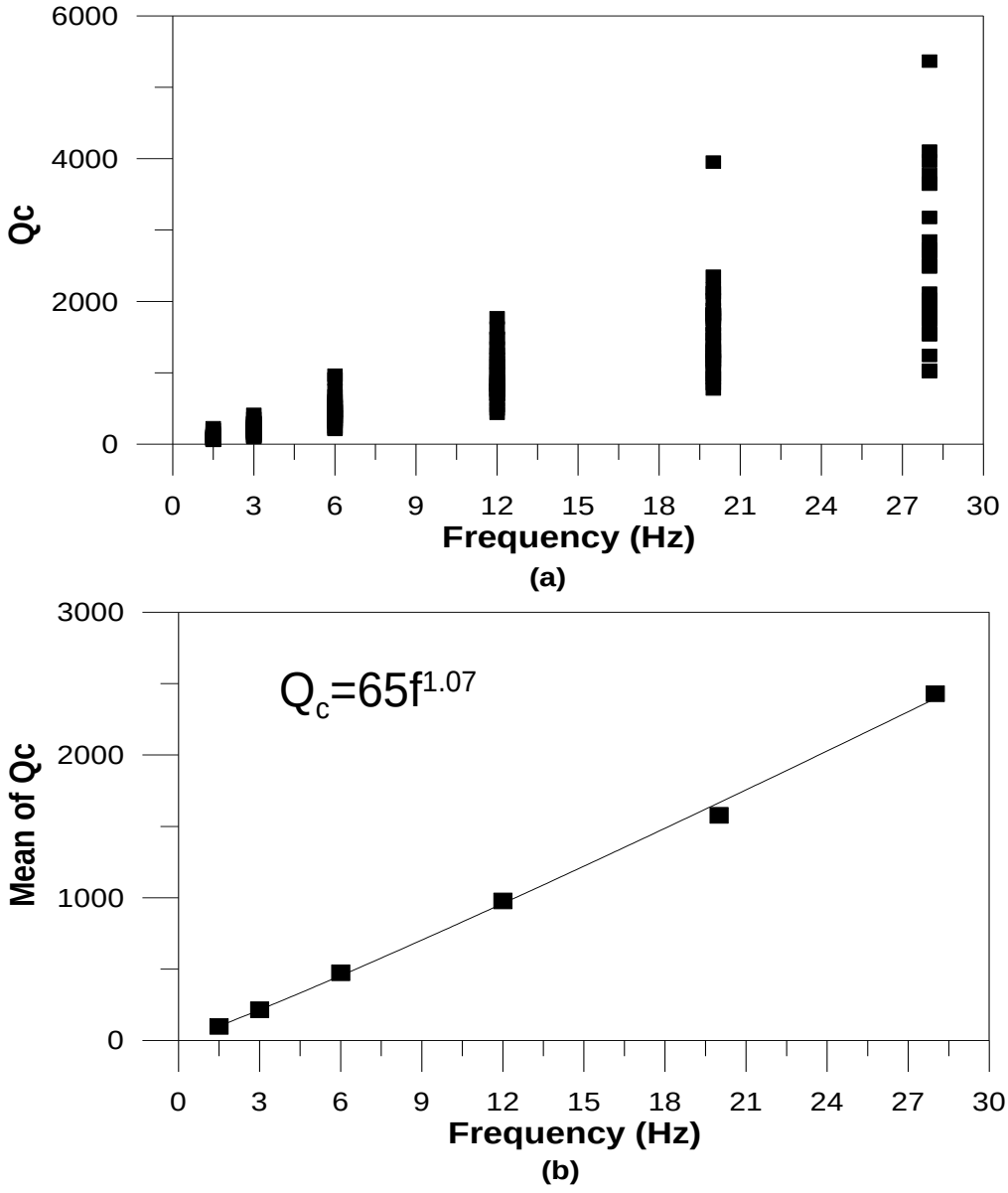

Figure 5.7 Plot for obtained (a) frequency dependent Q_c Values at different central frequencies. (b) Mean value of coda Q_c as a function of frequency for the Kumaon Himalaya.

5.5.2 Case Study: Coda Wave Quality Factor for the Garhwal Himalaya

Strong motion data of nine earthquakes recoded at six stations from the Garhwal Himalaya were taken from the website www.pesmos.in. Figure 5.8 shows location of earthquakes and recording stations used for determination of coda Q_c. Parameters of nine earthquakes used in this analysis are given in Table 5.5. Twenty accelerograms recorded at six stations formed part of the analysis, which was similar to that carried out for data from the Kumaon Himalaya. Figure 5.9 shows the filtered accelerogram at six different central frequencies. Fig. 5.10 gives the value of $Q_c(f)$ for one event recoded at the Uttarkashi station. Obtained coda $Q(f)$ relationship for various stations from the Garhwal Himalaya is given in Table 5.6 and is shown in Fig.5.11. Figure 5.12(a) shows the plot of estimated coda Q_c with different central frequency for the Garhwal region. Average value of Q_c obtained at different central frequency is further used to obtain regional $Q_c(f)$ relationship for this region and is given in Fig. 5.12(b). The regional $Q_c(f)$ relationship for the Garhwal Himalaya is obtained as $Q_c = (96 \pm 6.9)\, f^{(1.06 \pm .04)}$.

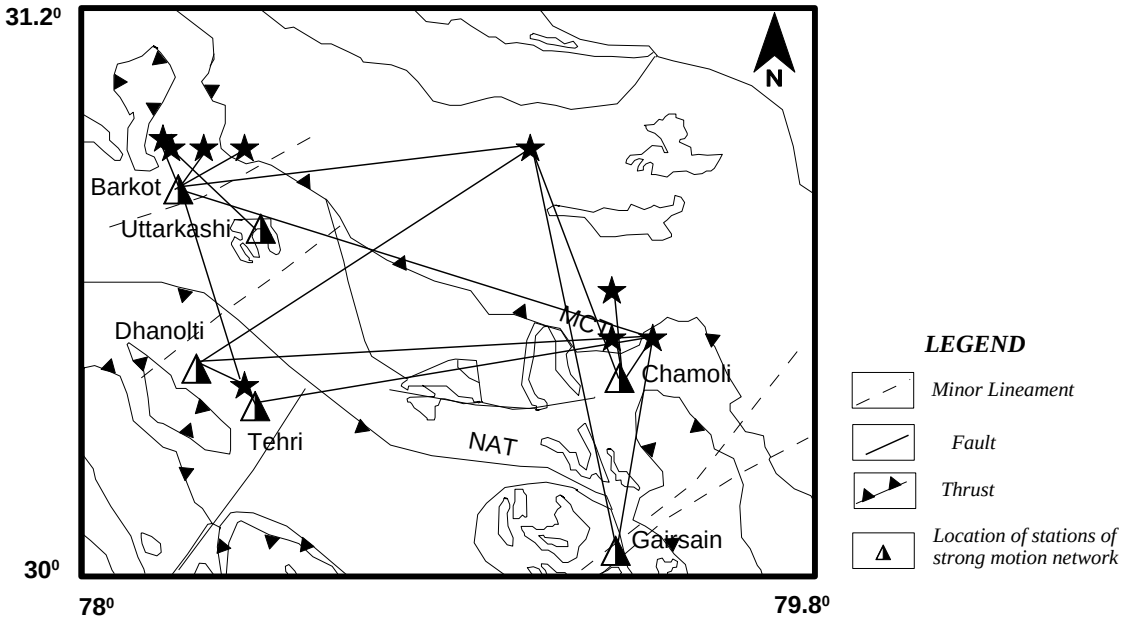

Figure 5.8 Projection of ray path of events recorded at different stations in the Garhwal region. Star shows epicenters of studied events and half filled triangles show the recording stations. Tectonics of the region has been taken after GSI (2000).

Table 5.5 Moment magnitude and hypocentral parameters of the events used in the present study for the Garhwal Himalaya taken from website www.pesmos.in

Date	Origin time (UTC)	Epicenter	Depth (km)	Moment magnitude M_w (IMD)
18/03/09	11:22:42	30.9N,78.2E	10	3.3
21/09/09	09:43:37	30.9N,79.1E	13	4.7
03/05/10	17:15:08	30.4N,78.4E	08	3.5
20/06/11	06:27:18	30.5N,79.4E	12	4.6
21/09/11	02:24:36	30.9N,78.4E	10	3.1
24/09/11	14:32:18	30.9N,78.3E	10	3.0
25/02/09	04:04:21	30.6N, 79.3E	10	3.7
15/05/09	18:39;22	30.5N,79.3E	15	4.1
9/02/12	19:17:29	30.9N, 78.2E	10	5.0

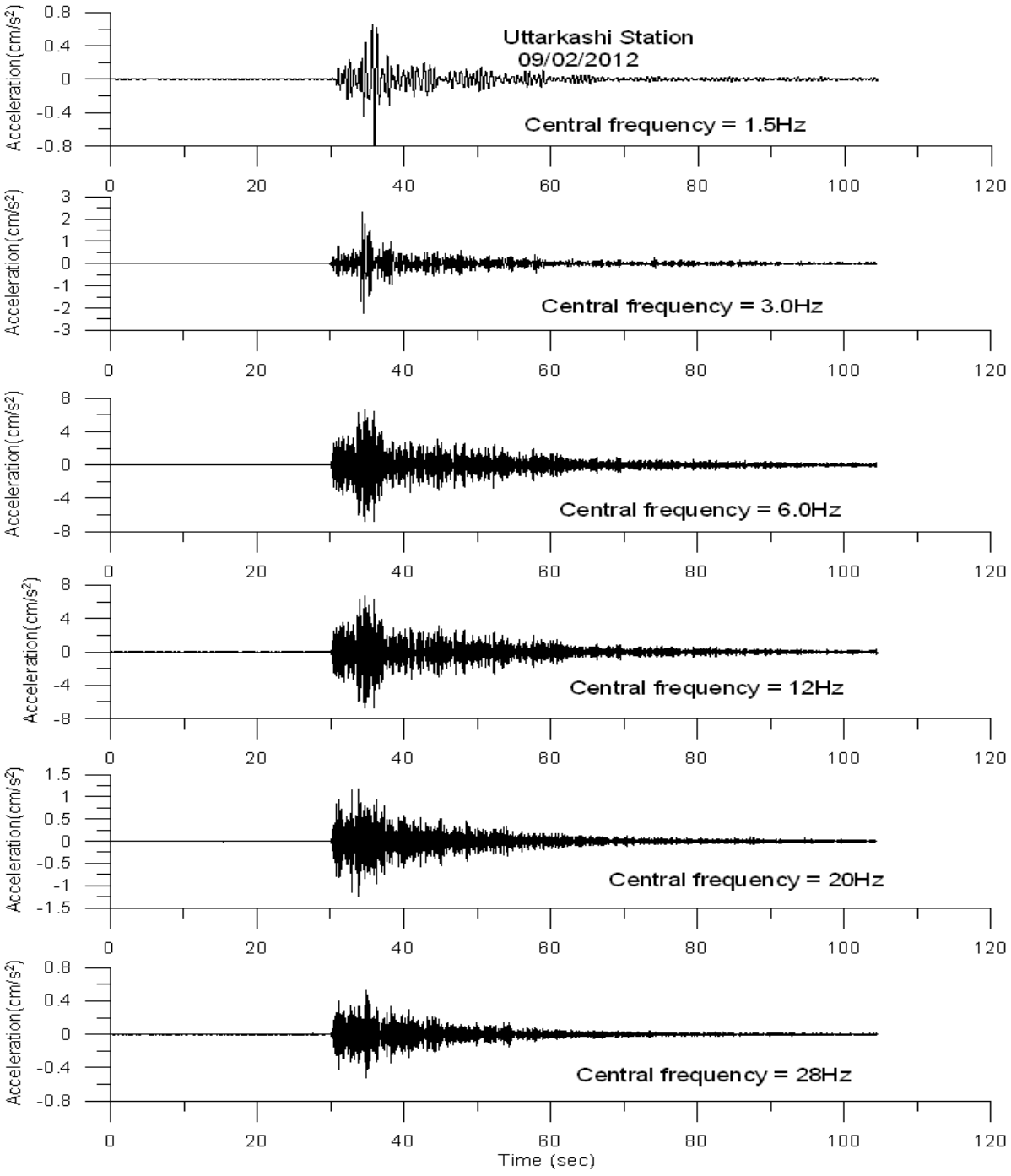

Figure 5.9 Strong motion record at the Uttarkashi station for event that occurred on 09/02/2012, filtered at different central frequencies.

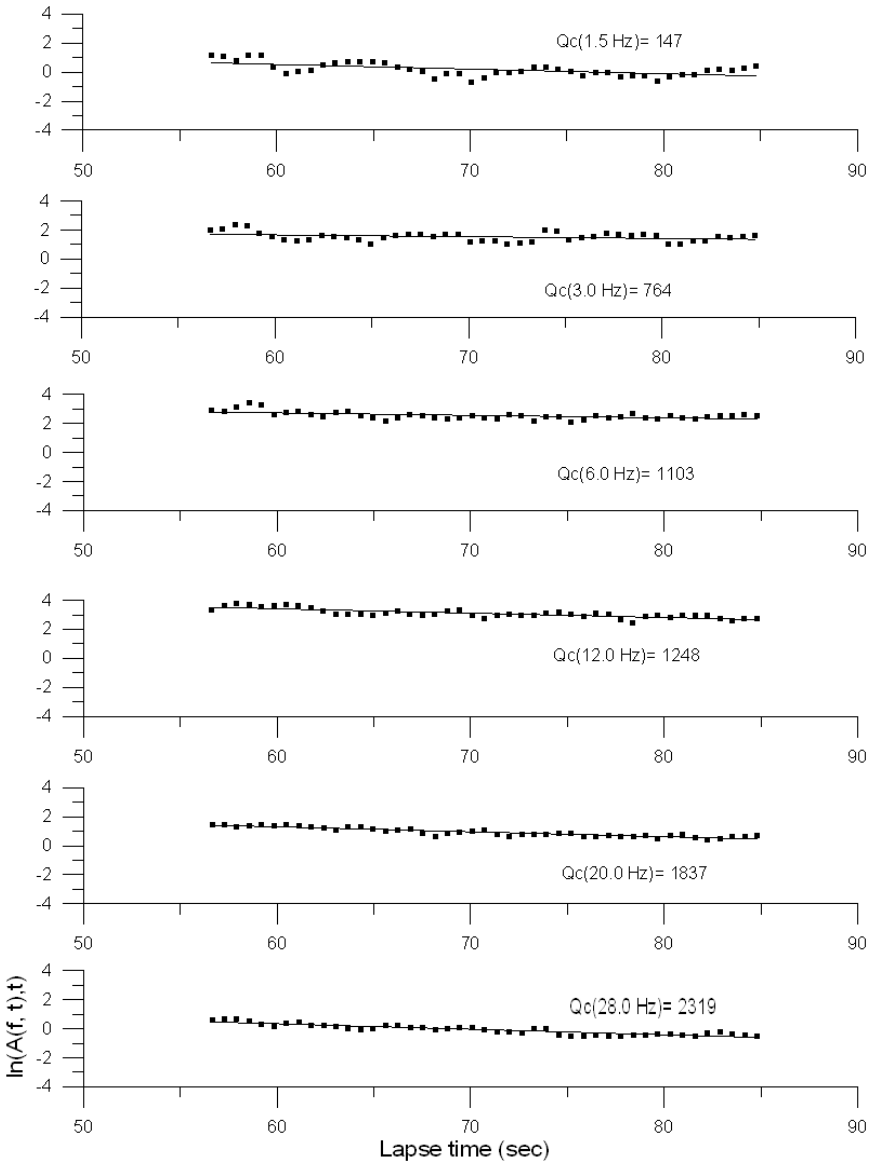

Figure 5.10 Linear equation fitted between logarithmic coda amplitudes and lapse time for estimation coda Q_c at the Uttarkashi station for the event recoded on 09/02/2012.

Table 5.6 Obtained coda *Q(f)* relationship for various stations of the Garhwal region.

S.N.	Station Name	Coda Qc Value
1.	Barkot	$87f^{1.06}$
2.	Chamoli	$72f^{1.15}$
3.	Tehri	$61f^{1.14}$
4.	Uttarkashi	$118f^{0.81}$
5.	Dhanaulti	$84f^{1.09}$
6.	Garsain	$107f^{1.05}$

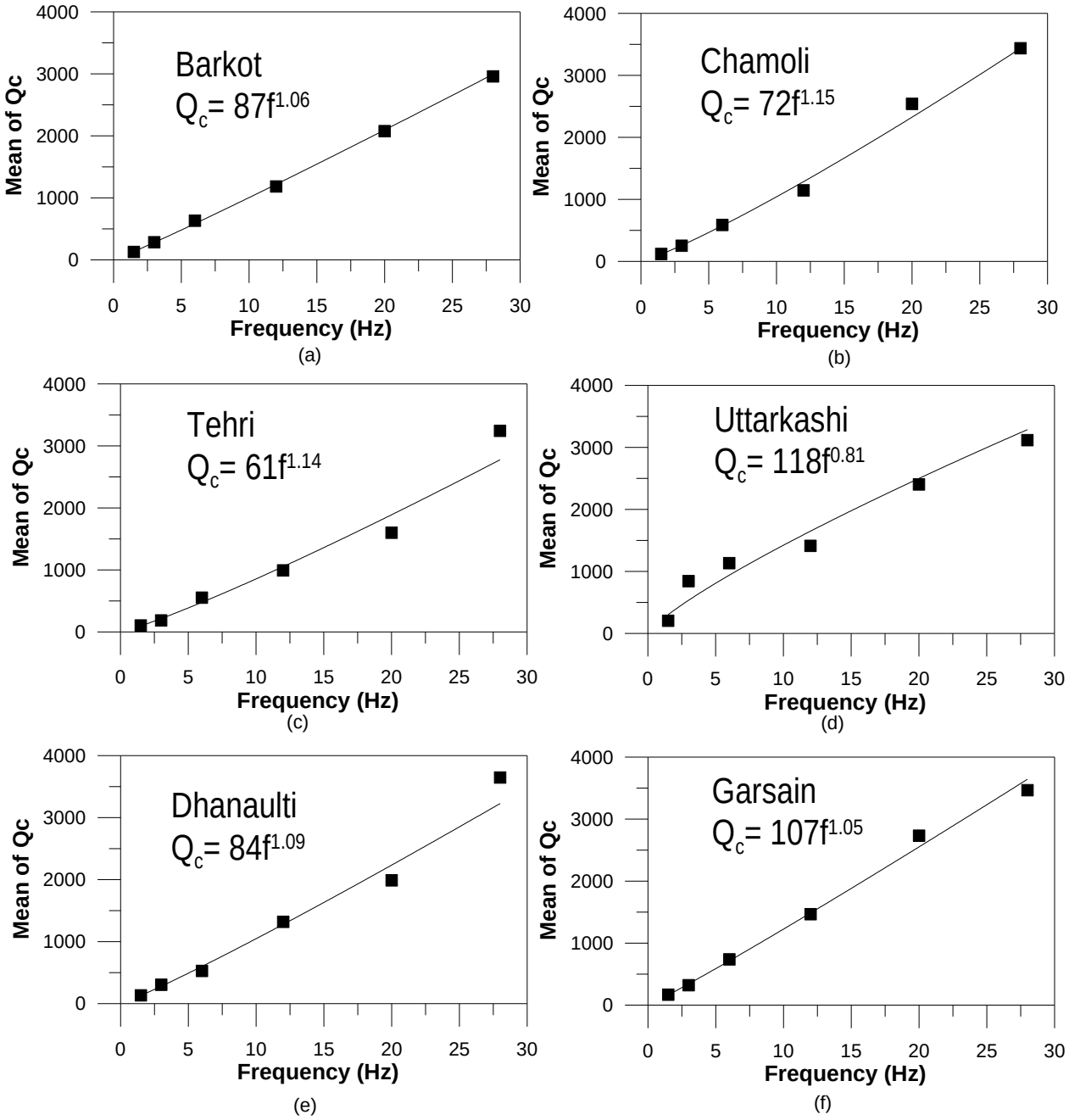

Figure 5.11 Plot for obtained frequency dependent *Q(f)* relationship for various stations of the Garhwal region.

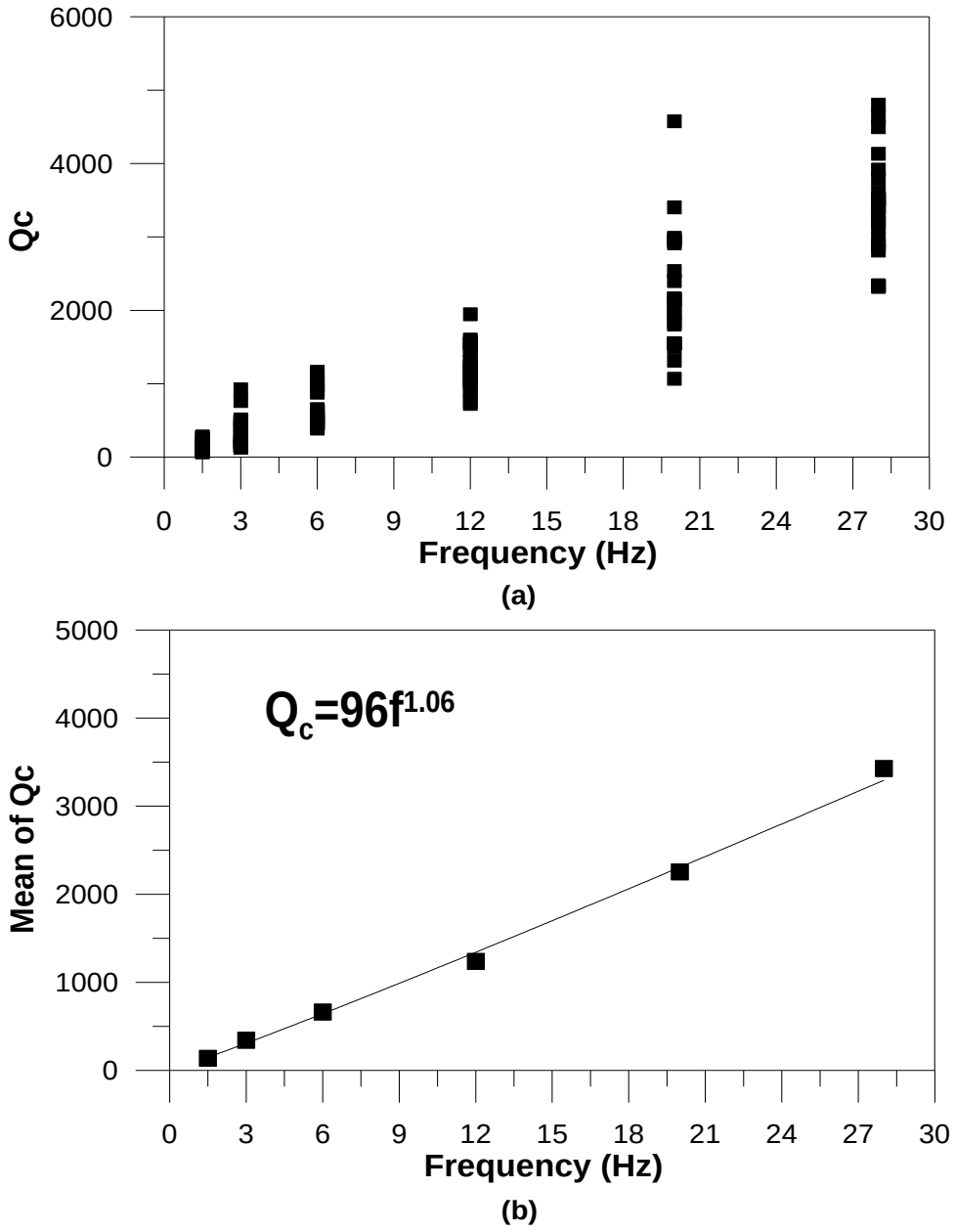

Figure 5.12 Plot for obtained (a) frequency dependent Q_c at different central frequencies for Garhwal Himalaya. (b) Mean value of coda Q_c as a function of frequency for Garhwal Himalaya.

5.6 Results and Discussion

The study of frequency dependent coda wave quality factor Q_c is interpreted as an important tectonic parameter. Regions of high tectonic activities are characterized by low values of Q_c compared to stable regions where Q_c is high. Further, the frequency dependent coda wave relationship, in the form of $Q_c = Q_0 f^n$, generally provides estimate of Q_0 (Q_c at 1 Hz) which represents the level of medium heterogeneities. The power of frequency dependence given by parameter *n* represents the level of tectonic activity of the region; high value of *n* indicates high tectonic activity. The Kumaon Himalaya is more heterogeneous and less stable tectonically as compared to the adjoining the Garhwal Himalaya (Paul et al. 2003, Gupta et al. 1995). The fitting of the power law $Q_c = Q_0 f^n$ gives the frequency dependent relationship for the Kumaon Himalaya as $Q_c = (65 \pm 2.4) f^{(1.07 \pm .04)}$ and for the Garhwal Himalaya and $Q_c = (96 \pm 6.9) f^{(1.06 \pm .04)}$. In the present study, as *n* has almost the same numerical value for both the Kumaon and Garhwal regions, it implies a similar tectonic activity in both regions. The coda wave quality factor obtained in the present work for two regions shows that these regions have different attenuation properties and almost similar level of tectonic activity. Several frequency dependent relationships for various Indian and worldwide regions are given in Table 5.7. A comparison of Q_c obtained in the present work, when made with available values obtained in other parts of India, and the world, shown in Fig. 5.13(a) and 5.13(b), respectively, indicates that the distribution falls within the range of values justified for tectonically active regions. The contours of Q_o values obtained at different stations are shown in Fig. 5.14. The contours of Q_o value shows that the region of Garhwal Himalaya is covered by high Q_o contours compared to the Kumaon Himalaya. This clearly indicates presence of high attenuating medium in the Kumaon Himalaya as compared to the Garhwal Himalaya.

The attenuation relations obtained for the Kumaon and Garhwal Himalaya support two different attenuation models which indicate two different attenuation properties for these regions. In order to confirm this attenuation trend we have compared the anelastic attenuation of shear wave and coda wave quality factor in the Kumaon and Garhwal Himalaya. The comparison of anelastic attenuation in terms of shear wave quality factor '$Q_\beta(f)$' obtained for the Garhwal and Kumaon Himalaya by Joshi (2006) and Joshi et al. (2010b) is shown in Fig. 5.15(a). The shear wave quality factors for these regions have been calculated using strong motion dataset from the Garhwal and

the Kumaon Himalaya by Joshi (2006) and Joshi et al. (2010b), respectively. It is seen from Fig.5.15 (a) and 5.15(b) that the shear wave quality factor $Q_{\beta}(f)$ and coda wave quality factor $Q_c(f)$ respectively, have comparative higher value in almost all frequencies in the Garhwal region as compared to the Kumaon Himalaya, indicating high attenuation in almost all frequencies in the Kumaon Himalaya. The estimate of shear wave and coda wave quality factor depends on characteristics of the medium between the source and station. Therefore, results obtained in the present work confirm the presence of a highly attenuating medium beneath the Kumaon Himalaya, as compared to the Garhwal Himalaya.

Table 5.7 Frequency dependent *Q(f)* relationship for various Indian and worldwide regions.

Relation	**Region**	**Reference**
$126f^{0.95}$	Garhwal Himalaya	Gupta et al. (1995)
$86f^{1.01}$	NE Himalaya	Gupta and Kumar (2002)
$92f^{1.07}$	Kumaon Himalaya	Paul et al. (2003)
$158f^{1.05}$	NW Himalaya	Kumar et al. (2005)
$117f^{0.97}$	Koyna region	Sharma et al. (2007)
$119f^{0.99}$	Garhwal-Kumaon Himalaya	Mukhopadhyay and Sharma (2010)
$80f^{1.10}$	Friuli Italy	Rovelli (1982)
$63f^{0.97}$	Washington state, USA	Havskov et al. (1989)
$155f^{0.89}$	South Spain	Ibanez et al. (1990)
$100f^{0.70}$	South Iberia	Pujades et al. (1991)
$79f^{0.74}$	Park field	Hellweg et al. (1995)
$152f^{0.84}$	South Central Alaska	Dutta et al. (2004)

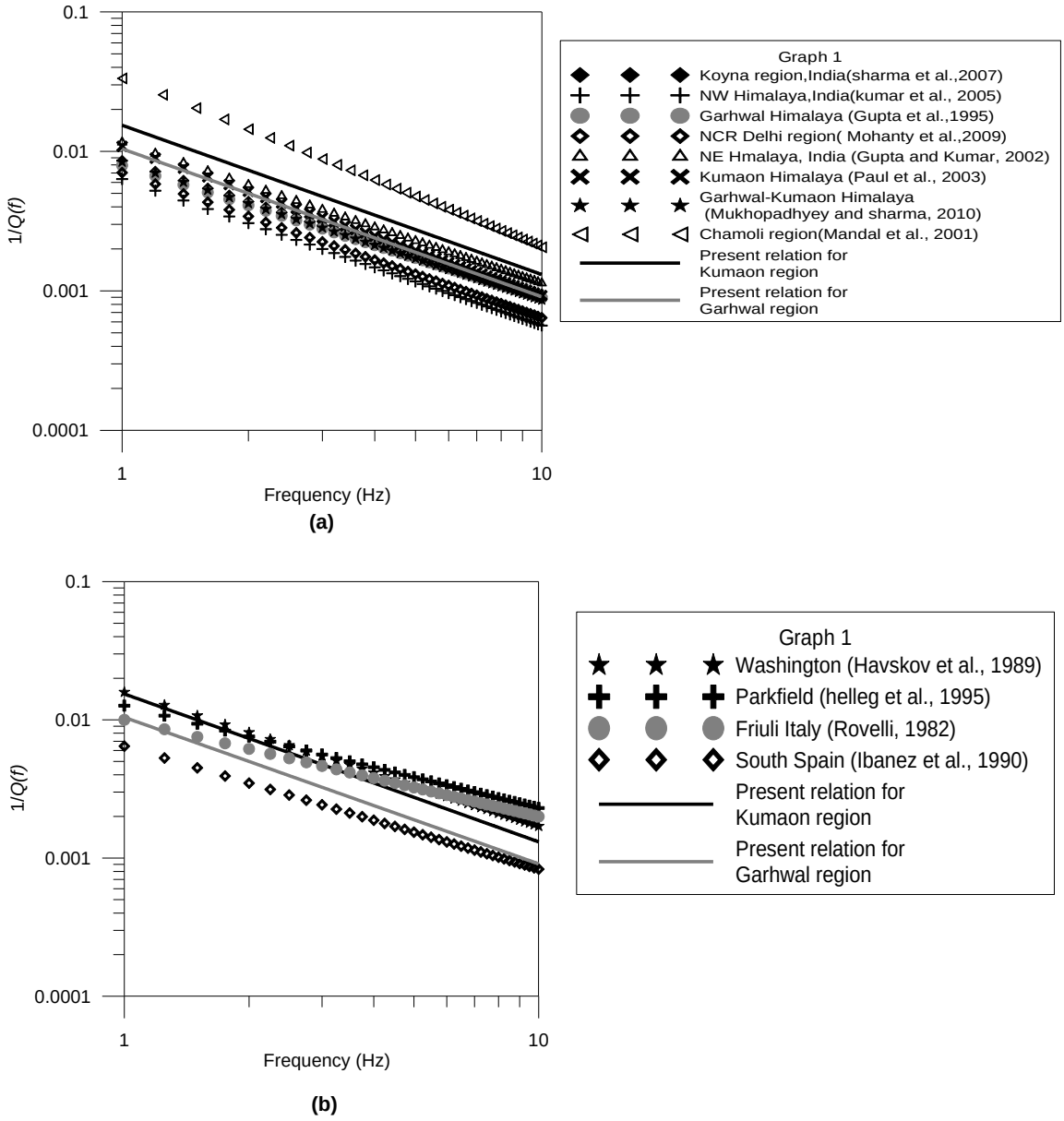

Figure 5.13 Comparison of $Q_c(f)$ relations developed in present work with (a) Indian region, and (b) for worldwide regions.

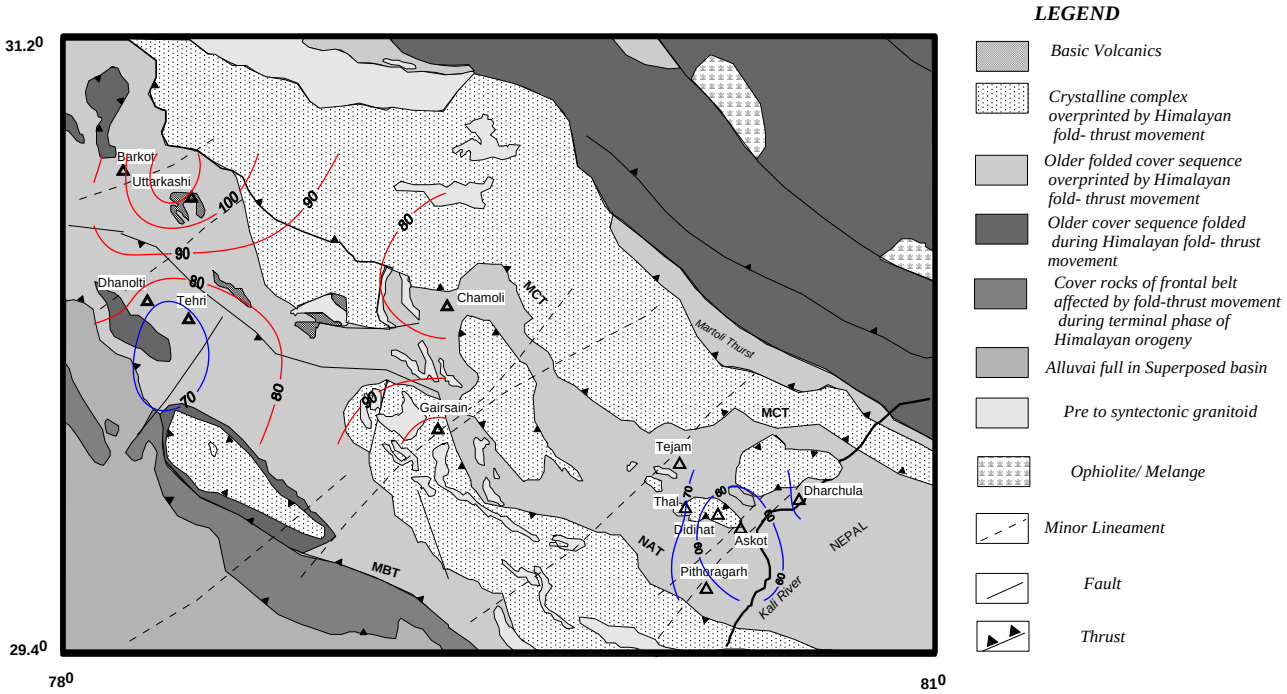

Figure 5.14 Contours of Q_o values obtained for the Kumaon and Garhwal Himalaya. Red and blue lines show the values of Q_o greater than and less than equal to 70, respectively.

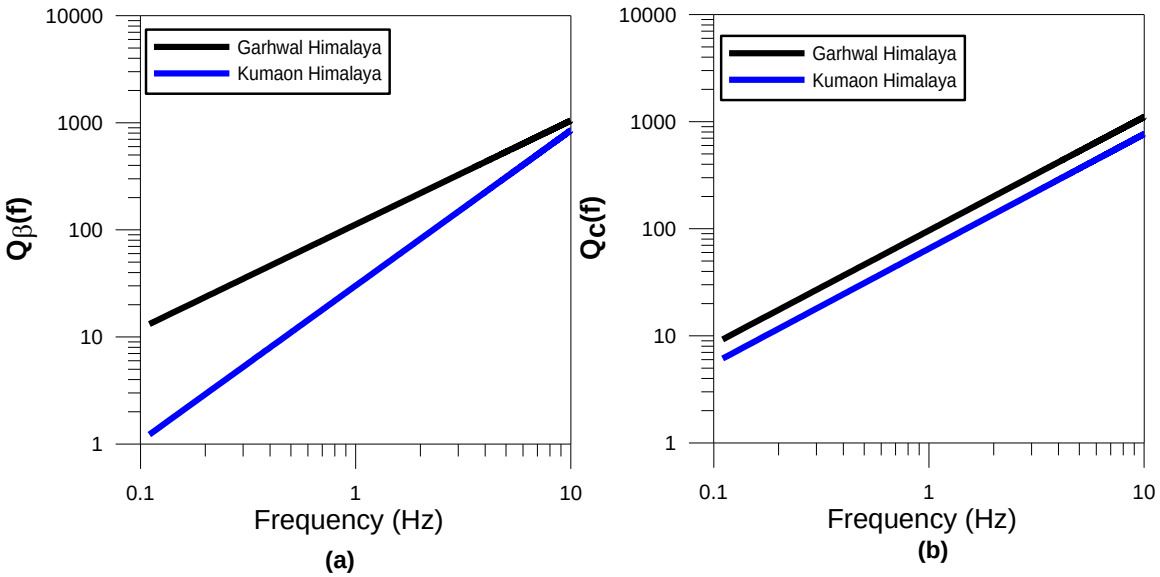

Figure 5.15 Comparisons of (a) $Q_\beta(f)$ relation and (b) $Q_c(f)$ relations developed in present study for the Garhwal and Kumaon Himalaya. The $Q_\beta(f)$ relationship for the Garhwal and Kumaon Himalaya has been used after Joshi (2006) and Joshi et al. (2010b), respectively.

5.7 Conclusion

In this Chapter coda wave quality factor for the Kumaon and Garhwal Himalaya has been investigated. Coda wave quality factor has been obtained using strong motion data recorded by two regional networks. Strong motion records were filtered using a band pass Butterworth filter at central frequencies of 1.5, 3.0, 6.0, 12.0, 20.0 and 28.0 Hz, respectively. Using single backscattering model the frequency dependent Q_c relationship for the Kumaon and Garhwal Himalaya were obtained as $Q_c = (65 \pm 2.4) f^{(1.07 \pm .04)}$ and $Q_c = (96 \pm 6.9) f^{(1.06 \pm .04)}$, respectively. Comparative study of attenuation characteristics of the Kumaon and Garhwal Himalaya indicate that the Kumaon Himalaya has a higher attenuation characteristic compared to the Garhwal Himalaya.

CHAPTER - 6

Seismic Hazard Assessment of the Uttarakhand Himalaya

6.1 Introduction

Seismic zoning can be defined as a process of demarcating or mapping areas of equal seismicity, or of equal hazard related to a characteristic of strong ground shaking and of site or structural response (Todorovska et al. 1995). An evaluation of seismic hazards, whether deterministic (scenario based) or probabilistic, requires an estimate of the expected ground motion at the site of interest. Seismic hazard in an area can be estimated by two approaches: (1) Probabilistic seismic hazard assessment approach (PSHA) and (2) Deterministic seismic hazard assessment approach (DSHA). Deterministic seismic hazard analysis (DSHA) is basically a method of engineering design that incorporates available data from geology leading to estimates of earthquake activity, plus everything else we know about a site and its environment, the tectonics, the past seismicity, the soil mechanics, the statistics and the sociology (Heriberta and Lomnitz 2002). Both approaches use the same datasets, which include earthquake sources, occurrence frequencies, and peak ground attenuation relationships. Due to the discontinuous recording of seismic activity within Himalaya, there is no continuous catalogue in this study area. This is a major drawback for any hazard study in this area no matter whether it is a probabilistic seismic hazard assessment approach (PSHA) or deterministic seismic hazard assessment approach (DSHA) technique. Joshi and Patel (Tectonophysics 283:289-310; 1997) have formulated a method of seismic hazard zonation, which is based on the modelling of finite rupture plane along identified lineaments in the region using the semi empirical simulation technique given by Midorikawa (1993). This method has advantage of using strong ground motion prediction equation of small magnitude earthquake to model strong motion parameters of large earthquake. The method of seismic zonation given by Joshi and Patel (1997) has been modified in this work to prepare seismic hazard zonation map of the Uttarakhand Himalaya region defined by the probability of exceedence of peak ground acceleration.

6.2 Method of Seismic Hazard Zonation

Seismic hazard zonation technique given by Joshi and Patel (1997) is based on the deterministic modeling of finite ruptures along identified probable fault in an area using semi empirical approach. The advantage of semi empirical simulation technique has been already discussed in Chapter 4. This technique of zonation has been applied for the Doon valley (Joshi and Patel 1997); NE part of India (Joshi et al. 2007); Assam valley (Joshi et al. 2007) and Uttarakhand Himalaya (Joshi and Mohan 2010). The technique of zonation presented by earlier researcher using the semi empirical simulation technique is based on the method given by Midorikawa (1993), which in turn is dependent on the attenuation relation applicable for the region under study. Applicability of attenuation relation is an important factor for successful implementation of this technique. Due to scarcity of enough strong motion data set in this region attenuation relation developed for worldwide earthquakes have been used in earlier study. The seismic hazard map prepared earlier by Joshi and Mohan (2010), Joshi and Patel (1997) for the Uttarakhand Himalaya is based on the attenuation relation given by Abrahamson and Litehiser (1989). Although attenuation relation given by Abrahamson and Litehiser (1989) is based on worldwide data it is seen that this relation also suffer from problem of overestimation and deviation from normality when used for predicting the Kumaon Himalayan earthquakes (Chapter 3). Besides using attenuation relation of worldwide applicability for preparing of seismic hazard zonation map for the Uttarakhand Himalaya, these map suffer a drawback of not including concept of probability of exceedence of specific peak ground acceleration (PGA) value. In the present study modification in earlier work by Joshi and Patel (1997) has been made to include the concept of probability of exceedence. Various steps in this modified technique are given as follows:

(i) The first step in the preparation of seismic hazard map is the identification of active lineaments. This identification is based on various geological information, satellite-imageries and geological field work done by other workers in the study area. The length of a possible rupture along these lineaments is measured from the same map. The lengths of possible ruptures along these lineaments are calculated using the following empirical relationship given by Wells and Coppersmith (1994):

$$\text{Log}\,(L) = -2.42 + 0.58M_w \qquad (6.1)$$

Where, 'M_w' is moment magnitude and 'L' is rupture length in kilometer.

Assuming the rectangular rupture model, the ruptured area (A) is calculated by using empirical relation given by Kanamori and Anderson (1975):

$$\text{Log (A)} = M_s - 4 \tag{6.2}$$

Where, A = Area of the rupture fault in square km.

M_s = Surface wave magnitude.

This area (A) is further used to compute the width (W) of the rupture plane i.e. W = A/L. the values of parameters L, W, L_e and W_e for each rupture model are computed from applicable empirical relations and self-similarity laws given by Kanamori and Anderson (1975).

$$L/L_e = W/W_e = T/\tau = D/d = \left(M_o/M_o'\right)^{1/3} = N \tag{6.3}$$

where,

L and L_e = Length of the rupture plane of the target and small earthquakes, respectively;

W and W_e = Width of the rupture plane of the target and small earthquakes, respectively;

T and τ = slip duration of the target and small earthquakes, respectively;

D and d = slip of the target and small earthquakes, respectively;

M_o and M_o' = seismic moment of the target and small earthquakes, respectively and

N = total number of sub-faults along the length or width of the rupture plane of target earthquake. Various parameters defined in equation (6.3) is shown in Fig. 6.1.

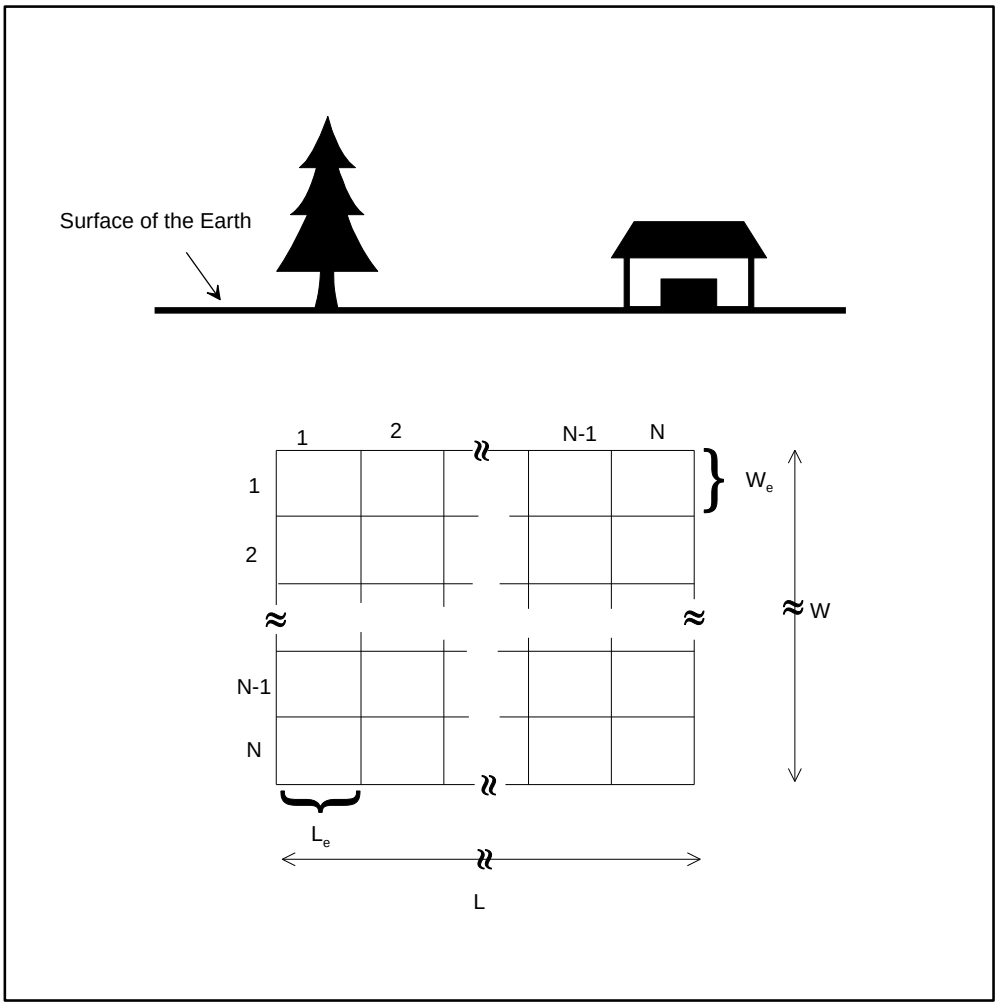

Figure 6.1 Various parameters of the rupture plane.

(ii) Number of subfaults along length or width is assumed as N and this is calculated by following relationship given by Sato (1989):

$$N = 10^{.5(M-m)} \tag{6.4}$$

where, 'M' and 'm' are the magnitude of target and small earthquakes, respectively.

(iii) Entire region is divided into a grid consisting of several observation points at which peak ground acceleration is computed from the simulated acceleration using semi empirical technique.

(iv) At each observation point acceleration records are simulated by modeling each rupture along selected lineament. For preparation of seismic zonation map of the Uttarakhand region two attenuation relations have been used. These are attenuation relations developed from database of small magnitude earthquakes in the Kumaon and Garhwal Himalaya, defined in Chapter 3. Following are two sets of attenuation relationships used in present work.

For Kumaon Himalaya:

$$\ln(PGA) = -0.336 + 2.58M_W + 0.018R - 2.96\ln(R+15) \tag{6.5}$$

$$\ln(PGA) = -5.8 + 2.62M_w - 0.16\ln R - 1.33\ln(E+15) \tag{6.6}$$

For Garhwal Himalaya:

$$\ln(PGA) = 2.29 + 2.07M_w + 1.95\ln R - 4.03\ln(R+15) \tag{6.7}$$

$$\ln(PGA) = -4.8 + 1.92M_w - 0.014R - 0.17\ln(E+15) \tag{6.8}$$

In above equations, PGA is peak ground acceleration in gals, M_w is moment magnitude, and R is hypocentral and E is epicentral distance in kilometers.

For 'm' number of lineaments 'm' values of peak ground accelerations i.e., P_{a1}, P_{a2},.....,P_{am} are obtained at a single observation point. In the present work acceleration records are simulated for various possibilities of nucleation point. For a rupture divided into subfualts of size n×n there are n×n possibilities of nucleation point. Therefore the process of simulation generates a dataset of peak ground acceleration which consists of n×n possibilities of ruptures for a single rupture model. The database includes contributions from ruptures within 100 km radius from the observation point. The probability of exceedence of peak ground acceleration is then computed from the developed database of peak ground acceleration values from several models at a given observation site.

(v) Since we are dealing with a small area having limited database therefore the similar frequency magnitude relation is expected in the region. The obtained frequency magnitude relation for this region is calculated on the basis of data from United States Geological Survey (USGS) shown in Fig. 6.2. The developed frequency magnitude relation is given as:

$$L\log_{10} N = 5.7 - 0.71M_w \tag{6.9}$$

Where, M_w is the magnitude of earthquake and N is number of earthquake equal or more than M_w. The plot of $Log_{10}N$ verses magnitude is shown in Fig. 6.2.

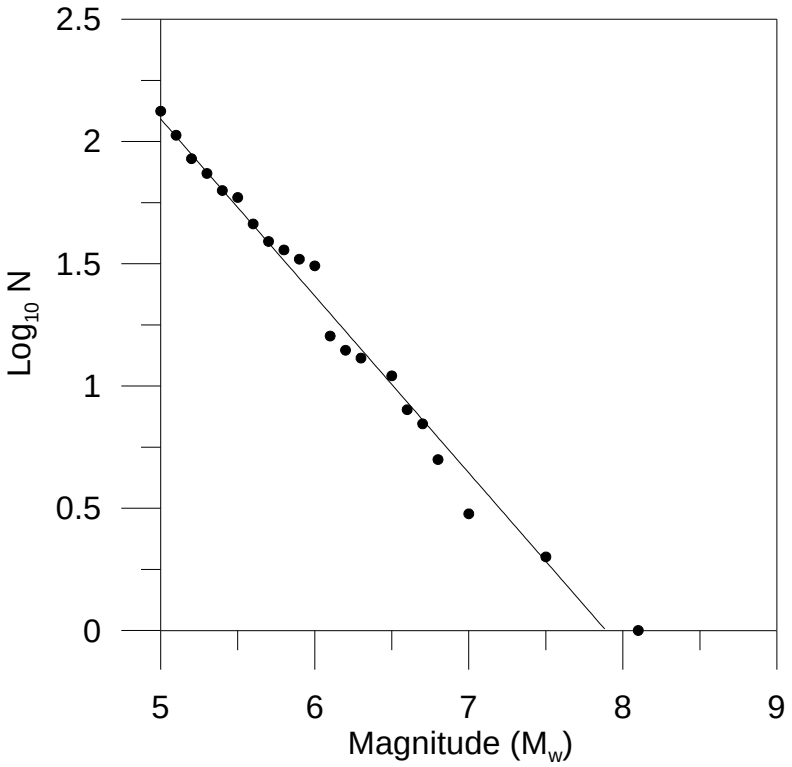

Figure 6.2 Frequency verses magnitude relationship for the Uttarakhand Himalaya region.

(vi) This process is repeated for all observation points and the probability of exceedence of peak ground acceleration at each point is computed. Contours of the expected acceleration are used in the preparation of a seismic hazard zonation map.

The flow diagram of this modified seismic zonation technique is shown in Fig. 6.3. For the purpose of preparation of the seismic hazard zonation map, the computer software 'EQHAZ' has been developed in the FORTRAN language. Required inputs to this software are parameters of the rupture plane, its location, velocity model of the region and attenuation relations applicable in the study region. The output from this software consists of the probability of exceedence of peak ground acceleration at each specified location on the map.

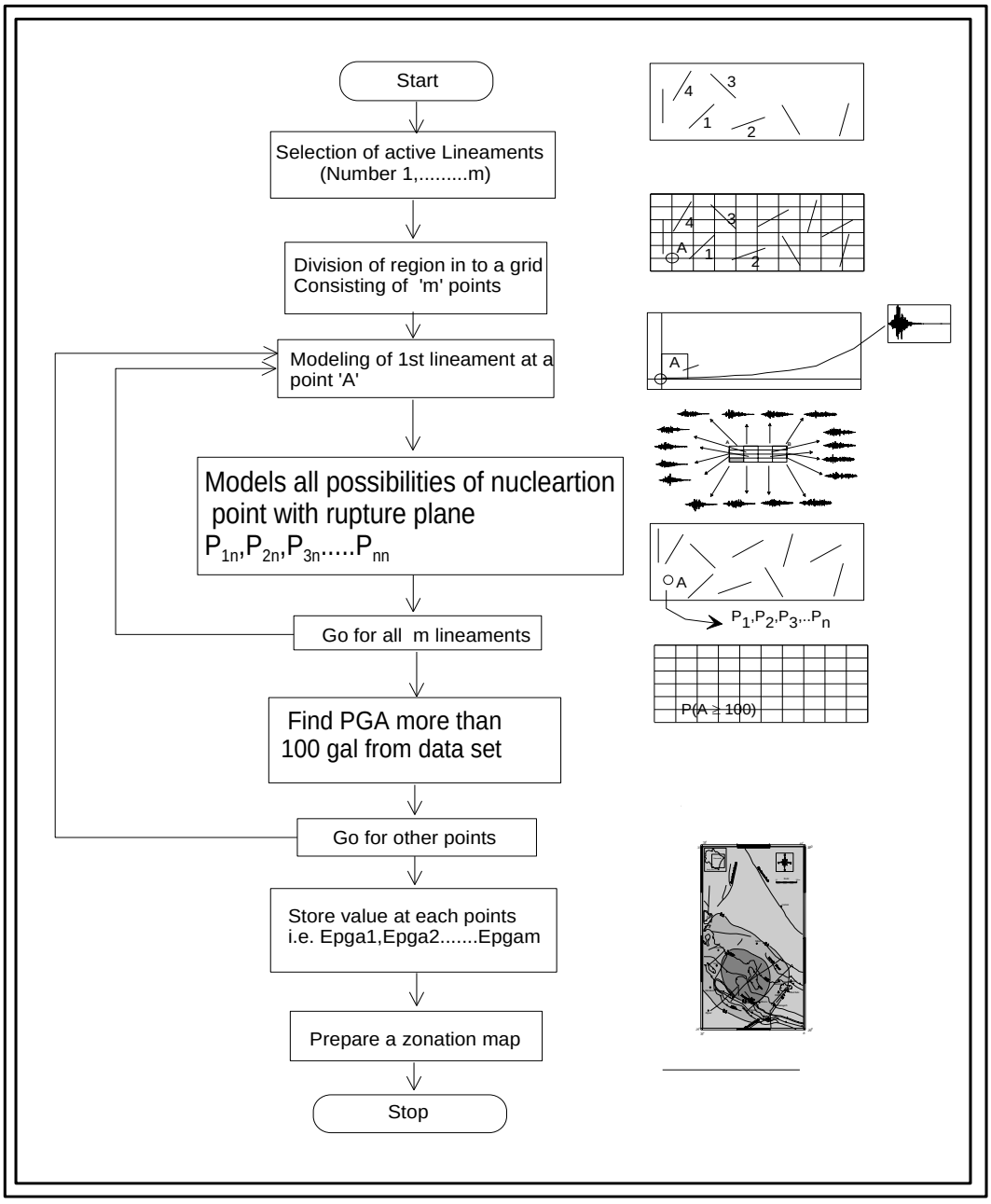

Figure 6.3 Flow diagram of modified seismic hazard zonation technique used in present work.

6.3 Seismic Zonation of the Uttarakhand Himalaya India

The Bureau of Indian Standard (BIS 2002) has divided entire India into four seismic zones (Zones II to Zone V). Unlike its previous edition which consisted of five or six zones for the country. Zone V and zone II expects the highest and lowest level of seismic hazard in the country, respectively. The Uttarakhand Himalayas lies in the northern part of the Indian subcontinent and falls under the highest zones IV and V of seismic zoning map of India. The Uttarakhand state has a total area of 53,484 km², of which 93% is mountainous and 65% is covered by forest. Most of the northern part of the state is covered by high Himalayan peaks and glaciers. The Tehri Dam which is the highest dam in India and one of the tallest in the world is located in this region. The area of study form part of the Kumaon and Garhwal region of the Uttarakhand Himalaya from latitude 29°N to 32°N and from longitude 78°E to 81°E. The main seismic zone extending from the Uttarkashi in the west to the Dharchula in the east is sub-parallel to Himalayan trend and lies in close proximity of Main Central Thrust (MCT). This zone is dominated by shallow focus (0-40 km) events, though some deeper events are also recorded from the Kaurik Fault Zone (GSI 2000). Within a period of 181 years from 1816 to 1997 a total of 297 seismic events have occurred in this region, out of which 32 events had magnitude, more than 5.5 (Yu et al. 1995). In the present work several ruptures have been identified from the tectonic and geological map of the region given by Geological Survey of India (GSI 2000). This map is shown in Fig. 6.4. A total of 67 lineaments have been identified as active lineaments by Joshi et al. (2007) for preparation of seismic hazard map of the region. In the present work the possibility of entire or portion of rupture along these lineaments that can generate earthquake of magnitude greater than or equal to 6.0 has been visualized. A total of 111 such possibilities were identified and are shown in Fig. 6.5.

The great and large earthquakes in the Himalaya occur at a shallow depth (10-20 Km) by thrust faulting on the Main Himalaya Thrust i.e. on the plane of detachment (Kayal 2014). The aftershock data of the Uttarkashi earthquake (1991) and the Chamoli earthquake (1999) has show that these shallow earthquakes (depth $\leq$ 20 km) occurred on the plane of detachment (Kayal 2014). The seismic rupture occurred at more than 20 km depth and did not break the surface (Lomnitz and Hofseth 2005). The average depth of events in this area reported from catalog of earthquake given by United State Geological Survey (USGS) is also around 20 kilometer. In the present work possible rupture for preparation of seismic hazard map is placed at a depth of 12 kilometer. The

strike of rupture is measured from the tectonic map, whereas the dip of modeled rupture plane is assumed as 15°. This dip coincides with the shallow dipping plane of detachment that has given rise to the Uttarkashi and the Chamoli earthquakes. Same dip has been also assumed in earlier study for modeling of the rupture plane of the Uttarkashi and the Chamoli earthquakes (Joshi 2004, Joshi and Midorikawa 2004). The rupture velocity for modeling rupture plane is assumed as 2.6 km/sec which is similar to that used for modeling of the Uttarkashi and the Chamoli earthquakes by Joshi (1997; 2004). The velocity model given by Yu et al. (1995) is used in the present work and is selected on the basis of its applicability for modeling of the Uttarkashi and the Chamoli earthquakes by Joshi (1997, 2001, 2004) and Yu et al. (1995). This velocity model is given in Table 6.1.

Table 6.1 Velocity model used for present work is given by Yu et al. (1995).

Depth to top of layer (km)	**Velocity V_s (km/sec)**
0.4	2.0
1.0	2.86
15.0	2.96

The entire region is divided into hundred grids and each center of each grid is assumed as an observation point for the purpose of preparation of seismic hazard map. In the present work all elements within the identified rupture plane are treated as nucleation point. Strong motion records have been simulated at each hundred observations point from different possibility of nucleation point using semi empirical method discussed in Chapter 4. At each observation point several strong motion records have been simulated using semi empirical technique. The semi empirical technique depends on attenuation relation that is applicable for the study area. In the present work different regression models defined in equation (6.5) to (6.8) have been used. The modeling parameters of rupture plane based self-similarity laws are given in Table 6.2.

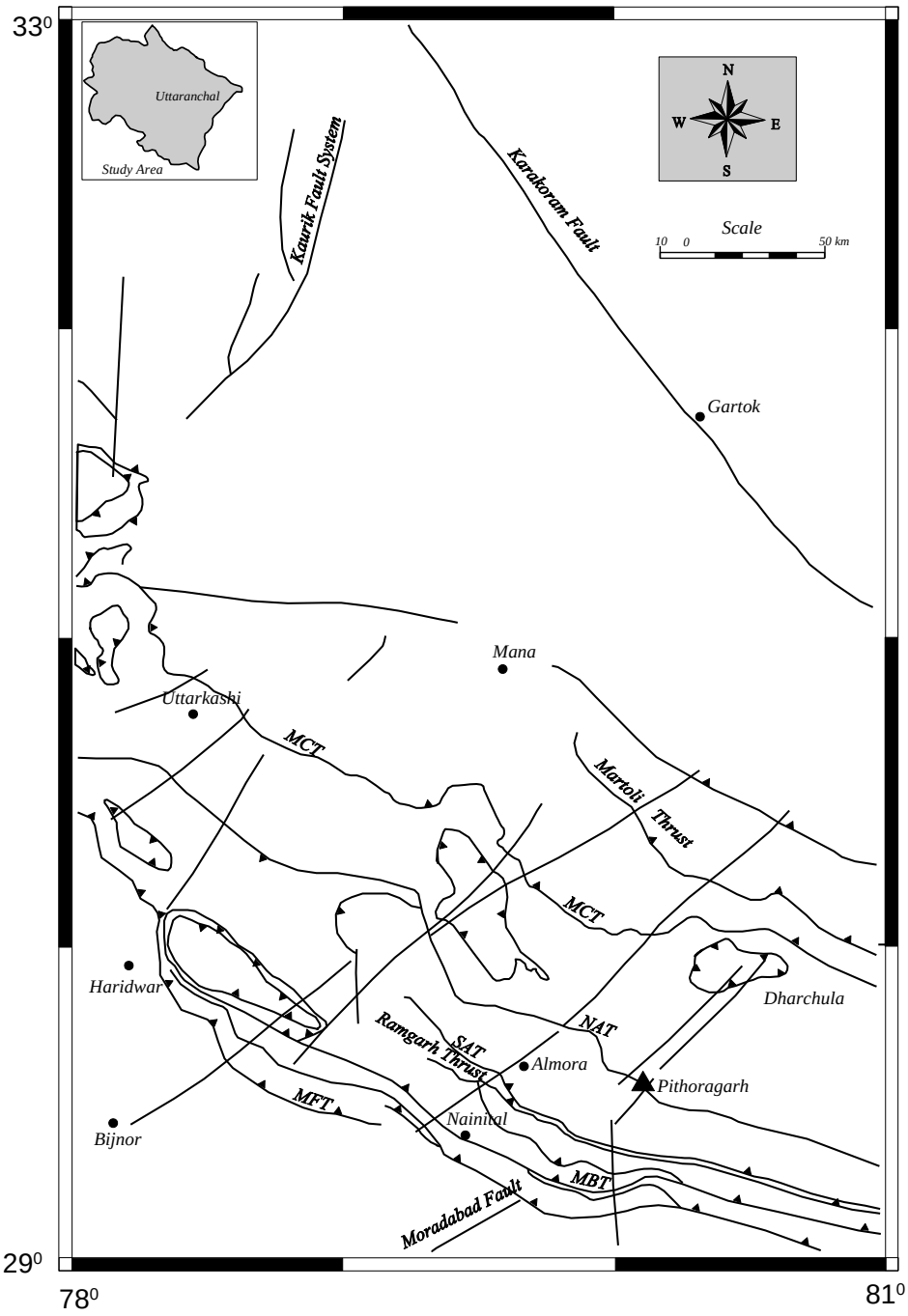

Figure 6.4 Tectonic map of the Uttarakhand Himalaya has been taken after Geological Survey of India (2000).

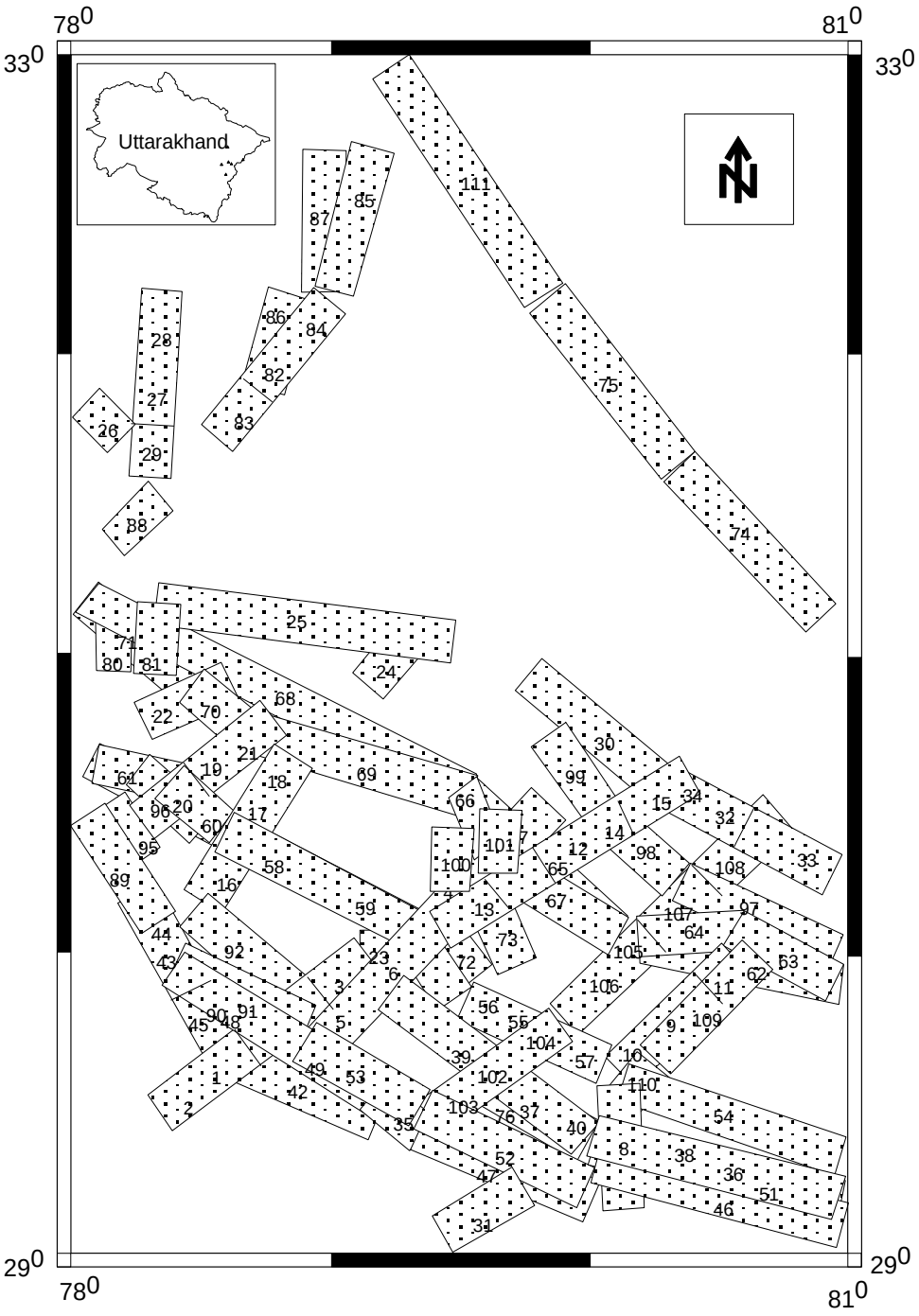

Figure 6.5 Location of rupture modeled for the Uttarakhand Himalaya for preparation of seismic hazard zonation map. The rupture is identified from seismotectonic map of the Uttarakhand region given by Geological Survey of India (GSI, 2000).

Table 6.2 The lineaments and modeling parameters of ruptures computed from various empirical relations.

Lineament No.	Length(km)	Downward Extension(km)	Magnitude (M_w)	Rupture area (sq. km)	L_e (km)	W_e(km)
1	107.1	34.32	7.7	3675.6	9.4	3
2	47.6	19.35	7.1	920.9	6.7	2.7
3	59.5	22.65	7.2	1347.7	7.3	2.8
4	133.28	40.06	7.8	5338.8	10.3	3.1
5	35.7	15.79	6.8	563.6	5.9	2.6
6	35.7	15.79	6.8	563.6	5.9	2.6
7	61.88	23.29	7.3	1441.1	7.4	2.8
8	47.6	19.35	7.1	920.9	6.7	2.7
9	61.88	23.29	7.3	1441.1	7.4	2.8
10	47.6	19.35	7.1	920.9	6.7	2.7
11	14.28	8.26	6.2	117.9	4	2.3
12	116.62	36.45	7.7	4250.7	9.8	3
13	40.46	17.25	6.9	697.8	6.2	2.6
14	28.56	13.48	6.7	385.1	5.4	2.5
15	47.6	19.35	7.1	920.9	6.7	2.7
16	38.08	16.52	6.9	629.2	6.1	2.6
17	38.08	16.52	6.9	629.2	6.1	2.6
18	28.56	13.48	6.7	385.1	5.4	2.5
19	64.26	23.92	7.3	1536.9	7.6	2.8
20	26.18	12.68	6.6	331.9	5.2	2.5
21	38.08	16.52	6.9	629.2	6.1	2.6
22	38.08	16.52	6.9	629.2	6.1	2.6
23	30.94	14.27	6.7	441.4	5.5	2.6
24	23.8	11.85	6.5	282.1	5	2.5
25	119	36.97	7.8	4399.8	9.8	3.1
26	21.42	11	6.5	235.6	4.7	2.4
27	76.16	26.97	7.4	2054	8.1	2.9

28	52.36	20.69	7.1	1083.5	6.9	2.7
29	23.8	11.85	6.5	282.1	5	2.5
30	71.4	25.77	7.4	1839.8	7.9	2.9
31	35.7	15.79	6.8	563.6	5.9	2.6
32	73.78	26.37	7.4	1945.7	8	2.9
33	35.7	15.79	6.8	563.6	5.9	2.6
34	38.08	16.52	6.9	629.2	6.1	2.6
35	26.18	12.68	6.6	331.9	5.2	2.5
36	99.96	32.69	7.6	3267.3	9.1	3
37	59.5	22.65	7.2	1347.7	7.3	2.8
38	99.96	32.69	7.6	3267.3	9.1	3
39	95.2	31.58	7.6	3006.2	8.9	3
40	45.22	18.66	7	843.7	6.5	2.7
41	49.98	20.02	7.1	1000.8	6.8	2.7
42	64.26	23.92	7.3	1536.9	7.6	2.8
43	61.88	23.29	7.3	1441.1	7.4	2.8
44	35.7	15.79	6.8	563.6	5.9	2.6
45	26.18	12.68	6.6	331.9	5.2	2.5
46	76.16	26.97	7.4	2054	8.1	2.9
47	76.16	26.97	7.4	2054	8.1	2.9
48	128.52	39.04	7.8	5017.5	10.2	3.1
49	42.84	17.96	7	769.3	6.4	2.7
50	85.68	29.31	7.5	2511.4	8.6	2.9
51	99.96	32.69	7.6	3267.3	9.1	3
52	71.4	25.77	7.4	1839.8	7.9	2.9
53	52.36	20.69	7.1	1083.5	6.9	2.7
54	92.82	31.02	7.6	2879.1	8.9	3
55	95.2	31.58	7.6	3006.2	8.9	3
56	59.5	22.65	7.2	1347.7	7.3	2.8

57	35.7	15.79	6.8	563.6	5.9	2.6
58	147.56	43.05	7.9	6351.8	10.8	3.1
59	35.7	15.79	6.8	563.6	5.9	2.6
60	26.18	12.68	6.6	331.9	5.2	2.5
61	85.68	29.31	7.5	2511.4	8.6	2.9
62	92.82	31.02	7.6	2879.1	8.9	3
63	47.6	19.35	7.1	920.9	6.7	2.7
64	45.22	18.66	7	843.7	6.5	2.7
65	90.44	30.45	7.5	2754.2	8.8	2.9
66	38.08	16.52	6.9	629.2	6.1	2.6
67	52.36	20.69	7.1	1083.5	6.9	2.7
68	190.4	51.54	8.1	9814	12	3.3
69	95.2	31.58	7.6	3006.2	8.9	3
70	23.8	11.85	6.5	282.1	5	2.5
71	71.4	25.77	7.4	1839.8	7.9	2.9
72	28.56	13.48	6.7	385.1	5.4	2.5
73	42.84	17.96	7	769.3	6.4	2.7
74	95.2	31.58	7.6	3006.2	8.9	3
75	95.2	31.58	7.6	3006.2	8.9	3
76	109.48	34.86	7.7	3816.1	9.5	3
77	19.04	10.12	6.4	192.7	4.5	2.4
78	66.64	24.54	7.3	1635.4	7.7	2.8
79	23.8	11.85	6.5	282.1	5	2.5
80	28.56	13.48	6.7	385.1	5.4	2.5
81	47.6	19.35	7.1	920.9	6.7	2.7
82	69.02	25.16	7.3	1736.3	7.8	2.8
83	23.8	11.85	6.5	282.1	5	2.5
84	45.22	18.66	7	843.7	6.5	2.7
85	57.12	22.01	7.2	1257	7.2	2.8

86	42.84	17.96	7	769.3	6.4	2.7
87	59.5	22.65	7.2	1347.7	7.3	2.8
88	47.6	19.35	7.1	920.9	6.7	2.7
89	47.6	19.35	7.1	920.9	6.7	2.7
90	71.4	25.77	7.4	1839.8	7.9	2.9
91	73.78	26.37	7.4	1945.7	8	2.9
92	76.16	26.97	7.4	2054	8.1	2.9
93	40.46	17.25	6.9	697.8	6.2	2.6
94	35.7	15.79	6.8	563.6	5.9	2.6
95	28.56	13.48	6.7	385.1	5.4	2.5
96	35.7	15.79	6.8	563.6	5.9	2.6
97	69.02	25.16	7.3	1736.3	7.8	2.8
98	38.08	16.52	6.9	629.2	6.1	2.6
99	38.08	16.52	6.9	629.2	6.1	2.6
100	28.56	13.48	6.7	385.1	5.4	2.5
101	33.32	15.03	6.8	500.9	5.7	2.6
102	61.8	23.27	7.3	1437.9	7.4	2.8
103	35.7	15.79	6.8	563.6	5.9	2.6
104	26.18	12.68	6.6	331.9	5.2	2.5
105	121	37.41	7.8	4526.8	9.9	3.1
106	47.6	19.35	7.1	920.9	6.7	2.7
107	33.32	15.03	6.8	500.9	5.7	2.6
108	40.46	17.25	6.9	697.8	6.2	2.6
109	57.12	22.01	7.2	1257	7.2	2.8
110	23.8	11.85	6.5	282.1	5	2.5
111	95.2	31.58	7.6	3006.2	8.9	3

At each observation point several strong motion records have been simulated for each possibility of nucleation point within identified 111 rupture plane in the area. A total of these 6569 records have been simulated at each observation point. From each simulated record peak ground acceleration value is stored in the dataset at each observation point. A dataset of 6569 peak ground accelerations values is obtained from different simulated records obtained after modeling various rupture plane at each observation point. This dataset has been used for preparation seismic zonation map. The data set is used to compute the seismic hazard map by calculating probability of exceedence of specific peak ground acceleration value. The processes of obtaining seismic hazard map is applied for both regression models given in equations (6.5) to (6.8), thereby two different seismic hazard maps for probability of exceedence of peak ground acceleration is obtained. These maps are shown in Fig. 6.6 to Fig. 6.9, respectively.

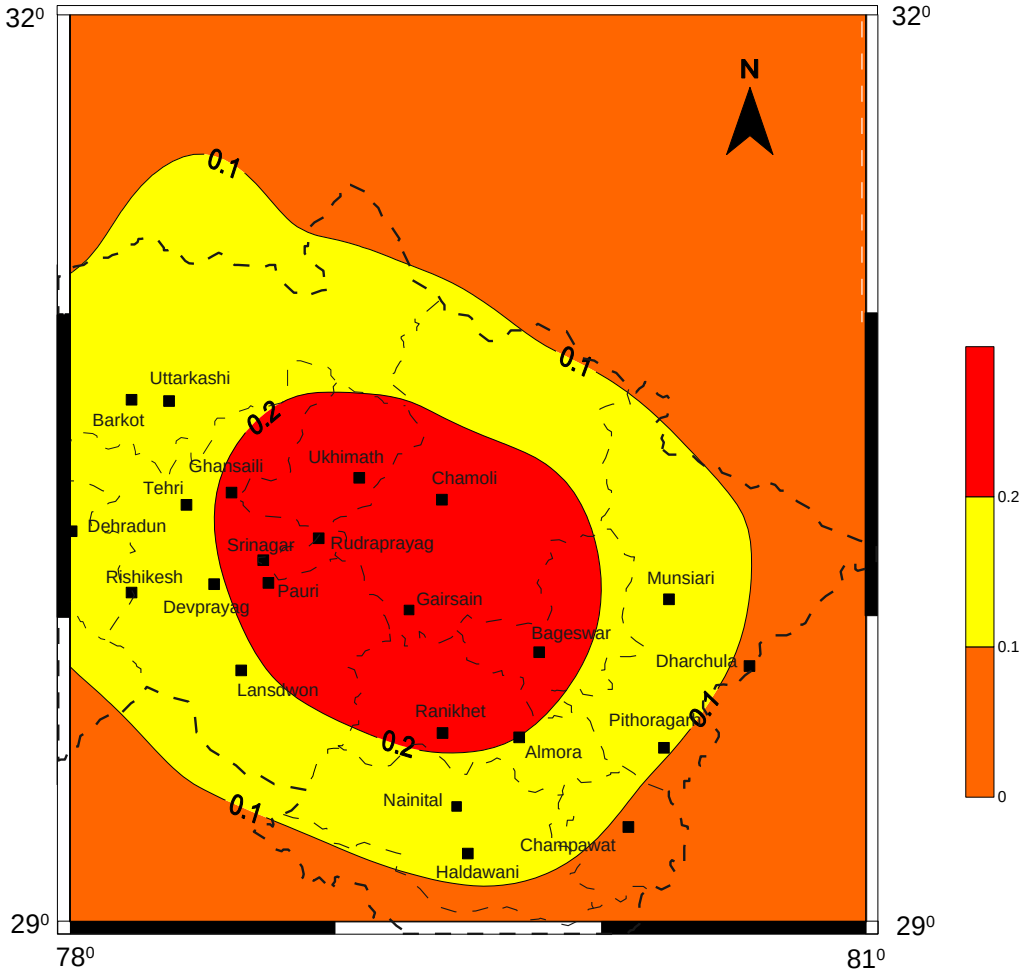

Figure 6.6 Seismic hazard map of Uttarakhand region showing 10% probability of exceedence of peak ground acceleration of 100 gals using developed attenuation relation for dependent of hypocentral distance.

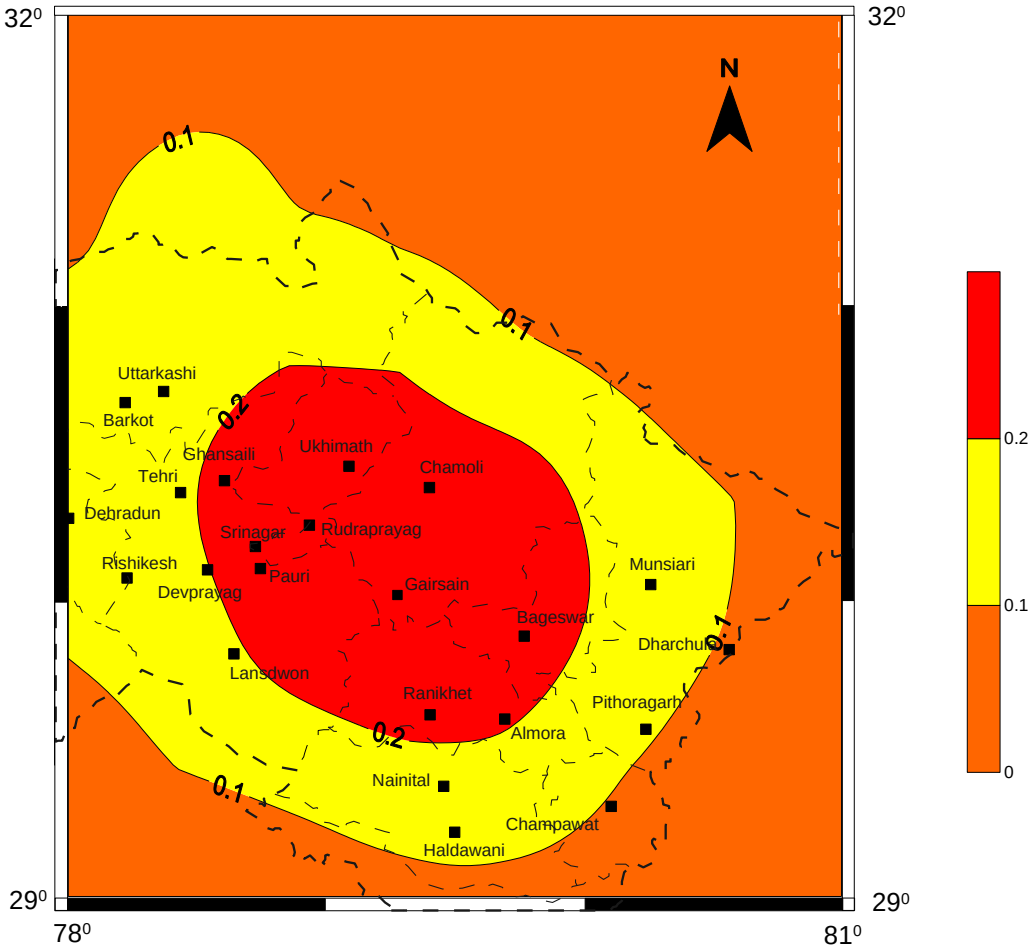

Figure 6.7 Seismic hazard map of Uttarakhand region showing 10% probability of exceedence of peak ground acceleration of 100 gals using developed attenuation relation for epicentral distance.

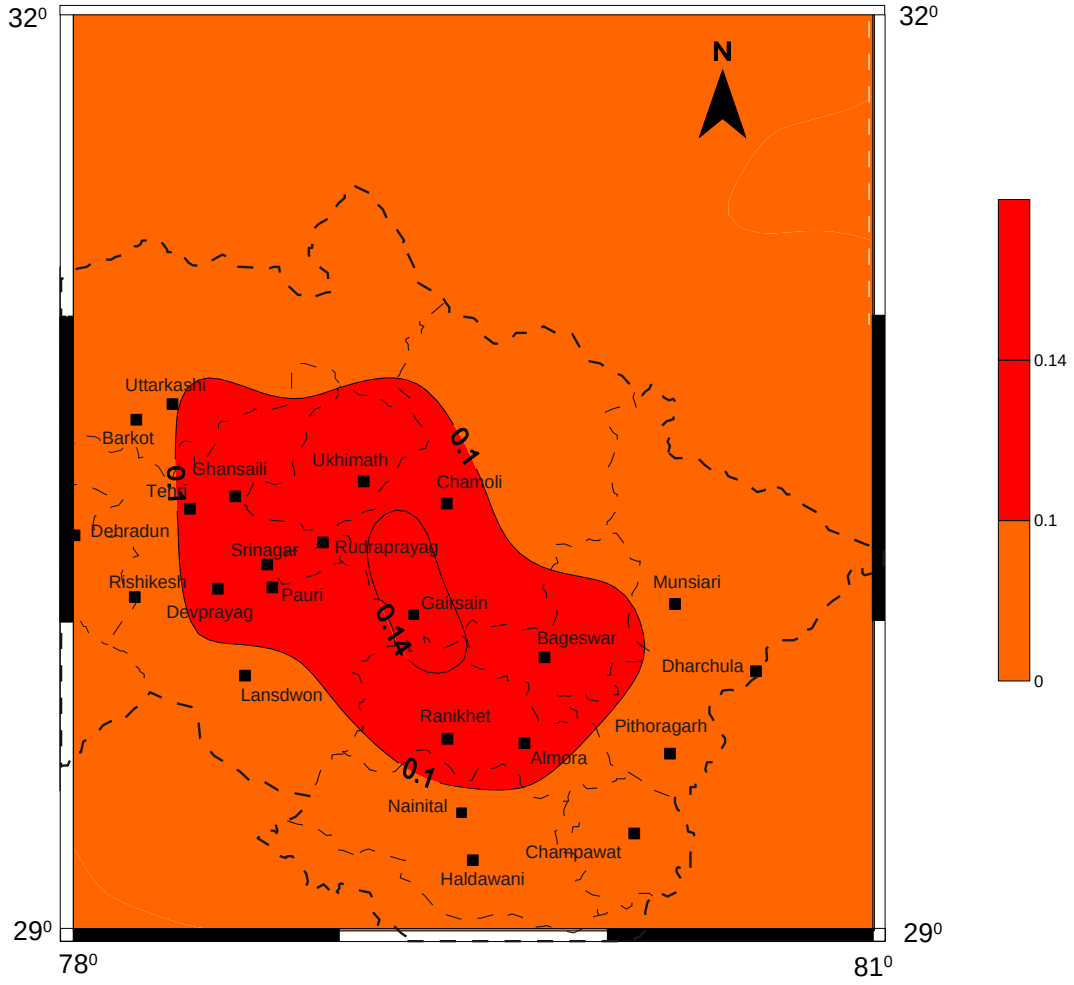

Figure 6.8 Seismic hazard zonation map of Uttarakhand region showing contours of 10% probability of exceedence of peak ground acceleration of value 200 gal using developed attenuation relations for hypocentral distance.

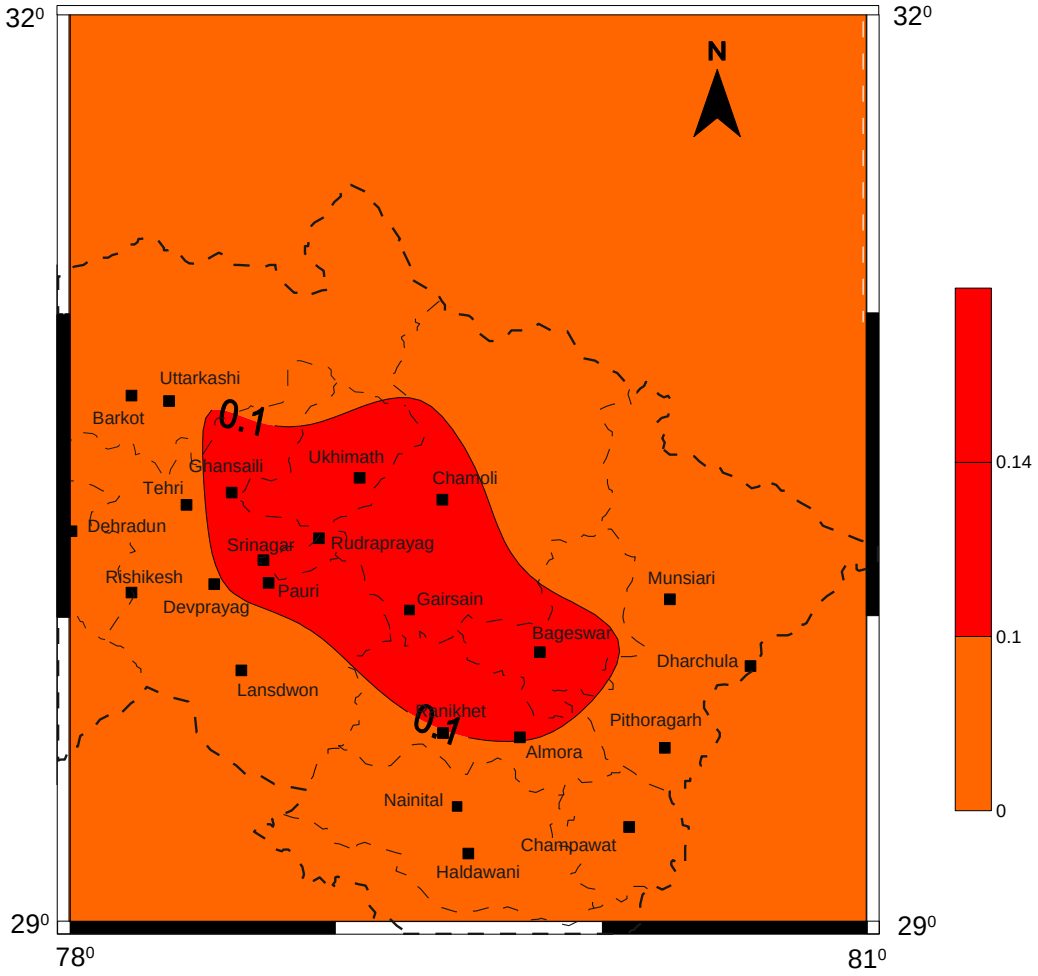

Figure 6.9 Seismic hazard zonation map of the Uttarakhand region showing contours of 10% probability of exceedence of peak ground acceleration of value 200 gal using developed attenuation relations for epicentral distance.

It is seen that appropriate choice of attenuation relations influence the value of predicted parameters. In an attempt to check how attenuation relation can influence seismic hazard map of the region, the seismic hazard map of the Uttarakhand Himalaya is prepared using different attenuation relations. The developed attenuation relations for different distance parameters have been used in this work. The prepared seismic hazard zonation maps using developed attenuation relations for various distance parameters are shown in Fig. 6.6, 6.7, 6.8 and 6.9, respectively. Further, the attenuation relation given by Abrahamson and Litehiser (1989) has been also used for preparation of seismic hazard zonation map and is shown in Fig. 6.10. The attenuation relation given by Abrahamson and Litehiser (1989) has been frequently used for modeling of great earthquakes in Indian region. Since attenuation relation given by Abrahamson and Litehiser (1989) clearly shows overestimation of peak ground acceleration (PGA) values with Himalaya dataset (Joshi et al. 2012). The zones of 10% probability of exceedence of peak ground acceleration of value 100 gal is shown in Fig. 6.10 has also increased drastically. It is seen that when attenuation relation prepared from regional database is used in preparation of seismic hazard zonation map there is no drastic difference in the obtained seismic hazards of the region using similar technique. However, strong difference in terms of shape of zones is observed when attenuation relation given by Abrahamson and Litehiser (1989) is used for preparation of seismic hazard zonation. This test clearly demonstrates importance of proper choice of attenuation relation used for seismic hazard zonation in any region.

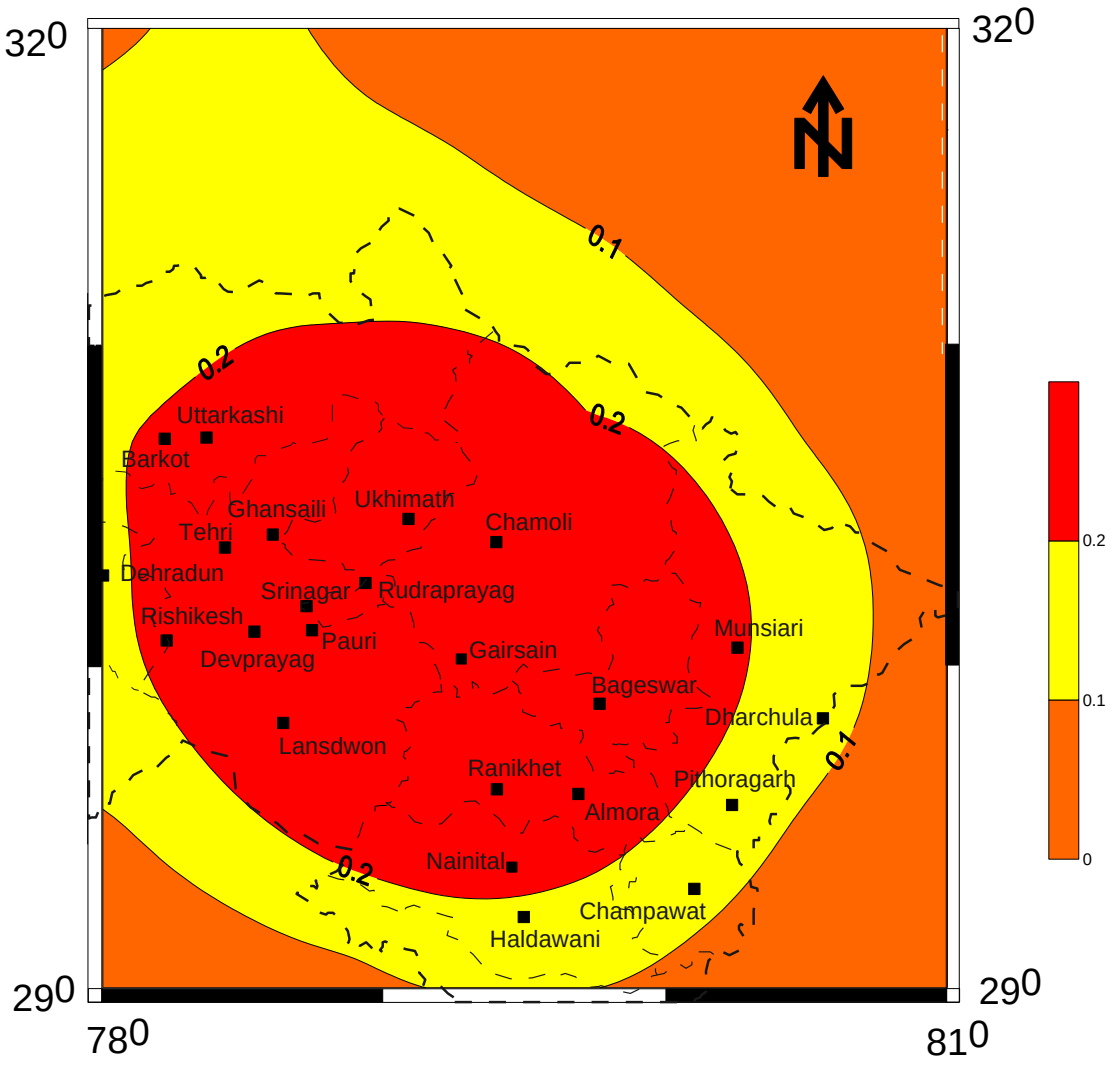

Figure 6.10 Seismic hazard zonation map of the Uttarakhand region showing 10% probability of exceedence of peak ground acceleration values of 100 gals using attenuation relation given by Abrahamson and Litehiser (1989).

The prepared zonation map for two different cases is shown in Fig. 6.5 and Fig. 6.6, respectively. It is shows from these maps that a large part of the region falls in the 10% probability of exceedence of the peak ground acceleration value of 100 gal. The area becomes smaller in the seismic hazard map for the 10% probability of exceedence of 200 gals (Fig. 6.8 and 6.9). The prepared seismic zonation maps for the Uttarakhand Himalaya shows that major area fall within 10% probability of exceedence of peak ground acceleration 100 gal and 200 gal, respectively. It is seen that many locations like Tehri, Chamoli, Almora, Srinagar, Devprayag, Bageshwar and Pauri fall in a zone of 10% probability of exceedence of peak ground acceleration value of 200 gals. The peak ground acceleration recorded during the Uttarkashi earthquake of 1991 and the Chamoli earthquake of 1999, at near source region is between 253 and 352 gal. These are two resent major earthquakes that occurred in the Uttarakhand Himalaya. The destruction during the Uttarkashi and the Chamoli earthquakes was severe in the near source region. This indicates that the area which falls under 10% probability of exceedence for the peak ground acceleration value of 200 gal in the present study can expect similar destruction in future earthquake and needs to be looked more carefully. This study indicates that the Uttarakhand Himalaya and the surrounding region are highly vulnerable to seismic hazard.

6.4 Conclusion

A modified technique of seismic zonation based on deterministic modeling of rupture plane is presented in this Chapter and is applied of the Uttarakhand Himalaya. The developed attenuation relations have been used for preparing the seismic hazard zonation maps of 10% probability of exceedence of peak ground acceleration values of 100 and 200 gals, respectively. It is seen that similar hazard maps are obtained when regional attenuation relations based on different regression model is used in this study. However, clear deviation in seismic hazard is seen when regression relation based on worldwide data is used. Therefore present study clearly demonstrates importance of regional regression relation is presenting seismic hazard map of the region.

CHAPTER - 7

Summary and Conclusions

7.1 Summary

Attenuation characteristics play an important role for safe deign of earthquake resistance building in a seismically active region. A seismic wave in a medium is affected by the three factors viz., source characteristics, travel path and medium. Different types of medium present in the earth crust behave differently for the similar seismic wave propagation. The effects of the propagation seismic wave in material on earthquake ground motion are associated with the attenuation properties of medium. Therefore estimation of attenuation characteristics is an important task for seismic hazard assessment of a region. Present research work is an attempt to understand and quantify the attenuation properties of earthquake ground motions in the seismically active Himalaya region. Further seismic hazard assessment has been carried out in this study. Following are the main objectives of this study:

1. Development of regression relations of peak ground acceleration for the Uttarakhand Himalaya using strong motion data of similar parametric constraints of independents variables.

2. Checking the suitability of developed attenuation relation to simulate large earthquake which occurred in this region.

3. Development of frequency dependent coda wave quality factor for both the Kumaon and the Garhwal Himalaya using similar strong motion data with similar techniques.

4. Preparation of seismic hazard map on the basis of developed attenuation relations for the Uttarakhand Himalaya.

In the present work, attenuation properties have been determined for two regions viz., the Kumaon Himalaya and Garhwal Himalaya, of the Uttarakhand Himalaya, India. In the Kumaon

Himalaya region very few studies have been carried out regarding the attenuation properties. Strong motion data have been used to achieve the above objectives. The strong motion data recorded on the Kumaon network consisting of eight stations, installed in the highly mountainous terrain of the Kumaon Himalaya, India have been used for in the present study. However, for the Garhwal Himalaya the strong motion data recorded on Garhwal network have been used. The average interspacing distance of station in the Kumaon Himalaya and Garhwal Himalaya region is approximately 11 km and 20 km, respectively.

First part of the present study is to determine the attenuation relations for peak ground acceleration using the strong motion data recorded by these networks. The strong motion array in the Garhwal Himalaya operating by the Department of Earthquake Engineering, Indian Institute of Technology Roorkee, provide an opportunity to obtain strong motion data recorded in this region. The method of regression analysis to obtain the attenuation relation has been described in the Chapter 3. The Kumaon and Garhwal Himalaya strong motion dataset has been used to develop attenuation relations for these regions. Developed attenuation relations for the Kumaon and Garhwal Himalaya region obtained two different models in this study. For checking the suitability of developed attenuation relations a test for normality and model adequacies with the Himalaya data set has been examined. Further, test of normality and model adequacies with worldwide attenuation relations has been also checked.

In the present work developed attenuation relation has been used for simulation of strong motion records of two resent earthquakes using semi empirical technique. Semi empirical simulation technique given by Midorikawa (1993) and modified by Joshi and Midorikawa (2004) has been used for simulation the record of two earthquakes viz. the 1991 Uttarkashi earthquake and the 1999 Chamoli earthquake which is occurred in the Garhwal Himalaya. This simulation technique is turn dependent on the attenuation relation applicable for the sturdy area. The semi empirical simulation technique is frequently used by many researchers. In the present work simulated acceleration time series of the Uttarkashi and the Chamoli earthquakes give the good agreement with observed one. This test is confirming the efficacy of developed attenuation relations for study area.

The frequency dependent attenuation property has been also investigated for these regions in the present study. Coda wave quality factor ($Q_c(f)$) has been computed using the strong motion dataset recorded by the Kumaon and the Garhwal Himalaya networks, India. In this study we have analyzed data from nine local events recorded on six stations for each networks separately. The single backscattering technique given by Aki and Chouet (1975) has been used for this work. The process of determination of frequency dependent coda wave quality factor ($Q_c(f)$) has been discussed in Chapter 5. The obtained results have been compared with worldwide relations given by many researchers, which fall within limits. This test is conformation of efficacy of obtained results.

Seismic hazard zonation of the Uttarakhand Himalaya has been done in the present study. Modified seismic hazard zonation technique has been used in this present study. Joshi and Patel (1997) has been formulated a method of seismic zonation which base on semi empirical technique given by Midorikawa (1993) and later modified Joshi and Midorikawa (2004). This method has been successfully used for Doon Valley, Northeast region and the Uttarakhand of the India. In this work seismic zonation method given by Joshi and Patel (1997) has been modified. The modified method of seismic hazard zonation is discussed in Chapter 6. In this approach rupture plane has been modelled as a rectangular plane. The length of the rupture plane has been determined with the help of map. The length of the rupture plane has been calculated using the empirical relation given by Wells and Coppersmith (1994).

The attenuation relations developed for the Uttarakhand Himalaya region with different distance parameters has been used and found no drastic difference with obtained results. Further, long difference in terms of shape of zones is observed when the worldwide attenuation relation given by Abrahamson and Litehiser (1989) has been used. The attenuation relation given by Abrahamson and Litehiser (1989) has been frequently used for simulation of past Himalayan earthquakes. The modified seismic zonation is strongly dependent on attenuation relations applicable for study region. The obtained result gives the good evidence with seismicity of the region.

7.2 Conclusions

Research work carried out in this thesis presents the attenuation characteristics of the Uttarakhand Himalaya based on strong motion data. The strong motion data recorded by two networks operating in the Kumaon and Garhwal Himalaya region has been used in present work. The source parameters of recorded events have been estimated and attenuation characteristics have been studies for both regions viz. the Kumaon Himalaya and the Garhwal Himalaya. Major conclusions drawn on the research work carried out in present thesis is listed as follow:

1. Regression models developed for the Kumaon and Garhwal Himalaya are tested with actual data. The comparison of actual and synthetic database shows that regression model presented in this thesis is suitable to define trend of peak ground acceleration obtained during several earthquakes. The developed models are tested for the assumption of normality and model adequacies and it is found that all regression models satisfy the criteria.
2. Study of peak ground acceleration trends and several regression models in the Uttarakhand region suggest regression model having dependency on epicentral distance gives less error as compared to other models.
3. Dependency of peak ground acceleration on other parameters clearly shows that distribution of PGA in the Uttarakhand region follows different trend for the Kumaon and Garhwal Himalaya, respectively.
4. The test of normality and model adequacies are performed on several regression models of worldwide applicability and it is seen that as long as data set remain similar to that used for obtaining coefficients of regression analysis normality and model adequacies are satisfied in the regression model, while for other cases sharp deviation from normality and model adequacies are observed.
5. Rate of attenuation of peak ground acceleration observed from the developed regression model is checked for both regions of the Kumaon and the Garhwal Himalaya and it seen that high rate of attenuation of peak ground acceleration is observed in the Kumaon Himalaya as compared to the Garhwal Himalaya.
6. The validity of developed attenuation relations has been checked by simulating strong motion records of two recent earthquakes viz. the Uttarkashi and Chamoli earthquake that occurred in the Garhwal Himalaya region using semi empirical simulation technique given by Midorikawa

(1993). The regression model developed for the Garhwal Himalaya has been used in this simulation technique. The simulation of strong ground motion of these two earthquakes gives a good match with observed records, which further supports the validity of developed attenuation relation.

7. The difference in attenuation trend of peak ground acceleration is checked by computing dimensionless quality factor '$Q_c(f)$' for these two regions using strong motion data. The obtained value of $Q_c(f)$ in these two regions has been compared with available values measured in other part of India and world. This comparison indicates that the distribution of $Q_c(f)$ in this region falls within the range of values justified for tectonically active regions.
8. The comparative study of obtained $Q_c(f)$ relation for the Kumaon and Garhwal Himalaya indicate that coda wave quality factor is less in the Kumaon region as compared to the Garhwal region, which indicate highly attenuating medium in the Kumaon Himalaya as compared to the Garhwal Himalaya.
9. Seismic hazards assessment of seismically active region of the Uttarakhand Himalaya has been made using modified seismic hazard zonation technique initially given by Joshi and Patel (1997). The maps of probability of exceedance of peak ground acceleration have been prepared using modified seismic hazard zonation technique. These maps show that many important cites in this region fall in highly hazardous zones.

References

[1] Abrahamson NA, Litehiser JJ (1989) Attenuation of vertical peak acceleration. Bull Seism Soc Am 79: 549-580

[2] Algermissen ST, Perkins DM (1976) A probabilistic estimate of maximum acceleration in rock in the contiguous United state. United States Dept. of the Interior, Geological survey, open file report 76-416

[3] Aki K (1967) Scaling law of seismic spectrum. J Geophys Res 72:1217-1231

[4] Aki K (1968) Seismic displacements near a fault. J Geophys Res 73:5359–5376

[5] Aki K (1969) Analysis of seismic coda of local earthquakes as scattered waves. J Geophys Res 74:615–631

[6] Aki K (1980) Attenuation of shear waves in the lithosphere for frequencies from 0.05 to 25 Hz. Phys Earth Planet Inter 21:50–60

[7] Aki K, Chouet B (1975) Origin of Coda wave: source, attenuation and scattering effects. J Geophys Res 80: 3322-3342

[8] Auden JB (1959) Earthquakes in relation to Damodar valley project. 1st symp on Earthquake Engineering, University of Roorkee, India

[9] Atkinson GM, Boore DM (1995) Ground motion relations for eastern North America. Bull Seism Soc Am 85:17-30

[10] Atkinson GM, Boore DM (1998) Evaluation of models for earthquake source spectra in eastern North America. Bull Seism Soc Am 88:917-934

[11] Atkinson GM, Boore DM (2006) Earthquake ground-motion prediction equations for Eastern North America. Bull Seism Soc Am 96(6):2181–2205

[12] Basu S, Nigam NC (1977) Seismic risk analysis of Indian Peninsula. Proc. 6th world Conf. Earthquake Eng. New Delhi Vol (I) :782-788

[13] Basu S, Nigam NC (1978) On Seismic zoning map of India. Proc. VI Symp Eathq Eng Roorkee Vol I: 83-90

[14] Bhatia SC, Kumar MR, Gupta HK, (1999) A probabilistic hazard map of India and adjoining regions. Ann Geofisica 42:1153-1164

[15] Bhattacharya AR (2008) Basement rocks of the Kumaon-Garhwal Himalaya: Implications for Himalayan Tectonics I(I):1-10

[16] Boore DM (1983) Stochastic simulation of high frequency ground motions based on seismological models of the radiated spectra. Bull Seism Soc Am 73: 1865-1894

[17] Boore DM, Atkinson GM (1987) Stochastic prediction of ground motion and spectral response parameters at hard-rock sites in eastern North America. Bull Seism Soc Am 77: 440-467

[18] Boore DM, Joyner WB (1982) The empirical prediction of ground motion. Bull Seism Soc Am 72 (6): S43-S60

[19] Boore DM, Joyner WB (1991) Estimation of ground motion at deep soil sites in eastern North America. Bull Seism Soc Am 81:2167–2185

[20] Boore DM, Bommer JJ (2005) Processing of strong motion accelerograms: needs, options and consequences. Soil Dyn and Earthq Eng 25: 93-115

[21] Boore DM, Atkinson GM (2008) Ground motion prediction equations for the average horizontal component of PGA, PGV and 5% damped PSA at spectral periods between 0.01s and 10.0s. Earthq Spectra 24(1): 99-138

[22] Boore DM, William B, Joyner, Fumal TE (1997) Equations for Estimating Horizontal Response Spectra and Peak Acceleration from Western North American Earthquakes: A Summary of recent Work. Seism Res Lett 68(1):128-153

[23] Brahma J (2012) Estimation of coda wave attenuation quality factor from digital seismogram using statistical approach. Sci and Tech 2(1):1-7

[24] Brune JM (1970) Tectonic stress and spectra of seismic shear waves from earthquakes. J Geophys Res 75: 4997-5009

[25] Brune JM (1971) Correction, J Geophys Res 76: 5002

[26] BIS (2002) Criteria for earthquake resistant Design of Structures, Part-I General provisions and Building, Bureau of Indian Standards, New Delhi

[27] Campbell KW (1981) Near source attenuation of peak horizontal acceleration. Bull Seism Soc Am 71(6): 2039–2070

[28] Campbell KW (1985) Strong motion attenuation relations: A ten year perspective, earthquake spectra 1: 759-804

[29] Campbell KW (2001) Strong motion attenuation relations (Draft Personnel communication).

[30] Chandrasekaran AR, Das JD (1992) Strong motion arrays in India and Analysis of data from Shillong array. Curr Sci 62:233-249

[31] Chandrasekaran AR, Das JD (1993) Strong earthquake ground motion data in EQINFOS for India part 1B (edited by Trifunac MD, Todorovska MI, Lee VW). Report No. CE 93-04, Univ of Southern California, Los Ageles, USA

[32] Chen D, Dong W, Shah HC (1988) Earthquake recurrence relationships from fuzzy earthquake magnitudes. Soil Dyn Earthq Eng 7(3): 136-142

[33] Castagna JP, Batzle ML, Eastwood RL (1985) Relationship between compressional-wave and shear wave velocities in elastic silicate rocks. Geophysics 50:571–581

[34] Coats DA, Kanamori H, Houston H (1984) Simulation of strong ground motion from the 1964 Alaskan earthquake (Abs.). Earthq Notes 55:18

[35] Costa G, Panza GF, Suhadolc P, Vaccari F (1993) Zoning of the Italian territory in term of expected peak ground acceleration derived from complete synthetic seismograms in Geophysical Exploration in area of complex Geology II. J Appl Geophys 30:149-160

[36] Cornell CA (1968) Engineering seismic risk analysis. Bull Seism Soc Am 58:1583-1606

[37] Deif A, Abed A, Rahman KA, Moneim EA (2011) Strong ground motion attenuation in Aswan area, Egypt. Arab J Geosci 4:855-861

[38] Demets C, Gordon RG, Argus DF, Stein S (1990) Current plate motions. Geophys J Inter 101: 425-478

[39] Dimri VP (1992) Deconvolution and Inverse Theory: Application to geophysical problems, Elsevier Science Publishers. Amsterdam, 230

[40] Domenico SN (1977) Elastic properties of unconsolidated porous sand reservoir. Geophysics 42:15–24

[41] Donovan NC (1973) A statistical evolution of strong motion data including the February 9, 1971 San Fernando earthquake. 5th world conf. Earthq Eng.

[42] Douglas J (2001) A comprehensive worldwide summary of strong-motion attenuation relationships for peak ground acceleration and spectral ordinates (1969-2000), Eng Seismol and Erthq Eng Report No. 01-1 January 2001

[43] Douglas J (2011) Investigating possible regional dependence in strong motions, in Earthquake data in Engineering Seismology. S. Skkar, P. Gulkan, T. Van Eck (eds.). Springer Ltd: 29-38

[44] Dutta U, Biswas NN, Adams DA, Papageorgiou A (2004) Analysis of S- wave attenuation in South Central Alaska. Bull Seism Soc Am 94:16-28

[45] Esteva L (1970) Seismic risk and seismic design decisions, in Seismic Design for Nuclear Power Plants. RJ Hansen (eds), MIT Press, Cambridge, Massachusetts:142–182

[46] Fukushima Y, Tanaka T (1990) A new attenuation relation for peak horizontal acceleration of strong earthquake ground motion. Bull Seism Soc Am 80: 757-783

[47] Gansser A (1964) Geology of the Himalayas – Interscience publishers john Wiley and Sons Ltd London New York Sydney:1-289

[48] Geological Survey of India (GSI) (2000) Seismotectonic atlas of India and its environs. (eds. Dasgupta S, Pande P, Ganguly D, Iqbal Z, Sanyal E, Venkatraman NV, Dasgupta S, Sural B, Harendranath L, Mazumdar K, Sanyal S, Roy A, Das LK., Mishra PS, Gupta) Geol Soc India : 43

[49] Gitis V, Yurkov E, Arora BR, Chabak S, Kumar N, Baidya P (2008) Analysis of seismicity in North India. Russ J Earth Sci 10 ES5002 doi: 10.220/2008ES000303

[50] Guha SK (1962) Seismic regionalization of India. 2nd sym Earthq Eng Roorkee, 191-207

[51] Gubin IE (1968) Seismic zoning of the Indian Peninsula. Bull Int Inst Seism Erthq Eng 5

[52] Gupta S, Gupta ID (2004) The prediction of earthquake peak ground acceleration in Koyna region India. 13th WCEE Vancouver BC Canada paper no. 1437

[53] Gupta SC, Singh VN, Kumar A (1995) Attenuation of coda waves in the Garhwal Himalaya, India. Phys Earth Planet Inter 87:247–253

[54] Gupta SC, Teotia SS, Rai SS, Gautam N (1998) Coda Q estimates in the Koyna region, India. Pure Applied Geophys 153:713-731

[55] Gupta SC, Kumar A (2002) Seismic wave attenuation characterises of three Indian regions: a comparative study. Curr Sci 83: 247-253

[56] Gupta AK, Sutar AK, Chopra S, Kumar S, Rastogi BK (2012) Attenuation characterizes of coda waves in Mainland Gujarat (India). Tectonophysics 530-531:264-271

[57] Hadley DM, Helmberger DV (1980) Simulation of strong ground motions. Bull Seism Soc Am 70: 610-617

[58] Hadley DM, Helmberger DV, Orcutt JA (1982) Peak ground acceleration scaling studies. Bull Seism Soc Am 72:959-978

[59] Hanks T, Kanamori H (1979) A moment magnitude scale. J Geophys Res 84:2348-2350

[60] Hanks TC, McGuire RK (1981) Character of high frequency ground motion. Bull Seism Soc Am 71:2071-2095

[61] Hartzell SM (1978) Earthquake aftershocks as Green Functions. Geophy Res Lett 5:1-4

[62] Hartzell SM (1982) Simulation of ground accelerations for May 1980, Mammoth Lakes, California earthquakes. Bull Seism Soc Am 72: 2381-2387

[63] Havskov J, Malone S, McClurg D, Crosson R (1989) Coda Q for the state of Washington. Bull Seism Soc Am 79:1024-1038

[64] Heaton TH, Helmberger DV (1977) A study of the strong ground motion of the Borrego Mountain, California, earthquake. Bull Seism Soc Am 67:315–330

[65] Helleg M, Spandich P, Fletcher JB, Baker LM (1995) Stability of coda Q in the region of Parkfield, California: view from the U.S. Geological Survey Parkfield dense seismograph array. J Geophys Res 100: 2089-2102

[66] Heriberta C, Lomnitz C (2002) PSHA: is it sciences?. Eng Geol 66:315-317

[67] Hermann RB (1980) Q estimates using the coda of local earthquakes. Bull Seism Soc Am 70: 447-468

[68] Holmes A (1965) Principles of physical geology. Ronald press, New York, NK: 1288

[69] Housner GW, Jennings PC (1964) Generation of Artificial earthquakes. Proc. ASCE 90:113-150

[70] Hutchings L (1985) Modeling earthquakes with empirical green's functions (abs). Earthq Notes 56: 14

[71] Ibanez JM, Del pezzo E, De Miguel F, Herraiz M, Alguaicil G, Morales J (1990) Depth dependent seismic attenuation in the Granada zone (southern Spain). Bull Seism Soc Am 80:1232–1244

[72] Irikura K (1983) Semi empirical estimation of ground motion during large earthquake. Bull Disaster Prevent Res Inst (Kyoto Univ) 33: 63-104

[73] Irikura K (1986) Prediction of strong acceleration motion empirical green's function. Proc 7th Japan Earthq Eng Sym:151-156

[74] Irikura K, Muramatu I (1982) Synthesis of strong ground motion from large earthquake using observed seismograms of small event. Proc of 3rd International Earthq Microzonation conf, Seattle :447-458

[75] Irikura K, Kagawa T, Sekiguchi H (1997) Revision of the Empirical Green's Function method by Irikura (1986), programme and abstracts. The Seismological Society of Japan 2, B25

[76] IS: 1893 (part1) (2002) Indian standards code of practice for earthquake resistant Design of Structures. Indian Standards Institution, New Delhi

[77] Iyengar RN, Raghukanth STG (2004) Attenuation of strong ground motion in Peninsular India. Seism Res Lett, 79(5): 530–540.

[78] Joshi A (1997) Modeling of peak ground acceleration for Uttarkashi earthquake of 20th Oct, 1991. Bull Ind Soc Earthq Tech 34: 75-96

[79] Joshi A, Patel RC (1997) Modeling of active lineaments for predicting possible earthquake scenario around Dehradun, Garhwal Himalaya, India. Tectonophysics 283: 289-310

[80] Joshi A (1998) Study of the Uttarkashi earthquake in terms of rupture model and isoseismals. J Geophys 19: 133-140

[81] Joshi A, Kumar B, Sinvhal A, Sinvhal H (1999) Generation of synthetic accelerograms by modelling of rupture plane. ISET Journal of Earthquake Technology

[82] Joshi A (2001) Strong motion envelope modelling of the source of the Chamoli earthquake of March 28, 1999 in the Garhwal Himalaya, India. J Seism 5: 499-518

[83] Joshi A, Singh S, Giroti K (2001) The simulation of ground motions using envelope summations. Pure App Geophy 158: 877-901

[84] Joshi A (2004) A simplified technique for simulating of ground motion for two recent Himalaya earthquakes. Pure App Geophy 8: 467-484

[85] Joshi A, Midorikawa S (2004) A simplified method for simulation of strong ground motion using finite rupture model of the earthquake source. J Seism 8: 467-484

[86] Joshi A (2006) Use of acceleration spectra for determining the frequency-dependent attenuation coefficient and source parameters. Bull Seism Soc Am 96: 2165-2180

[87] Joshi A, Mohan K, Patel RC (2007) A deterministic approach for preparation of seismic hazard maps in North East India. Nat Hazards 43: 129-146

[88] Joshi A, Mohan K (2008) Simulation of accelerograms from simplified deterministic approach for the 23rd October 2004 Niigata-ken Chuetsu, Japan earthquake. J Seism 12: 35-51

[89] Joshi A, Mohanty M, Teotia SS, Bansal AR, Dimri VP, Chadha RK (2009) Crustal attenuation of shear waves in Pithoragarh region. J Ind Geophys Union 13:137-146

[90] Joshi A, Mohanty M, Bansal AR, Dimri VP, Chadha RK (2010a) Use of spectral acceleration data for determination of three dimensional attenuation structure in the Pithoragarh region of

Kumaon Himalaya. J Seism 14:247-272

[91] Joshi A, Mohanty M, Bansal AR, Dimri VP, Chadha RK (2010b) Use of strong motion data for frequency dependent shear wave attenuation studies in the Pithoragarh region of Kumaon Himalaya. Indian Society of earthquake Technology 47(1):25-46

[92] Joshi A, Mohan K (2010) Expected peak ground acceleration in Uttarakhand Himalaya, India region from a deterministic hazard model. Nat Hazards 52:299-317

[93] Joshi A, Kumar A, Lomnitz C, Castanos H, Akhtar S (2012) Applicability of attenuation relations for regional studies. Geofisica Internacional Journal, 51(4): 349-363

[94] Joshi A, Kumar A, Mohan K, Rastogi BK (2013) Hybrid Attenuation Model for Estimation of Peak Ground Accelerations in the Kutch Region, India. Natural Hazard, 68: 249-269

[95] Johnston DH, Toksoz MN (1981) Seismic wave attenuation. Society of Exploration Geophysicists, pp 1-5.

[96] Jin A, Aki K (1986) Temporal change in the coda Q before the Tangshan earthquake of 1976 and the Haicheng earthquake of 1975. J Geophys Res 91: 665-673

[97] Joyner WB, Boore DM (1981) Peak horizontal acceleration and velocity from strong motion records including records from the 1979 Imperial valley, California earthquake. Bull Seism Soc Am 71(6):2011-2038

[98] Joyner WB, Boore DM (1988) Measurement, characterization and prediction of strong ground motion. Proc of Earthq Eng and Soil Dyn II, Utah, June 27-30: 43-100

[99] Kaila KL, Gaur VK, Narain H (1972) Quantitative seismicity map of India. Bull Seism Soc Am 62:1119-1132

[100] Kaila KL, Rao MN (1979) Seismic zoning maps of the Indian subcontinent. Geophy Res Bull NGRI Hyderabad 17:293-301

[101] Kamae K, Irikura K (1998) Source model of the 1995 Hyogoken Nanbu earthquake and simulation of near source ground motion. Bull Seism Soc Am 88: 400-412

[102] Kamae K, Irikura K, Pitarka A (1998) A technique for simulating strong ground motion using hybrid Green's function. Bull Seism Soc Am 88(2):357–367

[103] Kameda H, Sugito M (1978) Prediction of strong earthquake motion by evolutionary process model. Proc of 6th Japan Earthq Eng sym : 41-48

[104] Kanamori H (1979) A semi empirical approach to prediction of long period ground motions from great earthquake. Bull Seism Soc Am 69: 1645-1670

[105] Kanamori H (1977) The energy release in great earthquakes. J Geophys Res. 82: 2981-2987

[106] Kanamori H, Anderson DL (1975) Theoretical basis of come empirical relations in seismology. Bull Seism Soc Am 65:1073-1095

[107] Kanao M, Ito K (1992) Attenuation of coda waves in source area of the 1990 July 16 Luzon earthquake, Philippines. Disaster Prev Res Inst, Kyoto Uni, Bull 42(2,356):31-51

[108] Kayal JR, Reena De (1991) Microseismicity and tectonics in northeast India. Bull Seism Soc Am 81: 131-138

[109] Kayal JR (2014) Seismotectonics of the great and large earthquakes in Himalaya. Current Sci 106(2): 188-197

[110] Khattri KN (1987) Great earthquake, seismicity gaps and potential for earthquake disaster along the Himalaya plate boundary. Tectonophysics 138: 79-92

[111] Khattri KN, Rogers AM, Algermissen ST (1984) A seismic hazard map of India and adjacent areas. Tectonophysics 108:93-134

[112] Kiremidjian AS, Shah HC, Sutch PL (1982) Seismic hazard and uncertainty analysis of Honduras. Soil Dyn Earthq Eng 1(2): 83-94

[113] Knopoff L (1964) Q, Review. Geophysics 2:625–660

[114] Krishna J (1959) Seismic zoning of India. Earthq Eng seminar Roorkee Uni 32-38

[115] Kumar D, Teotia SS, Khattri KN (1997) The representation of attenuation characteristics of strong motions observed in the 1986 Dharamsala and 1991 Uttarkashi earthquakes by available empirical relations. Curr Sci 73: 543-548

[116] Kumar D, Khattri KN, Teotia SS, Rai SS (1999) Modeling of accelerograms for two Himalayan earthquakes using a novel semi-empirical method and estimation of accelerogram for a hypothetical great earthquake in the Himalaya. Current Science 76:819–830

[117] Kumar D, Teotia SS, Sriram V (2011) Modelling of strong ground motions from 1991 Uttarkashi India earthquakes using a hybrid technique. Pure Appl Geophys 168:1621-1643

[118] Kumar N, Parvez IA, Virk HS (2005) Estimation of coda wave attenuation for NW Himalayan region using local earthquakes. Physics of Earth and Planetary Interiors 151:243-258

[119] Kumar CHP, Sarma CSP, Shekar M, Chadha RK (2007) Attenuation studies based on local earthquake coda waves in the Southern Indian Peninsular shield. Natural Hazard 40:527-536

[120] Kumar S, Mahajan AK (2001) Seismotectonics of the Kangra region, Northwest Himalaya.

Tectonophysics 331: 359-371

[121] Kumar A, Mittal H, Sachdeva R, Kumar A (2012) Indian strong motion Instrumentation Network. Seism Res Lett 85:59-66

[122] Kuo CH, Wen KL, Hsieh HH, Chang TM, Lin CM, Chen CT (2011) Evaluating empirical regression equations for Vs and estimating Vs30 in northeastern Taiwan. *Soil Dyn Earthq Eng* 31(3):431-439

[123] Lai SP (1982) Statistical characterization of strong motions using power spectral density function. Bull Seism Soc Am 72: 259-274

[124] Lee WKH, Lahr JC (1972) HYPO71: A computer program for determination of hypocenter, magnitude, and first motion pattern of local earthquake. Open file report, U.S. Geological Survey: 100

[125] Levenberg K (1944) A method for the solution of certain non-linear problems in least squares. Q Appl. Math 2: 164-168

[126] Lin CM, Chang TM, Wen KL, Kuo CH, Hsieh HH (2014) Seismogenic structure beneath decollement inferred from 2009/11/5 M_L 6.2 Mingjian earthquake in central Taiwan. Terr Atmos Ocean Sci 25:27-38

[127] Lomnitz C, Hofseth SN (2005) The Indian ocean disaster: Tsunami physics and early warning dilemmas. EOS Transactions American Geophysical Union, 86:65-76

[128] Lyon CH, Molnar P (1983) Constraints on the structure of the Himalaya from an analysis of gravity anomalies and a flexural model of the lithosphere. Journal of Geophysical Research 88: 8171-8191

[129] Mahajan AK, Virdi NS (2001) Macroseismic field generated by 29 March, 1999 Chamoli earthquake and its seismotectonics. J Asian Earth Sci 19:507-516

[130] Mahajan AK, Thakur VC, Sharma ML, Chauhan M (2010) Probabilistic seismic hazard map of NW Himalaya and its adjoining area, India. 53:443-457

[131] Mahood M, Hamzehloo H (2009) Estimation of coda wave attenuation in east central Iran. J Seism 13:125-139

[132] Malischewsky Auning PG, Lomnitz C, Wuttke F, Saragoni R (2006) Prograde Rayleigh wave motion in the valley of Mexico. Geofisica Interna 45:149-162

[133] Mandal P, Rastogi BK (1998) A frequency dependent relation of coda Qc for Koyna Warna region India. Pure Appl Geophys 153:163-177

[134] Mandal P, Kumar N, Satyamurthy C, Raju IP (2009) Ground-motion Attenuation Relation from Strong-motion Records of the 2001 Mw 7.7 Bhuj Earthquake Sequence (2001–2006), Gujarat, India. Pure appl geophys, 166:1–19

[135] Mandal P, Padhy S, Rastogi BK, Satyanarayana HVS, Kousalya M, Vijayraghavan R, Srinivasan A (2001) Aftershock activity and frequency-dependent low coda Qc in the epicentral region of the 1999 Chamoli earthquake of Mw 6.4. Pure Appl Geophys 158:1719-1735

[136] Manglik A, Verma SK (1998) Delineation of sediments below flood basalts by joint inversion of seismic and magnetotelluric data. Geophy Res Lett 25: 4015-4018

[137] McGuire RK (1976) FORTRAN computer program for seismic risk analysis, U.S. Geol. Survey. Open-File Rept 76-67

[138] McGuire RK (1977) Seismic design spectra and mapping procedures using hazard analysis based directly on oscillator response. Earthq Eng Structural Dyn 5:211-234

[139] McGuire RK (1978) FRISK-Computer program for seismic risk analysis using faults as earthquake sources. United States Geological Survey-open file report 78-110

[140] McGuire RK, Becker AM, Donovan NC (1984) Spectral estimates of seismic shear waves. Bull Seism Soc Am 74:2167–2185

[141] Metcalfe RP (1993) Pressure, temperature and time constraints on metamorphism across the Main Central Thrust zone and High Himalayan slab in Garhwal Himalaya, Himalayan tectonics. Geological Society special publication No.74, Treloar PJ, Searle MP (eds) pp.485-510

[142] Midorikawa S (1993) Semi empirical estimation of peak ground acceleration from large earthquake. Tectonophysics 218: 287-295

[143] Mikumo T, Irikura K, Imagawa K (1981) Near field strong motion synthesis from foreshock and aftershock records and rupture process of the main shock fault (abs). IASPEI 21th General Assembly, London, July 20-30

[144] Mitchell BJ (1995) Anelastic structure and evolution of the continental crust and upper mantle from seismic surface wave attenuation. Rev Geophys 33:441-462

[145] Mittal H, Kumar A, Ramhmachhuani R (2012) Indian national strong motion instrumentation network and site characteristzation of its stations. Int J GeoSci 3:1151-1167

[146] Mithal RS, Srivastava LS (1959) Geotectonic position and earthquakes of Ganga-

Brahamputra region. 1st symp Earthq Eng Roorkee

[147] Mohan K, Joshi A, Patel RC (2008) The assessment of seismic hazard in two seismically active regions in Himalayas using deterministic approach. J Ind geophys Union 12: 97-107

[148] Mohanty WK, Prakash R, Suresh G, Shukla AK, Walling MY, Srivastva JP (2009) Estimation of coda wave attenuation for the national capital region, Delhi, India using local earthquakes. Pure and App Geophys 166:429-449

[149] Molnar P, Tapponnier P (1975) Cenozonic tectonics of Asia: effects of a continental collision. Science 189:419-426

[150] Molnar P, Chen WP (1983) Focal depths and fault plane solutions of earthquakes under the Tibetian Platean. J Geophys res 88:1180-1196

[151] Molas GL, Yamazaki F. (1995), Attenuation of earthquake ground motion in Japan including deep focus events. Bull Seism Soc Am 85:1343-1358

[152] Molnar P, Chen WP (1983) Focal depths and Fault-plane solutions of earthquakes under the Tibetian plateau. J Geophy Res 88:1180-1196

[153] Montgomery DC, Peck EA, Vining GG (2003) Introduction to linear regression analysis, John Wiley & Sons (ASIA) Pvt. Ltd, Clementi Loop, Singapore

[154] Mukhopadhyay S, Sharma J, Massey R, Kayal JR (2008) Lapse time dependence of coda Q in the source region of the 1999 chamoli earthquake. Bull Seismol Soc Am 98:2080–2086

[155] Mukhopadhyay S, Sharma J (2010) Attenuation characteristics of Garhwal-Kumaon Himalayas from analysis of coda of local earthquakes. J Seism 14:693-713

[156] Munguia L, Brune JM (1984) Simulations of strong ground motions for earthquakes in the Mexicali-Imperial Valley. Proc. of workshop on strong ground motion simulation and earthquake engineering applications. Pub. 85-02. Earthquake Engineering Research Institute, Los Altos, California 21-1−21-19

[157] Nakata T (1989) Active faults of the Himalaya of India and Nepal. In tectonics of the western Himalaya (Malinconico LL, Jr, Lillie RJ, eds) pp 232, 243-264). Geol Soc America Spl paper (Geological Society of America, Colorado, 1989)

[158] Nath SK, Vyas M, Pal I, Sengupta P (2005) A Seismic hazard scenario in the Sikkim Himalaya from seismotectonics, spectral amplification, source parameterization and spectral attenuation laws using strong motion seismometry. J Geophys Res 110:B01301. doi: 10.1029/2004JB003199

[159] Nath SK, Thingbaljam KKS, Raj A (2008) Earthquake hazard in Northeast India - A seismic microzonation approach with typical case studies from Sikkim Himalaya and Guwahati city. J Earth Syst Sci 117:809-831

[160] Ni J, Barazangi M (1984) Sesimotectonics of the Himalayan collision zone: Geometry of the underthrusting Indian plate beneath the Himalaya. J Geophys Res 89: 1147-63

[161] Norton IO, Sclater IG (1979) A model for the evolution of the Indian Ocean and the breakup of the Gondwanaland. J Geophys Res 84:6803-6830

[162] OASES. Offshore Alaska seismic exposure study, Woodward- Clyde Consultants, San Francisco, CA, 1978

[163] Panza GF (1985) Synthetic seismogram: the Rayleigh waves model summation. J Geophy 58: 125-145

[164] Papageorgiou, AS, Aki, K., (1983) A specific barrier model for the quantitative description of inhomogeneous faulting and the prediction of strong ground motion. I. Description of the model. Bull Seism Soc Am 73:693-722

[165] Parvez IA, Vaccari F, Panza GF (2003) A deterministic seismic hazard map of India and adjacent area. Geophys J Int 155:489-508

[166] Patriat P, Achache J (1984) Indian- Eurasia collision chronology has implications for crustal shorting and driving mechanisms of plats. Nature 311:615-621

[167] Paul A, Gupta SC, Pant CC (2003) Coda Q estimates for Kumaon Himalaya. Earth Planet Sci 112:569-576

[168] Pujades L, Canas JA, Egozcue JJ, Puigvi MA, Pous J, Gallart J, Lana X, Casas A (1991) Coda Q distribution in the Iberain Penisula. Geophys J Int 100:285-301

[169] Pulli JJ (1984) Attenuation of coda waves in New England Bull Seism Soc Am 74:1149-1166

[170] Powell CMcA (1979) A speculative tectonic history of Pakistan and surroundings: some constraints from the Indian Ocean. In Farah A, Dejong KA (Eds), Geodynamics of Pakistan. Geol Surv Pak Quetta :5-24

[171] Rahimi H, Hamzehloo H, Kamalian N (2009) Estimation of Coda and Shear wave attenuation in the volcanic area in SE Sabalan Mountain, NW Iran. Acta Geophysica 58(2): 244-268

[172] Rao PP, Thakur NK, Rajput S (2006) A case study on simulation of seismic reflections for

4C ocean bottom seismometer data in anisotropic media using gas hydrate model. 6th International conference & exposition on petroleum geophysics in Kolkata.

[173] Rautian TG (1976) Role of source and medium in the formation of seismic oscillations near local earthquakes, Investigations of the physics of earthquakes, Nauka Publishing House, Moscow (in Russian): 25-55

[174] Rautian TG, Khalturin VI (1976) Spectral structure of the coda of local earthquakes as an instrument of investigation of the source radiation. Doklady Acad. Sci. USSR 226 (in Russian): 566-569

[175] Rautian TG, Khalturin VI (1978) The use of the coda for the determination of the earthquake source spectrum. Bull Seism Soc Am 68:923–948

[176] Reha S (1984) Q determined from local earthquakes in the South Carolina coastal plain. Bull Seism Soc Am 74: 2257-2268

[177] Roecker SW, Tucker B, King J, Hatzfield D (1982) Estimates of *Q* in central Asia as a function of frequency and depth using the coda of locally recorded earthquakes. Bull Seism Soc Am 72:129-149

[178] Rovelli A (1982) On the frequency dependence of Q in Friuli from short period digital records. Bull Seism Soc Am 72: 2369-2372

[179] Ruff LJ (1999) Dynamic stress drop of resent earthquakes: Variations within subduction zones. Pure App Geophys 154: 409-431

[180] Sahin S (2008), Lateral variations of coda Q and attenuation of seismic waves in Southwest Anatolia. J Seism 12: 367-376

[181] Saikia CK (1993) Ground motion studies in great Los angles due to $M_w = 7.0$ earthquake on the Elysian Thrust fault. Bull Seism Soc Am 83: 780-810

[182] Saikia CK and Herrmann RB (1985) Application of waveform modeling to determine focal mechanisms of four 1982 Miramichi aftershocks. Bull Seism Soc Am 75: 1021-1040

[183] Sato H (1977) Energy propagation including scattering effect. J Phys Earth 25:27-41

[184] Sato R (ed.) (1989) Handbook of Fault parameters of Japanese earthquakes, Kajima, Tokyo (in Japanese)

[185] Satyabala SP, Gupta HK (1996) Is the Quiescene of major earthquakes (M > 7.5) scince 1952 in the Himalaya and Northeast India real?. Bull Seism Soc Am 86: 1983-1986

[186] Searle MP, Windley BF, Coward MP, Cooper DJW, Rex AD, Rex D, Tingdong L, Xuchang X, Jan MQ, Thakur V, Kumar S (1987) The closing of Tethys and the tectonics of the Himalayas. Geol Soc Am Bull 98:678-701

[187] Seeber L, Armbruster JG, Quittmeyer RC (1981) Seismicity and continental collision in the Himalayan arc. In Geodynamics series: Zargos, Hindukush, Himalaya, Geodynamic Evolution (Gupta HK, Delany FM eds.) Am Geophysical Union Washington 3:215-242

[188] Seeber L, Armbruster JG (1984) Some elements of continental subduction along the Himalayan Front. Tectonophysics 92:335-367

[189] Shafiee A, Kamalian M, Jafari MK, Hamzehloo H (2011) Ground motion studies for microzonation in Iran. Nat Haz 59:481-505

[190] Shah HC, Dong WM (1984) Reliability assessment of existing building subjected to probabilistic earthquake loadings. Soil Dyn Earthq Eng 3(1): 35-41

[191] Shakal AF, Huang MJ, Graizer VM (2004) CSMIP strong motion data processing. Proc. International workshop on strong motion record processing May 26-27,COSMOS, Richmond California

[192] Sharma B, Teotia SS, Kumar D (2007) Attenuation of P, S and coda waves in Koyna region, India. J Seism 11:327-344

[193] Sharma B, Gupta AK, Devi K., Kumar D, Teotia SS, Rastogi BK (2008) Attenuation of high frequency seismic waves in Kachchh region, Gujarat India. Bull Seism Soc Am 98:2325-2340

[194] Sharma B, Kumar D, Teotia SS, Rastogi BK, Gupta AK, Prajapati S (2012) Attenuation of Coda wave in the Saurashtra region, Gujarat (India). Pure Appl Geophys 169: 89-100

[195] Sharma ML (1998) Attenuation relationship for estimation of peak ground horizontal acceleration using data from strong motion arrays in India. Bull Seism Soc Am 88:1063–1069

[196] Sharma ML, Douglas J, Bungum H, Kotadia J (2009) Ground motion prediction equations based on data from the Himalayan and Zagros regions. J Earthq Eng 13:1191-1210

[197] Singh C, Singh A, Bharathi S, Bansal AR, Chadha RK (2012) Frequency-dependent body wave attenuation characteristics in the Kumaun Himalaya. Tectonophys 524-525:37-42

[198] Singh RP, Aman A, Prasad YJJ (1996) Attenuation relations for strong seismic ground motion in the Himalayan region. Pure App Geophys 147(1):161-180

[199] Singh SK, Ordaz M, Dattarayam RS, Gupta HK (1999) A spectral analysis of the 21 May 1997, Jabalpur India earthquake (Mw = 5.8) and estimation of ground motion from future earthquakes in the Indian Shield region. BSSA 89:1620-1630

[200] Singh S, Gupta DK, Rajput S (2014a) Full waveform modeling for converted waves seismic reflections in mountainous and Marine Environment. Advances in Petroleum exploration and development 7(2): 21-29

[201] Singh S, Gupta DK, Rajput S (2014b) Pre-stack seismic inversion and amplitude versus angle modeling reduces the risk in Hydrocarbon prospect evaluation. Advances in Petroleum exploration and development 7(2): 30-39

[202] Somerville PG, Sen MK, Cohece BP (1991) Simulation of strong ground motions recorded during the 1985 Michoacan, Mexico and Valparaiso Chile earthquakes. Bull Seism Soc Am 81:1–27

[203] Srivastava LS (1969) A note on seismic zoning map of India. Bull Ind Soc Earthq Tech 6(4):185-194

[204] Stepp JC (1973) Analysis of completeness of the earthquake sample in the Puget sound area. In ST Harding (editor) contributions to seismic zoning. NOAA Tech. Rep. ERL 267- ESL 30, US Dep commerce

[205] Tandon AN (1956) Zone of India liable to earthquake damage. Ind J Meteo Gephy 10:137-146

[206] Todorovska MI, Gupta ID, Gupta VK, Lee VW, Trifunac MD (1995) Selected Topics in seismic hazard analysis. Report published in University of South California, Deptt of civil Eng CE 95-08

[207] Trifunc MD (1977) Uniformly processed strong motion earthquake ground accelerations in the Western United State of America for period from 1993 to 1971: Pseudo relative spectra and processing noise. Report CE 77-44, Univ Southern California Los Angles

[208] Ulutas E, Ozer MF (2010) Empirical attenuation relation of peak ground acceleration for Eastern marmara region in Turkey. Arab J Sci Eng 35:187-204

[209] Valdiya KS (1977) Structural setup of the Kumaon lesser Himalaya, In: Himalayan Science de la terre. Centre Nationale Recherche Science, Paris 268: 449-462

[210] Varma MM, Gosavi PD, Guha SK (1970) Kothagudem (Andhra Pradesh) earthquake of April 13, 1969, Broach (Gujarat) earthquake of March 23, 1970 and seismicity of Peninsular India. Bull Ind Soc Earthq Tech Vol VII(4):207-218

[211] Wells DL, Coppersmith KJ (1994) New empirical relationships among magnitude, rupture length, rupture width, and surface displacements. Bull Seism Soc Am 84: 974-1002

[212] Wen KL, Chang TM, Lin CM, Chiang HJ (2006) Identification of nonlinear site response using the H/V spectral ratio method. Terr Atmos Ocean Sci 17:533-546

[213] West WD (1937) Earthquake in India. Presidential address, Indian Science Congress

[214] Yu G (1994) Some aspect of earthquake seismology: Slip partitioning along major convergent plane boundaries; Composite source model for estimation of strong motion; and nonlinear soil response modeling. Ph.D. Thesis, University of Nevada, Reno

[215] Yu G, Khattri KN, Anderson JG, Brune JN, Zeng Y (1995) Strong ground motion from the Uttarkashi earthquake, Himalaya, India, Earthquake: Comparison of observations with synthetics using the Composite source model. Bull Seism Soc Am 85: 31-59

[216] Zelt BC, Dotzev NT, Ellis RM, Roger GC (1999) Coda Q in Southwestern British Columbia Canada. Bull Seism Soc Am 89: 1083-1093

[217] Zeng Y, Anderson JG, Su F (1994) A composite source model for computing realistic synthetic strong ground motions. Geophys Res Lett 21: 725-728

Websites used

http://earthquake.usgs.gov

http://pesmos.in